Aus dem Institut Experimentelle Neurologie der Klinik für Neurologie
der Medizinischen Fakultät Charité – Universitätsmedizin Berlin

DISSERTATION

Identification of erythropoietin isoforms and evaluation of their biological importance.

zur Erlangung des akademischen Grades
Doctor of Philosophy in Medical Neurosciences
(PhD in Medical Neurosciences)

vorgelegt der Medizinischen Fakultät
Charité – Universitätsmedizin Berlin

von

Christel Barbara Bonnas

aus Hof/Saale (Germany)

Gutachter: 1.: Prof. Dr. med. J. Priller

2.: Prof. Dr. med. I. Bechmann

3.: Prof. Dr. med. G. Kempermann

Datum der Promotion: 14.06.2009

I INDEX

I.I Abbreviations

AsialoEPO	desialylated erythropoietin
ELISA	Enzyme Linked Immunosorbent Assay
EPO	erythropoietin
EPOR	erythropoietin receptor
CEPO	carbamylated erythropoietin
CFU-E	colony forming unit erythroid
CFU-G	colony forming unit granulocyte
CFU-M	colony forming unit macrophage
CHO	Chinese Hamster Ovary cells
DCX	doublecortin
DIV	day *in vitro*
GFAP	Glial fibrillary acidic protein
GST-tag	protein tag consisting of the protein glutathione-S-transferase
HEK 293	Human Embryonic Kidney cells
HIF	hypoxia inducible factor
His-tag	protein tag consisting of Histidine residues
hS3	human splice variant missing exon 3
hS4	human splice variant missing first half of exon 4
HSC/HPC	hematopoietic stem and progenitor cells
IPTG	Isopropyl β-D-1-thiogalactopyranoside
LDH	lactate dehydrogenase
LIF	leukemia inhibitory factor
mMSC	murine mesenchymal stem cell
mS	murine splice variant missing exon4
MAP2	major microtubule associated protein of brain tissue
MOCK	preparations from cells transfected with empty expression vectors
NMDA	N-Methyl-D-aspartate
NSC/NPC	neural stem and precursor cells
OGD	Oxygen Glucose Deprivation
OSM	oncostatin M

PCR	Polymerase Chain Reaction
rhEPO	recombinant human erythropoietin
rpm	round per minute
RT	room temperature
RT-PCR	reverse transcription Polymerase Chain Reaction
s.d.	standard deviation
vEPO	erythropoietin variant(s)

I.II Table of contents

I INDEX 3

I.I Abbreviations 3
I.II Table of contents 5

1 INTRODUCTION 8

1.1 Erythropoietin – a hematopoietic cytokine 8
1.2 Erythropoietin receptor 10
1.3 Erythropoietin – more than a hematopoietic cytokine 12

1.3.1 Erythropoietin as neuroprotectant in experimental models of ischemia 13
1.3.2 Erythropoietin as cytoprotectant 14
1.3.3 Use of Erythropoietin as neurotherapeutic agent 14

1.4 An alternate Erythropoietin receptor? 15
1.5 Erythropoietin isoforms 15
1.6 Short introduction to stem cells 16

2 AIMS OF THIS STUDY 17
3 MATERIAL AND METHODS 19

3.1 Materials 19

3.1.1 Chemicals and Reagents 19
3.1.2 Kits 20
3.1.3 Antibodies 21
3.1.4 Cell Culture Media and Supplements 21
3.1.5 Equipment 22
3.1.6 Media and buffer formulations 23

3.1.6.1 Media used for Microbiology 23
3.1.6.2 Buffers 24

3.2 Methods 25

3.2.1 Cloning strategy 25

3.2.1.1 Synthesis of murine and human EPO cDNA 25
3.2.1.2 Construction of the pZ/EG-vEPO-IRES-EGFP plasmids 27
3.2.1.3 Construction of His-tagged vEPO-constructs 28
3.2.1.4 Generation of human EPO A-helix derivatives 29
3.2.1.5 Construction of the GST-tagged EPO-constructs 30
3.2.1.6 Generation of the murine LIFR and gp130-constructs 30

3.2.2 Protein expression and purification strategies 31

3.2.2.1 Expression of recombinant proteins in HEK293 and CHO-S cells 31
3.2.2.2 Purification of His-tagged proteins 32
3.2.2.3 Western Blot Analysis of purified proteins 33

3.2.3 Erythroid Colony formation assay 33
3.2.4 Primary neuronal cultures 34

3.2.4.1 Preparation of rat primary cortical neurons 34
3.2.4.2 Preparation of culture plates 34
3.2.4.3 Induction of neuroprotection with EPO variants in an *in vitro* model of cerebral ischemia 35
3.2.4.4 Lactate dehydrogenase (LDH) assay 36

3.2.4.5 Signaling cascades in primary cortical neurons 36
3.2.4.6 Akt kinase assay 37
3.2.4.7 AG490 kinase inhibitor experiment 37
3.2.4.8 Neuroprotection assays in presence of soluble receptors and blocking antibodies 37
3.2.5 H9c2 - model of myocardial ischemia 38
3.2.6 Immunoprecipitation of endogenous erythropoietin from mice 39
3.2.7 Expression analysis of cytokine receptors 39
3.2.8 Neural stem and progenitor cells 41
3.2.8.1 Isolation of neural stem and progenitor cells 41
3.2.8.2 Differentiation and survival assays 41
3.2.8.3 Pretreatment of NSC cultures and clonogenic assays 42
3.2.8.4 Real time analysis of GFAP mRNA expression in NSC sphere cultures 43
3.2.9 Pulldown experiments 43
3.2.9.1 Generation of competent bacteria 44
3.2.9.2 Test for erythropoietin production in the different *E.coli* strains 44
3.2.9.3 GST-Pulldown assay 44
3.2.10 BaF3-cells 45
3.2.10.1 Baf3/EPOR survival experiments 45
3.2.10.2 MTT (Thiazolyl blue) assay 45
3.2.10.3 Radioactive binding assay 46
3.2.11 Bone marrow cell assays 46
3.2.12 Murine mesenchymal stem cells (mMSC) 47
3.2.13 M1 proliferation assay 48
3.2.14 *In vivo* hematopoiesis assay 48
3.2.15 Bioinformatics 49

4 RESULTS 50

4.1 Identification of alternatively spliced EPO transcripts 51
4.2 Expression and purification of recombinant EPO variants (rvEPO) 55
4.3 Erythropoietic potential of the EPO variants 58
4.4 Neuroprotection experiments 59
4.4.1 EPO variants are neuroprotective in an *in vitro* model of cerebral ischemia 59
4.4.2 Dose-survival curves of the human EPO splice variants 62
4.4.3 Derivatives of the A-helix of hEPO are sufficient to induce neuroprotection 63
4.4.4 Identification of neuroprotective EPO peptides 65
4.5 hEPO and hS3 mediated cytoprotection in an *in vitro* model of myocardial ischemia . 66
4.6 Immunoprecipitation reveals EPO splicing isoform in murine tissues 67
4.7 Pathways involved in neuroprotection 69
4.8 EPO variants promote diverse effects on stem cells 72
4.8.1 EPO variants promote divergent effects in neural stem and precursor cells 72
4.8.2 Human A-helix derived peptide P16 protects neural stem and progenitor cells 79
4.8.3 EPO isoforms have no colony-stimulating activity on murine HPC 81
4.8.4 EPO isoforms support survival of HPC in *ex vivo* cultures 83
4.8.5 Effects of EPO isoforms on murine mesenchymal stem cells (mMSC) 88
4.9 Receptor characterization 90
4.9.1 Analysis of EPO-A-helix-muteins 90
4.9.2 *In silico* prediction of $(EPOR)_2$-binding of EPO splice variants 91

4.9.3 BaF3 experiments: survival and proliferation assays 92
4.9.4 BAF3/EPOR Pulldown experiments 93
4.9.5 Radioactive binding experiments 94
4.9.6 Cytokine receptor screening in various cell types 96
4.9.7 Receptor blocking experiments 97
4.9.8 Pulldown experiments LIFR 99

4.10 *In vivo* hematopoietic activity of vEPO 101

4.10.1 *In vivo* biological activity of recombinant human erythropoietins 101
4.10.2 *In vivo* hematopoietic activity of the EPO variants 102

5 DISCUSSION 104

5.1 Identification of endogenous Erythropoietin variants 104
5.2 *In vitro* functional analysis of the erythropoietin variants 106

5.2.1 Non-hematopoietic neuroprotective erythropoietin splice variants 106
5.2.2 Protective effects of hS3 in an *in vitro* model of myocardial ischemia 109

5.3 Effects of EPO variants on adult stem cells 109

5.3.1 Hematopoietic stem and progenitor cells (HSC/HPC) 109
5.3.2 EPO variants effect on neural stem and progenitor cells 113
5.3.3 EPO variants promote survival of mesenchymal stem cells 117

5.4 The vEPO receptor 118

5.4.1 An alternate non-hematopoietic EPOR? 118
5.4.2 LIFR as receptor candidate for the human splice variant hS3 119

5.5 Identification of a new neurotrophic sequence derived from erythropoietin 122
5.6 Conclusion and outlook 124

6 SUMMARY 126
7 APPENDIX 128

7.1 List of human and murine EPO variants 128
7.2 Multiple Alignments of human and murine EPO variants (cDNA) 129

7.2.1 Multiple Alignment of human EPO variants 129
7.2.2 Multiple Alignment of murine EPO variants 131

7.3 Protein Sequences of murine and human EPO variants 133
7.4 Summary: biological activities of the EPO variants and EPO peptides 134

8 REFERENCES 135
9 LIST OF FIGURES AND TABLES 144

9.1 List of Tables 144
9.2 List of Figures 145

ACKNOWLEDGEMENTS 147
CURRICULUM VITAE 148
LIST OF PRESENTATIONS AND PUBLICATIONS 149
EIDESSTATTLICHE ERKLÄRUNG 150

1 INTRODUCTION

1.1 Erythropoietin – a hematopoietic cytokine

The name erythropoietin comes from the Greek words ἐρυθρός (ērythrós) and ποιεῖν (poieîn) that mean ’red’ and ‘do’, respectively. Erythropoietin (EPO) was identified as hematopoietic cytokine that functions as the main regulator of erythropoiesis. This function of EPO was first formulated in 1906 by the French scientist Paul Carnot (Carnot *et al.*, 1906). In 1948 the term 'erythropoietin' was introduced by Bonsdorff and Jalavisto, but only in 1977 was native human EPO isolated for the first time from human urine at the University of Chicago (Miyake *et al.*, 1977). The glycoprotein hormone is primarily produced by the fetal liver and by the tubular cell fraction of the adult kidney (Peschle *et al.*, 1975; Schuster *et al.*, 1987). The main roles of EPO are inhibiting the apoptosis of erythroid precursor cells and support of their proliferation and differentiation into normoblasts (Jelkmann, 1992).

The erythropoietin gene was successfully cloned in 1985 (Jacobs *et al.*, 1985). The human EPO gene, a single-copy gene located on chromosome 7 at position 99,929,820 bp to 99,932,720 bp from *pter*, consists of five exons and four introns. EPO is much conserved throughout the species. The human gene shares 91% identity to monkey EPO, 85% identity to cat and dog EPO, and 80% to 82% identity to pig, sheep, mouse, and rat EPO (Wen *et al.*, 1993). These levels of identity are reflected in the phylogenetic tree of erythropoietin (Figure 1).

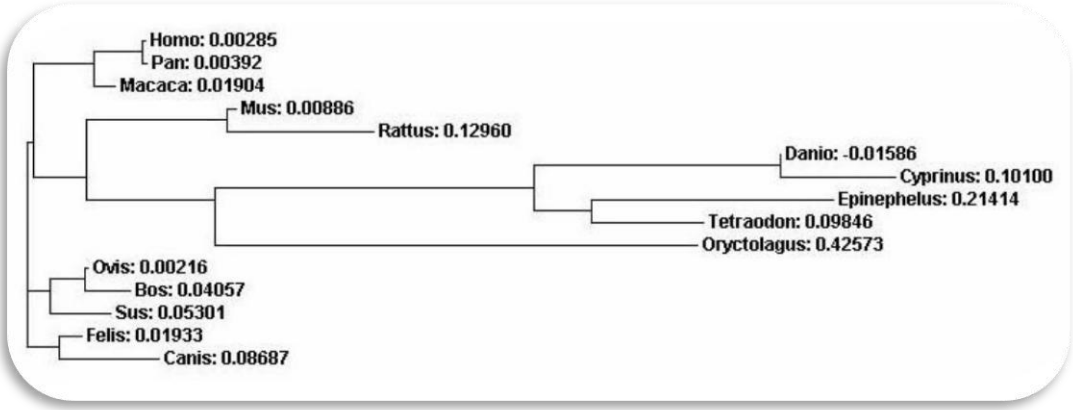

Figure 1: Phylogenetic tree of erythropoietin

A phylogenetic tree of erythropoietin was calculated from a Multiple Sequence Alignment (Clustal W) of the EPO coding sequences of different species using default parameters. Clustal W (at www.ebi.ac.uk) uses the neighbor-joining method of Saitou (Saitou et al., 1987) for phylogenetic calculations. The phylogenetic tree shows the evolutionary relationships among EPO of various species. Each node represents the most recent common ancestor of the descendants. The branch lengths are proportional to the amount of inferred evolutionary change. Negative branch lengths result from the algorithm.

Human EPO is a heavily glycosylated protein with a molecular weight of about 34,000 Da. It consists of one 165 amino acid chain and contains four oligosaccharide side chains: three N-linked and one O-linked. The carbohydrate moiety represents approximately 40% of the total molecular mass and is important for the stability and solubility of the protein (Narhi *et al.*, 1991), but not for receptor binding (Darling *et al.*, 2002). Thus, unglycosylated erythropoietin has a very low *in vivo* bioactivity due to rapid clearance from plasma by the liver (Tsuda *et al.*, 1990). EPO was predicted by Wen in 1994 and confirmed by NMR data in 1998 (Cheetham *et al.*, 1998) to have a four-antiparallel amphiphatic alpha-helical bundle structure (A, B, C and D), a structure shared with other members of the cytokine family (Figure 2).

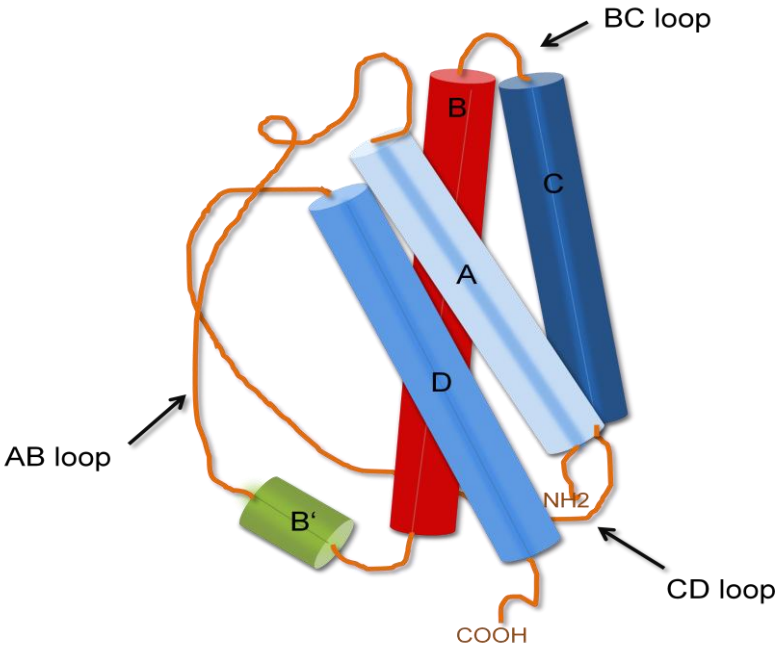

Figure 2: The average minimized NMR structure of EPO (modified according to Cheetham et al., 1998)

The NMR structure of erythropoietin is derived from a mutant MKLysEPO. This EPO analogue was generated by mutating the N-Linked glycosylation sites into Lys residues and by adding methionine and lysine residues to the N-terminus for higher expression yields in Escherichia coli. The view is taken perpendicular to the four-helical-bundle axis, parallel to the AD plane. The four alpha-helices are shown in red (helix B) and blue (helices A, C and D). The AB loop contains a short helix B' (green).

The A and D helices are linked by a disulfide bond between Cys7 and Cys161 and packed against the helices B and C. Near the carboxy end of the AB loop is a short alpha-helical segment (B') important for receptor binding (Cheetham *et al.*, 1998). The hydrophobic core of the protein is formed by aromatic residues of the D-helix that are packed against hydrophobic residues from the remaining helices. Species comparisons of EPO have shown that the core-forming amino acids are invariant. Mutations in these domains lead to marked effects on protein folding. Functionally important domains for $(EPOR)_2$-binding have been delineated in human

EPO by preparing amino acid replacement mutants and testing them in three cell bioassay systems based on the human UT7-EPO leukemia cell line, the murine HCD57 erythroleukemia cell line and murine erythroid spleen cells (Wen *et al.*, 1994). Two distinct patches were identified on the protein surface relevant for the formation of a 2:1 homodimeric (EPO receptor)$_2$:EPO complex. A high-affinity receptor binding site involves residues at the helix D:AB loop interface and a low affinity receptor binding site comprises residues Val11, Arg14, Tyr15, Ser100, Arg103, Ser104 and Leu108 (Wen *et al.*, 1994).

EPO expression in the fetal liver and adult kidney is induced under hypoxic conditions via the hypoxia-inducible factor 1 (HIF-1) (Semenza *et al.*, 1992). HIF proteins are transcriptional regulators targeting genes involved in angiogenesis, vasomotor control, energy metabolism, apoptosis and erythropoiesis (Marti, 2004). HIF-1 is a heterodimer composed of an α- and a β-subunit. The HIF-1β subunit is a constitutive nuclear factor. HIF-1α is an oxygen-labile protein containing two oxygen-dependent degradation domains (ODD) that is rapidly degraded under normoxic conditions (Huang *et al.*, 1998). Regulators of this proteasome-mediated degradation are three prolyl-4-hydroxylases (PHD 1-3) that require O_2, iron and oxoglutarate as cofactors. Under normoxic conditions the PHD proteins hydroxylase key prolines in the HIF-1α subunit, thus leading to their ubiquitylation and proteasomal degradation (Cai *et al.*, 2003). Under hypoxic conditions this hydroxylation cannot occur and HIF-1 accumulates in the nucleus. HIF-1 binds to a highly conserved region 120 bp 3' to the polyadenylation site of the EPO gene, the hypoxically inducible enhancer (Semenza *et al.*, 1991). Depending on the severity of hypoxia, EPO mRNA levels can increase about 100-fold *in vitro* (Marti *et al.*, 1996) and about 1000-fold *in vivo* (Fandrey *et al.*, 1993).

Hypoxic conditions, leading to transactivation of erythropoietin, can be mimicked by cobalt chloride ($CoCl_2$) and the iron chelator desferrioxamine (DSF). $CoCl_2$- and DSF-treatment of murine neuronal and astroglial cultures induced EPO mRNA expression of about 4- to 5-folds (Bernaudin *et al.*, 2000). Also *in vivo* application of $CoCl_2$ and DSF was found to stimulate EPO gene transcription in mice and rats (Bernaudin *et al.*, 2000; Prass *et al.*, 2002). A possible mechanism for the actions of the transition metal Co^{2+} is the substitution of the iron (Fe) atom in heme proteins, locking them thereby in a ‘deoxy’ state. In contrast, DSF binds intracellular iron and thereby inhibits the Fe-catalyzed formation of reactive oxygen species.

1.2 Erythropoietin receptor

First evidence for an erythropoietin binding receptor (EPOR) was published in 1987 from cross-linking experiments of iodinated EPO to immature murine erythroid cells (Sawyer *et al.*, 1987).

Two years later, the DNA sequence of this unidentified protein could be identified by expression cloning from a pXM expression library made from murine erythroleukemia cells (D'Andrea *et al.*, 1989). In 1990, the human erythropoietin receptor was finally cloned from an erythroleukemia line (OCIM1) and from fetal liver (Jones *et al.*, 1990).

On a genomic level the human EPOR gene has a size of 6 kb, contains 8 exons and is located on chromosome 19 (11,348,883 to 11,356,019 from *pter*). The corresponding glycoprotein has a size of approximately 66 kDa and belongs to the type I cytokine receptor family.

The binding of EPO to preformed $(EPOR)_2$-dimers induces a conformational change that brings constitutively associated Janus family tyrosine protein kinases 2 (Jak2) in close proximity and stimulates their activation by transphosphorylation (Witthuhn *et al.*, 1993). In turn, Jak2 phosphorylates residues in the cytoplasmic domain of EPOR, thereby inducing several downstream signaling cascades. Depending on the cell type, EPO binding activates pathways involving the Signal Transducers and Activators of Transcription (STATs), the Ras-mitogen-activated protein kinase (MAPK) or the phosphatidylinositol 3-kinase (PI3K) (Rossert *et al.*, 2005). Several domains are essential for receptor functioning: a WSXWS motif is necessary for proper protein folding and a box 1 motif in the cytoplasmic part of the receptor is required for Jak interaction and activation. Furthermore the protein contains a cytoplasmic immunoreceptor tyrosine-based inhibitor motif (ITIM) that is involved in modulation of cellular responses by binding the SH2-domains of several phosphatases. The existence of a fibronectin type-III domain is shared with other cytokine receptor.

A few years ago, several splice variants of the EPOR were reported in human primary cancers and cancer cell lines. Splicing is the crucial mechanism for messenger RNA (mRNA) maturation. This process removes introns and joins exons in a primary transcript (pre-mRNA). Introns usually contain a clear splicing signal, namely **gu** at the 5’ end of the splicing site, the splice donor, and **ag** at the 3’ end, the splice acceptor. These GU–AG dinucleotides flank more than 98% of known intron sequences. The third important element of the splice site is the branch site, which is located 20 - 50bp upstream of the acceptor site. The branch site contains a CU(A/G)**A**(C/U) motif, whereas **A** is conserved in all genes. Five snRNAs (U1, U2, U4, U5, and U6 snRNPs) and their associated proteins form the spliceosome that catalyses a two-step enzymatic reaction leading to removal of the intron and joining of the two neighboring exons (Figure 3).

Alternative splicing regulates differential inclusion or exclusion of regions in the immature mRNA, invalidating the old theory of ‘one-gene-one-protein’. Four modes of alternative splicing

are known: alternative selection of promoters; alternative polyadenylation; intron retaining and splicing out of exons.

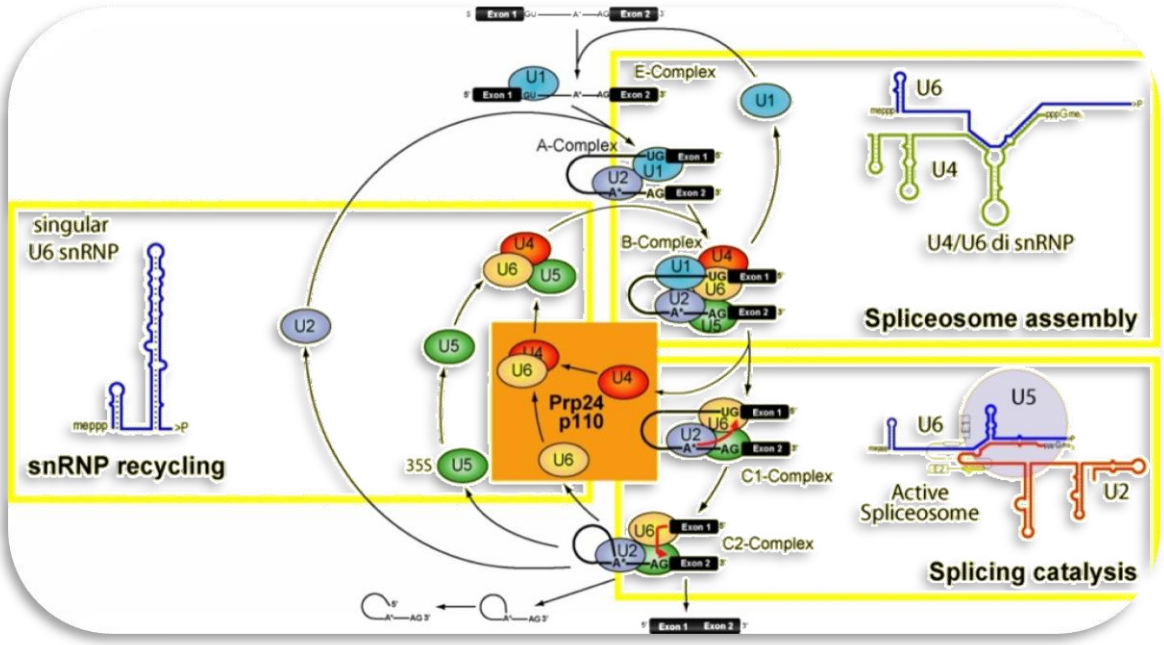

Figure 3: Spliceosome catalyses removal of introns in pre-mRNAs

Source: http://de.wikipedia.org/wiki/Bild:Spliceosome_ball_cycle_new2.jpg
The spliceosome is assembled in a stepwise process. In a first step, the U1 snRNP and non snRNP associated factors bind to the 5' splice site of the pre-mRNA forming thereby the early (E) ATP-independent complex committing the pre-mRNA to the splice process. U2 sRNP becomes tightly associated with the branch point sequence to form complex A. Recruitment of further snRNPs completes the spliceosome (complex C) activating it thereby for catalysis. The pre-mRNA splicing reaction proceeds in two steps: 5' splice site cleavage and ligation of the intron's 5' end to the branch site occurs in the first step. The 3' splice site cleavage with resulting excision of the intron takes place in the second step.

The first identified EPOR splice variants, reported by Nakamura in 1992, resulted from intron retaining leading to an early stop codon as in the case of the soluble EPO receptor (EPOR-S), or to a prolonged amino acid sequence as in the case of EPOR-T. In the last years, several more splice variants were revealed encoding soluble EPO receptors or membrane-bound EPO receptors with intracellular carboxy-terminal truncations (Arcasoy *et al.*, 2003).

1.3 Erythropoietin – more than a hematopoietic cytokine

EPO was long thought to be exclusively produced in kidney and fetal liver but recently brain and uterus have been identified as additional production sites that regulate EPO expression in a tissue-specific manner (Chikuma *et al.*, 2000). The finding of a hematopoietic factor in the brain raised the question if erythropoietin was merely a regulator of erythropoiesis. Furthermore, the homodimeric erythropoietin receptor $(EPOR)_2$ was not only found on erythroid colony-forming units but also on neurons, astrocytes and endothelial cells in the brain (Marti *et al.*, 1996). It

seems that a paracrine EPO/$(EPOR)_2$ system exists in the central nervous system independent of the endocrine system of adult erythropoiesis.

In recent years, EPO was found to have multiple functions outside of the bone marrow. Erythropoietin acts as an antiapoptotic and tissue-protective cytokine in multiple *in vitro* and *in vivo* studies.

1.3.1 Erythropoietin as neuroprotectant in experimental models of ischemia

In vitro it was shown that cortical neurons were protected by EPO against neurotoxic events such as NMDA (N-methyl-D-aspartate) or nitric oxide (Digicaylioglu *et al.*, 2001) and ischemic events such as oxygen and glucose deprivation (Sinor *et al.*, 2000).

The oxygen and glucose deprivation model (OGD-model) is an *in vitro* model of brain ischemia. In medicine, ischemia is a restriction of blood supply, resulting in damage or dysfunction of the affected tissue. The organs most sensitive to inadequate blood supply are the heart, the kidneys and the brain. The brain requires glucose and oxygen to maintain neuronal metabolism and function. Hypoxia refers to inadequate delivery of oxygen to the brain, and ischemia results from insufficient cerebral blood flow. The consequences of cerebral ischemia depend on the degree and the duration of reduced cerebral blood flow. Neurons can tolerate ischemia for 30 - 60 minutes. If flow is not re-established to the ischemic area, a cascade of metabolic processes ensues. The neurons become depleted of ATP and switch to anaerobic glycolysis, a much less efficient pathway. Lactate accumulates and the intracellular pH decreases. Without an adequate supply of ATP, ion pumps in the plasma membrane fail. The resulting influx of sodium, water and calcium into the cell causes rapid swelling of neurons and glial cells. Membrane depolarization also stimulates the massive release of the amino acids glutamate and aspartate, both of which act as excitatory neurotransmitters in the brain. Glutamate further activates sodium and calcium channels in the neuronal cell membrane, namely the well-characterized NMDA calcium channel. Excessive calcium influx causes the disordered activation of a wide range of enzyme systems such as proteases, lipases and nucleases. These enzymes and their metabolic products, such as oxygen free radicals, damage cell membranes, genetic material and structural proteins in the neurons, ultimately leading to cell death (Dirnagl *et al.*, 1999).

In vivo models of ischemia, performed in mouse, rat or gerbil, also revealed significant reduction in stroke volumes after erythropoietin treatment (Bernaudin *et al.*, 1999; Brines *et al.*, 2000; Morishita *et al.*, 1997). This finding was independent from the mode of application: intraventricularly in order to bypass the blood brain barrier (BBB) or systemically. Although the

BBB is considered impermeable to large molecules, EPO was demonstrated to cross the BBB (Brines *et al.*, 2000).

1.3.2 Erythropoietin as cytoprotectant

In addition to neuroprotective effects EPO also mediates robust cytoprotective effects in ischemic models of the retina (Junk *et al.*, 2002), the spinal cord (Celik *et al.*, 2002), the heart (Calvillo *et al.*, 2003), the skin (Saray *et al.*, 2003) and the intestine (Akisu *et al.*, 2001). Furthermore, EPO promotes endothelial cell proliferation and angiogenesis (Anagnostou *et al.*, 1990; Anagnostou *et al.*, 1994) and has immunomodulatory effects on B-cells and T-cells (Imiela *et al.*, 1993; Katz *et al.*, 2007). Recent *in vitro* experiments show that pharmacological doses of EPO have effects on neural stem cells, acting on their proliferation, survival, and differentiation (Shingo *et al.*, 2001; Studer *et al.*, 2000) and increasing neuroblast migration to areas exposed to ischemic damage *in vivo* (Zhang *et al.*, 2004).

1.3.3 Use of Erythropoietin as neurotherapeutic agent

Although endogenous brain EPO is crucial for neuronal survival in mild ischemia (Sakanaka *et al.*, 1998), it is not sufficient to significantly reduce brain injury after stroke. Therefore, exogenous administration of EPO has been considered. Promising results were obtained in animal models, since treatment of mice with exogenous EPO reduced brain damage after hypoxia (Marti *et al.*, 2000). In a pilot double-blind clinical trial using recombinant erythropoietin (rhEPO), Ehrenreich suggested that the protection may also apply to human stroke patients (Ehrenreich *et al.*, 2002). As erythropoietin is a general cytoprotective factor, its clinical application is not restricted to ischemia but might be considered for the treatment of chronic diseases associated with neuronal or cellular degeneration such as Parkinson's or Alzheimer's disease or for psychiatric disorders where neurodegenerative processes are likely to contribute to the pathophysiology of the disease. Actually, clinical trials for a psychiatric disorder, namely schizophrenia, are currently underway (Ehrenreich *et al.*, 2007).

One major drawback of erythropoietin in the treatment of chronic diseases is its hematopoietic property, leading to undesired rheological properties of the blood at chronic dosing. Thus, research focused in the last years on uncoupling the hematopoietic potential of EPO from its neuro- and cyto-protective characteristics. A first success was the invention of asialoerythropoietin (asialoEPO) but it's very short plasma half-life made *in vivo* applications inefficient (Erbayraktar *et al.*, 2003). In 2004, a carbamylated non-hematopoietic EPO-derivative (CEPO) was published by Leist et al., having preserved neuroprotective functions and a normal plasma half-life. Leist showed, in a rat cerebral infarct model, that CEPO had comparable tissue-

protection capacities at equal doses as reported for EPO. Analogous to EPO, CEPO was found to be cardioprotective in a rat ischemia-reperfusion model (Fiordaliso *et al.*, 2005), kidney-protective in a rat ischemia-reperfusion model (Imamura *et al.*, 2007) and ameliorated disease and neuroinflammation in a rat model of experimental autoimmune encephalomyelitis (Savino *et al.*, 2006).

1.4 An alternate Erythropoietin receptor?

The fundamental question is how neuroprotective actions can be independent from erythropoietic actions in EPO derivatives. The nonerythropoietic characteristic of asialoEPO, having only a short plasma half-life, is based on the fact that formation of red blood cells requires the continuous presence of EPO, whereas a brief exposure is sufficient for neuroprotection *in vitro* (Erbayraktar *et al.*, 2003). However, it is also conceivable that EPO derivatives do not mediate their neuroprotective activities via the classical erythropoietin receptor $(EPOR)_2$ as suggested for CEPO (M. Brines *et al.*, 2004). Brines et al. proposed a heterodimeric receptor complex as non-hematopoietic receptor mediating EPO protection, consisting of one EPOR chain and the beta common chain, the signaling subunit of many receptors such as the granulocyte macrophage colony-stimulating factor (GM-CSF) receptor, the interleukin-3 (IL-3) receptor and the IL-5 receptor. Recent findings in EPOR conditional knockdown mice suggest that the EPOR chain may not be involved in protection of neurons from ischemic injury (Tsai *et al.*, 2006). To this date, the existence and identity of a putative non-hematopoietic EPO receptor remains unclear.

1.5 Erythropoietin isoforms

No splice variants of EPO have been reported in mammalians so far. Hints for alternatively spliced EPO transcripts in the mouse were obtained during my diploma thesis (‘Neuroprotection by erythropoietin: isolation of novel isoforms and brain-specific expression in the mouse’, unpublished data). The aim of this work was to establish a Cre-loxed based vector system for the creation of a brain specific EPO overexpressing mouse. The alternative EPO transcripts were accidentally isolated by Nested PCR from murine brain and kidney cDNA. Most of the alternative EPO transcripts contained internal deletions at repetitive sequences, but one variant (mS) followed a GU-AG splice pattern. However, whether the alternative transcripts are translated into protein remained unclear to that date. Preliminary *in vitro* studies suggested a neuroprotective potential of the recombinant splice variant mS equivalent to recombinant murine erythropoietin but the function of the erythropoietin isoforms was not analyzed in more detail.

1.6 Short introduction to stem cells

A stem cell is defined as a cell possessing the capability of self-renewal, which is the ability to go through multiple cell cycles of cell division without entering differentiation, and possessing a differentiation potential in specialized cells, whereas this can be any mature cell type in the case of totipotent stem cells (e.g. fertilized egg) or only defined cell types in the case of pluripotent (e.g. embryonic stem cell), multipotent (e.g. hematopoietic stem cell) or unipotent cell types (e.g. muscle stem cell). Two classes of stem cells are found in mammalians, namely embryonic stem cells derived from the inner cell mass of a blastocyst and adult stem cells that are found in multiple adult tissues acting as a repair system of the body, such as neural stem cells (NSC), hematopoietic stem cells (HSC) and mesenchymal stem cells (MSC). NSC exist in the adult human mammalian brain throughout the entire lifetime. This cell type is capable of self-renewal, proliferation, and differentiation into brain cells, most predominantly neurons and astrocytes. Two defined areas of ongoing neurogenesis have been identified in the adult mammalian brain namely the subgranular layer of hippocampal dentate gyrus and the subventricular zone of the forebrain (Zhao *et al.*, 2008). From the latter, NSC migrate tangentially along the rostral migratory stream towards the olfactory bulb before they undergo differentiation into all types of neural cells, including neurons, astrocytes, and oligodendrocytes (Zhao *et al.*, 2008). Neural stem cells and further determined neural progenitors or precursor cells (NPC), can be dissected from the defined brain regions and taken into culture. Primary cultures of adult NSC/NPC are potent tools to investigate signals controlling adult neurogenesis. Addition of fibroblast growth factor beta (β-FGF) and epidermal growth factor (EGF) are sufficient for expansion of adult NSC/NPC as sphere cultures and maintenance of their multipotent feature. HSC and MSC can both be isolated from adult bone marrow (Ratajczak *et al.*, 2007). HSC give rise to all blood cell types including myeloid and lymphoid lineages. *In vivo* transplantation of HSC into adult recipient mice depleted of endogenous HSC by high dose irradiation has been shown to lead to the complete, long-term engraftment of all blood lineages by donor-derived stem cells. Thus, human HSC are of clinical importance in transplantation scenarios for blood-related genetic deficiencies and leukemias. Hence, *ex vivo* expansion of HSC is of intense interest (Durand *et al.*, 2005). MSC are a rare stromal population that has the capacity to differentiate into several tissues of mesenchymal origin, such as bone, fat and cartilage. However, recent studies show also successful induction of myogenesis and tenogenesis (Kolf *et al.*, 2007). MSC are usually isolated by adherence to plastic and constitutive passages, and acquire a fibroblast-like appearance. Because MSCs are multipotent and easily expanded in culture, there is much interest in their clinical potential for tissue repair and gene therapy.

2 AIMS OF THIS STUDY

The principal aims of this study were:

1. To provide experimental evidence for the existence of the murine EPO variants identified during my diploma thesis.
2. To screen for EPO variants in human tissues and to isolate possible transcripts.
3. To generate recombinant human and murine EPO variants in eukaryotic expression systems for analysis of possible hematopoietic and cytoprotective features in appropriate *in vitro* models.
4. To analyze the mechanisms underlying the neuroprotective effects of the EPO variants.
5. To investigate possible effects of the EPO variants on different types of adult stem cells.

The first aim of this study was the characterization of the murine erythropoietin variants identified during my diploma thesis. The promising results of my diploma thesis concening the neuroprotective potential of the splice variant mS encouraged me to study more closely the biological functions of the murine erythropoietin variants. Thus, a main goal was to provide evidence for their existence on a protein level.

Furthermore I supposed that erythropoietin splice variants might not be unique to the murine organism. During this study, two EPO splice variants, hS3 and hS4, being structurally different from the murine splice variant mS, were isolated from human kidney and brain cDNA.

Due to the very low abundance of the murine and human EPO variants further characterization required the generation of recombinant proteins. Thus, this project aimed to establish a protocol for production of the EPO variants in a eukaryotic expression system and subsequent purification of the recombinant proteins.

Since EPO has been shown to be neuro- and tissue-protective, a study of possible hematopoietic, neuroprotective and cytoprotective actions of the recombinant EPO variants in appropriate *in vitro* models was attempt. These experimental results raised the question about the mechanisms underlying EPO-mediated neuroprotection. To answer the question about the minimal protein domains required for neuroprotective actions, I intended to generate EPO mutants and EPO peptides and to analyze them in our *in vitro* models of neuroprotection and hematopoiesis. Furthermore, I planned to examine cellular signaling pathways in primary cortical neurons.

A major interest in this study was to investigate potential antiapoptotic effects of the EPO variants exerted on adult stem cells. I focused on three types of murine adult stem cells already established in our laboratory, namely neural stem cells, hematopoietic stem cells and mesenchymal stem cells. Putative differentiation effects of the EPO isoforms were analyzed in more detail in stem and precursor cultures of neural and hematopoietic origins.

Receptor studies performed in the last part of this study emerged from the unexpected result that the classical EPO receptor is not involved in mediating the functions of the EPO variants.

3 MATERIAL AND METHODS

3.1 Materials

3.1.1 Chemicals and Reagents

Product	Supplier
Agar-Agar (pure)	Roth, Karlsruhe (Germany)
Agarose NEEO Ultra	Roth, Karlsruhe (Germany)
Albumine from bovine serum, >= 96% purity	Sigma-Aldrich, Taufkirchen (Germany)
Ammoniumpersulfate, > 98% purity	Sigma-Aldrich, Taufkirchen (Germany)
BD TALON columns	BD Biosciences, Heidelberg (Germany)
BD TALON™ Metal Affinity Resin	BD Biosciences, Heidelberg (Germany)
β-mercaptoethanol ($HSCH_2CH_2OH$)	Merck, Darmstadt (Germany)
β-Nicotinamide adenine dinucleotide, reduced	Sigma-Aldrich, Taufkirchen (Germany)
Bromophenol blue ($C_{19}H_{10}Br_4O_5S$)	Sigma-Aldrich, Taufkirchen (Germany)
Chloroform ($CHCl_3$)	Sigma-Aldrich, Taufkirchen (Germany)
Cobalt Chloride ($CoCl_2$)	Sigma-Aldrich, Taufkirchen (Germany)
Coomassie Brilliant Blue G solution	Sigma-Aldrich, Taufkirchen (Germany)
Crystal violet ($C_{25}H_{30}N_3Cl$)	Sigma-Aldrich, Taufkirchen (Germany)
Diethylpyrocarbonate (DEPC)	Sigma-Aldrich, Taufkirchen (Germany)
DNase RQ1	Promega, Mannheim (Germany)
dNTP-mix	Promega, Mannheim (Germany)
EDTA, Ethylenediaminetetraacetic acid	Sigma-Aldrich, Taufkirchen (Germany)
Ethanol	Baker, Deventer (Netherlands)
Ethidium bromide	Roth, Karlsruhe (Germany)
Glycine	Sigma-Aldrich, Taufkirchen (Germany)
Glycerol, >99% purity	Sigma-Aldrich, Taufkirchen (Germany)
4-(2-Hydroxyethyl)piperazine-1-ethanesulfonic acid (HEPES) >99.5% purity	Sigma-Aldrich, Taufkirchen (Germany)
Imidazole ($C_3H_4N_2$)	Sigma-Aldrich, Taufkirchen (Germany)
Isopropanol	Sigma-Aldrich, Taufkirchen (Germany)
Isopropyl β-D-1-thiogalactopyranoside (IPTG), >99% purity	Sigma-Aldrich, Taufkirchen (Germany)
Lithium chloride (LiCl)	Roth, Karlsruhe (Germany)
Magnesium sulphate heptahydrate ($MgSO_47H_2O$)	Merck, Darmstadt (Germany)
Milk powder blocking grade	Roth, Karlsruhe (Germany)
M-MuLV reverse transcriptase	Promega, Mannheim (Germany)
Paraformaldehyde, extra pure	Merck, Darmstadt (Germany)
Peptone	Roth, Karlsruhe (Germany)
Phenol:Chloroform:Isoamyl Alcohol (25:24:1, v/v), UltraPure™	Invitrogen, Karlsruhe (Germany)
Phenylmethanesulfonylfluoride (PMSF)	Sigma-Aldrich, Taufkirchen (Germany)
Pfu Turbo Hotstart Polymerase	Stratagene, Amsterdam(Netherlands)
Ponceau S solution	Sigma-Aldrich, Taufkirchen (Germany)

Product	Supplier
Potassium chloride (KCl)	Merck, Darmstadt (Germany)
Potassiumphosphate dibasic (K_2HPO_4)	Merck, Darmstadt (Germany)
Potassiumphosphate monobasic (KH_2PO_4)	Merck, Darmstadt (Germany)
Pyruvic acid	Sigma-Aldrich, Taufkirchen (Germany)
Random hexameres	Promega, Mannheim (Germany)
Rotiphorese Gel 30	Roth, Karlsruhe (Germany)
RNasin	Promega, Mannheim (Germany)
RQ1 DNase	Promega, Mannheim (Germany)
SeeBlue Plus2 Prestained Standard	Pierce, Bonn (Germany)
Sodiumchloride, >99.8% purity (NaCl)	Roth, Karlsruhe (Germany)
Sodium dodecyl sulphate, 99% purity (SDS)	Sigma-Aldrich, Taufkirchen (Germany)
Sodiumhydrogencarbonate ($NaHCO_3$)	Sigma-Aldrich, Taufkirchen (Germany)
Sodium dihydrogenphosphate ($NaH_2PO_{4)}$	Merck, Darmstadt (Germany)
Sodium hydroxide pellets, extra pure	Merck, Darmstadt (Germany)
Soluble EPOR (sEPOR)	R&D Systems, Wiesbaden-Nordenstadt (Germany)
Soluble LIFR (sLIFR)	R&D Systems, Wiesbaden-Nordenstadt (Germany)
Streptavidin-agarose	Pierce, Bonn (Germany)
SYBR®Gold (10,000x)	Molecular Probes, Invitrogen, Karlsruhe (Germany)
T4 DNA Ligase	Roche, Mannheim (Germany)
TEMED	Roth, Karlsruhe (Germany)
Thiazolyl Blue Tetrazolium Bromide, ~98% purity	Sigma-Aldrich, Taufkirchen (Germany)
Tris-hydrochloride, >99% purity	Roth, Karlsruhe (Germany)
Triton®X-100	Sigma-Aldrich, Taufkirchen (Germany)
Trizol Reagent	Invitrogen, Karlsruhe (Germany)
Tween 20	Sigma-Aldrich, Taufkirchen (Germany)
Western Blotting Luminol Reagent	Santa-Cruz, Heidelberg (Germany)
Yeast extract	Roth, Karlsruhe (Germany)

Table 1: List of Chemicals and Reagents

3.1.2 Kits

Kit	Supplier
Access-RT-PCR Kit	Promega, Mannheim (Germany)
Akt assay Kit	Cell Signaling, NEB, Schwalbach (Germany)
BCA assay	Pierce, Bonn (Germany)
Color Silver Stain Kit	Pierce, Bonn (Germany)
ELISA hEPO	Roche, Mannheim (Germany)
ELISA mEPO	R&D Systems, Wiesbaden-Nordenstadt (Germany)
ELISA pSer-Akt	R&D Systems, Wiesbaden-Nordenstadt (Germany)
Light Cycler Fast Start DNA Master SYBRGreen I kit	Roche, Mannheim (Germany)
Slide-A-Lyzer (10K MWCO)	Pierce, Bonn (Germany)
Spectra/Por Dispo Dialyzer	Spectrum Laboratories, DG Breda (Netherlands)
Thermo Sequenase™ Primer Cycle Sequencing Kit	GE Healthcare, München (Germany)
QIAGEN Endofree Maxiprep Kit	QIAGEN, Hilden (Germany)

QIAGEN Plasmid Midi Kit	QIAGEN, Hilden (Germany)
QIAquick Gel extraction Kit	QIAGEN, Hilden (Germany)
QIAprep Spin Miniprep Kit	QIAGEN, Hilden (Germany)

Table 2: List of commercial Kits

3.1.3 Antibodies

Antibody	Supplier
α-BAD, rabbit	Cell Signaling, NEB, Schwalbach (Germany)
α-doublecortin (DCX), goat	Santa-Cruz, Heidelberg (Germany)
α-GFAP, rabbit	DAKO, Hamburg (Germany)
α-goat Alexa 594, donkey	Molecular Probes, Invitrogen, Karlsruhe (Germany)
α-gp130, rabbit	Santa-Cruz, Heidelberg (Germany)
α-gp130, rabbit	Hypromatrix, Worcester (USA)
α-IL-3/IL-5/GM-CSFRβ	Santa-Cruz, Heidelberg (Germany)
α-Jak2, rabbit	Santa-Cruz, Heidelberg (Germany)
α-LIFR, rabbit	Santa-Cruz, Heidelberg (Germany)
α-LIFR, rabbit	Hypromatrix, Worcester (USA)
α-MAP2, mouse	Sigma-Aldrich, St. Louis (USA)
α-mEPO, goat	R&D Systems, Wiesbaden-Nordenstadt (Germany)
α-mouse HRP, goat	GE Healthcare, München (Germany)
α-mouse Alexa 488, donkey	Molecular Probes, Invitrogen, Karlsruhe (Germany)
α-olig α-Myelin CNPase	Sternberger Monoclonals, Lutherville, Maryland (USA)
α-pBad-Ser112, rabbit	Cell Signaling, NEB, Schwalbach (Germany)
α-pBad-Ser136, rabbit	Cell Signaling, NEB, Schwalbach (Germany)
α-pIKK, rabbit	Cell Signaling, NEB, Schwalbach (Germany)
α-pJak1, rabbit	Santa-Cruz, Heidelberg (Germany)
α-pJak2, rabbit	Santa-Cruz, Heidelberg (Germany)
α-pStat5, rabbit	Santa-Cruz, Heidelberg (Germany)
α-rabbit Alexa 488, donkey	Molecular Probes, Invitrogen, Karlsruhe (Germany)
α-rabbit HRP, goat	GE Healthcare, München (Germany)
α-rhEPO, rabbit (H-162)	Santa-Cruz, Heidelberg (Germany)
α-RIP, mouse (MAB 1580)	Chemicon, Hofheim (Germany)
α-V5, rabbit	Serotec, Martinsried (Germany)

Table 3: List of antibodies

3.1.4 Cell Culture Media and Supplements

Product	Supplier
B27 supplement	Gibco, Karlsruhe (Germany)
B27 supplement w/o retinoic acid	Gibco, Karlsruhe (Germany)
Collagen G	Biochrom, Berlin (Germany)
CD-CHO medium	Gibco, Karlsruhe (Germany)
D-(+)-Glucose >99.5% purity	Sigma-Aldrich, St. Louis (USA)
DMEM High Glucose	Gibco, Karlsruhe (Germany)

Product	Supplier
EBSS	Gibco, Karlsruhe (Germany)
ECGS/H	PromoCell, Heidelberg (Germany)
ERYPO (rhEPO)	Janssen-Cilag, Neuss (Germany)
FCS (fetal calf serum)	Biochrom, Berlin (Germany)
FCS (fetal calf serum) GOLD	PAA, Linz (Austria)
Fecturin™	Polyplus Transfection, Illkirch (France)
Freestyle HEK293 Expression medium	Invitrogen, Karlsruhe (Germany)
Glutamate	Sigma-Aldrich, Taufkirchen (Germany)
Glutamax	Invitrogen, Karlsruhe (Germany)
HEPES 1M	Biochrom, Berlin (Germany)
Horse Serum	Gibco, Karlsruhe (Germany)
Insuline	Aventis, Frankfurt (Germany)
L-glutamine	Biochrom, Berlin (Germany)
MEM-Earle	Gibco, Karlsruhe (Germany)
MEM/HamF10	Gibco, Karlsruhe (Germany)
MEM non-essential amino acids	Gibco, Karlsruhe (Germany)
MEM vitamins	Biochrom, Berlin (Germany)
MethoCult 03534	StemCell Technologies, St Katharinen (Germany)
MethoCult SF 3236	StemCell Technologies, St Katharinen (Germany)
Na-pyruvate	Sigma-Aldrich, Taufkirchen (Germany)
Neurobasal A medium	Gibco, Karlsruhe (Germany)
Neurobasal medium	Gibco, Karlsruhe (Germany)
Nu-serum	BD Biosciences, Heidelberg (Germany)
Penicillin 10,000IE/ Streptomycin 10,000 µg/ml (Pen/Strep)	Biochrom, Berlin (Germany)
PBS w/o	Biochrom, Berlin (Germany)
Poly-L-Lysine (0.1 mg/ml)	Biochrom, Berlin (Germany)
Pro293a-CDM	Cambrex, Verviers (Belgium)
rhEPO (Roche)	Roche, Mannheim (Germany)
Serum Supreme	BioWhittaker, Lonza, Basel (Switzerland)
Trypan Blue	Biochrom, Berlin (Germany)
Trypsin/EDTA (10x)	Biochrom, Berlin (Germany)
VLE RPMI	Biochrom, Berlin (Germany)

Table 4: List of Cell Culture Media and Supplements

3.1.5 Equipment

Equipment	Supplier
Bacteria incubator	Minitron, Infors AG, Bottmingen (Switzerland)
Balance	CP225D Sartorius, Göttingen (Germany) BL150 Sartorius, Göttingen (Germany)
Blotting chamber	Biorad Trans-Blot®SD Semi-Dry Transfer Cell, Biorad, München (Germany)
Cell incubator	Nuaire, COTECH Berlin (Germany)
Centrifuges	Biofuge pico, Heraeus, Hanau (Germany)

Equipment	Supplier
	Hettich Universal 30RF, Hettich Universal 32R, Thermo Electron, Oberhausen (Germany)
Electrophoresis – Horizontal	Biorad Mini-Sub Cell, Biorad, München (Germany)
Electrophoresis – Vertical	Biorad Criterion, Biorad, München (Germany) Biorad Miniprotean 3 cell, Biorad, München (Germany)
Fluorescence microscope	DmRA2, Leica, Wetzlar (Germany)
Fuchs-Rosenthal, Counting chamber	Lo Laboroptik, Friedrichsdorf (Germany)
Imager	Typhoon 8600, GE Healthcare, München (Germany)
Inverse microscope	DM IL, Leica, Wetzlar (Germany)
Laminar Flow Box	Nuaire, COTECH Berlin (Germany)
Light Cycler	Roche, Mannheim (Germany)
OGD chamber	Concept 400, Ruskinn Technologies, Bridgend (UK)
PCR machines	Mastercycler gradient, Eppendorf, Wesseling-Berzdorf (Germany) Thermocycler, Invitrogen, Karlsruhe (Germany)
pH meter	pH100, VWR International, Darmstadt (Germany)
Plate reader	MRX^{TC} Revelation, Thermo Labsystems, Dreieich (Germany)
Vertical Shaker	Edmund Bühler Lab Tec, Tübingen (Germany)
Shaker for Freestyle293 cultures (GFL 3005)	GFL - Gesellschaft für Labortechnik, Burgwedel (Germany)
Sonicator	Sonorex Super 10P, Bandelin electronic, Berlin (Germany)

Table 5: List of Laboratory Equipment

3.1.6 Media and buffer formulations

3.1.6.1 Media used for Microbiology

Medium / Reagent	Preparation
SOB-medium	2% (w/v) peptone, 0.5% (w/v) Yeast extract, 10 mM NaCl, 2.5 mM KCl, 10 mM $MgCl_2$, 10 mM $MgSO_4$, pH 7.0
SOC-medium	2% (w/v) peptone, 0.5% (w/v) Yeast extract, 10 mM NaCl, 2.5 mM KCl, 10 mM $MgCl_2$, 10 mM $MgSO_4$, 20 mM Glucose, pH 7.0
LB-medium	1% w/v NaCl, 1% w/v tryptone, 0.05% w/v yeast extract, pH 7.0
LB-agar	2% (w/v) agar in LB-medium
Ampicillin	100 µg/ml working concentration
Chloramphenicol	25 µg/ml working concentration
Kanamicin	50 µg/ml working concentration
Tetracycline	50 µg/ml working concentration
TB-medium	10 mM PIPES, 55 mM $MnCl_2$, 15 mM $CaCl_2$, 250 mM KCl, pH 6.7

Table 6: List of media used for Microbiology

3.1.6.2 Buffers

Buffer	Preparation
BSS_0	6.8 g/l NaCl, 5.4 g/l KCl, 0.8 g/l $MgSO_47H_2O$, 1.0 g/l NaH_2PO_4, 26.2 g/l $NaHCO_3$, 0.265 g/l $CaCl_2$, 0.0001 g/l glycine in double distilled water (ddH_2O), pH 7.4
BSS_{20}	6.8 g/l NaCl, 5.4 g/l KCl, 0.8 g/l $MgSO_47H_2O$, 1.0 g/l NaH_2PO_4, 26.2 g/l $NaHCO_3$, 0.265 g/l $CaCl_2$, 0.0001 g/l glycine, 4.5 g/l D-Glucose in ddH_2O, pH 7.4
LDH buffer (10x)	45.3 g/l KH_2PO_4, 116.1 g/l K_2HPO_4 in ddH_2O, pH 7.4
5xTBE	54 g/l Tris-HCl, 27.5 g/l borat acid, 10 mM EDTA
RIPA buffer	50 mM Tris pH 7.4, 150 mM NaCl, 1% Triton-X-100, 0.1% SDS, 1% Na-Deoxycholate, 1x Protease Inhibitor Cocktail from Roche
NP-40 lysis buffer	50 mM HEPES-KOH pH 7.4, 10% glycerol, 100 mM NaCl, 1% NP-40, 200 U/l Benzonase from Sigma-Aldrich, 1.5 mM MgCl2, 1x Protease-Inhibitor-Cocktail from Roche
IP buffer	50 mM HEPES-KOH pH 7.4, 10% glycerol, 100 mM NaCl, 1% NP-40, 1.5 mM MgCl2, 1x Protease-Inhibitor-Cocktail from Roche
Protein sample buffer (2x)	125 mM Tris-HCl (pH 6.8), 1% SDS, 20% glycerol, 10% β-mercaptoethanol, 0.008% bromophenol blue
5x Laemmli electrophoresis running buffer	1.86 M glycine, 0.25 M Tris-base, 17.6 mM SDS
TBST	0.05% Tween 20, 10 mM Tris pH 8, 150 mM NaCl
Transfer buffer (1x)	0.37 M glycine, 0.05 M Tris-base, 3.5 mM SDS, 20% methanol
GST binding buffer	50 mM Hepes pH 7.4, 150 mM NaCl, 10% glycerine, 1% NP-40, 20 mM NaF, 1 mM DTT, 5 mM EDTA
TAE buffer (50x)	1 l: 240 g Tris-Base, 57.1 ml glacial acetic acid, 100 ml 0.5 M EDTA in ddH_2O

Table 7: List of standard buffers

3.2 Methods

3.2.1 Cloning strategy

3.2.1.1 Synthesis of murine and human EPO cDNA

Human adult kidney (male) and fetal brain (male) poly A+ RNA was purchased from Stratagene. Total RNA from kidney and brain of C57BL/6 mice (Charles River Laboratories) and 129/Sv mice (Bundesinstitut für Risikobewertung, Berlin) was extracted according to the Trizol Reagent protocol from Invitrogen. To minimize the risk of contamination with genomic DNA, DNA digestion was performed using 1 U RQ1 RNase-free DNase in the presence of RQ1 DNase buffer and 40 units of ribonuclease inhibitor (RNasin) according to the RQ1 RNase-free DNase protocol from Promega. Samples were incubated for 30 min at 37°C, followed by cool-down to 4°C. After addition of 200 µl phenol/chloroform/isopropyl alcohol (25/24/1) to the reaction mix, samples were centrifuged at 10,000 rpm and 10°C for 10 min. The supernatant was mixed with 200 µl chloroform/isopropyl alcohol (24/1) and centrifuged for a further 10 min. 20 µl 8 M lithium chloride and 550 µl of absolute ethanol were added to the supernatant. This mix was incubated for 1 h at -70°C and RNA was subsequently precipitated by centrifugation at 11,000 rpm and 0°C for 30 min. The resulting pellet was washed with 600 µl 75% ethanol, centrifuged at 8000 rpm (4°C, 10 min) and dried at RT. The RNA was dissolved in 20 µl double distilled water containing Diethylene Pyrocarbonate (DEPC-H_2O). The quantity of RNA was measured by its absorbance at 260 nm.

For cDNA synthesis 3 µg total RNA or 200 – 250 ng polyA+ RNA and 3 µl random hexamer primers (10 µM) in a final volume of 15 µl of DEPC-treated water were heated to 70°C for 10 min. Components added to the reaction mix included 6 µl of 5x reaction buffer, 2 µl of 2.5 mM dNTPs, 1 µl of RNase inhibitor (1 U/µl) and 1 µl of Moloney murine leukemia virus (MMLV) RNase H^- reverse transcriptase. The RT reaction was incubated for 5 min at 21°C, 1 h at 37°C and 5 min at 95°C. The resulting murine and human cDNA was used to amplify the open-reading frame of mEPO and hEPO using *Pfu* Turbo Hotstart Polymerase according to the manufacturer's protocol (Stratagene). All primers were obtained from MWG-Biotech AG. Nested PCR approaches were established consisting of two amplification rounds designated as PCR1 and PCR2 (Table 8). The second DNA amplification was set up in fresh tubes using 'PCR2-primers' and 2 µl of the PCR product obtained in the first PCR round.

The PCR products were separated by gel electrophoresis on 1.2% TAE-agarose gels, visualized by SYBRGold staining and purified using the Gel Extraction Kit from Qiagen according to the manufacturer's intructions.

	Human brain	Human kidney	Mouse brain	Mouse kidney
PCR1-primers	hepo_sense: GAT GGG GGT GCA CGA ATG TCC TGC hepo_antisense: CAC ACC TGG TCA TCT GTC CCC TGT C	hepo_sense: GAT GGG GGT GCA CGA ATG TCC TGC hepo_antisense: CAC ACC TGG TCA TCT GTC CCC TGT C	genepo_sense: GAA CTT CCA AGG ATG AAG ACT TGC AGC genepo_antisense: GTG GCA GCA GCA TGT CAC CTG TC	genepo_sense: GAA CTT CCA AGG ATG AAG ACT TGC AGC genepo_antisense: GTG GCA GCA GCA TGT CAC CTG TC
PCR1-protocol	3 min at 95°C; 35 cycles: 30 sec at 67°C, 1 min at 72°C, 30 sec at 95°C; 10 min at 72°C	3 min at 95°C; 35 cycles: 30 sec at 67°C, 1 min at 72°C, 30 sec at 95°C; 10 min at 72°C	3 min at 95°C; 35 cycles: 30 sec at 65°C, 1 min at 72°C, 30 sec at 95°C; 10 min at 72°C	3min at 95°C; 35 cycles: 30 sec at 65°C, 1 min at 72°C, 30 sec at 95°C; 10 min at 72°C
PCR2-primers	hepo_sense: GAT GGG GGT GCA CGA ATG TCC TGC hepo_antisense: CAC ACC TGG TCA TCT GTC CCC TGT C		epo_sense: TAT GGA TCC ATG GGG GTG CCC GAA CGT CCC AC epo_antisense: TAT GGA TCC TCA CCT GTC CCC TCT CCT GCA GAC	epo_sense: TAT GGA TCC ATG GGG GTG CCC GAA CGT CCC AC epo_antisense: TAT GGA TCC TCA CCT GTC CCC TCT CCT GCA GAC
PCR2-protocol	3 min at 95°C; 20 cycles: 30 sec at 67°C, 1 min at 72°C, 30 sec at 95°C; 10 min at 72°C		3 min at 95°C; 5 cycles: 30 sec at 67°C, 1 min at 72°C, 30 sec at 95°C; 15 cycles: 30 sec at 70°C, 1 min at 72°C, 30 sec at 95°C; 10 min at 72°C	3 min at 95°C; 5 cycles: 30 sec at 67°C, 1 min at 72°C, 30 sec at 95°C; 15 cycles: 30 sec at 70°C, 1 min at 72°C, 30 sec at 95°C; 10 min at 72°C

Table 8: List of PCR strategies used to amplify the EPO variants

The purified cDNA was subcloned into the pCR-Blunt II-TOPO Vector from Invitrogen. The ligation reaction was transferred to chemically competent Top10 One Shot Cells and transformation was performed for 30 sec at 42 °C. For selection of positive transformants cells were plated onto LB-agar plates supplemented with Kanamycin (50 µg/ml). Plasmid-DNA was isolated from single colonies using the QIA prep Kit from Qiagen. In brief, 5 ml LB-medium supplemented with appropriate antibiotics was inoculated with a single colony and grown over-night at 37°C. 2 ml of this culture were harvested by centrifugation (10 min, 3,500 rpm, 4°C) and resuspended in 250 µl buffer P1 of the Miniprep Kit. Isolation of plasmid DNA was performed according to the manufacturer's protocol. Inserts in the pCR-Blunt II-TOPO Vector were

analyzed in an ALFexpress™ DNA sequencer from Pharmacia Biotech using the Thermo Sequenase™ Primer Cycle Sequencing Kit from Amersham Biosciences which is based on the dideoxynucleotide chain termination method. The sequencing primers 'M13FWDCY' (5'-GTC GTG ACT GGG AAA ACC CTG GCG-3') and 'M13REVCY' (5'-AGC GGA TAA CAA TTT CAC ACA GGA-3') were labeled with the fluorescent dye Cy5 for detection purposes. The termination reactions were performed according to the protocol provided by the supplier and analyzed on acrylamide-gels. Parameters for electrophoretic runs were as follows: t = 900 min; T = 55°C; U = 800 V; I = 55 mA and P = 30 W. Sequence analysis and homology searches were performed using the BLAST software available at www.ncbi.nim.nih.gov/Blast/.

An Access-RT-PCR System from Promega, used as alternative PCR method, was performed according to manufacturer's instructions. The Access RT-PCR System allows reverse transcription and PCR amplification of a specific target RNA from total RNA or mRNA in a single tube. The system uses Avian Myeloblastosis Virus (AMV) Reverse Transcriptase for first-strand cDNA synthesis and the thermostable *Tfl* DNA Polymerase from *Thermus flavus* for second-strand cDNA synthesis and amplification. PCR products were analyzed by sequencing as described previously. All PCR reactions were realized in Thermocyclers from Invitrogen or Eppendorf.

3.2.1.2 Construction of the pZ/EG-vEPO-IRES-EGFP plasmids

The pZ/EG-vEPO-IRES-EGFP plasmids were designed as expression vectors for production of recombinant erythropoietin variants (vEPO) in eukaryotic cell lines and as future tools for the generation of transgenic animals. The original plasmid pZ/EG, a gift from Dr. U. Schweizer (Institut für Experimentelle Endokrinologie, Charité, Berlin), contains loxP sites derived from the Bacteriophage P1 allowing site specific recombination events catalyzed by the Cyclization Recombination protein Cre. The Cre/loxP system is used as a genetic tool for the generation of animal models expressing the gene of interest in a tissue-specific manner. The IRES-EGFP (internal ribosomal entry site - enhanced green fluorescent protein) cassette was introduced into the pZ/EG plasmid as tool for the identification of transfected cells.

The pZ/EG-vEPO-IRES-EGFP plasmids were generated by oriented subcloning of the vEPO cDNA sequences into the *Bam*HI cloning site of the pIRES2-EGFP cloning vector from BD Biosciences Clontech and subsequent excision of the whole cassette 'vEPO-IRES-EGFP' using the restriction enzymes *Bgl*II and *Not*I. This cassette was finally cloned into the pZ/EG-vector using the same restriction enzymes. Ligations were performed over-night using the T4 DNA Ligase from Roche according to the manufacturer's protocol. Plasmids were amplified in XL-1

Blue Competent Cells (recA1 endA1 gyrA96 thi-1 hsdR17 supE44 relA1 lac [F' proAB $lac^qZ\Delta M15$ Tn10 (Tet^R)]) from Stratagene. The XL-1 Blue Competent Cells transformation protocol was performed without β-mercaptoethanol and with a prolonged heat pulse of 60 sec. Bacteria were grown on LB-Agar plates containing selection antibiotics. Single colonies were picked and grown in liquid LB-medium over-night. Plasmids were purified using the QIAprep Spin Miniprep Kit from Qiagen and analyzed by restriction digestion. Preparative isolation of plasmids from positive *E.coli* clones was carried out using the EndoFree Plasmid Maxi Kit from Qiagen. All restriction enzymes used for cloning were purchased from New England Biolabs.

3.2.1.3 Construction of His-tagged vEPO-constructs

The His-tagged vEPO-constructs were generated for purification purposes of the recombinant vEPO proteins. The His-tag, consisting of six Histidine residues, binds to metal-chelate columns and can be easily eluted with imidazole, thus simplifying protein purification tasks. Three different plasmid backbones were used: the pcDNA3.1V5/His vector family (Invitrogen), a modified pDRIVE vector (pCAG, InvivoGen) and pVITRO4 (InvivoGen). For construction of the pcDNA3.1-vEPO-V5/His plasmids, *Bam*HI and *Eco*RI restriction sites were added to the PCR products by using appropriate overhang primers. The primer pair 'epo_sense' / 'epoeco_antisense' was used for generation of the murine constructs, the primer pair 'Hepobam_se' / 'Hepoeco_as' was used for generation of the human constructs (Table 9).

Primer	Sequence	
epo_sense	TAT GGA TCC ATG GGG GTG CCC GAA CGT CCC AC	*Bam*HI
epoeco_antisense	TCG GAA TTC TCA CCT GTC CCC TCT CCT GCA GAC	*Eco*RI
Hepobam_se	TAT GGA TCC ATG GGG GTGCAC GAA TGT	*Bam*HI
Hepoeco_as	AGA GAA TTC TCT GTC CCC TGT CCT GCA	*Eco*RI
pVITRO-hvEPO-fwd	AAC CAT GGG GGT GCA CGA ATG TCC TGC CTG	*Nco*I
pVITRO-HISV5-rev	AAG GAT CCT CAA TGG TGA TGG TGA TGA TGA CCG GTA C	*Bam*HI

Table 9: List of primers used for the generation of the His-tag expression vectors

The resulting PCR products were introduced in frame with the V5/His-tag into the appropriate pcDNA3.1V5/His vector (A, B or C) via *Bam*HI and *Eco*RI restriction sites. The pCAG-vEPO-V5/His plasmids were generated by subcloning of the 'vEPO-His-V5 cassettes' derived from pcDNA3.1-vEPO-V5/His constructs into the modified pDRIVE vector pCAG. An alternative multiple cloning site was inserted into pDRIVE in order to facilitate cloning tasks by providing more restriction sites for commercial restriction enzymes (gift from P. Mergenthaler, Institut für

Experimentelle Neurologie, Charité, Berlin). For generation of the pVITRO4-vEPO-V5/His constructs, the ‘vEPO-V5-His’ cassettes were amplified from the pcDNA3.1-V5/His-constructs using the primer pair ‘pVITRO-hvEPO-fwd‘ / ‘pVITRO-HISV5-rev’ and inserted into the pVITRO4 vector via *Nco*I and *Bam*HI restriction sites. Cloning and plasmid purification protocols were performed as described previously (see 3.2.1.2 Construction of the pZ/EG-vEPO-IRES-EGFP).

3.2.1.4 Generation of human EPO A-helix derivatives

Plasmids coding for several human EPO A-helix derivatives were generated for expression in eukaryotic cell lines. The hEPO A-helix motif was amplified from the hEPO cDNA template using the forward primer ‘hepobam_se’ containing a *Bam*HI site and the reverse primer ‘hEPO-HelA-STOP_rev’ containing a *Eco*RV site and a stop codon. The PCR product was purified as described previously and introduced into the pcDNA3.1/V5-His vector from Invitrogen using *Bam*HI and *Eco*RV restriction sites leading to the pcDNA3.1-hEPO-HelixA construct.

The human EPO A-helix muteins mutant A (MutA) and mutant E (MutE) were generated by site-directed mutagenesis using pcDNA3.1-hEPO-helixA as template. Amino acid changes at Arg14 were introduced by combination of two separate PCR reactions for each mutein. Mismatch primers were designed to change the hEPO A-helix cDNA sequence from AGG to GCG for mutant A or from AGG to GAG for mutant E. The first round PCRs were performed using the flanking primers ‘hepobam_se’ or ‘hEPO-HelA-STOP_rev’ and the appropriate mismatch primers (‘hEPO-helA-mutA_for’, ‘hEPO-helA-mutA_rev’, ‘hEPO-helA-mutE_for’ or ‘hEPO-helA-mutE_rev’) summarized in Table 10.

Primer	Sequence	
hepobam_se	TAT GGA TCC ATG GGG GTGCAC GAA TGT	*Bam*HI
hEPO-HelA-STOP_rev	CAA GAT ATC TCA CGT GAT ATT CTC GGC CTC C	*EcoR*V
hEPO-helA-mutA_for	AGT CCT GGA GGC GTA CCT C	internal
hEPO-helA-mutA_rev	GAG GTA CGC CTC CAG GAC T	internal
hEPO-helA-mutE_for	GAG TCC TGG AGG AGT ACC TC	internal
hEPO-helA-mutE_rev	GAG GTA CTC CTC CAG GAC T	internal
hEPO_helA-20_re	CAA GAT ATC TCA GAT GAG GCG TGG TGG GG	*EcoR*V
hEPO_helA-10_re	CAA GAT ATC TCA GAG GTA CCT CTC CAG GAC TC	*EcoR*V

Table 10: List of primers used for the generation of the A-helix mutants

The products from the first PCR reactions were used in equal amounts as templates for the second PCR using the flanking primers ‘hepobam_se’ and ‘hEPO-HelA-STOP_rev’. PCR

products were introduced into pcDNA3.1/V5-His vector leading to pcDNA3.1-hEPO-mutA and pcDNA3.1-hEPO-mutE constructs.

'-20aa' and '-10aa' are deletion variants of the human EPO A-helix missing 20 amino acids or 10 amino acids respectively at the C-terminus. These mutants were generated by insertion of stop-codons into the open-reading frame of hEPO using site-directed mutagenesis ('hepobam_se' with either 'hEPO_helA-10_re' or 'hEPO_helA-20_re'). PCR products were introduced into pcDNA3.1/V5-His vector leading to the pcDNA3.1-helA-10 and pcDNA3.1-helA-20 constructs. All PCR reactions were conducted with *Pfu* Turbo Hotstart Polymerase (Stratagene) as described previously.

3.2.1.5 Construction of the GST-tagged EPO-constructs

EPO variants were produced as fusion proteins to glutathione-S-transferase (GST) for pulldown assays. For expression in *E.coli* strains the N-terminal protein part, acting as secretion signal in eukaryotic cells, was deleted. The resulting proteins are named hereafter as 'mature' EPO variants. The 5'-truncated mEPO, mS and hS3 isoforms were generated by site-directed mutagenesis from pcDNA3.1/V5-His-vEPO constructs using the primers summarized in Table 11 (matmE and matmS: 'Mat_mEpo_sense' / 'Epostopp_antisense'; mathS3: 'Mat_hEpo_sense' / 'hEpostopp_antise'). PCR products were introduced in frame with the GST-tag into pGEX-6P- from Amersham via *Bam*HI and *Eco*RI restriction sites. Resulting constructs were naimed pGEX-6P1-matmE, pGEX-6P1matmS and pGEX-6P1mathS3.

Primer	Sequence	
Mat_mEpo_sense	TAT GGA TCC GCT CCC CCA CGC CTC ATC TGC	*Bam*HI
Mat_hEpo_sense	TAT GGA TCC GCC CCA CCA CGC CTC ATC TGT	*Bam*HI
hEpostopp_antise	TCG GAA TTC TCA TCT GTC CCC TGT CCT GCA GG	*Eco*RI
Epostopp_antisense	TCG GAA TTC TCA CCT GTC CCC TCT CCT GCA GAC	*Eco*RI

Table 11: List of primers used for the generation of the GST-tag expression vectors

3.2.1.6 Generation of the murine LIFR and gp130-constructs

Two LIFR isoforms were cloned: murine LIFRα (mLIFR) and murine soluble LIFR (msLIFR). Primers used for the isolation of LIFR isoforms from murine brain cDNA contained *Eco*RI and *Xho*I restriction sites (Table 12). Murine LIFRα was amplified using the primers 'mLIFR_forward' and 'mLIFR_reverse'. msLIFR was generated by truncation of the C-terminal protein part using the primers 'mLIFR_forward' and 'msLIFR_reverse' and cloned in frame with the V5-His-tag for later detection purposes. Amplification of murine gp130 from brain cDNA,

the signal transduction sub-unit of several receptors, was achieved with the primers ‘Gp130_fw’ and ‘Gp130_rev’, which contained *Xho*I and *Pme*I restriction sites (Table 12). The PCR products were purified as described previously and inserted into the pcDNA3.1/V5-His vector using *EcoR*I and *Xho*I or *Xho*I and *Pme*I restriction sites, respectively.

Primer	Sequence	
mLIFR_forward	GAC GAA TTC ATG GCA GCT TAC TCA TGG TGG AGA C	*Eco*RI
mLIFR_reverse	AGA CTC GAG TTA GTC ATT TGG TTT GTT CTG GAA GAA GTT TG	*Xho*I
msLIFR_reverse	AGA CTC GAG AAT AAT CAA TCC CAC AGA GTT TTC CTT GGT C	*Xho*I
Gp130_fw	ATC TCG AGA TGT CAG CAC CAA GGA TTT GGC TAG CG	*Xho*I
Gp130_rev	AGG TTT AAA CTC ACT GCG GCA TGT AGC CAC CTT G	*Pme*I

Table 12: List of primers used for the generation of the murine LIFR- and gp130-constructs

3.2.2 Protein expression and purification strategies

3.2.2.1 Expression of recombinant proteins in HEK293 and CHO-S cells

Recombinant erythropoietin variants were produced in eukaryotic expression systems: Human Embryonic Kidney (HEK) 293 cells from BD Biosciences, Freestyle HEK293 cells from Invitrogen and Chinese Hamster Ovary cells (CHO-S) from Gibco.

HEK 293 cells from BD Biosciences were grown in Dulbecco’s modified Eagle’s medium (DMEM, Biochrom, Berlin, 1 g/l glucose, 3.7 g/l $NaHCO_3$) supplemented with 10% fetal calf serum GOLD, 1% Pen/Strep and 1% L-glutamine in tissue culture flasks at 37°C and 5% CO_2. When reaching 80 - 90% confluency, cells were lifted with Trypsin/EDTA and seeded in fresh culture flasks. For transient transfections, cells were plated in poly-L-lysine (PLL) coated 12-well plates at a density of 120,000 cells per well. After 48 h, transfection was performed with Lipofectamine 2000 (Invitrogen) according to the manufacturer’s instructions. Shortly before adding the Lipofectamine-DNA complexes plating medium was replaced with serum-free Pro293a-CDM medium (Cambrex). Freestyle HEK293 cells (Invitrogen) were grown as agitated suspension cultures in Freestyle293 Expression Medium at 37°C and 8% CO_2 on an orbital shaker platform rotating at 125 rpm. Cells were subcultured every 2 to 3 days in disposable sterile Erlenmeyer flasks (Corning). Transient transfection was performed according to manufacturer’s protocol using 293fectin™ (Invitrogen).

CHO-S cells adapted to serum-free medium were grown as agitated suspension culture in chemically-defined, protein-free CD-CHO medium (BD Biosciences) supplemented with 100 µM hypoxanthine, 16 µM thymidine and 8 mM L-glutamine under same CO_2- and shaking conditions as Freestyle HEK293 cells. CHO-S cells were transfected using Fecturin™ as indicated by the supplier (Polyplus transfection).

3.2.2.2 Purification of His-tagged proteins

Three days after transient transfection of eukaryotic expression cell lines with Endotoxin-free plasmidic DNA coding for His-tagged EPO variants (pcDNA3.1-V5/His, pCAG or pVITRO4) culture supernatants were collected and cell debris was pelleted for 15 min at 3500 rpm and 4°C. Harvested medium was concentrated by means of the Vivapore 10/20 ultrafiltration system (Sartorius AG) at 4°C over-night. Purification was achieved in a single chromatographic step using BD TALON™ Metal Affinity Resin (BD Biosciences) according to the workflow shown in Figure 4.

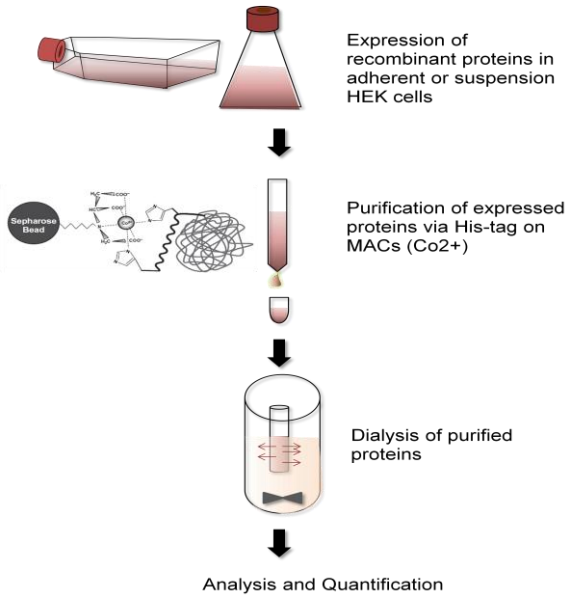

Figure 4: Workflow: protein purification of His-tagged proteins expressed in HEK293 cells

Metal ion affinity chromatography (IMAC) was used to purify recombinant proteins expressed in HEK293 cells or CHO-S cells. Crude supernatant was incubated with Co^{2+}-matrix to bind the His-tagged proteins. Elution was performed in a column-based format using imidazole. Fractions containing the His-tagged proteins were dialyzed against PBS.

All steps (equilibration, washing and elution) were performed at pH 7.1 and 4°C according to manufacturer's instructions. In brief, protein binding to the resin was carried out in a batch format under slight agitation for 1 h. Thorough washing of the agarose was repeated three times using 50 mM sodium phosphate buffer containing 300 mM NaCl before transferring the resin into 2 ml disposable columns (CellThru, BD Biosciences). Elution was performed with

imidazole and eluate was collected in 500 µl-fractions and stored on ice before dialysis. Fractions containing His-tagged recombinant proteins were identified by Western Blot and pooled for further processing. Imidazole was removed from pooled fractions via dialysis against PBS (pH 7.4) using cellulose membranes from Spectrapor (Spectrum Laboratories) having an exclusion limit of 15,000 Da or Slide-A-Lyzer Dialysis Cassettes (Pierce) with a molecular weight cut-off of 10,000 Da. Regardless from the dialysis system, PBS was replaced two times during dialysis and used in a 100 time surplus to the sample volume. In first experiments, bovine serum albumin (BSA) was added for stabilization of the purified protein samples at a final concentration of 0.1%. Due to problems in immunological assays (not mentioned in this thesis) BSA was not added in later experiments. After dialysis, protein samples were aliquoted in LOW-BIND tubes (Eppendorf), frozen in liquid nitrogen and stored at -80°C.

3.2.2.3 Western Blot Analysis of purified proteins

Discontinuous Tris Glycine SDS Polyacrylamide-gels were prepared using western blot standard protocols by layering a stacking gel (Tris-Glycine buffer pH 6.8; 5% Polyacrylamide) on top of a separating gel (Tris-Glycine buffer pH 8.8; 7.5% - 16% Polyacrylamide). Protein samples were mixed with equal volumes of protein sample buffer (2x) and boiled for 5 min before loading. Polyacrylamide gels were run at 120 V in Laemmli buffer (1x). A semi-dry blotting system was used for the electrophoretic transfer of proteins from the polyacrylamide gels to nitrocellulose sheets (Whatman). In brief, the nitrocellulose membrane, soaked in transfer buffer (10% methanol in 1x Laemmli buffer), was assembled together with the polyacrylamide gel and four Whatmann sheets to form a ‘sandwich’. Transfer was done for 45 min at 200 mA. Nitrocellulose membranes were blocked for at least one hour in blocking buffer containing 5% non-fat dry milk powder in Tris-buffered saline, 0.1% Triton (TBST) at RT. Incubation with the first antibody (anti-rhEPO 1:500 or anti-V5 1:1000) was performed over-night at 4°C in 3% non-fat dry milk in TBST. The secondary horseradish peroxidase-conjugated antibody (1:1000) was added for 2 h at RT in 1% non-fat dry milk in TBST. The blot was developed by use of Luminol reagent (Santa Cruz Biotechnology). Films (Kodak) were exposed for 2 - 10 min and processed with developer and fixer chemicals from Sigma according to standard protocols. Membranes were stained with Ponceau Red according to manufacturer’s protocol.

3.2.3 Erythroid Colony formation assay

Erythroid colony formation assays were performed using bone marrow cells harvested from tibia and femur of male C57BL/6 mice (8 - 10 weeks, Bundesinstitut für Risikobewertung, Berlin). In brief, hind legs were removed from euthanized mice and tibias and femurs were carefully

cleaned from fur and flesh. Bone marrow cells were harvested by flushing the marrow out of the bones with PBS. Cells were pelleted for 5 min at 1200 rpm and 4°C. PBS was discarded and pellets were resuspended in α-medium (supplemented with 20% fetal calf serum GOLD, 1% Pen/Strep and 1% L-glutamine). Cells were counted in the presence of 1% acetic acid to lyse the erythrocytes and seeded in 35 mm^2 Petri dishes at a density of 225,000 cells per dish. Assays contained 8 parts MethoCult SF 3236 methyl cellulose (StemCell Technologie Inc), 1 part cells, 2 parts α-medium and 200 U/l rhEPO from Roche or equimolar concentrations of EPO or the EPO splice variants (60 pM), respectively. Plates were incubated for 48 h at 37°C in a humified atmosphere containing 5% CO_2. For evaluation only reddish colonies containing at least six hemoglobinised cells were counted.

3.2.4 Primary neuronal cultures

Possible neuroprotective characteristics of the EPO isoforms were analyzed in an *in vitro* model of cerebral ischemia in primary cortical neurons of the rat. The *in vitro* model simulates the restriction in blood supply occurring in brain ischemia by an oxygen and glucose deprivation (OGD) in neuronal cultures containing less than 10% astrocytes.

3.2.4.1 Preparation of rat primary cortical neurons

Rat primary neuronal cultures were obtained from E17 to E18 embryos from Wistar rats (Bundesinstitut für gesundheitlichen Verbraucherschutz und Veterinärmedizin, Berlin, Germany). Cultures were prepared according to a modified protocol from Brewer (Brewer, 1995). In brief, cerebral cortex was isolated after removal of meninges and rinsed twice in PBS. After 15 min incubation in Trypsin/EDTA at 37°C, tissues were rinsed twice in N-Med (modified Eagle's medium from Gibco with 10% fetal calf serum, 1% Pen/Strep, 2mM L-glutamine, 100 IE/l insulin, 10 mM HEPES and 44 mM glucose) and carefully dissociated in a small volume of N-Med using a fire-polished Pasteur pipette. Cells were pelleted at RT at 210 g and resuspended in NBM starter medium (Neurobasal medium from Gibco with 2% B27 supplement, 1% Pen/Strep, 0.5 mM L-glutamine and 25 µM glutamate). The cell suspension was stored at 4°C and plated up to 5 days after preparation without significant increase in cell death.

3.2.4.2 Preparation of culture plates

24-well Falcon plates (BD Biosciences) and 6-well Falcon plates were pretreated by over-night incubation at 4°C with poly-L-lysine (2.5 µg/ml in PBS w/o). After rinsing the wells with PBS, plates were coated with collagen for 1 h at 37°C (modified Eagle's medium supplemented with 5% FCS GOLD, 1% Pen/Strep, 10 mM HEPES and 0.03 w/v collagen G). Before filling the

wells with starter medium the coated plates were carefully rinsed twice with PBS to wash out unbound collagen.

3.2.4.3 Induction of neuroprotection with EPO variants in an *in vitro* model of cerebral ischemia

Neurons used in neuroprotection assays (Figure 5) were plated in 24-well plates at a density of 300,000 cells per well in a final volume of 600 µl NBM starter medium. After 4 days, 200 µl of the medium was replaced with 250 µl of fresh NBM/B27 (same as NBM starter medium without glutamate). For pretreatment with EPO variants at *in vitro* day 8 (DIV 8) the medium was removed to an end volume of 200 µl and filled up with 200 µl fresh NBM/B27 containing the EPO variants at defined concentrations. The medium removed at this step was pooled and stored at 4°C (conditioned medium). For oxygen-glucose deprivation (OGD), an *in vitro* model of cerebral ischemia, the culture medium was washed out by rinsing the plates once with pre-warmed PBS. OGD was induced with 500 µl of a deoxygenated aglycaemic solution (BSS_0) in a hypoxic atmosphere generated by a dedicated humified gas-tight incubator (Concept 400) flushed with a gas mix containing 5% CO_2, 85% N_2 and 10% H_2

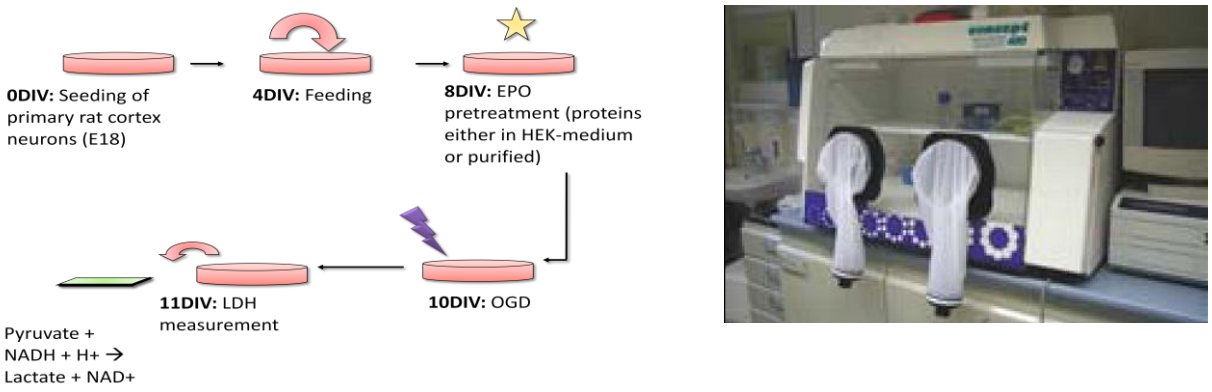

Figure 5: Oxygen glucose deprivation (OGD) assay as model of cerebral ischemia (Ruscher et al., 2002)

Primary cortical neurons were prepared from rat embryos (E17 to E18) and seeded in coated 24 well plates. Cells were grown for 8 days in a humified atmosphere containing 5% CO_2. At DIV 8, neuronal cultures were treated with EPO or EPO variants. After 48 h, cultures were deprived from oxygen and glucose for two to three hours. Cell death was evaluated by the 24 h release of lactate dehydrogenase into the medium.

The length of the oxygen glucose deprivation in the chamber varied between 2.5 h and 3 h depending on the density of the cultures. In control experiments, cultures were treated with 500 µl per well of the oxygenated glycaemic BSS_0 solution (BSS_{20}) and incubated at 37°C in a normoxic atmosphere containing 5% CO_2. Immediately after OGD, treated cultures and control cultures were changed from BSS solution to medium containing 50% fresh NBM/B27 and 50% conditioned medium (400 µl per well). 24 h after termination of OGD, lactate dehydrogenase (LDH) activity was measured in the supernatants as an indicator of cell death.

3.2.4.4 Lactate dehydrogenase (LDH) assay

LDH is a stable enzyme present in all cell types that is rapidly released upon damage of the plasma membrane. The LDH assay measures the pyruvate-dependent oxidation of NADH to NAD+. The reaction velocity is determined by a decrease in absorbance at 340 nm corresponding to the excitation wave-length of reduced NADH.

Culture supernatants (20 – 25 µl per assay) were transferred in 96-well plates (Sarstedt) and mixed with 100 µl of a fresh pre-warmed (37°C) β-NADH solution (0.15 mg/ml in 1x LDH-buffer). Enzymatic reaction was started by adding 25 µl of a 22.7 mM pyruvate-solution. Optical density was measured at 340 nm using a microplate reader. The kinetic of the reaction was established from 10 counts with 30 sec intervals. The maximal releasable LDH was obtained in each well by 30 min incubation with 0.5%. Triton X-100. All measures were performed at least in duplicates. LDH-standard was purchased from Greiner (system calibrator).

3.2.4.5 Signaling cascades in primary cortical neurons

For analysis of signaling pathways, primary cortical neurons were grown for eight days in 6-well plates and starved for 60 min by changing the cell culture medium to the aglycaemic BSS_{20} solution. Human EPO and the human splice variant hS3 were added at a final concentration of 90 pM for indicated time points. After stimulation, cells were washed twice in PBS and harvested in 1x cell lysis buffer (New England Biolabs) supplemented with 1mM PMSF. Lysates were incubated on ice for 5 min, sonicated for 1 min at 4°C and centrifuged at 18,000 g for 10 min at 4°C. Whole protein concentration was determined by using a bicinchoninic acid (BCA) protein assay according to manufacturer's instructions (Pierce). Cell lysates were diluted in protein sample buffer and boiled for 5 min before loading. Equivalent amounts of protein were separated on 12% SDS-polyacrylamid gels. Proteins were blotted onto nitrocellulose membranes for 35 - 90 min at 200 mA. Blocking was performed for 1 h in Tris-buffered saline containing 0.1% Triton (TBST) and 5% bovine serum albumin (BSA). Primary polyclonal antibodies against Bad (1:500), phospho-Bad Ser 136 (1:100), phospho-Bad Ser 112 (1:500), and phospho-pIKK (1:500) were purchased from New England Biolabs, primary polyclonal antibodies against phospho-Jak2 (1:200), phospho-Jak1 (1:200), phospho-Stat5 (1:200) and Jak2 (1:250) were purchased from Santa Cruz Biotechnology. Incubations with primary antibodies were performed over-night at 4°C in 5% BSA in TBST. The secondary antibody (goat anti-rabbit HRP, 1:1000) was added for 2 h at RT in 1% non fat-dry milk in TBST. Blots were developed as described previously (see 3.2.2.3 Western Blot Analysis of purified proteins).

3.2.4.6 Akt kinase assay

To measure Akt kinase activity in neuronal cell cultures, a non-radioactive Akt kinase assay (New England Biolabs) was performed. In this assay, an immobilized Akt antibody is used to immunoprecipitate Akt proteins from cell extracts in an over-night step at 4°C. After thorough washing, the agarose beads having bound Akt are incubated for 30 min with the Akt substrate, a GSK-3 fusion protein. Phosphorylated fusion protein can then be visualized by Western blotting, using a Phospho-GSK-3alpha/beta (Ser21/9) antibody.

In brief, primary cortical neurons from the rat were grown in 6-well plates. At DIV 8, cortical neurons were treated with 30 pM hS3, hEPO or rhEPO (Roche) for 30 min at 37°C. This was equivalent to 100 U/l rhEPO as indicated by the supplier. Preparation of lysates and determination of protein concentrations was performed as described previously. Akt kinase assays were performed immediately using same amounts of proteins in each condition.

3.2.4.7 AG490 kinase inhibitor experiment

AG490, a specific inhibitor of the Janus kinase 2, was obtained from Calbiochem. Primary cortical neurons were grown in 24-well plates. At DIV 8, cultures were preincubated for 1 h with 5 µM AG490 before preconditioning with human EPO (30 pM) or human EPO splice variant (30 pM). AG490 remained in the cultures until induction of OGD according to the protocol described previously (see 3.2.4.3 Induction of neuroprotection with EPO variants in an in vitro model of cerebral ischemia).

3.2.4.8 Neuroprotection assays in presence of soluble receptors and blocking antibodies

Human soluble receptors sLIFR and sEPOR were purchased from R&D Systems. The soluble receptors were preincubated with preconditioning medium containing hEPO (60 pM) or human splice variant hS3 (60 pM) for 60 min on a rotating shaker at 4°C before application to neuronal cultures. Soluble receptors were added to a final concentration of 1.5 µg/ml sEPOR or 2.5 µg/ml sLIFR, respectively. Antibodies directed against epitopes in the N-termini of gp130 and LIFRα antibodies were purchased from Hypromatrix (Worcester MA). Neuronal cultures were preincubated for 30 min with 1 µg/ml antibody before preconditioning with 30 pM of hEPO or hS3, respectively. Soluble receptors and antibodies were washed out with the NBM culture medium immediately before OGD. OGD was then performed as described previously (see 3.2.4.3 Induction of neuroprotection with EPO variants in an in vitro model of cerebral ischemia).

3.2.5 H9c2 - model of myocardial ischemia

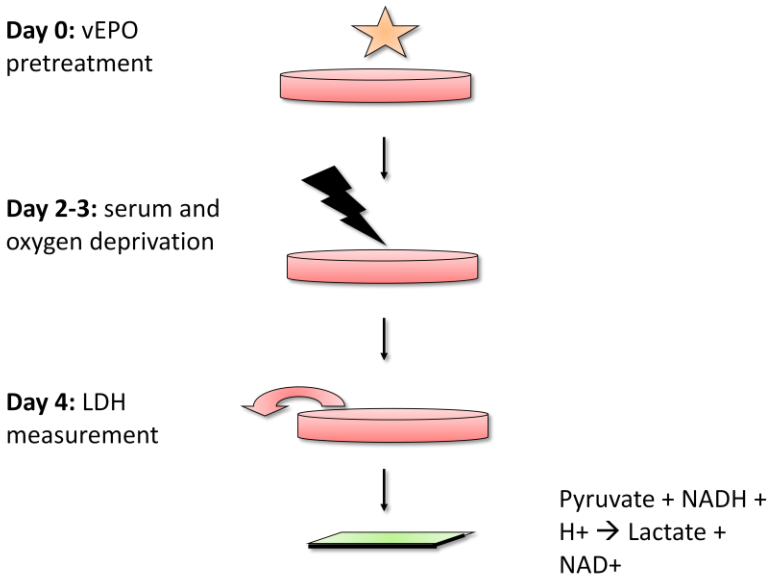

Figure 6: Serum and oxygen deprivation in the H9c2 myoblast cell line

H9c2 cells (rat myoblast cell line) were seeded in 24-well plates and cultured for 48 h in medium containing hEPO or hS3. Cells were transferred to serum and oxygen deprived conditions for defined time points. 24 h after end of the deprivation state, lactate dehydrogenase release into the medium was measured as a marker of cell death.

In order to analyze possible cytoprotective characteristics of the EPO splicing variants, an *in vitro* model of myocardial ischemia was established (Figure 6). A rat heart myoblast cell line (H9c2), obtained from the European Collection of Cell Cultures, was grown in 25 cm^2 and 75 cm^2 culture flasks containing DMEM (4.5 g/l glucose) supplemented with 2 mM L-glutamine, 10% FCS Gold and 1% Pen/Strep. Subconfluent cultures (70%) were subcultured at the ratio 1:4. After rinsing with PBS, cells were incubated in Trypsin/EDTA solution at 37°C for 5 min until cells detached. For experiments, cells were plated in 400 µl medium containing 120 pM hEPO or hS3 respectively at the density of 15,000 cells per well in 24-well plates. After 48 h, cells were deprived of serum and oxygen by changing the medium into serum-deficient DMEM and left for approximately 24 h in an anaerobic workstation saturated with a gas mix containing 5% CO_2, 85% N_2 and 10% H_2 at 37°C. Control cells were incubated in serum-deficient DMEM in a normoxic incubator. At the end of the experiment medium was replaced to 400 µl fresh serum-deficient DMEM and LDH was measured 24 h later as described previously (3.2.4.4 Lactate dehydrogenase (LDH) assay).

3.2.6 Immunoprecipitation of endogenous erythropoietin from mice

Proof of the existence of the erythropoietin splice variants on a protein level was obtained from immunoprecipitation (IP) experiments. Male 129/Sv mice or male C57BL/6 mice (8 - 10 weeks, Bundesinstituts für Risikobewertung, Berlin) were used for the experiments. Cobalt chloride ($CoCl_2$) was dissolved in saline and injected subcutaneously in a single dose of 60 mg/kg body weight. Animals were sacrificed 18 hours after $CoCl_2$-administration. Brains and kidneys were instantly removed, frozen in liquid nitrogen and stored at -80°C until use. Organs were homogenized in NP-40 lysis-buffer (2.5 ml/g) and lysates were centrifuged for 30 min at 14,000 rpm (Hettich) and 4°C. Supernatants were carefully removed and stored at -80°C. Blood was collected from hearts of anesthetized mice in 10% EDTA and centrifuged for 15 min at 5000 rpm (Hettich) at 4°C. The plasma supernatants were stored at -80°C. Whole protein concentration was determined by the BCA method (Pierce). Erythropoietin concentrations in EDTA-plasma, kidney and brain protein extracts were measured in a commercial ELISA assay (R&D, mEPO) according to supplier's protocol.

To precipitate the EPO variants tissue samples were adjusted to a volume of 200 µl to 250 µl and 10 µl (50µg/ml) of an anti-mEPO antibody (R&D) or an anti-rhEPO antibody (Santa-Cruz) was added. The samples were incubated over-night at 4°C with constant gentle mixing on a rotarod. 40 µl Streptavidin-agarose was added and samples were incubated for 1 h at RT. The samples were centrifuged at 700 g for 1 min and the supernatant was removed. The pellets were washed three times with 0.5 ml of PBS (pH 7.4). After removing the final wash, the pellet was resuspended in 40 µl of protein sample buffer, and placed for 5 min in a boiling water bath. The samples were then centrifuged to pellet the agarose and loaded onto polyacrylamide gels. Western blot analysis from IP-samples was performed as described previously using an anti-rhEPO antibody from Santa-Cruz (1:500). To show specificity of the western blot signals the anti-rhEPO antibody was incubated with 10 µg of rhEPO (DarbepoetinA, Amgen) for 2 h at RT before applying the antibody solution to the membranes.

3.2.7 Expression analysis of cytokine receptors

A screening approach was used to identify potential receptor candidates for the so the as yet unknown receptor complex mediating the effects of the EPO variants. Different cell lines were analyzed for expression levels of receptor candidates in a real-time PCR approach. Real-time PCR allows a highly sensitive relative quantification of transcriptional levels of the gene of interest within a few hours. Selected cell lines were cultivated using standard protocols as described in Table 13.

Cell line	Culture medium	Splitting
HT22 (murine hippocampal cell line)	DMEM containing 4.5 g/l glucose (Biochrom) supplemented with 10% FCS, 1% Pen/Strep, 1% L-glutamine	1:10 twice a week
SH-SY5Y (human neuroblastoma cell line)	MEM/Ham F10 supplemented with 10% FCS, 1% Pen/Strep, 1% L-glutamine, 1% non-essential amino acids	Splitted at confluency; seeded at 1,000 – 10,000 cells per cm^2

Table 13: Cultivation protocols of cell lines

Cells were grown to confluence in 25 cm^2 tissue culture flasks at 37°C in a humified atmosphere containing 5% CO_2. Total RNA was prepared by the Trizol isolation method as described previously (3.2.1 Cloning strategy). Relative quantification of mRNA was performed by real-time RT-PCR using the LightCycler System from Roche. PCR reactions were set up with the LightCycler FastStart DNA Master SYBR Green I kit (Roche) according to the protocol from the supplier. All samples were measured in duplets. The house-keeping gene β-actin was used for relative quantification. Primers used in real-time RT-PCR are given in Table 14.

Primer	Sequence	Gene of interest
mEPO_REC_FWD	CCC AAG TTT GAG AGC AAA GC	EPOR (mouse)
mEPO_REC_REV	TGC AGG CTA CAT GAC TTT CG	EPOR (mouse)
OSMR-FWD	GAA TTA TAG CAC CAC TGT GAA G	alpha chain of OSM receptor (mouse, human, rat)
OSMR-REV	GGA ACT CCA GTT GCC CCA G	alpha chain of OSM receptor (mouse, human, rat)
GP130-FWD	GAA GCT GTC TTA GCG TGG GAC C	Gp130 chain (mouse, human, rat)
GP130-REV	GAG GTG ACC ACT GGG CAA TAT G	Gp130 chain (mouse, human, rat)
LIFR-FWD	CTG ACA TAT CCC AGA AGA CAC	alpha chain of LIF receptor (mouse, human, rat)
LIFR-REV	CCA TTC TCG CTT CCG ATA GC	alpha chain of LIFreceptor (mouse, human, rat)
bActin_FWD	ACC CAC ACT GTG CCC ATC TA	β-actin (mouse, human, rat)
bActin-REV	ATC GGA ACC GCT CGT TGC C	β-actin (mouse, human, rat)

Table 14: Primers used in LightCycler experiments for the establishment of receptor expression profiles of different cell lines

FWD = forward primer; REV = reverse primer

3.2.8 Neural stem and progenitor cells

3.2.8.1 Isolation of neural stem and progenitor cells

Brains from male C57BL/6 mice aged 8 – 10 weeks were rinsed twice in PBS before dissection of the subventricular region embodying the lateral ventricles from 2 mm thick acute slices. A thin layer surrounding the ventricles excluding striatum and corpus callosum was prepared, cut into small pieces and incubated for 30 - 60 min in a papain-DNase-solution (47.2 mg papain, 9 mg cystein, 9 mg EDTA in 50 ml EBSS) at 37°C. Cells were pelleted by centrifugation at 110 g for 10 min. Supernatant was removed and tissue was dissociated in an ovomucoid solution (0.7 mg/ml ovomucoid in NBM-A, 2% B27 w/o Retinoic acid, 1% L-Glutamine). Single cells were pelleted by centrifugation at 110 g for 10 min and resuspended in growth medium (NBM-A, 2% B27 w/o Retinoic acid, 1% L-Glutamine, 10 ng/ml EGF, 20 ng/ml β-FGF). Cells were seeded in 25 cm^2 flasks (Falcon, BD Biosciences) at a density of 4,000 cells per cm^2 in order to obtain neurospheres. After first splitting of neurospheres, cells were cultivated in low-attachment flasks (Corning). Experiments were performed with cells from first passage up to passage 10.

3.2.8.2 Differentiation and survival assays

Neurosphere cultures were differentiated by removing the growth factors EGF and β-FGF from the culture medium. Spheres were washed in growth factor-free medium and dissociated into single cells by trituration with a 200 µl pipette tip. Cells were plated onto poly-L-lysine-coated coverslips at the density of 65,000 or 130,000 cells per well either in presence of MOCK (control), hEPO (300 pM), hS3 (300 pM) or P16 (1,000 – 100,000 pM). After 24 h cultures were analyzed for survival rate and morphology of the differentiating cells (Figure 7).

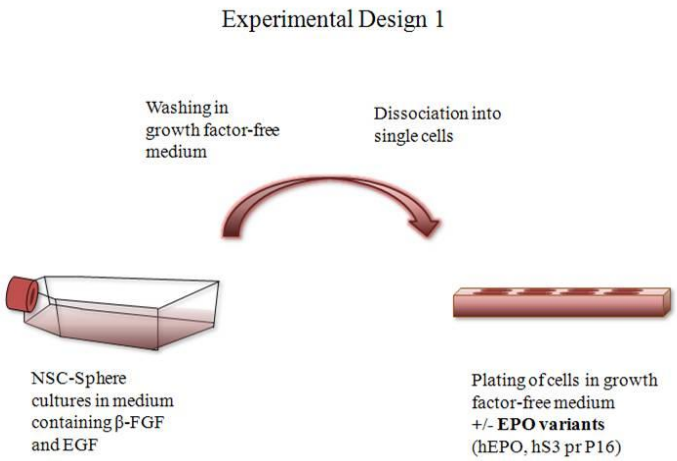

Figure 7: Experimental Design 1 of NSC experiments

Living cells were counted and analyzed for length and number of branches on minimum three randomly chosen areas per well. After 7 days, coverslips were fixed with 4% paraformaldehyde in PBS. Coverslips were blocked with 10% normal donkey serum and 0.3% Triton X-100 in PBS for 1 h at RT. Incubations with primary antibodies (anti-DCX 1:1000, anti-GFAP 1:1000) were performed at 4°C overnight. After washing with PBS, coverslips were blocked with 0.1% BSA for 1 h at RT. Secondary antibodies (Alexa594 donkey anti-goat and Alexa488 donkey anti-rabbit, 1:500) were added for 1 h at RT in the dark. Coverslips were mounted using Vectashield mounting medium supplemented with 4',6-diamidino-2-phenylindole (DAPI, Vector Laboratories) or with Mowiol after an additional DAPI-staining step. For DAPI-staining, cells were incubated with DAPI-solution (1:50,000) for 5 min at RT. After an additional quick washing step in PBS coverslips were mounted with Mowiol.

3.2.8.3 Pretreatment of NSC cultures and clonogenic assays

Neuronal stem and progenitor cells were seeded in 25 cm^2 low-attachment flasks (Nunc) at a density of 4,000 cells per cm^2 in NSC growth medium containing 10 ng/ml EGF, 20 ng/ml β-FGF and hS3 (3 nM), P16 (100,000 pM) or equivalent volumes MOCK. 48 h after seeding cultures were fed with hS3-, P16- or MOCK-containing medium and grown for 5 more days. At the day of experiment spheres were harvested at 110 g for 10 min (Hettich), washed once in growth-factor-free NSC-medium and dissociated into single cells using a 200 µM pipette tip (Figure 8). Cells were differentiated as described previously either in NSC-medium containing low concentrations of β-FGF and EGF (0.86 ng/ml EGF, 1.72 ng/ml β-FGF; 65,000 cells per well) or in growth-factor-free NSC-medium (100,000 cells per well).

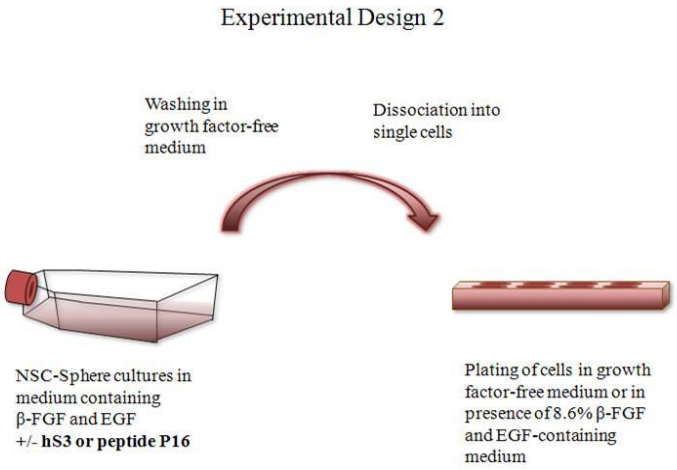

Figure 8: Experimental Design 2 of NSC experiments

After 7 days, coverslips were fixed and stained for DCX, GFAP and MAP2 (1:1000) as described previously. For clonogenic assays, cells derived from pretreated sphere cultures were resuspended in growth medium containing β-FGF and EGF and subjected to serial twofold dilutions. Cell suspensions (200 µl per well) of different concentrations were pipetted as duplets in 96-well plates (Falcon). The number of sphere-forming units was counted for each well after 7 days and 12 days. Spheres were only taken into account when they contained at minimum 10 cells to ensure multicellular collections.

3.2.8.4 Real time analysis of GFAP mRNA expression in NSC sphere cultures

NSC sphere cultures were grown for 7 days in NSC-medium containing 20 ng/ml β-FGF and 10 ng/ml EGF. Spheres were harvested at 810 rpm and transferred to growth-factor free NSC medium. Spheres were treated with 3 nM hS3 or 100,000 pM P16 for 2, 4 or 6 h, respectively. MOCK-medium was used in equal volumes as control. In experiments with peptide P16, PBS was used as control. Spheres were pelleted at 810 rpm for 5 min, washed once in PBS and lysed in Trizol. RNA extraction was performed as described previously.

GFAP-mRNA expression levels were quantified in a real-time RT-PCR as also described previously. All samples were measured in duplets. The house-keeping gene β-actin was used as internal standard for quantification. Primers used are summarized in Table 15.

Primer	Sequence	Gene of interest
GFAP-LC-FWD	GAG GGA CAA CTT TGC ACA GGA C	GFAP (mouse)
GFAP-LC-REV	GAT CTC CTC CTC CAG CGA TTC	GFAP (mouse)
bActin_FWD	ACC CAC ACT GTG CCC ATC TA	β-actin
bActin-REV	ATC GGA ACC GCT CGT TGC C	β-actin

Table 15: Primers used in LightCycler experiments for quantification of GFAP-mRNA levels in NSC sphere cultures

FWD = forward primer; REV = reverse primer

3.2.9 Pulldown experiments

Pulldown experiments were performed in order to study ligand-receptor interactions. Pulldown assays are very similar to immunoprecipitation except that a bait protein is used instead of an antibody. The tagged bait protein is captured on a support having specific affinity for the tag. For that purpose, the EPO variants mEPO, mS and hS3 were expressed in an appropriate *E.coli*-strain as GST fusion proteins.

3.2.9.1 Generation of competent bacteria

BL-21, BL-21-RIL and BL-21-RP strains (gift from AG Wanker, Berlin) were tested as producer lines. The BL21 strain is by far the most widely used bacterial gene expression host. BL-21-RIL cells contain extra copies of the *argU*, *ileY*, and *leuW* tRNA genes. Therefore this strain is used for the expression of AT-rich genes. BL-21-RP competent cells contain extra copies of *argU* and *proL* tRNA genes. These codons appear frequently in GC-rich genomes, such as mammals.

50 ml SOB-Medium was inoculated with 50 µl over-night cultures of BL-21, BL-21-RIL and BL-21-RP. Bacterial cultures were grown at 37°C to an optical density (OD 600) of 0.6. Optical density was measured in a spectrophotometer from Eppendorf at 600 nm wave length. Cells were pelleted for 20 min at 2500 rpm and 4°C. Pellets were carefully resuspended in 3 ml ice-cold TB-medium mixed with 7% DMSO and stored at -70°C.

3.2.9.2 Test for erythropoietin production in the different *E.coli* strains

1 ml LB-medium was inoculated with over-night cultures of BL-21, BL-21-RIL and BL-21-RP bacteria transformed with pGEX-6P1-matmE, pGEX-6P1matmS, pGEX-6P1-mathS3 and pGEX-6P1. Cultures transformed with the empty plasmid pGEX-6P1 expressed only the gluthation-S-transferase-tag (MOCK). Tranformed cultures were agitated for 2 h at 37°C before addition of 1 mM Isopropyl-β-D-1-thiogalactopyranosid (IPTG). Then, cultures were agitated for additional 2 h at 37°C. Samples taken before induction and at the end of the cultivation were mixed with sample buffer, boiled for 5 min and separated on 10% SDS-acrylamid gels. Gels were stained with Coomassie-blue and destained with a solution containing 30% methanol and 10% acetic acid. This solution was replaced several times until protein bands became clearly visible. Clones with high expression levels of the GST-tagged mature erythropoietin variants were used for the subsequent GST-Pulldown assays.

3.2.9.3 GST-Pulldown assay

LB-medium (200 ml per construct) was inoculated with over-night cultures and grown at 37°C to an optical density of OD 600 = 0.6. Induction of protein expression was done with 1 mM IPTG and cultures were agitated for additional 3.5 h. Cells were pelleted for 20 min at 2500 rpm and 4°C. Pellets were resuspended in 13 ml PBS containing protease inhibitors (Protease Inhibitor Cocktail Tablets without EDTA). After sonication, 0.5% triton was added to the cell suspensions. Lysates were incubated on ice for 5 min before centrifugation for 30 min at 14,000 rpm and 4°C (Hettich).

50 µl GST-beads (Santa-Cruz) were prepared for each pulldown and washed with PBS and GST-binding buffer. Beads were incubated with the bacterial lysates at least for 1 h at 4°C, washed

once with PBS and incubated with cell lysates containing prey proteins over-night at 4°C. The next day, beads were washed four times with PBS (2500 rpm, 4°C), resuspended in SDS sample buffer and boiled for 5 min. Captured proteins were analyzed on Western blots using the protocol described previously (see 3.2.2.3 Western Blot Analysis of purified proteins). Primary antibodies were purchased from Santa Cruz Biotechnology (anti-EPOR, anti-LIFR, anti-gp130, anti-IL-3/IL-5/GM-CSFRβ) and used at final dilutions of 1:1000 in TBST containing 3% non-fat dried milk.

3.2.10 BaF3-cells

A cell line over-expressing the homodimeric EPOR was used to analyze possible binding of the splice variant hS3 to the $(EPOR)_2$ in a functional assay (survival in presence of hS3) and in a radioactive competition experiments against ^{125}I-rhEPO.

3.2.10.1 Baf3/EPOR survival experiments

A murine pro-B IL-3 dependent cell line stably transfected with the erythropoietin receptor (Baf3/EPOR, provided by PD Dr. rer. nat. Ursula Klingmüller from the Systems Biology of Signal Transduction lab at the Deutsches Krebsforschungszentrum Heidelberg) was cultured in RPMI medium (10% fetal calf serum GOLD, 1% Pen/Strep, 1% glutamine) supplied with 1 ng/ml IL-3 and 1.5 mg/ml Puromycin (Invivo Gen) for positive selection.

For the survival experiment cells were seeded at a density of 10^4 cells per well of a 96 well plate in presence or absence of IL-3 and / or hEPO or hS3 (300 pM). Cell death and vitality of the cultures under the different experimental conditions were determined 48 h after treatment using LDH and MTT (Thiazolyl blue) assays.

3.2.10.2 MTT (Thiazolyl blue) assay

The MTT assay is a standard colorimetric assay for measuring cellular growth and cell vitality. Yellow MTT (3-(4,5-Dimethylthiazol-2-yl)-2,5-diphenyltetrazolium bromide) is reduced to insoluble purple formazan in the mitochondria of living cells that has to be dissolved either in DMSO or in SDS.

For MTT-assay cells were incubated for defined durations at 37°C with 0.05 mg/ml Thiazolyl blue (Sigma) before addition of equal volumes of 10% SDS in 0.01 M HCl. Incubation times with MTT were adjusted to 2 h for Baf3 cells and to 2.5 h for M1 cells. The next day, optical density was measured in a plate reader (Thermo Labsystems, MRX^{TC} Revelation) at 550 nm wave length.

3.2.10.3 Radioactive binding assay

Radioactive ^{125}I-rhEPO was purchased from Amersham (GE Healthcare).

Binding assays were performed with 10^6 BAF3/EPOR cells per assay in a total volume of 200µl. In a first step, cells were incubated for 45 min at 37°C with 1nM ^{125}I-rhEPO in order to saturate the available binding sites (EPOR) with radioactive EPO. In a second step defined concentrations of cold (non-radioactive) EPO variants were added and cells were incubated for further 90 min at 37°C. The binding/competition reaction was terminated by washing the cells with PBS (pH 7.4) and pelleting the cells by centrifugation at 1200 rpm for 5 min. Cell pellets were dissolved in 2 ml scintillator-medium 'Hisafe3' (Amersham Biosciences) and counted for their content of radioactivity.

3.2.11 Bone marrow cell assays

Bone marrow of male C57/Bl6 mice was prepared as described previously (see 3.2.3 Erythroid Colony formation assay). Effects of erythropoietin variants on murine bone marrow cells were tested using two different approaches. Survival effects were tested in growth factor deprived bone marrow cultures. Primary bone marrow cells were cultivated in presence of hEPO (3 nM), hS3 (3 nM) or peptide P16 (100 nM) but in total absence of additional cytokines in α-medium at a density of 10^6 cells per ml. After 2 or 5 days, floating cells were harvested and seeded in growth factor-containing MethoCult 03534 methylcellulose (mSCF, mIL-3, hIL-6; StemCell Technologie Inc) at a density of 20,000 cells per plate. In the 5 days survival assay cells were fed at DIV 2 with medium containing hEPO, hS3 or P16, respectively. Colonies on methylcellulose plates were evaluated after 7 days using an inverted microscope (Leica) at 2.5x magnification (Figure 9).

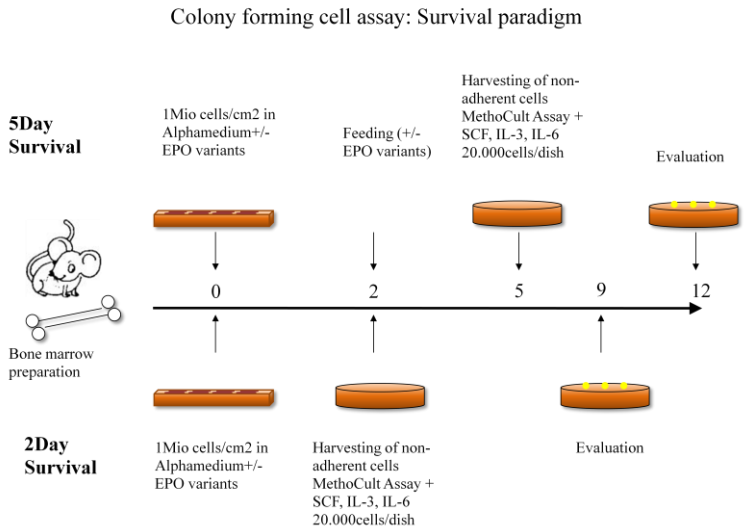

Figure 9: Survival paradigm in a hematopoietic stem cell system derived from murine bone marrow

Differentiation effects of the EPO variants on hematopoietic progenitor cells (HPC) were tested in combination with other cytokines. Freshly prepared bone marrow cells were seeded in 12-well plates (10,000 cells/dish) containing 8 parts MethoCult SF 3236 methyl cellulose (StemCell Technologie Inc) 1 part cells suspension and 2 parts α-medium containing hEPO (3 nM), hS3 (3 nM) or peptide P16 (100 nM). Methylcellulose was supplemented with either 20 ng/ml IL-3 or 20 ng/ml IL-3 and 50 ng/ml SCF, respectively. After 48 h plates were evaluated for growth of erythroid colony forming units (CFU-E). Myeloid colony forming units including CFU-M (colony forming unit macrophage), CFU-G (colony forming unit granulocyte) and CFU-GM (colony forming unit granulocyte and macrophage) were counted after 7 days (Figure 10).

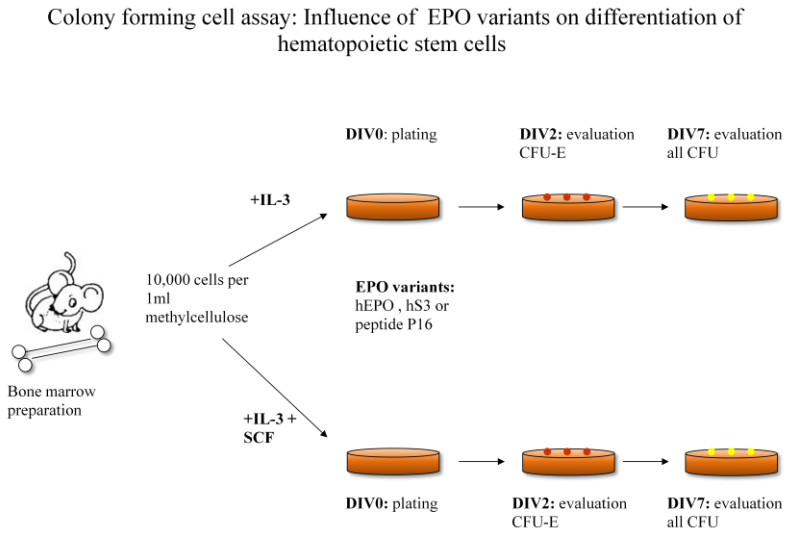

Figure 10: Differentiation assay with hematopoietic stem cells derived from murine bone marrow

3.2.12 Murine mesenchymal stem cells (mMSC)

Murine MSCs (mesenchymal stem cells) were obtained from Tulane University (T-mMSC, New Orleans, USA). Mesenchymal stem cells were cultivated as low density cultures (50 cells / cm^2) in α-medium supplemented with 10% serum Supreme, 10% horse serum (HS) and 1% L-glutamine.

For experiments, cells were lifted by trypsination and seeded at low density (50 cells / cm^2) in medium containing 20% serum (serum-containing condition) or 0.5% serum (low serum-condition) in presence of EPO variants. Equivalent volumes of PBS or MOCK were added to control cultures. Colonies were stained with crystal violet after 6 days in serum-containing conditions or after 8 days in low-serum conditions. Staining was performed by removing the medium, washing the plates once with PBS and incubation of the cells with a 3% crystal violet-solution in methanol for 10 min at RT. Plates were washed severalfold with ddH_2O until colonies

were easily distinguishable from background. For evaluation, only colonies of defined size (equal or > 1mm diameter) were taken into account. For feeding experiments cells were seeded as described previously. Two days after seeding, medium was completely exchanged to fresh medium containing 0.5% or 20% serum and +/- 100 nM peptide P16 according to the experimental condition.

3.2.13 M1 proliferation assay

The mouse myeloid leukemia M1 cell line is known to differentiate into mature macrophages and granulocytes *in vitro* when treated with various stimulators such as bacterial LPS (lipopolysaccharide), dexamethasone, LIF, OSM or IL-6. This differentiation is accompanied with growth arrest.

The mouse myeloid leukemia M1 cell line was purchased from the cell culture collection ECACC. Suspension cultures were maintained at a density of 200,000 to 900,000 cells per ml in RPMI 1640 supplemented with 10% FCS GOLD, 2 mM L-Glutamine and 1% Pen/Strep in 25 cm^2 or 75 cm^2 culture flasks (Sarstedt). For proliferation experiments in presence of the EPO variants, cells were seeded at the density of 150,000 cells per ml in presence or absence of 15 nM hEPO, hS3 or equivalent volumes of MOCK-medium or in presence or absence of 500 nM peptide P16 in 96 well plates (Falcon, BD Biosciences). Each condition was repeated in presence of 50 ng/ml murine LIF (Chemicon). Proliferation of the cells was evaluated by measuring the vitality by means of the MTT-test as this test was shown to correlate with the level of LIF used for stimulation (Ohno *et al.*, 1991). The MTT test was performed as described previously (see: 3.2.10.2 MTT (Thiazolyl blue) assay).

3.2.14 *In vivo* hematopoiesis assay

In vivo hematopoietic activity of vEPO was assayed in male C57Bl/6 mice of age 8 – 10 weeks. Mice were injected intraperitoneally with 5000 U/kg recombinant human erythropoietin, either commercial rhEPO (ERYPO, Janssen Cilag), purified hEPO produced in Freestyle HEK293 (hEPO-HEK) or purified hEPO produced in CHO-S (hEPO-CHO), equivalent volumes of PBS as control or equivalent concentrations of purified hS3 produced in CHO-S. Injections were done on day 0, day 2 and day 5 with 5 to 10 mice per group. Hematocrit was measured 48h after the last injection using hematocrit capillaries.

Briefly, blood was taken retro-orbitally from anesthetized mice by means of heparinized microcapillaries. Two capillaries were taken per mouse each filled to two-thirds with blood. Capillaries were sealed at one end and centrifuged for 10 min at 5000 rpm. The hematocrit was determined as percentage of red blood cells to total blood volume (red zone (red blood cells),

buff zone (white blood cells), and plasma layer). Hemoglobin-levels were determined in the QuantiChrom™ Hemoglobin Assay Kit from BioAssay Systems (Biotrend Chemicalien GmbH, Köln) according to manufacturer's protocol.

3.2.15 Bioinformatics

The Multiple Sequence Alignment of the erythropoietins of different species was performed using the ClustalW software at www.ebi.ac.uk. Default parameters were not changed for construction of the phylogenetic tree. EPO cDNA sequences of the different species were obtained from the NCBI database (http://www.ncbi.nlm.nih.gov).

The Homology modeling of mS and hS3 was performed at the SWISS-MODEL Protein Modeling Server database (SWISS-MODEL Version 36.0003) accessible via 'http://swissmodel.expasy.org/' (Arnold *et al.*, 2006; Guex *et al.*, 1997; Kopp *et al.*, 2004; Peitsch, 1995; Schwede *et al.*, 2003). The templates '1eerA.pdb' (rhEPO), '1buyA.pdb' (rhEPO) and '1cn4C.pdb' (mEPO) were used as scaffolds. The templates were obtained from the RCSB Protein database at 'http://www.rcsb.org/pdb/home/home.do'. Default parameters were not changed for construction of the 3D models of mS and hS3. Manual corrections were not performed.

Visualization of structure predictions were done in the Astex Viewer ™, a program for displaying molecular structures and electron density maps. This software has been developed by Astex Technology Limited (Cambridge, UK) and has been modified by the Macromolecular Structure Database Group of the European Bioinformatics Institute, under license from Astex Technology Limited.

The visualizations of the splice variants complexed to the EPOR were performed using the Swiss-PdbViewer (version 3.7) from EMBL (European Molecular Biology Laboratory). The crystal structure of human erythropoietin complexed to its receptor (1eerA.pdb) was used as template. Predictions were made by hiding amino acids not present in the splice variants.

4 RESULTS

The results disclosed in this section will be structured as follows:

The first chapter describes the finding of unknown erythropoietin variants (vEPO) in a Nested PCR approach on human and murine tissues. The variants will be analyzed on a cDNA level for the existence of splice sites and on the protein level in order to predict primary protein structures and three dimensional structures for the most important variants.

The second chapter deals with problems encountered in the production of recombinant erythropoietin variants. Different plasmid and expression systems will be compared that were used for the establishment of a final protein expression and purification protocol.

Chapters 3 to 5 describe functional characterization of the erythropoietin variants in different cell culture models. Hematopoietic, neuroprotective and cytoprotective capacities of the murine and human EPO isoforms will be analyzed *in vitro*. Comparative analysis of the variants will lead to the identification of minimal protein structures relevant for neuroprotective actions. Neuroprotective EPO-peptides will be designed and their functionality will be verified in an *in vitro* model of cerebral ischemia.

The confirmation of the spliced EPO variants on a protein level will be performed exemplarily for the murine splice variant from tissue extracts of $CoCl_2$-treated mice using an immunoprecipitation technique and will be further explained in chapter 6.

Next, signaling pathways of the EPO variants will be analyzed in more detail. The study will be focused on the signal transduction pathways induced by hEPO and hS3 in cortical neuronal cultures of the rat. Several techniques will be used such as Western Blots for phosphorylated proteins, functional kinase assays and use of kinase inhibitors in neuroprotection assays.

Chapter 8 deals with the effects of the EPO variants on diverse stem and progenitor cell populations. In the first part, survival and differentiation effects of the EPO variants hEPO, hS3 and P16 on murine neural stem and progenitor cells (NSC) will be analyzed. In the two following parts survival effects will be studied on bone marrow derived cells namely murine hematopoietic progenitor cells and murine mesenchymal stem cells.

Chapter 9 tries to elucidate the receptor mediating the observed effects of the EPO variants on diverse cell types described beforehand. After ruling out the classical homodimeric EPOR as receptor mediating the effects of the EPO variants, other receptor candidates will be analyzed, in particular members of the LIFR family.

The last chapter of this section shows the first *in vivo* results supporting the *in vitro* findings about hematopoietic activities of the EPO variants.

4.1 Identification of alternatively spliced EPO transcripts

Nested PCRs on human and murine brain and kidney cDNA using primers specific for the open-reading frame of erythropoietin allowed amplification of a major product (600 bp) corresponding to EPO and several products of smaller sizes (Figure 11A and Figure 11B). Sequencing of these fragments revealed incomplete EPO transcripts containing internal deletions. Several variants had deletions between short direct repeats of three to six nucleotides: the murine deletion variants were named mG3, mG5, m300-1 and mK3; the human deletion variants were named h1-1, h1-2, h1-4 and h1-5 (see Table 17, 7.1 List of human and murine EPO variants). Among these incomplete transcripts were transcripts identified as having typical splice patterns: one splice variant of murine EPO (mS) and two splice variants of human EPO (hS3 and hS4). The cDNA sequences of the murine and human splice and deletion variants are summarized as Multiple Alignments in Figure 62 and Figure 63 in the Appendix.

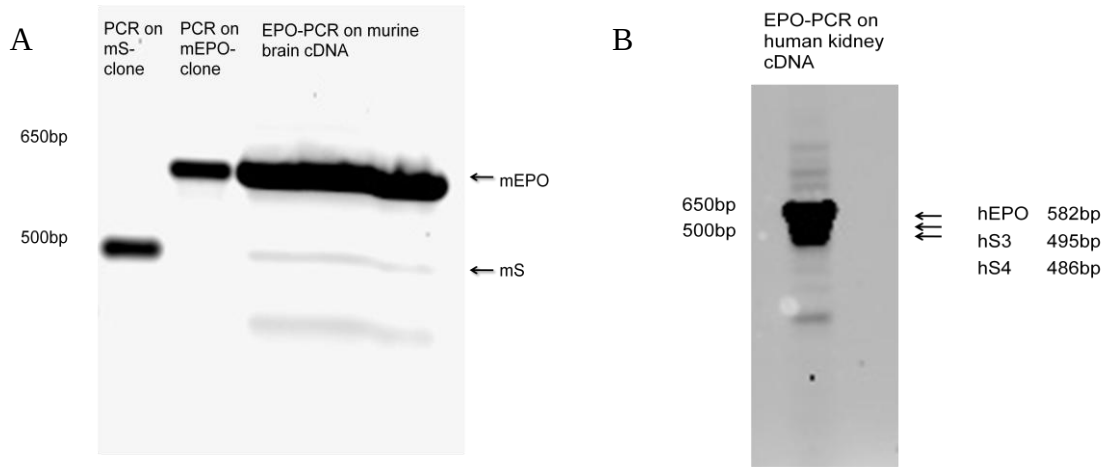

Figure 11: Agarose gels visualizing products of EPO-PCRs on murine and human tissues

A: Agarose gel (1.2 %) stained with ethidium bromide showing Nested PCR products generated from murine brain cDNA by primers flanking the murine EPO mRNA. The major product corresponds in size to the murine EPO transcript (mEPO clone) loaded as control. The faint second product coincidises with the murine spliced EPO transcript (mS clone).
B: PCR products generated by using primers flanking the human EPO mRNA. cDNA was prepared from human kidney poly (A)+ RNA (Stratagene). Three products were amplified corresponding to hEPO (582 bp), the splicing variant hS3 (495 bp) and the splicing variant hS4 (486 bp).

To confirm the finding of spliced EPO transcripts an alternative PCR approach using the Access RT PCR System from Promega was performed. This system allows cDNA generation and PCR amplification in one tube. The system uses Avian Myeloblastosis Virus (AMV) Reverse Transcriptase for first-strand cDNA synthesis and the thermostable *Tfl* DNA polymerase from *Thermus flavus* for second-strand cDNA synthesis and amplification. The reverse transcription step at the elevated temperature of 45°C instead of 37°C minimizes problems encountered with

RNA secondary structures. RNA with complex secondary structures can cause the reverse transcriptase to dissociate from the RNA template leading to truncated cDNAs or to skip over looped-out regions leading to internal deletions. This source of error is reduced using the Access RT PCR System since RNA secondary structures are denatured at higher temperatures. This approach removed a number of bands but the prominent smaller sized PCR products of approximately 490 bp and 400 bp length for human and mouse kidney, respectively, were retained. Subcloning and sequencing of these PCR products revealed the EPO splice variants mS and hS3. No deletion isoforms following the direct repeat pattern were found in Access RT PCR experiments on human or murine cDNA.

The human and murine EPO genes consist of five exons and four introns, respectively. In the alternatively spliced murine EPO transcript mS, detected in RNA obtained from brain and kidney of ischemic and non-ischemic mice, exon 4 is deleted (Figure 12A). The human splice variant hS3 misses exon 3 and was detected in poly A RNA from fetal brain and adult kidney whereas the second splice form hS4 was only detected in poly A RNA from adult kidney (Figure 12B). The hS4 rearrangement occurs at a splice acceptor site in exon 4 leading to a loss of the first 30 nucleotides of exon 4. The intra-exonic splice acceptor site contains a conserved **ag** dinucleotide typical for splice sites (see: Figure 3).

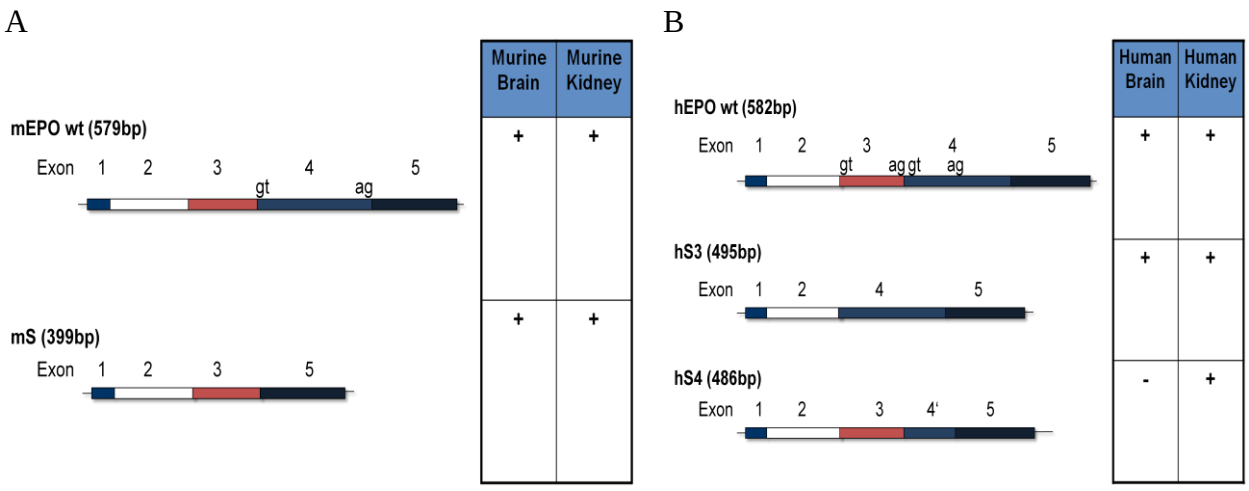

Figure 12: cDNA structure of EPO splice variants

Structures of alternatively spliced transcripts of human and murine EPO, discovered by PCR. Human and murine EPO transcripts consist of five exons, respectively. Exons deleted in the splice variants contain classical 5' donor and 3' acceptor splice sites (GU-AG rule of splicing).
A: Murine EPO splice variant mS, discovered in brain and kidney, contains a deletion of exon4.
B The spliced hEPO transcript hS3, discovered in human brain and kidney polyA RNA-derived cDNA, contains a deletion of exon3. The alternatively spliced hS4 was only detected in human kidney cDNA and lacks the N-terminal part of exon 4.

EPO has a four-alpha-helical bundle structure (helices A, B, C and D) similar to other members of the cytokine family. A fifth mini-helix B' near the carboxy end of the AB loop is important

for binding to the EPOR. Two distinct patches on the protein surface have been identified to be relevant for the formation of a 2:1 homodimeric $(EPOR)_2$:EPO complex. Residues at the D:AB loop interface build the high-affinity receptor binding site. The low affinity binding site comprises residues Val 11, Arg 14, Tyr 15, Ser 100, Arg 103, Ser 104 and Leu 108.

The predicted protein mS encoded by the murine spliced EPO transcript misses helices B and C and may form a structure similar to the classical helix-turn-helix motif (Figure 13). In the human variant hS3 loss of the AB loop and the mini-helix B' destroys the parallel bundle structure. Helices A and B may fuse to a single helix AB. The alternatively spliced EPO transcript hS4 codes only for helices A, C and D. The resulting protein is predicted to have a three-helix-structure with conservation of the mini-helix B'. Concerning receptor binding sites, the murine splice form retains the residues building up the high affinity binding site but loses residues of the low affinity binding site. The human splice form hS3 loses the residues in the AB loop building up the D:AB high affinity receptor binding interface whereas in hS4 no residues having contact to the receptor in the $(EPOR)_2$:EPO complex are lost.

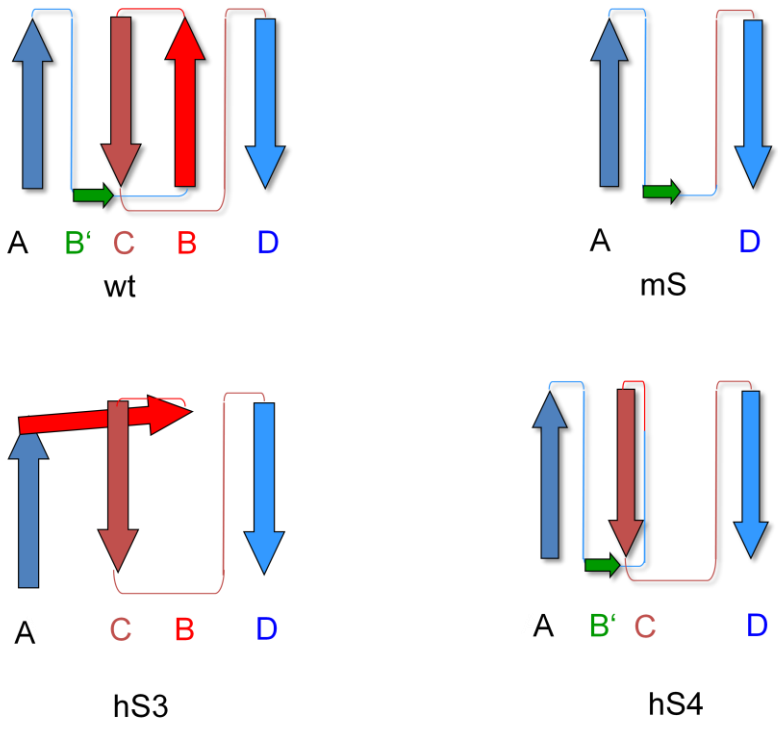

Figure 13: Predicted secondary protein structures of EPO splice variants

The figure shows the important structural changes in the human and murine splice variants. The secondary protein structures of the splice variants were deduced from the EPO structure without using modeling tools. In the murine splice variant mS the deletion of protein helices B and C leads to a classical helix-turn-helix motif. Loss of exon 3 in human hS3 results in deletion of the AB loop and the mini-helix B'. This brings helices A and B in direct contact. Human splice variant hS4 misses helix B and has probably a three-helix protein structure.

All splicing variants have a tremendously changed protein structure compared to the four-alpha-helical bundle structure of erythropoietin making binding to the EPO receptor questionable due to changed three-dimensional configurations.

Computational analysis of the EPO isoforms was focused on the splice variants hS3 and mS. Automated homology modeling was performed at the SWISS-MODEL Protein Modeling Server (SWISS-MODEL Version 36.0003) database using the templates 1eerA.pdb (rhEPO), 1buyA.pdb (rhEPO) and 1cn4C.pdb (murine erythropoietin) as scaffolds. SWISS-MODEL is a homology modeling server at the Swiss Institute of Bioinformatics accessible to everyone. It uses a standard protocol for homology modeling. In a first step appropriate protein structures are searched for in protein structure databases using BLAST. In a second step a model is build according to the chosen structure and optimized using energy minimization tools. The calculated models obtained from SWISS-MODEL were visualized in AstexViewer™, a Java molecular graphics program that can be used for visualization in many aspects of structure-based drug design. The NMR minimized rhEPO-model '1buyA.pdb' confirms the predicted four-antiparallel amphiphatic alpha-helical bundle structure of EPO (Figure 14A).

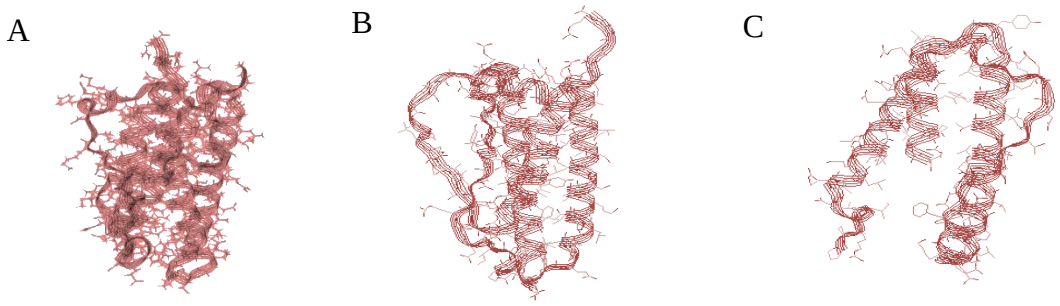

Figure 14: Structure prediction of hS3 and mS using an automated comparative protein modeling approach

A: NMR minimized rhEPO-model '1buyA.pdb' visualized in AstexViewer ™.
B: Structure prediction of hS3 based on model 1eerA.pdb (1.90Å). E-value: 5.80704e-62. Sequence identity 80%. Visualization in AstexViewer ™.
C: Structure prediction of mS based on model 1cn4C.pdb (2.80Å). E-value: 3.01905e-29. Sequence identity 48%. Visualization in AstexViewer ™.

The *in silico* generated 3D-models of the EPO splice reflect the assumptions made on the primary protein structures: a mainly two-helical protein mS (Figure 14C) and a three helical protein hS3 (Figure 14B). It should be noted, that the calculated protein structures are only predictions. Manual optimizations were not performed. However, the calculated structures have very low Expect (E)-values. The E-value is a parameter that describes the number of hits one can 'expect' to see just by chance, typically the lower the E-value, the higher the prediction accuracy. In the case of mS and hS3 one can therefore expect an accurate prediction of the protein structures.

4.2 Expression and purification of recombinant EPO variants (rvEPO)

The functional characterization of the alternatively spliced erythropoietin transcripts was of high interest in this study. As purification of the endogenous proteins from tissue extracts was unfeasible in view of low expression levels and the absence of appropriate purification tools, such as EPO variant specific antibodies for affinity purification or a specific multi-step purification protocol, recombinant proteins were generated. Recombinant proteins are proteins that are produced in genetically modified organisms such as bacteria, yeast, filamentous fungi, plants, insect cells or mammalian cells. While bacterial and yeast cells have some great advantages because of their rapid growth and high expression levels, mammalian cells are becoming a preferred choice in the biomanufacturing of human proteins due to their ability to perform proper posttranslational processing essential for many of the most promising protein therapeutics. In the case of erythropoietin, post-translational modifications comprise cleavage of a signal peptide (secretion signal) at the N-terminus of the immature protein and attachment of glycan groups. EPO contains four glycosylation sites, namely three N-glycosylation sites at Asn 24, Asn 38 and Asn 83 respectively and one O-glycosylation site at Ser 126. Glycosylation of EPO was shown to be essential for the protein's stability, solubility and *in vivo* bioactivity but is not required for *in vitro* activity (Sytkowski *et al.*, 1991) and receptor binding (Narhi *et al.*, 1991). Nevertheless receptor binding affinities are affected as glycosylated EPO has a 20-fold smaller association rate constant (k_{on}) than nonglycosylated EPO (Darling *et al.*, 2002). O-glycosylation is particularly important for biosynthesis and secretion (Dube *et al.*, 1988), the *in vivo* half-life of 4 - 5h (Salmonson, 1990) and physical stability (Tsuda *et al.*, 1990), whereas the importance of the N-linked glycans lies in decreasing the rate of EPO clearance.

Biologicals such as interleukins or vaccines are usually produced in Chinese hamster ovary (CHO) cells which generate glycosylation patterns very similar to natural human proteins. Nevertheless, in a first approach we selected human embryonic kidney cells (HEK) as producer cell line, as pilot experiments showed much higher productivity of HEK 293 cells compared to CHO cells. Transient gene expression by transfection, which is commonly known as a technique employed at a small scale for obtaining micrograms of recombinant protein, was preferred to the time-consuming generation of stably transfected producer lines. During the establishment and optimization process of the expression and purification protocol for the EPO variants, expression vectors and cell systems were changed multiple times in order to facilitate protein purification, enhance protein yield or improve protein quality. The history of expression vector improvement is summarized in Table 16.

Expression vector / host cell	EPO yield	Advantages	Disadvantages
pZ/EG in adherent HEK293	up to 15 ng/ml unpurified protein		co-tranfection of an expression vector coding for the cre recombinase necessary; purification of untagged proteins not possible; very low expression levels
pcDNA3.1-hEPO-V5/His in adherent HEK293	up to 100 - 200 ng/ml of purified protein	easy purification via His-tag; sensitive detection via V5-epitope	very low expression levels (CMV-promoter)
pcDNA3.1-hEPO-V5/His in HEK Freestyle	up to 500 ng/ml of purified protein	Suspension culture allows better yield	expression levels are higher compared to adherent cultures but too low for *in vivo* experiments
pCAG in HEK Freestyle	~ 750 µg/ml of purified protein	high expression levels due to CAG-promoter	bad protein quality (second product of higher molecular weight)
pVITRO4 in HEK Freestyle	up to 750 µg/ml of purified protein	high expression levels due to CAG-promoter; good protein quality	no or very low biological activity *in vivo*
pVITRO4 in CHO suspension cell line	up to 250 µg/ml of purified protein	high expression levels due to CAG-promoter; good protein quality; active *in vivo*	

Table 16: Improvements in protein expression systems

Attachment of a histidine tag at the C-terminus of the recombinant proteins allowed the use of metal affinity chromatography for protein purification as Histidine residues form complexes with transition metal ions such as Cu^{-}, Zn^{2+}, Ni^{2+}, Co^{2+} or Fe^{3+}. Using this technique, successful purification could be achieved in a single chromatographic step. A batch cultivation process was established in serum-free medium as fetal calf serum (FCS) contained in standard HEK medium had a negative impact on purity and yield of purified proteins. Furthermore serum-free and protein-free media are preferred in view of standardization of protein expression protocols. Addition of a V5-epitope-tag allowed comparative quantification of the different erythropoietin variants using Western Blot techniques by providing a common epitope for all variants (Figure 15A+B). The V5 epitope tag is derived from a small epitope present on the P and V proteins of the paramyxovirus of simian virus 5 (SV5). Many high-affinity antibodies are available to detect V5-tagged recombinant proteins.

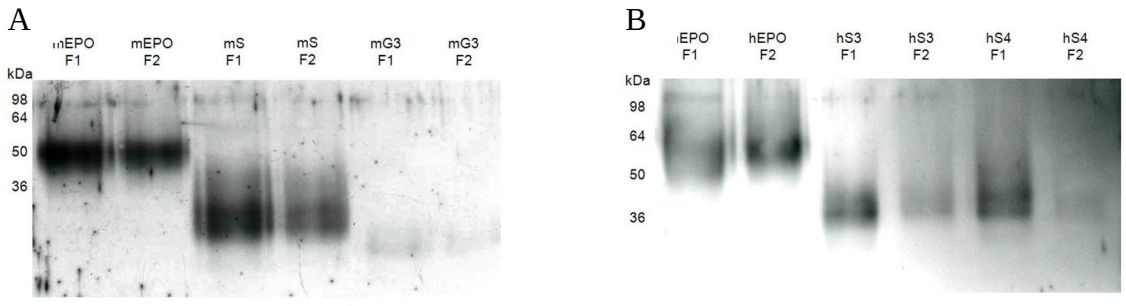

Figure 15: Purification of His-tagged murine and human EPO variants

Analysis of purified His-tagged murine (A) and human (B) EPO variants by Western Blot using a specific V5-antibody. All proteins were mainly eluted in fraction 1 but elution-peaks were unsharp. Eluted proteins were also detected in very late fractions (data not shown).

In the course of this work, the static HEK293 cultures were changed to shake flask cultures using the Freestyle Hek293 system from Invitrogen, a high-producing clonal variant of HEK293 cells. This cell line expresses the E1A adenovirus gene that participates in transactivation of some viral promoters, allowing these cells to produce very high levels of protein. Furthermore cultivation of cells in suspension enables high-density growth in appropriate culture media. By use of this system volumetric productivity was doubled.

Protein yields could additionally be enhanced by optimization of expression vectors. The change from a cytomegalovirus-promoter (CMV) to a composite promoter (CAG) that combines the human cytomegalovirus immediate-early enhancer and a modified chicken beta-actin promoter (Niwa *et al.*, 1991) improved yields significantly. The CAG promoter is a strong promoter that is known to produce high levels of expression *in vitro* and *in vivo*. In view of protein quality problems the vector pCAG, a modified form of the vector pDRIVE from InvivoGen, was finally changed to the pVITRO4 from InvivoGen. The low quality of the pCAG-derived proteins might be explained by distortions in the function of the poly A sequence due to modifications in the vector backbone. Use of the pVITRO4 expression vector in the agitated Freestyle HEK293 system systematically improved volumetric productivity up to levels necessary for *in vivo* assays. Furthermore, with the pVITRO4 expression vector acceptable protein yields were also reached in transiently transfected CHO-S suspension cultures.

The downstream process could be optimized by harvesting supernatants 72 h after transfection. At this time point high concentrations of recombinant proteins were detected but contaminating proteins in the supernatant, released from dying cells, were low (data not shown). Concentration of the harvested medium (up to 10x) using ultrafiltration systems significantly enhanced binding of His-tagged proteins to the resin (data not shown). From silvergel analysis the purity of the

recombinant EPO variants was estimated to 70 - 80% (data not shown). Compared to commercially available recombinant erythropoietin products for clinical use, our recombinant proteins were of much less purity, but sufficient for our purposes. Metal affinity chromatography of recombinant his-tagged proteins expressed from higher organisms such as yeast, insect cells or other eukaryotes does not generate pure products due to endogenous histidine-rich proteins in eukaryotes binding equally to the resin. In conclusion, our protein expression and purification strategy provides us with sufficient amounts of biological active recombinant proteins as illustrated in the following chapters.

4.3 Erythropoietic potential of the EPO variants

Recombinant proteins provided the tool to characterize the biological functions of the EPO variants. In a first approach, the erythropoietic potential of the EPO isoforms was tested, since this is the main biological function of erythropoietin.

A colony forming unit (CFU) assay is a common approach used to study hematopoiesis. It assesses the proliferative capacity of the bone marrow at a given point in time and in different conditions by addition of appropriate cytokines. For erythropoiesis assays a serum- and cytokine-free MethoCult SF 3236 methylcellulose was used that triggers the formation of colonies of various types such as CFU-M (colony forming unit-macrophage), CFU-G (colony forming unit-granulocyte) or CFU-E (colony forming unit-erythroblast) only after addition of the appropriate cytokines. Thus, the formation of CFU-E can only be observed in presence of erythropoietin. These small irregular reddish colonies appear by day 2 and disappear by day 3.

The hematopoietic potential of the murine and human splice variants was tested in comparison to recombinant murine erythropoietin from HEK cells (mEPO) and commercially available recombinant human erythropoietin from Roche (rhEPO). Proteins were expressed in adherent HEK 293 cells as tag-free pZ/EG constructs (recombinant murine proteins) or as pcDNA3-V5/His constructs (recombinant human proteins). After 48 h in culture, only reddish colonies were counted containing at least six hemoglobinised cells as defined in standard protocols for CFU-E assays. CFU-E formation was strongly induced by 200 U/l of rhEPO and by equimolar concentrations of mEPO produced in HEK293 cells. In three independent experiments mEPO and rhEPO had comparable *in vitro* bioactivities triggering the formation of approximately CFU-E per 100,000 plated cells (Figure 16 A+B). In contrast, we observed no formation of CFU-E in presence of the murine EPO variants mS and mG3 (Figure 16A) and the human splice variants hS3 and hS4 (Figure 16A), respectively.

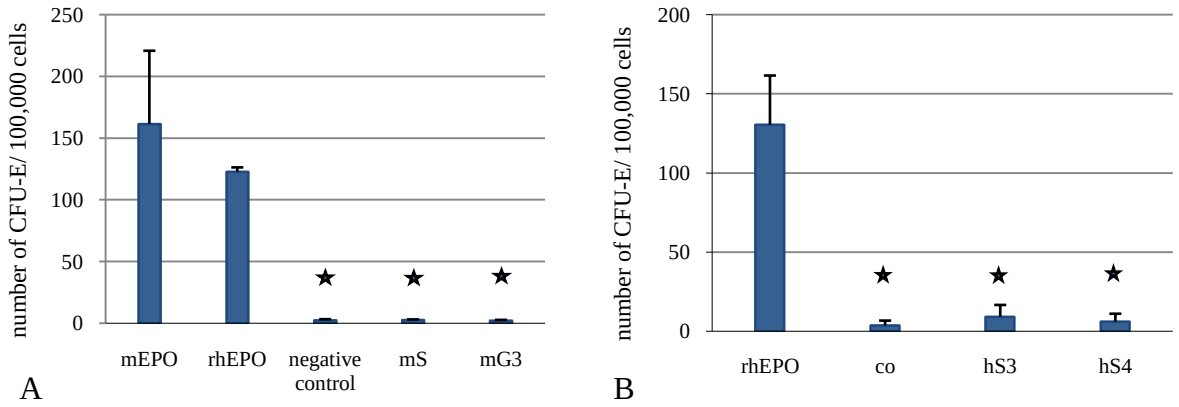

Figure 16: Colony forming assays

Murine bone marrow cells were seeded on methylcellulose in presence of 200 U/l rhEPO or equivalent concentrations of EPO variants, respectively. Small reddish colonies, the erythroid colony forming units (CFU-E), were counted 48 h after seeding. Colony counts were assessed on each individual sample at least three times and results are presented as average for colonies counted under each condition + s.d. Asterix: differences from rhEPO-treated controls (= p<0.05, Mann-Whitney).*
A: Murine EPO and EPO variants were used as unpurified proteins contained in HEK293-medium; control experiments were performed with supernatants of MOCK-transfected HEK 293 cells (negative control).
B: Human EPO variants were expressed as fusion proteins to a V5-His-tag inHEK293 cells and purified via Metal affinity chromatography.

The small human and murine erythropoietin deletion variants, generated as PCR-artefacts, were also non-hematopoietic in a single CFU-assay. Per 100,000 plated bone marrow cells formation of 39.1 CFU-E were counted in presence of h1-4; 8.9 CFU-E in presence of h1-5; 32.0 CFU-E in presence of mG5; 8.0 CFU-E in presence of m300-1 and 8.9 CFU-E in the negative control condition (MOCK-medium). On EPO-containing control plates (200 U/l) considerably higher CFU-formation rates were observed, that is 183.0 CFU-E in presence of rhEPO (Roche) and 195.6 CFU-E in presence of hEPO produced in HEK293 cells. These experiments suggest that all EPO variants are devoid of hematopoietic activity *in vitro*.

4.4 Neuroprotection experiments

4.4.1 EPO variants are neuroprotective in an *in vitro* model of cerebral ischemia

The neuroprotective ability of the EPO variants was tested in an *in vitro* model of cerebral ischemia (Ruscher *et al.*, 2002). This model consists of exposing primary cortical neuronal cultures of rodents to oxygen- and glucose-deprivation (OGD). The resulting energy deficiency leads to failure of ion pumps in the plasma membranes of the cells. Hence, influx of sodium, water and calcium into the cell causes rapid swelling which becomes visible under the microscope. The associated glutamate release triggers apoptotic pathways in neighboring neurons. The intracellular enzyme lactate dehydrogenase (LDH) is found to be released into the culture medium from dying neurons due to defects in the plasma membranes. In this model a

reduction in LDH release indicates reduced apoptotic neuronal death. However, the protective range is strongly dependent on the quality of neuronal cultures and on the amount of damage in vehicle-treated cultures. Thus, the variability between experiments can result in high standard deviations

Primary rat cortical neurons were pretreated for 48 h with EPO or EPO variants before induction of OGD (Ruscher *et al.*, 2002). In a first set of experiments, neuronal cultures were fed with supernatants of transiently transfected HEK293 cells. Expression and secretion of the untagged EPO variants into the supernatant was verified on Western Blots using an anti-rhEPO antibody from Santa-Cruz Biotechnologies (Figure 17D).

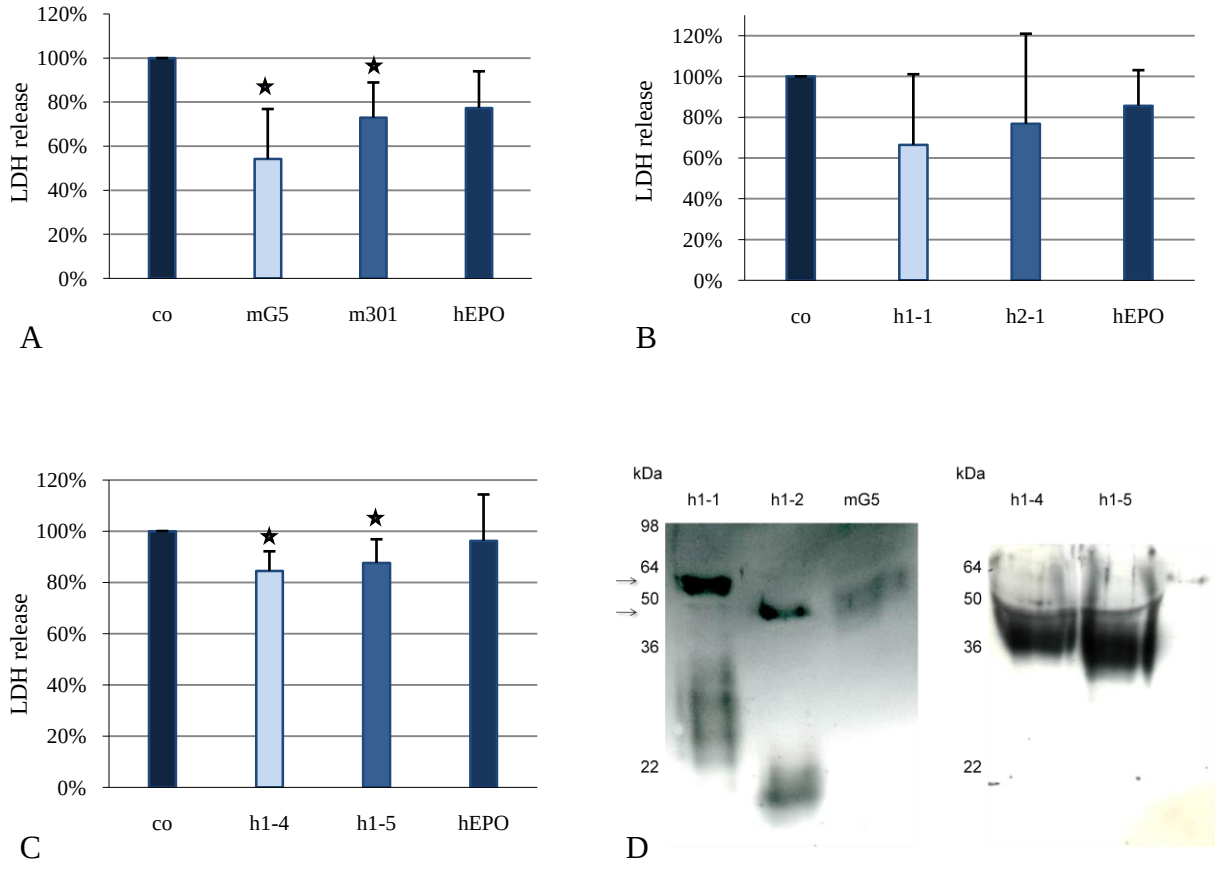

Figure 17: Human and murine EPO variants are neuroprotective.

A-C: EPO and the EPO variants induce tolerance against OGD in rat primary cortical neurons. Primary cortical neurons were pretreated for 48 h with unpurified hEPO (30 pM) or EPO variants (30 pM) contained in HEK293-medium respectively. Control cultures were treated with equal volumes of supernatants of MOCK-transfected HEK293 cultures. Recombinant hEPO and EPO variants protected primary cortical neurons from cell death induced by a 120 min OGD. Cell death was measured as LDH release for 24 h after OGD. Data were obtained from three to four independent experiments (A: n=3, B: n=3, C: n=4). Data were normalized and presented as means + s.d. Asterix: differences from MOCK treated controls (=p<0.1, Mann-Whitney).*
D: Western Blots of small untagged murine and human EPO variants secreted into the supernatants from transiently transfected HEK293 cultures. Proteins were detected with rabbit anti-rhEPO antibody from Santa-Cruz (1:500). The small proteins h1-1 and h1-2 seemed to aggregate easily (arrows).

Sister cultures were treated with equal amounts of supernatants from MOCK-transfected HEK293 cells to control for other substances contained in HEK293 medium. Interestingly, all tested human und murine EPO splice and deletion variants protected neuronal cultures from apoptotic cell death. Pretreatment of neuronal cultures with the EPO deletion variants mG5, m301, h1-4, and h1-5 led to statistically significant reductions in LDH release of 20 - 50% compared to untreated control cultures (Figure 17A, Figure 17C). Although the experiments were not repeated to significant values, the data obtained from three independent trials suggested also neuroprotective activities for the short human variants h2-1 and h1-1 (Figure 17B).

In a second study, neuronal cultures were pretreated for 48 h with the murine EPO isoforms mS, mG3 and mEPO (Figure 18A) or the human EPO isoforms rhEPO (Roche), hS3 and hS4 (Figure 18B) and exposed to different durations of OGD. The percentage of cell death in control cultures increased with prolonged duration of OGD. In agreement with previous results neuroprotective effects were observed for all EPO isoforms. However, the neuroprotective effects provided by the EPO splice variants and mG3 seemed to be more robust than protection provided by hEPO or mEPO. Neuroprotection mediated by EPO was only observed at medium damage levels (time point T1), whereas the protective window was prolonged for the EPO variants. Neuroprotective effects provided by mS, mG3, hS3 or hS4 was observed at both time points T1 and T2.

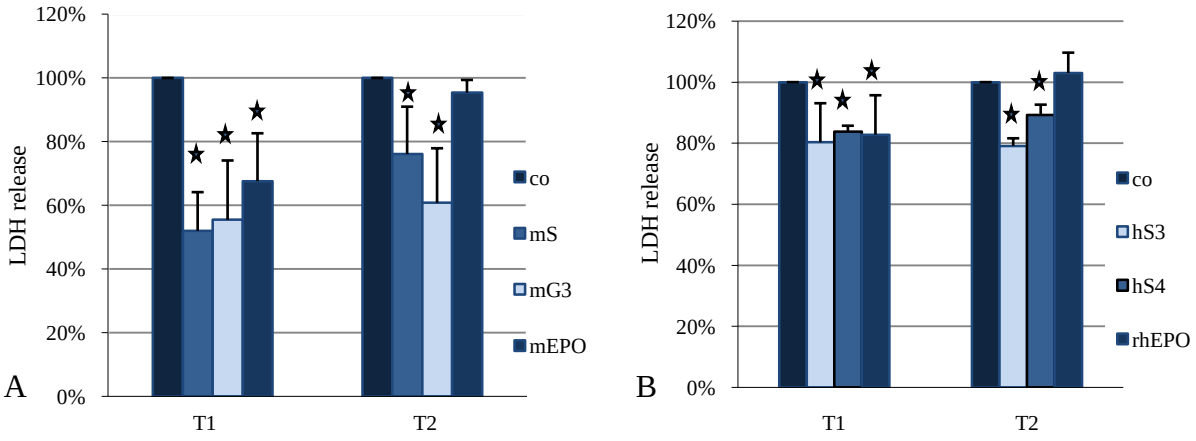

Figure 18: The EPO variants induce a more robust tolerance against OGD compared to EPO

Primary cortical neurons were pretreated for 48 h with human and murine EPO or EPO variants, respectively, and subjected to 120 min (T1) or 140 min OGD (T2). Cell death was measured as LDH release for 24 h after OGD. Pretreatment with 90 pM murine EPO variants or 30 pM human splice variants induced a more pronounced tolerance against OGD compared to 90 pM mEPO or 30 pM rhEPO. Data were obtained from three independent experiments. Data were normalized and presented as means + s.d. Asterix: differences from MOCK treated controls (=p<0.1, Mann-Whitney).*

4.4.2 Dose-survival curves of the human EPO splice variants

To determine the therapeutic doses of the human EPO splice variants, that were estimated to be of a higher clinical importance than the murine splice variant, dose-effect curves were generated in the *in vitro* model of cerebral ischemia. A dose-effect curve shows the relationship between the dose of a drug and the magnitude of the graded effect that it produces. Moreover, from these curves one can determine the specific dose that leads to a maximal effect (E_{max}).

To ensure comparability of the dose-effect curves, sister cultures of primary cortical neurons were pretreated with 0, 0.03, 0.3, 3, 8, 15, 30, 75 and 150 pM of purified hEPO expressed in HEK293, commercial rhEPO from Roche or purified human splice variants hS3 or hS4, respectively. In this study, 30 pM rhEPO corresponded to a biological activity of 100 U/l as declared by the supplier. The neuroprotective effect was determined from measures of LDH release into the culture medium 24 h after end of OGD. For presentation purposes neuroprotection was plotted as delta LDH release of treated cultures in comparison to untreated cultures in which LDH release was set to 100%.

Interestingly, no differences in the dose-survival curves of hEPO, rhEPO and the human EPO splice variants were observed (Figure 19).

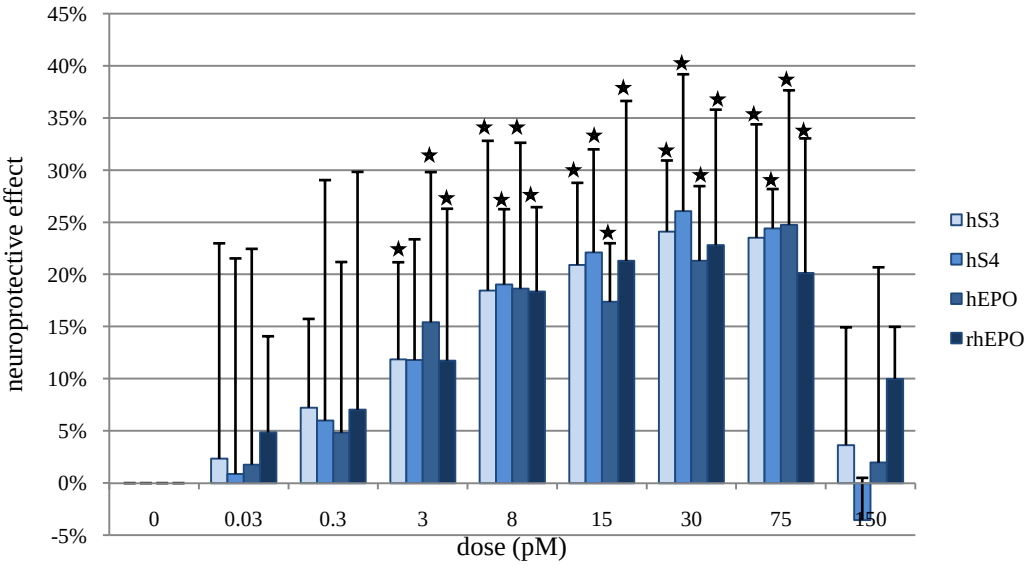

Figure 19: Human EPO and EPO splice variants have similar dose-survival curves

*Dose-effect curves of the human erythropoietin variants hEPO, hS3 and hS4 and the recombinant human erythropoietin from Roche (rhEPO) in an in vitro model of cerebral ischemia. Primary cortical neurons were pretreated for 48 h with 0, 0.03, 0.3, 3, 8, 15, 30, 75 or 150 pM rhEPO (Roche), hEPO or the human EPO splice variants hS3 and hS4, respectively, as indicated on the horizontal axis. The vertical axis represents the protective effect from cell death induced by a 120 min OGD. The neuroprotective effect was evaluated as reduction in the 24 h lasting LDH release after OGD. For all EPO derivatives an inverted u-shaped dose effect curve was obtained as described in literature for rhEPO. The maximal effect was obtained with doses from 30 - 75 pM. Data obtained from 7 to 21 experiments were normalized and presented as average + s.d. Asterix: differences from untreated controls (*p<0.05, ANOVA1, Dunn's method.)*

In accordance to literature the curves had an inverted u-shape with a maximal effect E_{max} between 30 and 75 pM. Significant neuroprotective effects of more than 10% were achieved with doses between 3 and 75 pM. Doses from 150 pM on were not protective anymore in the OGD-model. However, toxic effects of human EPO or EPO splice variants were not observed even at the highest dose of 150 pM.

4.4.3 Derivatives of the A-helix of hEPO are sufficient to induce neuroprotection

When comparing the primary protein structures of the so far identified neuroprotective erythropoietin variants the A-helix was found to be shared as common substructure by all variants (Figure 20).

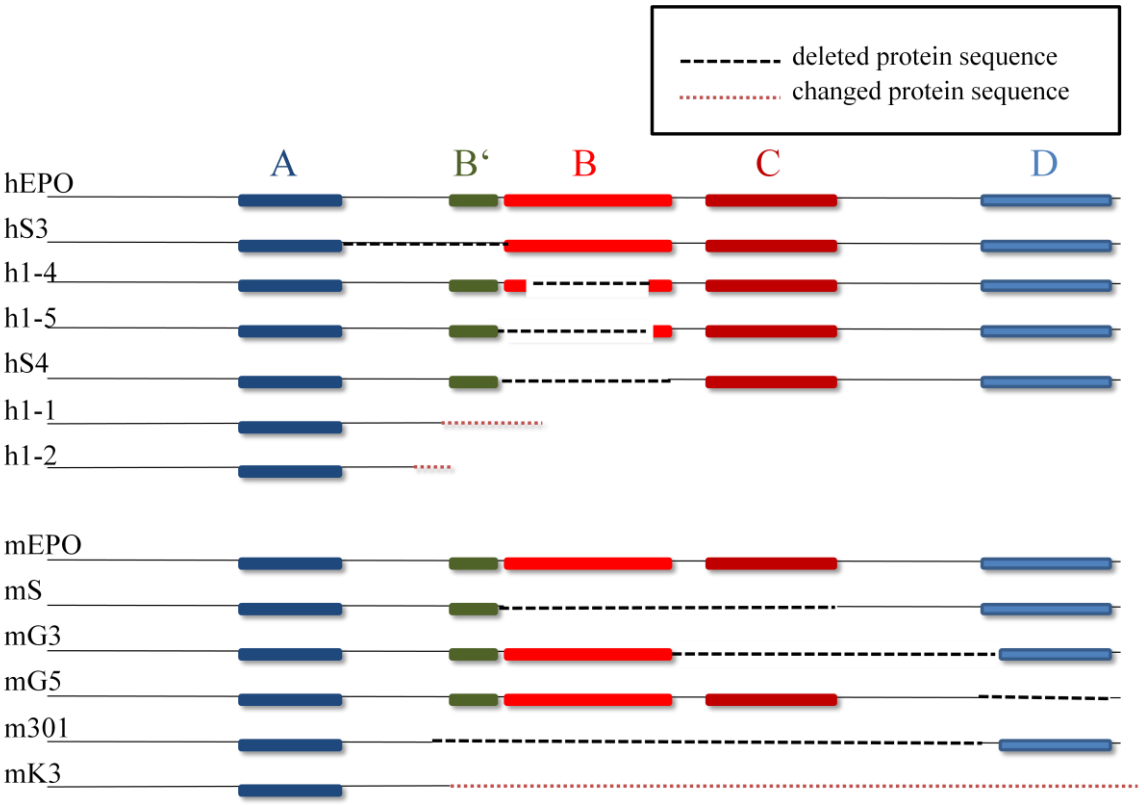

Figure 20: Primary protein structures of the EPO variants

Schematic view of the primary protein structures of the human and murine EPO variants. Helices are represented as boxes: dark blue=protein-helix A, red=protein-helix B, ruby-colored=protein-helix C, light blue=protein-helix D, green=mini-helix B'. Deleted protein parts are represented as dotted lines.

Therefore, the A-helix was supposed to be the functionally important domain for the neuroprotective character of erythropoietin. The open-reading frame of the human EPO A-helix was isolated and expressed in HEK293 cells as tag-free protein to avoid possible steric hindrance. To test the neuroprotective ability of the A-helix primary cortical neurons were pretreated for 48 h with supernatants of transiently transfected HEK293 cells before induction of OGD.

In four independent experiments, the A-helix provided significant neuroprotection. In cultures pretreated with 15 pM and 30 pM of the A-helix, LDH release was reduced by 20 – 30% compared to MOCK-treated controls (Figure 21).

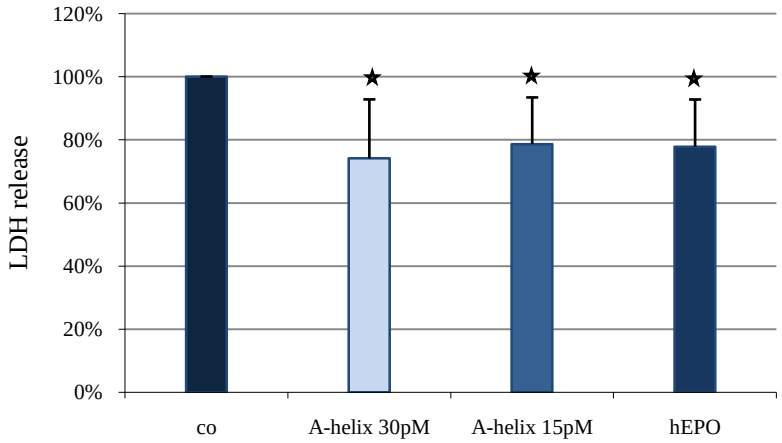

Figure 21: The A-helix of erythropoietin is sufficient to induce ischemic tolerance in neuronal cultures

*Primary cortical neurons were pretreated for 48 h with 15 pM or 30 pM hEPO-derived A-helix expressed in HEK-medium. Control cultures were pretreated with equivalent volumes of medium of MOCK-transfected HEK293 cells (negative control) or 30 pM hEPO expressed in HEK293 cells (positive control). OGD was applied for 120 min. LDH release was measured 24 h after reoxygenation. Data were obtained from four independent experiments. Data were normalized and plotted as means + s.d. Asterix: differences from control cultures (*p<0.05, t-test).*

To determine if the A-helix was the smallest possible substructure mediating neuroprotective effects, this structure was further shortened. A-helix derivatives were generated by truncation of the C-terminus and expressed in HEK293 cells (‘-10aa’ and ‘-20aa’). Interestingly, the mutant ‘-10aa’, shortened by ten aminoacids, still provided significant neuroprotection in the OGD-model. Pretreatment of cultures with ‘-10aa’ or hS3 reduced LDH release after OGD by nearly 40% compared to control cultures, whereas neuroprotective activity was lost in the deletion variant shortened by 20 amino acids (‘-20aa’) (Figure 22A).

Hence, an erythropoietin peptide of 16 amino acids length had been identified mediating neuroprotection *in vitro*. In order to confirm this finding, experiments were repeated with a commercial peptide from Bachem. This peptide herein after called P16 consisted of the amino acid sequence of the mature ‘-10aa’ peptide with a Biotin-label at the N-terminus.

When performing dose-effect experiments in the OGD paradigm using concentrations of 0, 60, 200 and 2000 pM, the maximal neuroprotective effect of P16 was found in the range of 60 to 200 pM (Figure 22B). In agreement with hEPO, hS3 and hS4 the predicted dose-survival curve of P16 in the *in vitro* model of cerebral ischemia was u-shaped. Neuroprotective effects were lost at concentrations above 2000 pM.

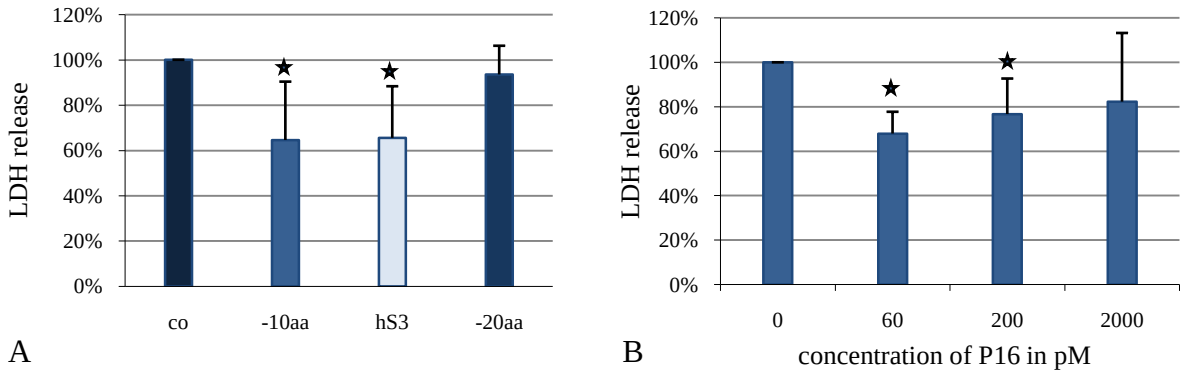

MATURE PEPTIDE	PROTEIN STRUCTURE
APPRLICDSRVLQRYLLEAKEAENIT	HelixA (hA)
APPRLICDSRVLQRYL	hA-**10aa** (P16)
APPRLI	hA-**20aa** (P6)

MATURE PEPTIDE	PROTEIN STRUCTURE
Biotin-APPRLICDSRVLQRYL	Biotin-hA-**10aa** (P16)

Figure 22: Erythropoietin A-helix deletion variants are neuroprotective

Neuroprotection assays were performed in an in vitro model of cerebral ischemia. Pretreatment of primary cortical neurons was performed for 48h induction of OGD. LDH release was measured 24 h after reoxygenation. Data were normalized and plotted as means + s.d.
A: Primary cortical neurons were pretreated with equal amounts of hS3 and the peptides '-10aa' and '-20aa' expressed in HEK-medium (n=9). hS3 was used at a final concentration of 30 pM. Control cultures were pretreated with equal volumes of medium of MOCK-transfected HEK293 cells. Asterix: differences from control cultures (p<0.05; ANOVA1, Dunn's method).*
*B: Primary cortical neurons were pretreated with different concentrations of the Bachem-peptide P16 corresponding to the peptide '-10aa' (n=6). The dose-effect curve of P16 was found to be u-shaped. Asterix: differences from cultures treated with 0 pM P16 (*p<0.001, t-test).*

4.4.4 Identification of neuroprotective EPO peptides

Having identified a neuroprotective peptide of only 16 amino acid length (P16) the interest was to determine the critical size of A-helix derived neuroprotective EPO peptides. Intermediate peptides of 8, 10, 12 and 14 amino acid length were tested in the OGD-model in primary cortical neurons (Figure 23A). The peptides were obtained from the company Bachem (Bubendorf, Switzerland) as non-biotinylated molecules to avoid any experimental artefacts. Peptides P8 to P14 were used in the dose of 200 pM previously shown to be the maximal neuroprotective dose for P16. Surprisingly the stepwise shortened peptides P14 and P12 were not protective in the OGD-model whereas P8 and P10 showed significant effects comparable to P16 in nine independent experiments (Figure 23B). The mean LDH release was lowered by approximately 20% compared to control cultures in P8, P10 and P16 pretreated cultures.

Exemplarily, a dose-survival curve was generated for the shortest peptide P8 using concentrations from 0 to 1000 pM (Figure 23C). The dose-effect curve of P8 was found to be

nearly identical to the dose-effect curve of P16 having maximal neuroprotective effects in the range of 60 to 200 pM.

Name	Sequence
P8	APPRLICD
P10	APPRLICDSR
P12	APPRLICDSRVL
P14	APPRLICDSRVLQR
P16	APPRLICDSRVLQRYL

A

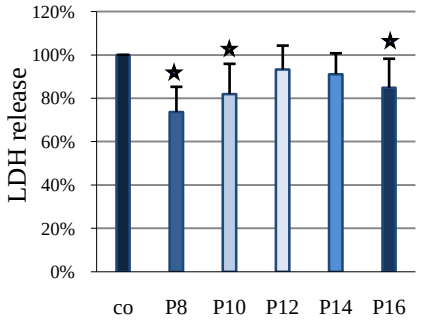

B 200 pM Bachem-peptides

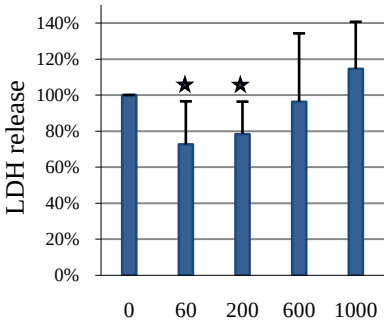

C concentration of P8 in pM

Figure 23: Neuroprotective EPO peptides

Primary cortical neurons were pretreated for 48 h with peptides derived from the human erythropoietin A-helix provided by Bachem before induction of oxygen-glucose deprivation.
A: The table summarizes the peptides P6 to P16 derived from the hEPO-A-helix. Shown are the amino acid sequences of the peptides.
B: Comparison of neuroprotective effects provided by the peptides P8, P10, P12 and P16. 24h LDH release after OGD was measured as marker of cell death. LDH release was normalized and averages were plotted + s.d. In nine independent experiments significant neuroprotection was observed after pretreatment with peptides P8, P10 and P16. P12 and P14 did not provide protection in this model. Asterix: differences from control cultures (p<0.05; ANOVA1, Dunn's method.)*
C: Dose-effect curve of the peptide P8 in primary cortical neurons from rat (n=7). Cultures were pretreated with growing concentrations of the Bachem-peptide P16 from 60 pM to 1000 pM. LDH release in control cultures was considered 100%. Averages were plotted + s.d. Asterix: differences from cultures treated with 0 pM P8 (p<0.05; ANOVA1, Dunn's method).*

4.5 hEPO and hS3 mediated cytoprotection in an *in vitro* model of myocardial ischemia

Recent evidence has shown that EPO is able to sustain antiapoptotic responses in several tissues outside of the central nervous system e.g. in the heart, the skin or the intestine. Therefore it can be regarded as a general tissue-protective cytokine.

The cytoprotective potential of the EPO variants was analyzed exemplarily for purified hEPO and hS3 in an *in vitro* model of myocardial ischemia. Myocardial ischemia is a disease characterized by reduced blood supply to the heart muscle inducing apoptosis and necrosis of the tissue. In the *in vitro* model, a long lasting serum and oxygen deprivation induced apoptotic cell death in the rat cardiac myoblasts cell line H9c2. LDH release into the medium after reoxygenation was shown to correlate with cell damage as hEPO or hS3 treatment had no proliferative effect in this experimental paradigm (data not shown). Therefore LDH release was assessed as a marker of cell death.

Interestingly, the degree of myoblast cell death was significantly attenuated by hEPO and hS3 compared with controls (Figure 24).

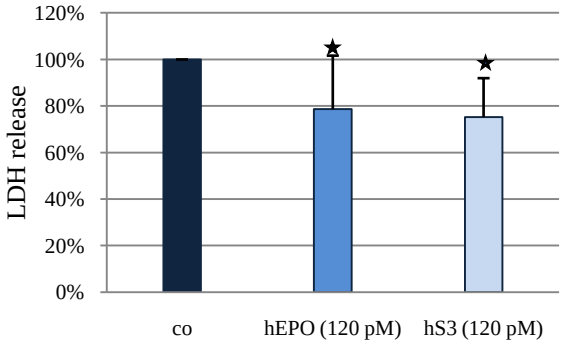

Figure 24: hEPO and hS3 mediated cytoprotection in an in vitro model of myocard ischemia

The rat cardiac myoblast cell line H9c2 cells was pretreated with 120 pM hEPO or hS3, respectively before induction of a 24 h serum and oxygen deprivation. Apoptosis was assessed after reoxygenation by determing the LDH activity in the medium. Mean LDH release from seven independent experiments was normalized and plotted + s.d. Asterix: differences from control cultures (p<0.001, ANOVA1, Dunn's method).*

The rate of LDH release was lowered by 20% after hEPO pretreatment and by 25% after preconditioning with hS3. This *in vitro* model of myocardial ischemia suggests equal cytoprotective capacities for hEPO and hS3.

4.6 Immunoprecipitation reveals EPO splicing isoform in murine tissues

To strengthen the finding of EPO splicing isoforms in human and murine tissues by a PCR-based approach, immunoprecipitations were performed on murine plasma, brain and kidney protein extracts of $CoCl_2$ treated mice using antibodies tested to recognize both isoforms, namely mEPO and mS. Subcutaneous injection of $CoCl_2$ in 129/Sv mice increased erythropoietin levels 5 - 60 times in plasma, 22 - 25 times in kidney and up to 3 times in brain tissue 18 h after injection compared to untreated mice as designated using a murine erythropoietin ELISA based test from R&D. When using large amounts (up to 6 mg total protein) of crude tissue extracts for immunoprecipitation we were able to detect erythropoietin (approximately 40 kDa) in plasma, brain and kidney of $CoCl_2$-treated mice (Figure 25A). Precipitation of erythropoietin from kidney extracts of untreated mice failed due to the very low expression level.

Importantly, in addition to mEPO a smaller protein (approximately 30 kDa) was precipitated from kidney and brain protein extracts of $CoCl_2$ treated mice (Figure 25A). Two immunoprecipitation experiments revealed the existence of the smaller protein also in murine plasma (Figure 25B). This protein was specifically recognized by the anti-rhEPO antibody as

shown by complete blocking of the antibody-antigen interaction with commercial rhEPO (Darbepoietin A) (Figure 25A). Furthermore, the unknown protein correlated in protein weight with recombinant mS expressed in HEK293 cells. This result strongly supports the existence of a murine erythropoietin splicing isoform on a protein level.

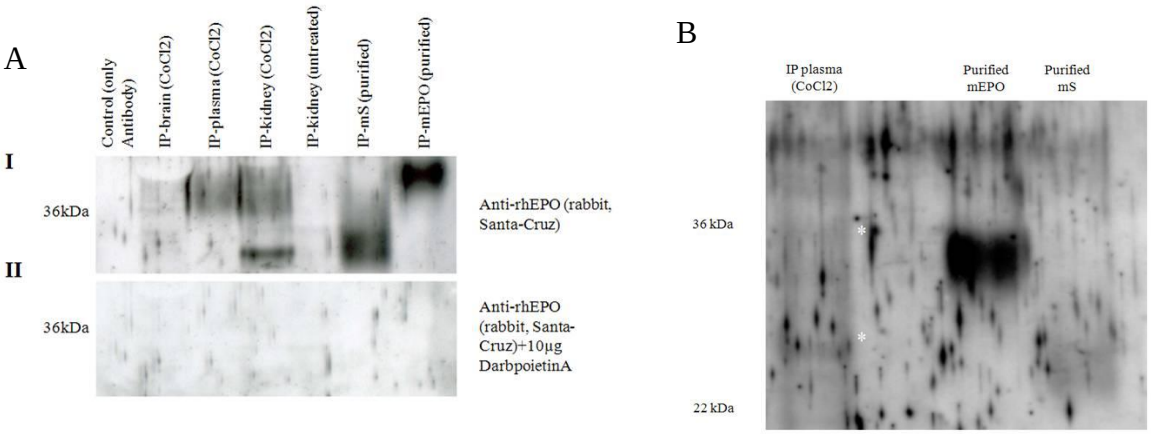

Figure 25: Anti-EPO antibodies immunoprecipitate two proteins from murine tissue extracts

Immunoprecipitations (IP) were performed using an anti-mEPO antibody from R&D (A) or an anti-rhEPO from Santa-Cruz (B). A:I: Two proteins were immunoprecipitated from murine tissue samples. Western Blot analysis of precipitates using anti-rhEPO from Santa-Cruz revealed one protein of 40 kDa corresponding in size to mEPO and a second protein of 30 kDa corresponding in size to mS. II: The specificity of the Western Blot was shown by blocking the antibody-antigen interaction. The anti-rhEPO was preincubated with large amounts of rhEPO (DarbepoietinA) before application to the membrane.
B: The existence of the smaller protein was also revealed in murine plasma samples.

The immunoprecipitation experiment was repeated in a second mouse strain, namely C57/Bl6 (Figure 26).

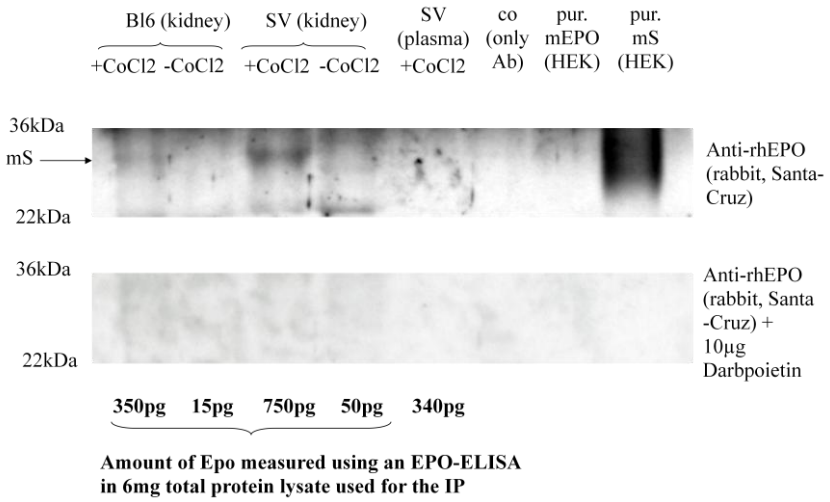

Figure 26: The expression of the smaller protein seems to be co-regulated with mEPO-expression

Immunoprecipitation experiment in the mouse strains SV and C57/Bl6. Amounts of the precipitated smaller protein correlated with measured levels of mEPO. (pur.=purified, Ab = antibody)

The finding of a second smaller protein specifically recognized by the anti-rhEPO antibody was reproduced in the C57BL/6 and the 129/Sv strain indicating that this protein is not mouse strain specific. The expression of the 30 kDa protein seemed to be co-regulated with mEPO expression. From samples containing high mEPO levels we were able to precipitate higher amounts of the 30 kDa protein that we assume to be our murine splice variant mS than from samples containing lower EPO concentrations (Figure 26).

4.7 Pathways involved in neuroprotection

The binding of erythropoietin to its preformed dimeric receptor is known to lead to a conformational change and thereby to activation of Janus kinase 2 (Jak2) by transphosphorylation (Remy *et al.*, 1999; Watowich *et al.*, 1994; Witthuhn *et al.*, 1993). In turn, pJak2 phosphorylates tyrosine residues in the cytoplasmic domains of the erythropoietin receptor. Phosphorylation of $(EPOR)_2$ attracts other intracellular proteins implicated in signaling pathways, which bind via their src homology 2 (SH2) domains (He *et al.*, 1995). At least three different signaling pathways are characterized for antiapoptotic actions mediated by erythropoietin.

In red blood cells erythropoietin induces the Ras/MAP kinase pathway and the Stat (signal transducer and activator of transcription) pathway. Ras is a G-protein attached to the cell membrane that plays a major role in many pathways for cell proliferation or differentiation (Reuter *et al.*, 2000). RAS is activated by exchange of GDP to GTP mediated by SOS (Son of sevenless), a RAS guanine nucleotide exchange factor. Translocation of SOS to RAS is dependent from pJak2 mediated phosphorylation of the adapter protein Shc (He *et al.*, 1995) and activation of the second adapter protein Gbr2. The second signaling pathway involving Stat5 has been well studied in models of red blood cell differentiation and proliferation and in antiapoptotic events mediated by erythropoietin in non-neuronal tissues as for example in cardiac cells (Parsa *et al.*, 2003). The activated Jak2 leads to tyrosine phosphorylation and thereby to dimerization of Stat5. The active protein then translocates to the nucleus and leads to expression of specific antiapoptotic genes by binding to the DNA. The third signaling pathway has as key mediators the phosphoinositide-3 kinase (PI3K) and the serine/threonine protein kinase B (Akt). This pathway seems to be critical for tissue protective actions of erythropoietin.

In primary cortical neurons activation of Akt leads to phosphorylation of BAD, a proapoptotic member of the Bcl-2 family, which dissociates subsequently from the cell survival factor Bcl-XL, resulting in protection from apoptosis (Ruscher *et al.*, 2002). Digicaylioglu proposes additional involvement of the NF-kB-pathway via phosphorylation of I-kB (inhibitor of NF-kB)

mediated by Akt and subsequent transcription of antiapoptotic genes such as XIAP or c-IAP-2 (Digicaylioglu *et al.*, 2001).

In this study, the focus was on the Jak2/Stat5 pathway and the Akt pathway previously described to be active in neuronal cells and already well studied by Ruscher *et al.* in my laboratory. For investigation of possible involvement of Akt in the antiapoptotic actions of the human EPO variant hS3 an Akt kinase assay was performed on cell lysates of primary cortical neuronal cultures of DIV 8 treated for 30 min with 30 pM hEPO, rhEPO (100 U/l, Roche) or hS3, respectively. GSK-3α/β is a substrate protein of Akt and analyzed as activation marker of Akt in this assay (Figure 27A). Significantly more phosphorylated product pGSK-3α/β was found in the cultures treated with hS3, hEPO or rhEPO than in control cultures (Figure 27B).

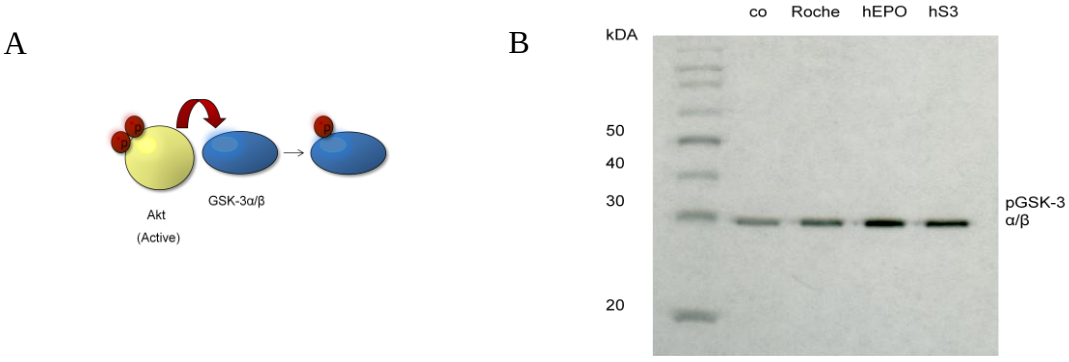

Figure 27: Akt kinase assay

A: Principle of the Akt kinase assay. Akt is immunoprecipitated from cell lysates and incubated with its substrate GSK-3α/β. Phosphorylated p GSK-3α/β is subsequently analyzed on Western Blots.
B: Akt kinase assay on lysates of neurons treated for 30 min with 30 pM hEPO, rhEPO or hS3. The representative Western Blot shows an upregulation of Akt activity after treatment with EPO or hS3.

Other members putatively involved in the signaling pathway of the hS3 were analyzed by Western Blot. Primary cortical neurons of DIV 8 were stimulated with 90 pM hS3 or hEPO for defined time lengths and lysed in appropriate buffers. Proteins were separated on acrylamide gels and analyzed using phospho-specific antibodies that recognize the activated forms of the putatively involved proteins. After 15 min stimulation with hEPO and hS3, Stat5 (data not shown) and Jak1 (Figure 28) were not found to be activated, but pJak2 was found to be slightly upregulated compared to untreated control cultures (Figure 28). BAD, a protein of the EPO signaling pathway in neurons downstream from AKT, was also analyzed. Phosphorylation of BAD at Ser112 and Ser136 was only found in hEPO and hS3 treated cultures (90 pM) after 15 min stimulation but not in control cultures (Figure 28). Another target of Akt, the kinase IKK which controls activation of the transcription factor NF-kB was slightly upregulated in cultures treated for 15 min with EPO variants (Figure 28). This hints at erythropoietin-mediated activation of the NF-kB-pathway in primary cortical neurons.

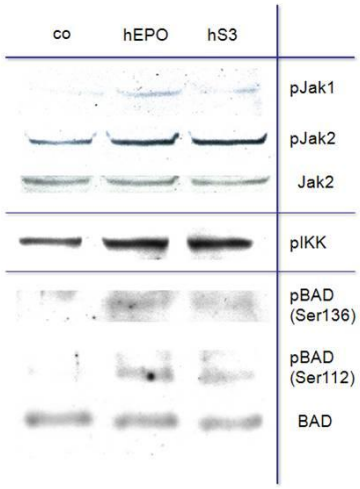

Figure 28: Signaling in primary cortical neurons

Primary cortex neurons were treated for 15 min with 30 pM hEPO or 30 pM hS3, respectively. Lysates were stained in western blots for different phosphorylated proteins being mediators in intracellular signaling cascades. pJak1 signals were not observed in primary cortical neurons. pJak2 seemed to be upregulated after hEPO and hS3 treatment in some experiments. More reliable upregulations were found for pIKK, a member of the NF-kB pathway, and for pBAD after treatment with hEPO and hS3.

To clarify the role of Jak2 in hS3 mediated neuroprotective effects, neuronal cultures were pretreated with the specific Jak2 inhibitor AG490 (5 µM) one hour before pretreatment with hEPO or hS3. In the OGD model, AG490 alone had no effect on neuronal viability but blocked antiapoptotic effects of hEPO and hS3 (Figure 29). This result suggests a central role of Jak2 in the signaling pathways of both hEPO and hS3, but does not exclude the possibility of different receptor kinetics or dissociation constants.

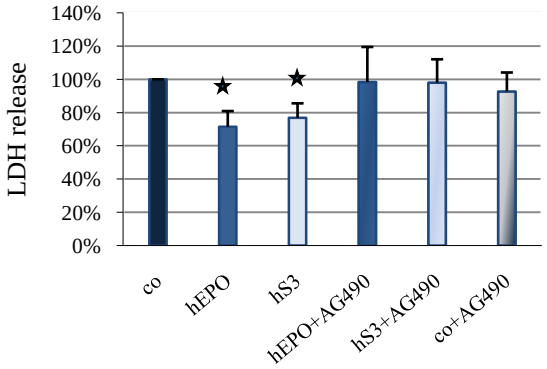

Figure 29: AG490 treatment of cortical neurons inhibits neuroprotection mediated by hS3 and hEPO

*Primary cortical neurons were pretreated for 48 h with 30 pM hEPO and hS3 before induction of OGD. Sister cultures were in addition pretreated with the specific Jak2 inhibitor AG490. Control cultures were untreated or treated with AG490 alone. LDH release in untreated control cultures was considered 100%. In three independent experiments abolishment of neuroprotective actions mediated by hEPO and hS3 was observed in presence of AG490. AG490 itself had no toxic effects on the neurons. Mean LDH releases were plotted + s.d. Asterix: differences from untreated control cultures (*p<0.05, ANOVA1, Dunn's method).*

4.8 EPO variants promote diverse effects on stem cells

A major interest in this study was to investigate potential antiapoptotic effects of the EPO variants exerted on adult stem cells. The study was focused on hEPO, the human splice form hS3 and the human A-helix derived peptide P16.

4.8.1 EPO variants promote divergent effects in neural stem and precursor cells

Neural stem and precursor cells (NSC/NPC) were isolated from male adult mice. Deficient trophic factor supply is known to rapidly activate apoptotic signaling cascades in NSC/NPC, similarly to apoptosis in mature neurons after trophic factor withdrawal (Eom *et al.*, 2007). Thus, to test possible antiapoptotic effects of EPO isoforms on NSC/NPC, isolated NSC/NPC were expanded as neurospheres and then plated as monolayers on PLL-coated coverslips in absence of the growth factors EGF and β-FGF. Purified recombinant proteins produced in HEK293 cells (300 pM) or Bachem-peptide P16 (1000 pM) were added immediately (see Experimental Design 1, chapter 3.2.8.2 Differentiation and survival assay). Withdrawal of the growth factors from the Neural Stem Cell Basal Medium resulted in massive cell death but also in the spontaneous differentiation of the rodent neural stem cells. 24 h hours after seeding, outgrowth of adhered cells was observed. Strikingly, the addition of EPO isoforms to the cultures had a positive effect on cell viability (Figure 30). This effect appeared to be most pronounced in hS3 treated cultures as viable cells had also longer branches.

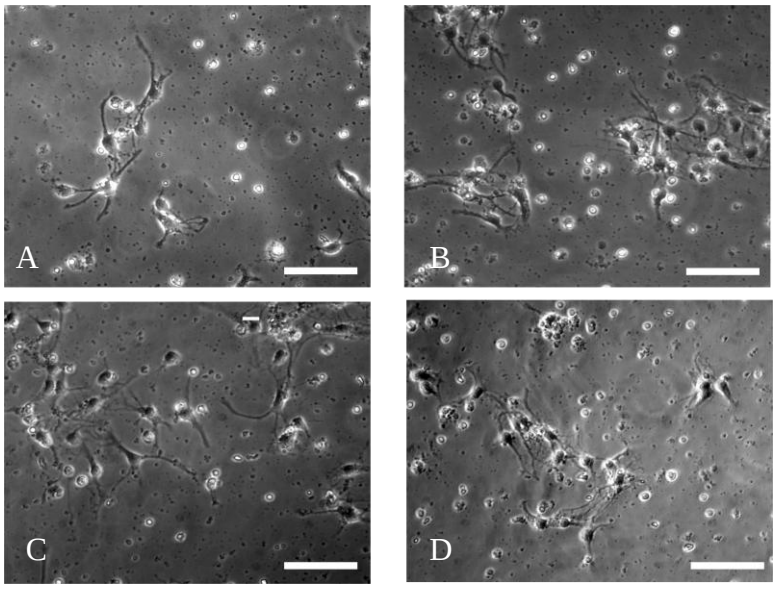

Figure 30: Recombinant EPO isoforms effect on cell viability of NSC/NPC

Dissociated murine neural stem and progenitor cells were seeded at the density of 130.000 cells/well on PLL-coated coverslips in absence of β-FGF and EGF. Addition of EPO isoforms had a positive effect on the viability of the cultures as observed 24 h after seeding. A: control culture, MOCK; B: hEPO (300 pM); C: hS3 (300 pM); D: peptide P16 (1000 pM) (400x magnification).

Viable cells were quantified in each well 24 h after seeding. Three randomly chosen fields were counted at a 200x magnification with a phase-contrast microscope. Cell viability in untreated cultures was considered as 100% (control, co). Addition of hEPO and hS3 improved the survival of NSC/NPC significantly. The survival rate was increased to approximately 170% in presence of hEPO and to 260% in presence of hS3. Only a weak effect on the survival rate was determined for 1000 pM of the peptide P16, whereas the lower concentration (300 pM) had no effect on viability (Figure 31E).

To determine whether the EPO isoforms influence the fate of NSC/NPC, cells were differentiated for 1 week in the presence of hEPO, hS3 or P16. Cultures were fixed with 4% paraformaldehyde (PFA) and stained for neuron (DCX), astroglia (GFAP) and oligodendrocyte (RIP, OLIG) specific markers (Figure 31A-D).

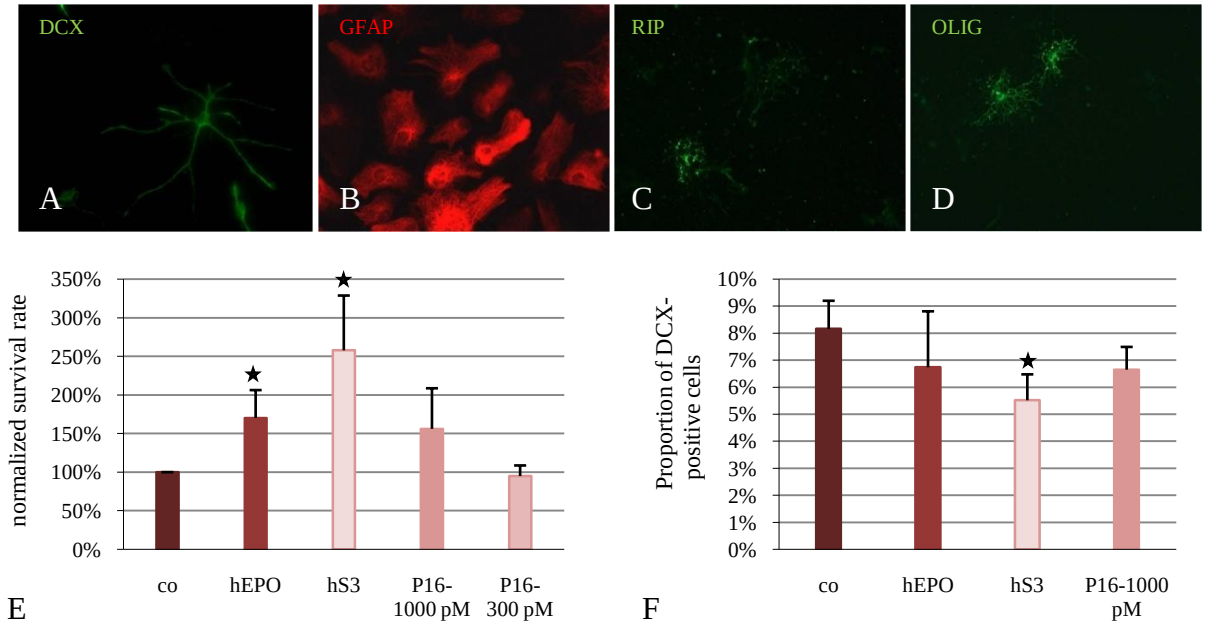

Figure 31: hS3 mediates survival and differentiation effects on NSC/NPC

NSCs were differentiated in absence of β-FGF and EGF but in presence of hEPO (300 pM), hS3 (300 pM) or peptide P16.
A-D: Staining of the major cell types, in which neural progenitor cells differentiate. A: neuronal phenotype (anti-DCX); B: astroglial phenotype (anti-GFAP); C: young oligodendrocytes (anti-RIP); D: mature oligodendrocytes (anti-OLIG).
*E: NSC cultures were evaluated 24 h after seeding for cell survival rates (n=6). The number of living cells counted in control cultures was considered as 100% survival and plotted + s.d. Significantly more surviving cells were counted in hS3-treated cultures. Asterix: differences from control cultures (*p<0.05, ANOVA1, Dunn's method).*
*F: NSC cultures were fixed seven days after seeding and stained for the astroglial marker GFAP and the early neuronal marker DCX (n=5). The proportion of DCX-positive cells in each condition was determined from minimum four randomly chosen fields (+ s.d.). Significant less DCX-positive cells were counted in the hS3-treated cultures (*p<0.01, t-test compared to co).*

Doublecortin (DCX) is a microtubule-associated protein expressed almost exclusively in immature neurons. Glial fibrillary acidic protein (GFAP) is an intermediate filament protein that is found in glial cells such as astrocytes. It is involved in maintaining structure and function of

the cytoskeleton. RIP is a marker for both immature and mature oligodendrocytes, in that it stains pre-ensheathing oligodendrocytes through myelinating stages and associated myelin. The OLIG antibody stains CNPase, an enzyme almost exclusively found in oligodendrocytes and Schwann cells. Oligodendrocytes were found at low percentage (<1%) only in cultures derived from very early passage NSC. Thus, analysis was focused on neuronal and astroglial phenotypes, the two major neural lineages in which NSC differentiate. In each well the percentage of DCX-positive cells was determined from a minimum of four randomly chosen fields at a 200x magnification. Surprisingly, a significant decrease in the proportion of DCX-positive neurons was observed in cultures differentiated in presence of hS3 compared to sister cultures differentiated in presence of hEPO, P16 or in absence of EPO isoforms (Figure 31F). In MOCK-, P16- and hEPO-treated cultures 7 to 8% of the cells were found to express DCX whereas after hS3 treatment only 5.5% of the cells were positive for this early neuronal marker. Consistent with the previous finding of enhanced viability 24 h after growth factor withdrawal, more healthy unfragmented nuclei were observed in DAPI stainings of hS3-treated cultures (data not shown).

To determine whether the hS3-mediated survival and differentiation effects on NSC/NPC were only existent under acute treatment conditions, cells were pretreated for 7 days with hS3 before differentiation (see Experimental Design 2, chapter 3.2.8.2 Differentiation and survival assay). Cells were seeded at 3500 cells/cm^2 in T-25 flasks (Corning) and grown in the presence of β-FGF and EGF, either with or without 3 nM or 0.3 nM hS3. After 7 days of incubation cultures grown in presence of 3 nM hS3 contained approximately 20% more cells than control cultures fed with equivalent volumes of MOCK-medium. This effect was statistically significant and reproducible in four independent experiments (Figure 32).

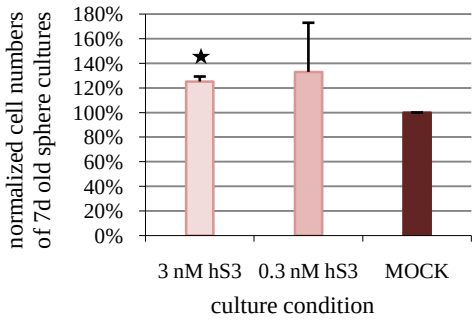

Figure 32: Sphere cultures cultivated in presence of hS3 contain higher cell numbers

*Neural stem and progenitor cells were grown as sphere cultures for seven days in medium containing 0 (MOCK-medium), 0.3 or 3 nM of the human splice variant hS3. Spheres were harvested, dissociated and cell numbers of total sphere cultures were evaluated. Four individual experiments were pooled. Absolute cell numbers assigned in control cultures (MOCK) were considered as 100% and plotted s.d. In sphere cultures grown in presence of 3 nM hS3 significantly higher cell numbers were determined. Asterix: differences from MOCK-treatment (*p<0.05, ANOVA1, Dunn's method).*

To assess the self-renewal capacity of cells derived with hS3, clonogenic assays were performed. These assays are routinely used in neural stem cell research to demonstrate the 'stem cell' nature of the candidate cell. The efficiency of secondary neurosphere formation was compared between neurospheres obtained in presence of 3 nM or 0.3 nM hS3 compared to neurospheres grown in MOCK-treated control cultures. Relevant sphere cultures were dissociated and single cells were seeded in 96 well plates at a density of 400, 200, 100, 50 or 25 cells per well in presence of β-FGF and EGF. After seven or twelve days of culture sphere-forming units were counted at a 25x magnification with a phase-contrast microscope. Cells adhered to the plate but still formed clear sphere-shaped colonies. Pretreatment with hS3 did not change the number of formed neurospheres significantly in four independent experiments (Figure 33A+B). However, there may be a weak tendency to an enhanced self-renewal potency of NSC after a 3 nM hS3 treatment.

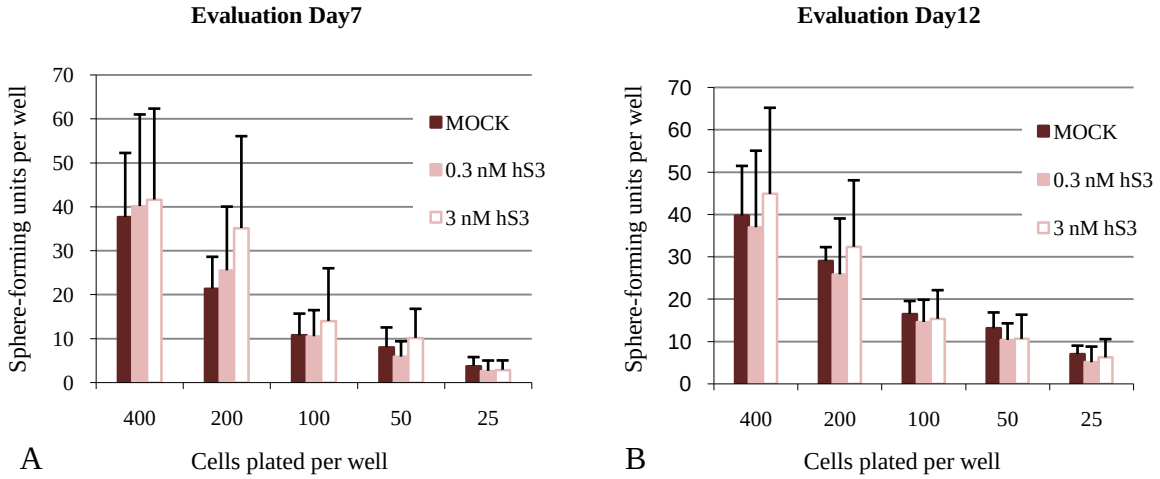

Figure 33: Clonogenic assay on neural stem cell cultures pretreated with hS3.

Treatment of neural stem cell cultures with hS3 does not potentiate self-renewal nor decreases clonogenicity. Neural precursor cells from dissociated neurospheres were plated at clonal densities in 96-well plates by limiting dilutions and cultures in growth-factor containing medium. After 7 days (A) or 12 days (B) the number of sphere forming units per well was assessed + s.d.. The addition of hS3 to neural stem cell cultures did not have any significant effect on the number of sphere-forming units (ANOVA1).

Although no loss of clonogenicity was observed in the clonogenic assays, one could not exclude changes in the multipotentiality of cells derived from hS3-treated sphere cultures. Thus, putative pretreatment-effects on the differentiation fate were analyzed. Cultures were washed with growth-factor free medium, dissociated and replated as single-cell suspensions on PLL-coated coverslips at a density of 65,000 cells per well. Cells were differentiated either in presence of low doses of EGF and β-FGF or in growth factor deprived conditions. In the latter condition higher levels of cell mortality were observed compared to reduced growth factor cultures (data not shown). Interestingly, in the growth-factor deprived paradigm, cells derived from hS3-

pretreated cultures developed faster compared to cells derived from MOCK-cultures (Figure 34A+B).

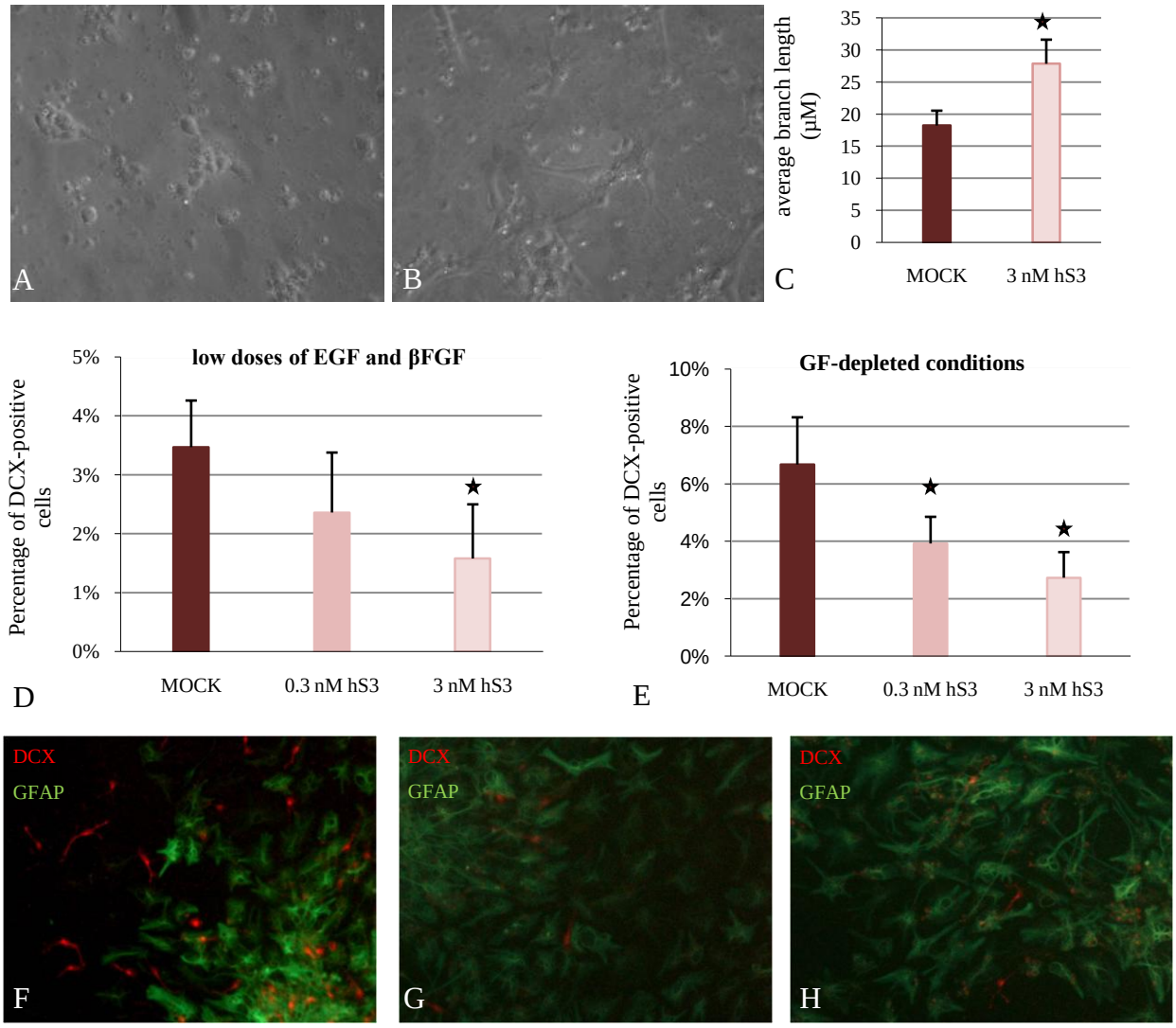

Figure 34: hS3 influences the differentiation of NSC/NPC

Neural stem and progenitor cells were grown as sphere cultures for seven days in medium containing 0, 0.3 or 3 nM of the human splice variant hS3. Spheres were dissociated and single cells were differentiated at low concentrations of β-FGF and EGF (GF-containing cultures) or depleted from growth factors (GF-free cultures).
*A-C: In the GF-free paradigm, cultures derived from spheres grown in presence of high hS3 concentrations seemed to be more mature (B) than control cultures (A) 24 h after seeding. The single cells had apparently longer branches. C: Length of branches of 100 - 300 randomly chosen neurons was measured. On average cultures derived from hS3 treated spheres had longer branches having a mean of 27.86 µM in comparison to a mean of 18.23 µM in controls. Mean branch lengths are plotted +s.d. (*p<0.05. t-test).*
*D-E: NSC cultures were fixed seven days after seeding and stained for the astroglial marker GFAP and the early neuronal marker DCX. Percentages of DCX-positive cells were evaluated and plotted +s.d. Significant less DCX-positive cells were observed in the hS3pre-treated cultures for both GF-free (A) and GF-containing conditions (B). Asterix: differences from MOCK-treated cultures (*p<0.05, ANOVA1, Bonferroni t-test).*
F-H: Representative pictures of cultures differentiated at low doses of β-FGF and EGF. F: MOCK; G: 0.3 nM hS3; H: 3 nM hS3.

This effect was quantified by measuring the length of all branches on each cell from minimum three randomly chosen fields at a 200x magnification. Cells derived from hS3 pretreated cultures possessed on average 1.5 times longer branches than cells derived from untreated cultures (Figure 34C). In addition, the average number of branches was slightly higher (data not shown).

Differentiated cultures were fixed seven days after plating with 4% PFA and stained for the early neuronal marker doublecortin and the glial marker GFAP. The proportion of DCX-positive cells in each well was determined from a minimum of four randomly chosen fields at a 200x magnification. Cultures derived from untreated spheres contained on a percentage basis more DCX-positive cells than cultures derived from hS3-treated spheres (Figure 34A+B). In both differentiation conditions, low doses of EGF and β-FGF or growth factor deprived, prior culture in 0.3 nM or 3 nM hS3 led to a reduction of approximately 30% to 60% of DCX-positive cells, respectively, compared to control cultures.

This observation may be explained by faster maturation of neuronal cells and therefore loss of the early neuronal marker doublecortin or by enhanced astroglial differentiation. To assess neural maturation, differentiated cultures generated from spheres prior grown in presence of MOCK or 3 nM hS3 were fixed after 7 days and were doublestained for the early neuronal marker DCX and the more mature neuronal marker MAP2. All cells in each condition were classified into DCX-positive immature neurons, DCX/MAP2 double-positive maturating neurons or MAP2-positive mature neurons.

The proportions of mature and immature neurons were not significantly different between cultures derived from hS3-pretreated or untreated NSC/NPC (Figure 35A+B).

In general, the percentage of immature DCX-positive cells was higher in cultures differentiated in growth factor-deprived conditions (approximately 50%) compared to cultures differentiated in presence of low doses of EGF and β-FGF (approximately 40%). In cultures derived from hS3-pretreated spheres slightly more MAP2-positive cells were counted. In both differentiation conditions approximately 7% more cells of neuronal phenotype were found to be mature with prior hS3 treatment compared to MOCK treatment. A faster maturation process after hS3 treatment may also explain the observation of longer branches 24 h after seeding.

Consistent with the previous findings, coverslips from control cultures contained approximately 40% more neuronal cells (Σ (DCX+, MAP2+, DCX/MAP2++)) than cultures prior treated with 3 nM hS3 (Figure 35C+D). These results suggest that hS3 promotes astrocyte differentiation of NSC/NPC. However, its cytoprotective property may favor also slightly faster maturation of neural cells.

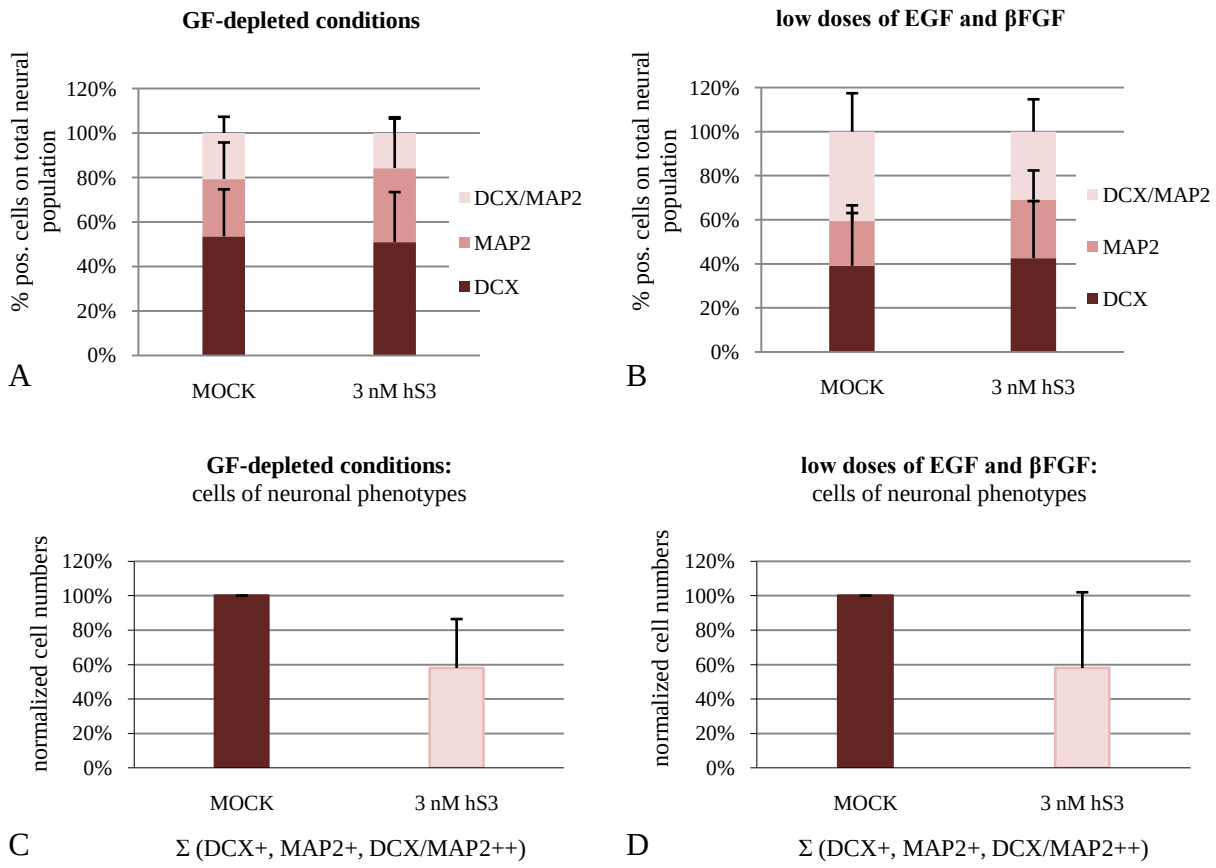

Figure 35: MAP2 and DCX staining of cultures derived from hS3 treated spheres

Neural stem and progenitor cells, prior grown in presence of MOCK or 3 nM hS3, were differentiated in presence of low doses of β-FGF and EGF or in growth factor depleted conditions. Cultures were fixed 7 days after plating and stained for the neuronal markers DCX (immature neurons) and MAP2 (mature neurons).
A+B: Neural cells were classified according to marker expression into immature (DCX), maturing (double-positive) or mature (MAP2) neurons. The mean percentage of each cell type was plotted + s.d. No significant differences due to prior treatment were found in both differentiation paradigms (n=3 each).
C+D: In both differentiation paradigms prior hS3-treatment led to a significant decrease in total numbers of cells having a neural phenotype. Mean normalized cell numbers were plotted +s.d. Significance was not reached in three single experiments, respectively.

Other gliogenesis regulating factors, such as LIF or CNTF are known to induce expression of GFAP protein and mRNA in precursor cells (Bonni *et al.*, 1997). Thus, GFAP mRNA expression was determined in sphere cultures after hS3 treatment. 3 nM hS3 induced the expression of GFAP mRNA within 4 h exposure of NSC/NPC spheres to the recombinant purified protein (Figure 36). Compared to control cells the relative GFAP mRNA expression was found to be upregulated by a factor of 1.3. A single experiment with a prolonged exposure of 7 h suggested that this induction may be only transient.

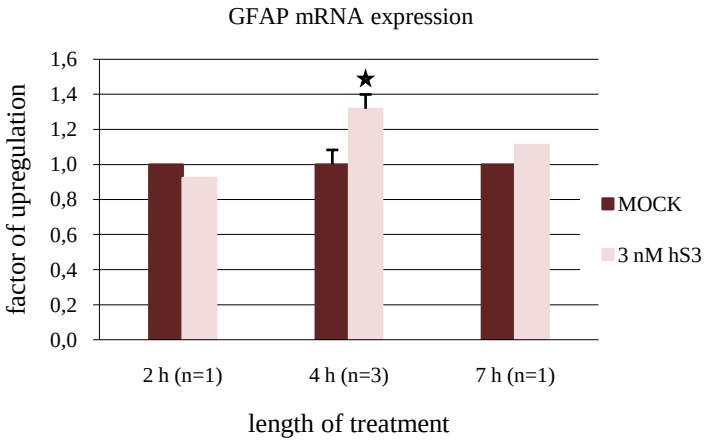

Figure 36: NSC/NPC exposure to hS3 enhances GFAP mRNA expression

*Spheres were treated with 3 nM hS3 for 2 h, 4 h or 7 h. RNA was extracted and cDNA was generated according to standard protocols. GFAP mRNA levels were determined in a Light cycler based real time PCR assay and standardized to β-actin mRNA levels amplified from the same sample. Three independent experiments showed significant upregulation in GFAP mRNA levels after a 4 h exposure to hS3 (data plotted +s.d.). Asterix: difference from MOCK-cells (*p<0.05; t-test).*

In summary, hS3 enhances survival of NSC/NPC and promotes the presence of astrocytes over neurons.

4.8.2 Human A-helix derived peptide P16 protects neural stem and progenitor cells

Previous experiments suggested the human A-helix derived peptide P16 to have a weak protective effect on NSC/NPC upon growth factor withdrawal. To confirm this finding, experiments were repeated with growing concentrations of the peptide from 0 pM (co) to 100,000 pM. As predicted, a dose-dependent protective effect of P16 was observed on NSC/NPC. Cell death was significantly decreased with doses beyond 10,000 pM (Figure 37).

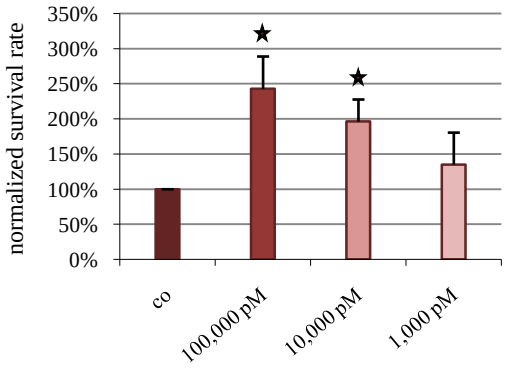

Figure 37: Human A-helix derived peptide P16 protects NSC/NPC from growth factor withdrawal in a dose-dependent manner

*NSCs were differentiated in absence of β-FGF and EGF but in presence of growing concentrations of the peptide P16.Cultures were evaluated 24 h after seeding. The number of living cells counted in control cultures was considered as 100% survival. Normalized survival rates were plotted +s.d. Asterix: differences from control cultures (co) (*p<0.05; ANOVA1, Bonferroni t-test).*

The next question was, whether the peptide had a proliferative effect on NSC/NPC cultures as observed for hS3. Thus, single cell suspensions of NSC/NPC were seeded at 3500 cells/cm^2 in T-25 flasks (Corning) and grown in the presence of β-FGF, EGF and 0 pM (co) or 100,000 pM peptide P16 for seven days. Similar to previous experiments in presence of 3 nM hS3, P16-treatment enhanced total cell numbers up to 150%. Due to high variations between experiments statistical significance was not achieved in four independent trials (Figure 38A).

In previous experiments with 1000 pM P16, differentiation patterns of NSC/NPC were not found to be influenced by the peptide. However, possible effects on cell fate could not be excluded for high doses of the peptide. Thus, it was intended to analyze the possible effects resulting from prior treatment with high doses of P16. Therefore cells grown for 7 days in presence of 0 or 100,000 pM P16 were dissociated and seeded at 65,000 cells/well onto PLL-coated coverslips in NSC-medium containing low concentrations of EGF and β-FGF. Cultures were fixed after 6 days with 4% PFA and stained for the neuronal marker DCX and the glial marker GFAP. In contrast to prior treatment with hS3, no differences in the proportion of DCX positive cells were observed between cultures derived from cells grown in presence or absence of the peptide (Figure 38B).

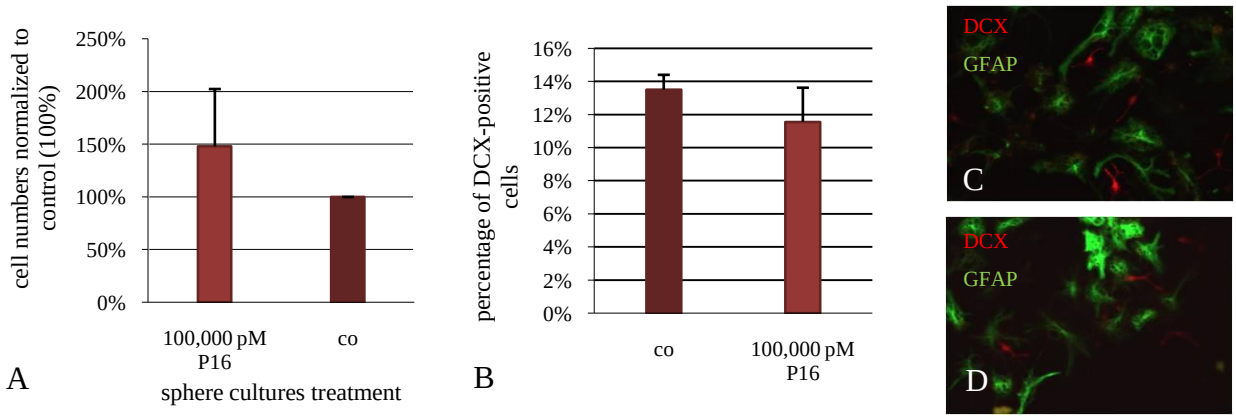

Figure 38: Effects of peptide P16 on NSC/NPC cultures

A: Neural stem and progenitor cells were grown for seven days in presence of 0 (co) or 100,000 pM of the A-helix derived peptide P16. Spheres were harvested, dissociated and cell numbers of total sphere cultures were evaluated. Four individual experiments were pooled. Absolute cell numbers in control cultures (co) were considered as 100% and plotted + s.d. In cultures grown in presence of high concentrations of P16 we observed a trend to higher cell numbers.
B-D: Single cells derived from spheres were differentiated in medium containing low concentrations of β-FGF and EGF. Cultures were fixed after 7 days and stained for the neuronal marker DCX and the astroglial marker GFAP. The percentage of DCX-positive cells in the total cell population was not found to be influenced by P16. Mean values from three independent experiments were plotted + s.d. (B). C-D: Representative pictures of slides. C = 0 pM P16; D = 100,000 pM P16.

As P16 seemed not to promote astrocytic differentiation from NSC/NPC a semiquantitative RT-PCR was performed for GFAP mRNA. As expected and in clear contrast to previous findings for

hS3, GFAP mRNA-expression after 4 h exposure of sphere cultures to 100,000 pM P16 remained unchanged compared to levels in control cultures (Figure 39).

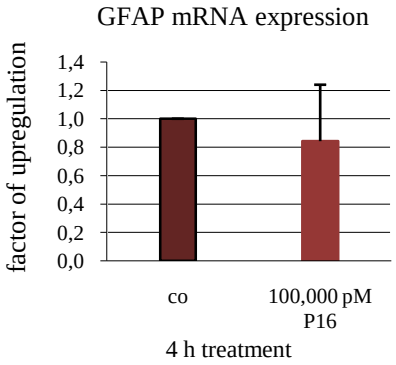

Figure 39: Light cycler real time PCR experiment for 4 h treatment of spheres with peptide P16

Spheres were exposed for 4 h to 100,000 pM peptide P16. RNA was extracted and cDNA was generated according to standard protocols. GFAP mRNA levels were determined in a Light cycler based real time PCR assay and standardized to β-actin mRNA levels amplified from the same sample. Four independent experiments showed no significant changes in GFAP mRNA levels between treatment and control group.

In summary, the peptide P16 seems to act as an antiapoptotic factor in NSC/NPC. However, a differentiation effect on NSC can be excluded from our experiments.

4.8.3 EPO isoforms have no colony-stimulating activity on murine HPC

Many cytokines are pleiotropic with a wide spectrum of biological activities. Frequently they affect the action of other cytokines in an additive, synergistic or antagonistic manner. As the EPO variants are derived from a hematopoietic factor, this study intended to analyze possible effects on hematopoietic stem and progenitor cells (HSC/HPC) apart from erythropoiesis. The study was again focused on hEPO, the human splice form hS3 and the human A-helix derived peptide P16.

To reveal potential colony stimulating activities of hEPO, hS3 and P16, their capacity to induce hematopoietic progenitor cells of murine bone marrow to develop colonies of differentiated cells was tested. The previous erythropoiesis experiments (see chapter 3.2.3 Erythroid Colony formation assay) were designed to solely support the formation of CFU-E in the presence of erythropoietin. Growth of other types of colonies was not supported due to the absence of appropriate hematopoietic stimulating factors. In the presence of the hematopoietic stimulating factors IL-3 (interleukin-3) and SCF (stem cell factor) one can observe the formation of colonies of type CFU-G (colony forming unit granulocyte), CFU-M (colony forming unit macrophage) or CFU-GM (colony forming unit granulocyte and macrophage) as both cytokines act on the survival of hematopoietic progenitor cells. Since many cytokines do not show direct colony-

stimulating activity as a single factor, it was intended to perform these assays in combination with other cytokines, namely in presence of IL-3 or IL-3 and SCF.

Freshly prepared murine bone marrow was plated at low density in presence of the EPO isoforms hEPO (3 nM), hS3 (3 nM) or P16 (100 nM) and either IL-3 or IL-3 and SCF. Plates were evaluated after 48 h for CFU-E formation and after seven days for myeloid colony formation namely CFU-G, CFU-GM and CFU-M.

As expected from erythropoiesis experiments significant formation of CFU-E was only observed in plates containing hEPO (Figure 41 A+B).

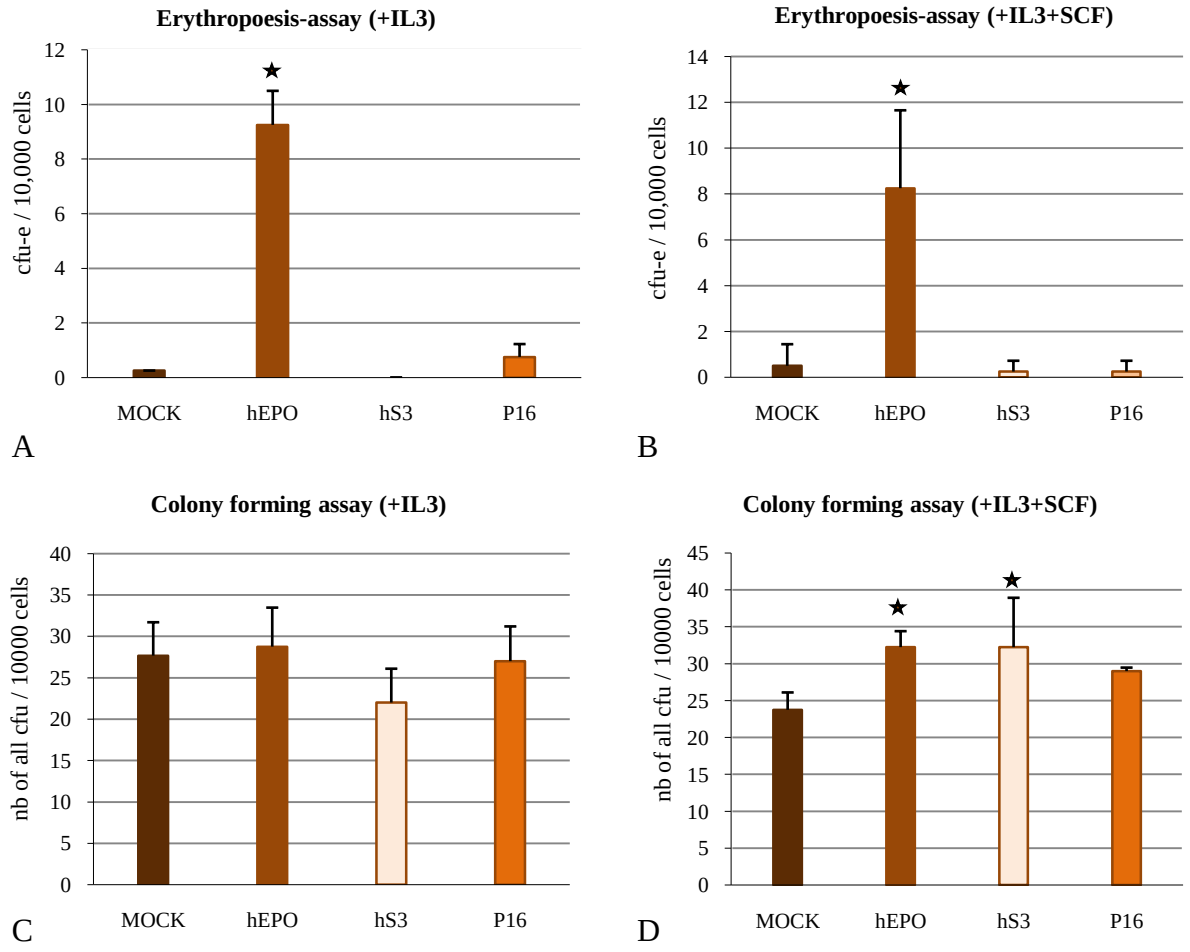

Figure 40: Influence of IL-3 or IL-3+SCF in combination with vEPO on the formation of CFU-E and myeloid CFU

Whole bone marrow was prepared and seeded at a concentration of 10,000 cells/ml in serum-free methylcellulose enriched with either 20 ng/ml IL-3 (A and C) or 20 ng/ml IL-3 and 50 ng/ml SCF (B and D) respectively. EPO isoforms were added at concentrations of 3nM for hEPO and hS3 or 100nM for the peptide P16. MOCK-medium was added in equal volumes in control cultures.
*A and B: Numbers of colonies of type CFU-E two days after plating (+s.d.). Formation of CFU-E was only observed in presence of hEPO. Asterix: differences from MOCK-treatment (*p<0.05, ANOVA1).*
*C and D: Numbers of myeloid colonies seven days after plating (+s.d.). No significant differences in numbers of CFU were observed in the IL-3 experiment. In the IL-3+SCF experiment, significant higher numbers of CFU per 10,000 plated cells were observed in presence of hS3 and hEPO. Asterix: differences from MOCK-treatment (*p<0.05, ANOVA1).*

Formation of approximately 10 colonies per 10,000 plated cells was counted in presence of IL-3 + hEPO and approximately 8 colonies per 10,000 cells in presence of IL-3 + SCF + hEPO. In respect of types of colonies evaluated at seven days after plating no differences were observed in the tested conditions. Colonies were mainly identified as CFU-GM (granulocyte-macrophage colonies) or CFU-G (granulocyte colonies) from shape and size of the single cells. Additional identification strategies were not performed. Numbers of CFU were significantly enhanced in cultures treated with SCF + IL-3 + hEPO or SCF + IL-3 + hS3 compared to control cultures treated with SCF + IL-3. The combination of hEPO or hS3 with only IL-3 had no effect on numbers of CFU. Thus, the EPO isoforms hS3 and P16 were supposed to have no colony-stimulating activity as single factors or in combination with IL-3. Only hEPO was found to have an erythropoiesis-stimulating activity. In presence of IL-3 and SCF, hEPO and hS3 may have a positive synergistic effect on myeloid colony formation of type CFU-G and CFU-GM.

4.8.4 EPO isoforms support survival of HPC in *ex vivo* cultures

Hematopoietic progenitor cells (HPC) progressively undergo apoptotic cell death in the absence of appropriate growth factors. To study putative pro-survival effects of the EPO isoforms on HPC, liquid *ex vivo* cultures were established from murine bone marrow. Liquid cultures consist of adherent cell populations containing phagocytic mononuclear cells, epithelial cells, and giant fat cells, and non-adherent populations containing the hematopoietic stem cell population (Dexter *et al.*, 1977). When murine bone marrow cells are incubated *in vitro* in absence of appropriate cytokines, a gradual decline of cell numbers and CFU-activity occurs (Spivak *et al.*, 1985).

Freshly prepared bone marrow cells were cultivated in absence of cytokines but in presence of the EPO isoforms hEPO (3 nM), hS3 (3 nM) or P16 (100 nM). After 2 days in culture survival of progenitor cells was analyzed using a methylcellulose based colony-formation assay. Thus, non-adherent cells were harvested from liquid bone marrow cultures and seeded at low density on methylcellulose containing IL-3, IL-6 and SCF, the factors needed for the formation of CFU-G, CFU-M and CFU-GM. (Figure 41A)

When counting non-adherent cell populations after two days in culture, no significant differences in cell numbers were observed between the treatment conditions (Figure 41B).

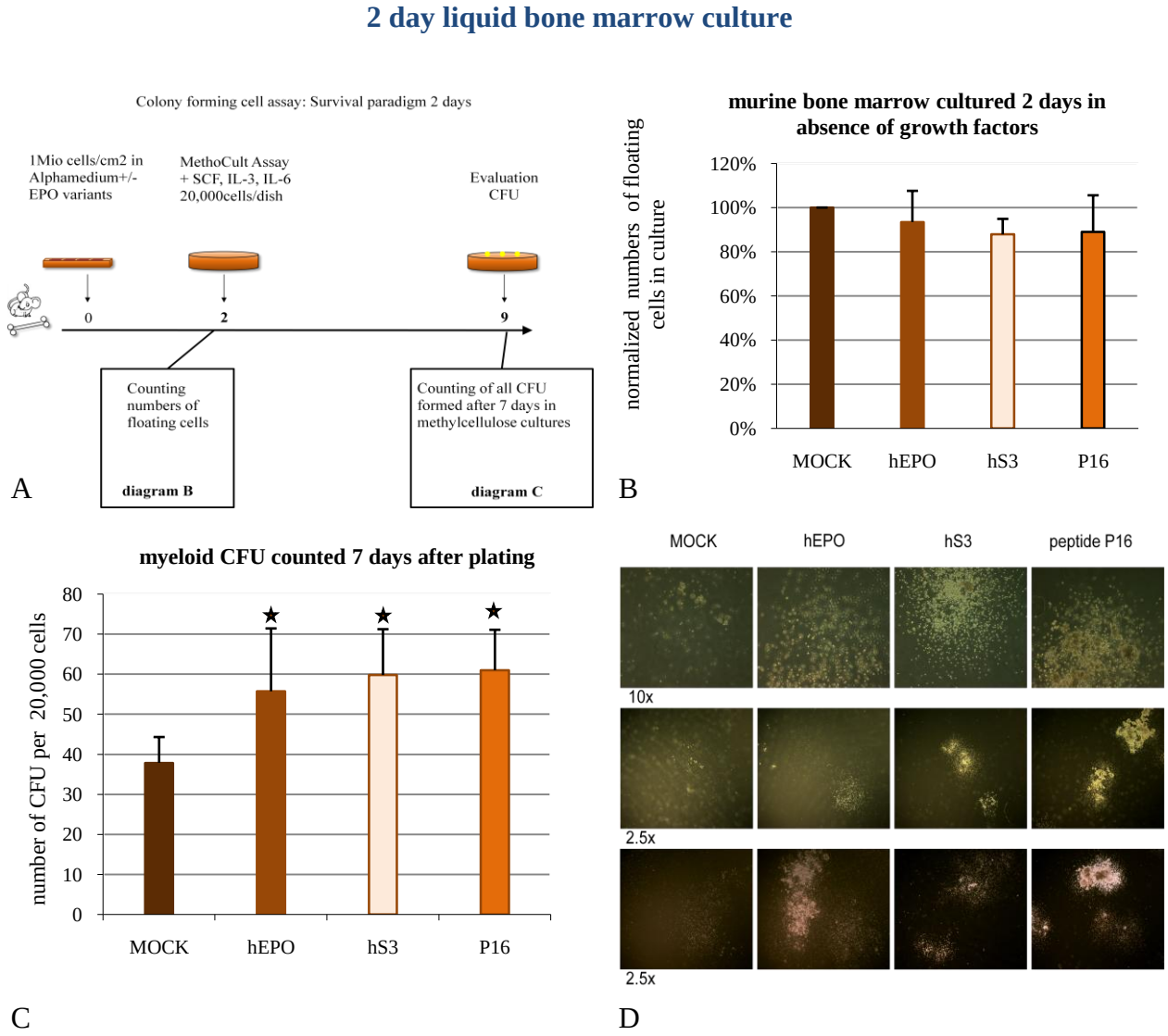

Figure 41: EPO isoforms enhance survival of HPC in 2 day liquid bone marrow cultures

A: Whole murine bone marrow was cultivated for 48 h in absence of the cytokines IL-3, IL-6 and SCF but in presence of 3nM hEPO or hS3 or 100 nM peptide P16 at the density of $4*10^6$ cells per well (4 cm^2). Non-adherent cells containing the hematopoietic stem and progenitor cells were harvested and seeded at a density of 20,000 cells in 1 ml methylcellulose containing cytokines IL-3, IL-6 and SCF. Colonies were evaluated at DIV7.
B: Number of non-adherent cells containing the hematopoietic stem cell population 48 h after cultivation in absence of cytokines IL-3, IL-6 and SCF but in presence of 3 nM hEPO or hS3 or 100 nM peptide P16. Cell numbers in MOCK conditions were considered 100%. Normalized cell numbers were plotted +s.d.
*C: 20,000 cells of the non-adherent HSC-containing bone marrow population were seeded in methylcellulose supplemented with IL-3, IL-6 and SCF. Colonies formed after 7 days were counted. Data from five individual experiments were pooled and plotted +s.d. Asterix: differences from MOCK-condition (*p<0.05, ANOVA1, Bonferroni t-test).*
D: In 100x magnification one can observe bigger colonies in plates seeded with hematopoietic progenitor cells prior cultivated in presence of EPO isoforms. No differences in type of colonies were sighted. All colonies were of type CFU-G or CFU-GM as determined from type and size of single cells in 25x magnification.

Equal numbers of non-adherent cells were seeded in methylcellulose for colony-forming assays and the number of formed colonies was evaluated after 7 days. Importantly, significantly higher numbers of colonies were counted in dishes containing cells prior cultivated in presence of

hEPO, hS3 or P16. In plates containing cells prior cultivated in MOCK-medium 38 colonies were formed on average, whereas in plates containing cells prior cultivated in presence of EPO isoforms around 55 colonies were counted, respectively. Among the EPO isoforms hEPO, hS3 and P16, no differences concerning colony numbers were observed; hEPO treatment was presumably slightly less effective than treatment with the smaller EPO variants (Figure 41C). Regarding type of colonies no differences were observed between the treatment groups. Colonies were mainly identified as CFU-GM (granulocyte-macrophage colonies) or CFU-G (granulocyte colonies) from shape and size of the single cells. Notably differences were observed in the mean size of the colonies. In general, colonies formed in plates seeded with hEPO, hS3 or P16-pretreated cells grew larger in size than on control plates (Figure 41D). This data suggest that the EPO isoforms provide better survival of myeloid progenitor cells and have a positive effect on conservation of the proliferative capacity of HPC.

To gauge the effectiveness of the EPO variants as protective agents on this cell population the same experimental setup was repeated with a prolonged starving period (Figure 42A). After 5 days in growth factor depleted medium containing the EPO variants hEPO (3 nM), hS3 (3 nM) or P16 (100 nM), non-adherent cells were harvested and cell numbers were evaluated. As expected from literature, cell numbers had dramatically declined from approximately $1*10^6$ cells at day 2 to approximately $2*10^5$ cells at day 5. Interestingly, significantly more cells were counted in hEPO-treated cultures, compared to hS3-, P16- and MOCK-treated cultures: This was supposed to be due to erythroblasts surviving in presence of hEPO (Figure 42B).

Importantly, when plating equal numbers of cells on growth factor-free methylcellulose supplemented with 200 U/l rhEPO, the emergence of colonies of type CFU-E was only observed on plates seeded with cells grown in hEPO-containing medium (Figure 42C). This indicates that the higher number of non-adherent cells after the five days starvation period in hEPO containing liquid bone marrow cultures is due to survival and proliferation of erythroid progenitor cells, which are not surviving in MOCK, hS3 and P16-conditions.

To study survival of hematopoietic progenitor cells types, 20,000 cells/dish were plated in methylcellulose according to the experimental protocol from previous experiments. Colony formation was evaluated after 7 days. Consistent with the previous experiments, more myeloid colonies were found in cultures derived from bone marrow grown in presence of hEPO, hS3 or P16 compared to control cultures. However, the peptide P16 performed much better in this setup than hS3 and hEPO. Nearly 50% more colonies emerged from cells cultivated in presence of P16 than from cells prior cultivated in presence of hS3 or hEPO. In comparison to control dishes the number of myeloid CFUs was nearly doubled (Figure 42D).

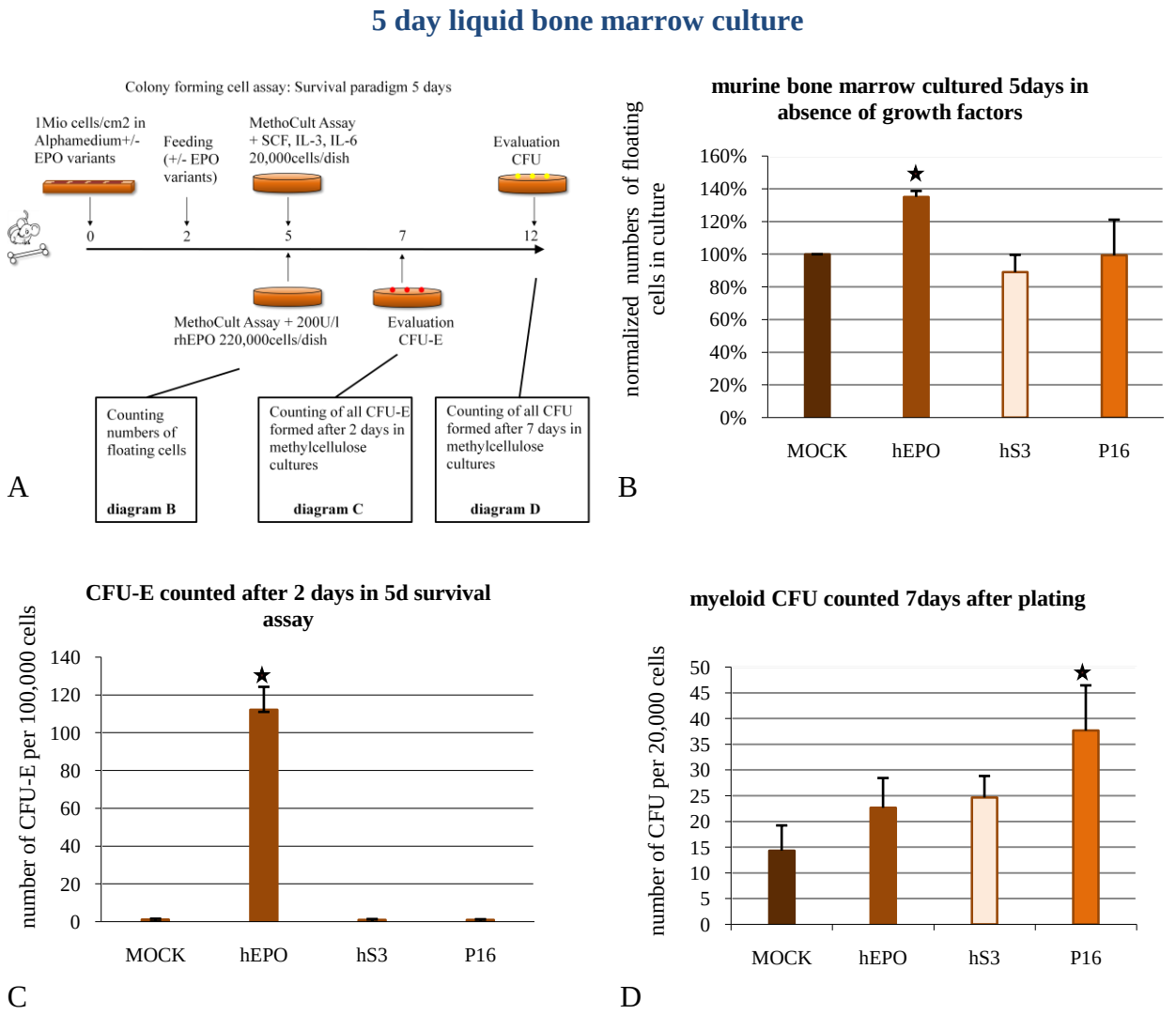

Figure 42: P16 is most effective in enhancing survival of HPC in 5 day liquid bone marrow cultures

A: Whole murine bone marrow was cultivated for 5 days in absence of the cytokines IL-3, IL-6 and SCF but in presence of 3 nM hEPO or hS3 or 100 nM peptide P16 at the density of $4*10^6$ cells per well (4 cm^2). Non-adherent cells containing the hematopoietic stem and progenitor cells were harvested and seeded at a density of 20,000 cells in 1 ml methylcellulose containing the cytokines IL-3, IL-6 and SCF or at a density of 220,000 cells in 2 ml methylcellulose containing 200 U/l rhEPO (Roche).
*B: Numbers of non-adherent cells after 5 days in liquid bone marrow culture. Cell numbers in MOCK conditions were considered 100%. Data from three individual experiments were pooled and plotted + s.d. Asterix: differences from MOCK-condition (*p<0.001, t-test).*
*C: 220,000 cells of the non-adherent HSC-containing bone marrow population were seeded in serum-free methylcellulose containing 200 U/l rhEPO (Roche). Data from four independent experiments was plotted + s.d. Asterix: differences from MOCK-condition (*p<0.05. t-test).*
*D: 20,000 cells of the non-adherent HSC-containing bone marrow population were seeded in methylcellulose supplemented with IL-3, IL-6 and SCF. Colonies formed after 7 DIV were counted. Data from five individual experiments were pooled and plotted + s.d. Asterix: differences from MOCK-condition (*p<0.05, ANOVA1, Bonferroni t-test).*

Again no differences in type of colonies were observed in the four conditions but colonies grown from P16-treated cultures were on average larger and denser. The smallest colonies were again found in the MOCK condition (Figure 43).

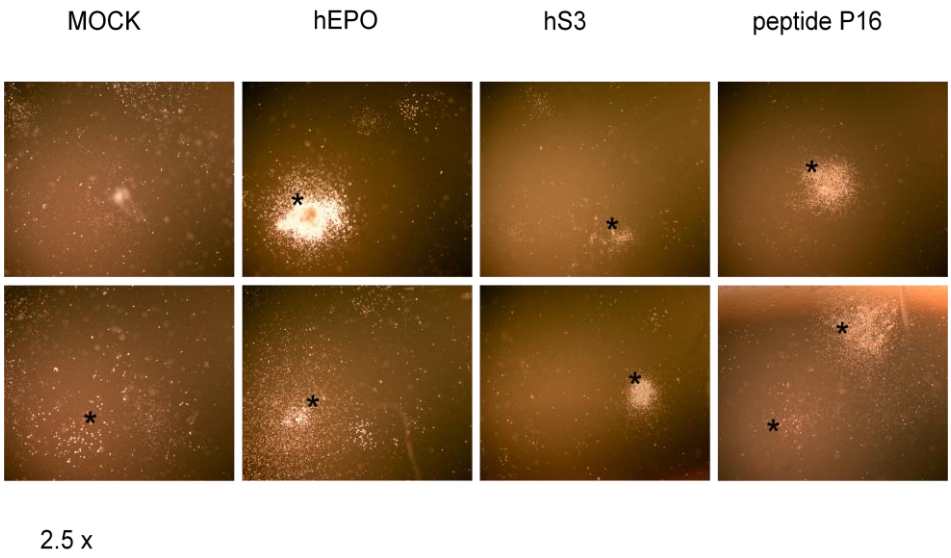

Figure 43: Colonies grown from P16-treated cultures are on average larger and denser

Representative pictures of methylcellulose-cultures. In 25x magnification one can observe bigger colonies in plates seeded with hEPO, hS3 or P16 pretreated cells. No differences in type of colonies were observed. All colonies were of type CFU-G or CFU-GM as determined from type and size of single cells.=colony*

4.8.5 Effects of EPO isoforms on murine mesenchymal stem cells (mMSC)

Mesenchymal stem cells (MSC) can be easily isolated from bone marrow of patients and exhibit enormous plasticity. In addition to their role in supporting HSC, they give rise to bone cells, fat cells, muscles, neural cells, liver cells, etc. Furthermore MSC have immunomodulatory functions, e.g. by reducing the incidence and severity of graft-versus-host disease during allogeneic transplantations. The ability to scale up hMSC production will be critical for any viable cell therapy.

In this study the focus was on putative prosurvival effects of the EPO isoforms hEPO, hS3 and P16 on murine MSC. Studies have shown that MSC require a minimum of 10% FCS in the culture medium (Stute *et al.*, 2004). Thus, murine MSC were grown either in high (20%) or in low (0.5%) serum conditions in presence or absence of EPO isoforms at low cell densities.

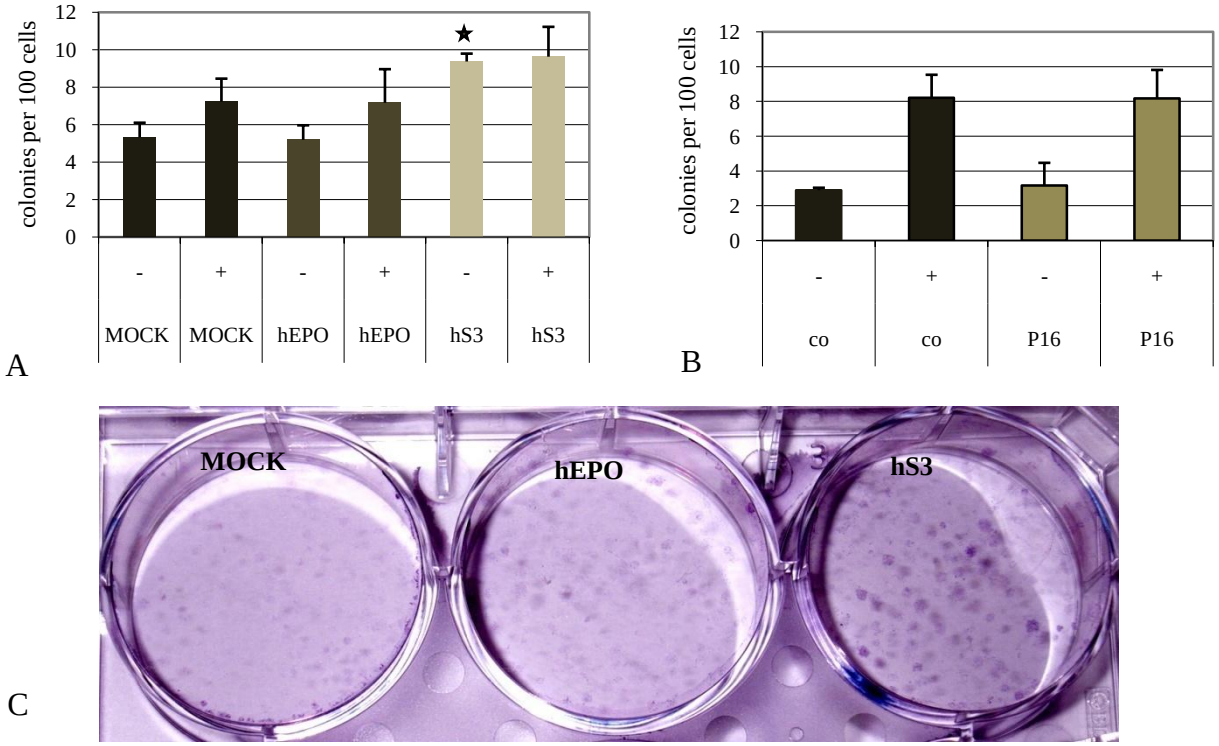

Figure 44: The splice variant hS3 mediates survival effects on murine mesenchymal stem cells.
mMSC were seeded at low density in high-serum-medium (20% serum, '+') or low-serum medium (0.5% serum '-'). EPO and EPO variants were added at final concentrations of 3 nM for hEPO and hS3 or 100nM for peptide P16. After 6 days for high-serum plates or 8 days for low-serum plates formed colonies were stained with crystal violet Only colonies were counted having a diameter of min. 1mm.
*A: mMSC plated in presence or absence of 3 nM hEPO or hS3, respectively. When comparing the high-serum groups no significant differences were observed (p=0.272). In the low-serum group hS3-treated wells contained significantly more colonies of defined size. Data is plotted + s.d Asterix: differences compared to MOCK-treatment (*p<0.050, ANOVA1, Bonferroni t-test).*
B: mMSC plated in presence or absence of 100 nM P16. No significant differences were observed between high-serum plates (t-test: p=0.983) or low-serum plates (t-test: p=0.788).
C: Representative pictures of mMSC seeded at low density in low-serum medium in presence or absence of 3 nM hEPO or hS3, respectively. Colonies stained after 8 days in culture with crystal violet.

When colonies reached confluence, dishes were stained with crystal violet and numbers of colonies having a diameter of minimum 1 mm were evaluated in each condition. In low serum conditions significantly higher numbers of colonies were observed when cells were grown in presence of 3 nM hS3 (Figure 44A). Number of colonies was nearly doubled compared to cultures containing 3 nM hEPO or equivalent amounts of MOCK-medium (Figure 44A). In conditions containing 20% serum no differences were observed between treatment groups. The peptide P16 had no positive effects on colony formation compared to PBS-containing control plates, neither in high (20% serum) nor in low (0.5% serum) serum conditions (Figure 44B). Assuming that the failure of the peptide P16 to promote colony formation may result from the instability of the peptide *in vitro*, the experimental protocol was changed to a feeding paradigm, where the medium was completely replaced after two days to fresh medium containing 0.5% or 20% serum and 100 nM P16 in the peptide treatment group (Figure 45A+B). In this feeding experiment a positive effect of the peptide on cell survival was observed in the low-serum condition, leading to nearly two-fold higher colony numbers compared to control wells. In six independent experiments statistically significance was not achieved (p=0.247) due to high variances in number of formed colonies between the individual experiments.

However, the experimental results indicate that the human EPO splice variant hS3, and presumably also the peptide P16, are survival factors for murine MSC in nutrient-deficient conditions.

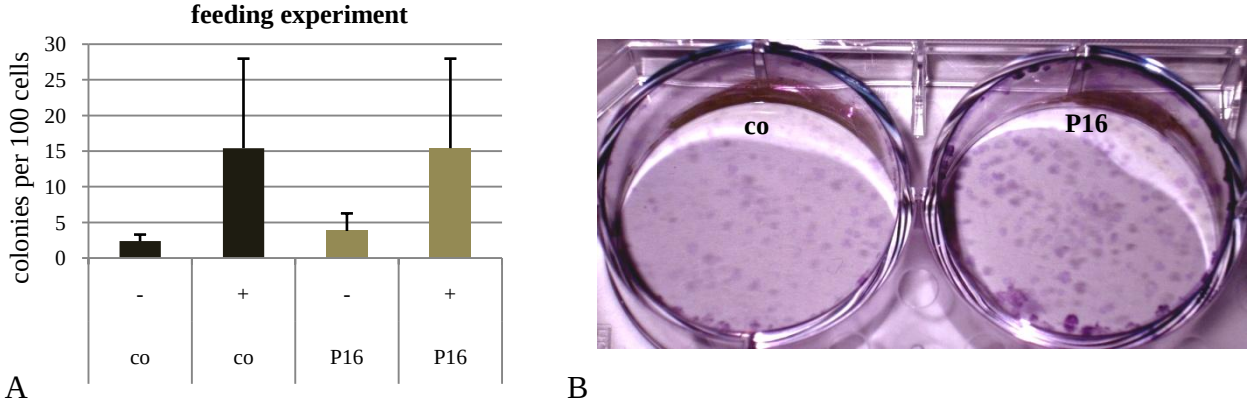

Figure 45: P16 provides survival effects on murine mesenchymal stem cells in a feeding paradigm.

mMSC were seeded at low density in low-serum medium (0.5% serum, '-') or high-serum medium (20%, '+'). Peptide P16 was added at a final concentrations of 100nM. After 2 days medium was replaced to fresh medium containing 0.5% serum or 20% serum respectively and 100 nM peptide P16 in the peptide treatment group.
A: Colonies were stained with crystal violet. Only colonies having a diameter of minimum 1 mm were counted Data from six independent experiments was plotted +s.d.
B: Representative pictures of mMSC seeded at low density in low-serum medium in presence or absence of 100 nM P16. Colonies were stained after 8 days with crystal violet.

4.9 Receptor characterization

4.9.1 Analysis of EPO-A-helix-muteins

In the present work, several murine and human EPO derivatives have been isolated, which have neuroprotective but no erythropoietic activities. Thus, we assumed the EPO derivatives not to bind the classical $(EPOR)_2$.

To test $(EPOR)_2$-binding of EPO isoforms, we generated human erythropoietin A-helix muteins comprising aminoacid exchanges at position 14. The A-helix was previously shown to be the functionally important domain for the neuroprotective character of EPO and to be shared by all EPO variants (see 4.4.3 Derivatives of the A-helix of hEPO are sufficient to induce neuroprotection). Replacement of Arg14 to Ala14 or Glu14 was demonstrated to generate almost inactive EPO muteins (Wen *et al.*, 1994). Erythropoietin A-helix muteins containing either a neutral (MutA) or an acidic amino acid exchange (MutE) at position 14 were expressed in HEK293 cells. Supernatants of transfected HEK293 cultures, containing the secreted A-helix muteins, were used for preconditioning of rat primary cortex neurons in our OGD-model. Supernatants of HEK293 cells transfected with hEPO, hS3 or MOCK-constructs were used as controls. LDH release was measured 24 h after reoxygenation as a marker of neuronal cell death. Interestingly, the acidic amino acid exchange at position 14 was not able to destroy the neuroprotective potential of the A-helix in our OGD model in six independent experiments (Figure 46).

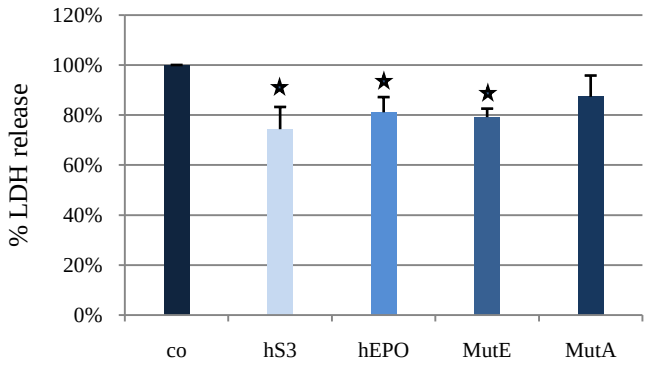

Figure 46: Neuroprotection mediated by A-helix mutants

Primary cortical neurons were pretreated for 48h with equal volumes of HEK293 supernatants, containing hS3, hEPO, MutE mutein (amino acid exchange at position 14 to Glu) or Mut A mutein (amino acid exchange at position 14 to Ala), respectively. Control cultures were supplemented with medium of MOCK-transfected HEK293 cells (co). OGD was applied for 120 min. 24 h LDH release after reoxygenation was determined as marker of cell death. LDH release in control cultures was considered 100%. Normalized LDH release was plotted + s.d. In six independent experiments, the neuroprotective potential of the A-helix due was not found to be abolished due to the acidic amino acid exchange. The A-helix mutant containing the neutral amino acid exchange did not provide significant but strong tendencies to neuroprotection. Asterix: differences to control cultures (p<0.05; ANOVA1).*

The MutE mutein mediated significant neuroprotective effects equivalent to hS3 and hEPO. The MutA mutein, containing a neutral amino acid exchange, showed also neuroprotective potential even though not to statistical significance. These results suggest that the $(EPOR)_2$ may not mediate the neuroprotective effects of the A-helix.

4.9.2 *In silico* prediction of $(EPOR)_2$-binding of EPO splice variants

A crystal structure of human erythropoietin complexed to its receptor (Syed *et al.*, 1998) was used to predict the effects of protein domain deletions in the erythropoietin splice variants. The murine EPO-$(EPOR)_2$ complex is supposed to be very similar to the human model. The crystal structure '1eer.pdb' used in the following analysis has a resolution of 1.9 angstroms. Analysis was performed with help of the Swiss-Pdb Viewer from EMBL (version 3.7).

In the EPO-$(EPOR)_2$ model, the protein domain deleted in the human splice variant hS3 was highlighted in orange and the A helix was highlighted in green (Figure 47A). The labeling showed that the amino acids deleted in hS3 form the interaction site with one of the EPOR chains in the EPO-$(EPOR)_2$ complex, whereas the helix A stained in green contains the most relevant amino acids for interaction with the second EPOR chain. Thus, in the putative hS3-$(EPOR)_2$ complex, hS3 is predicted to lose contact sites to one EPOR chain due to the deletion of the AB loop. In the putative model of the murine splice variant mS complexed to the $(EPOR)_2$, the murine splice variant seems to completely lose contact to the second receptor chain (Figure 47B). In summary, one can deduce from the *in silico* analysis that in all likelihood the EPO splice variants do not mediate their effects via the classical $(EPOR)_2$.

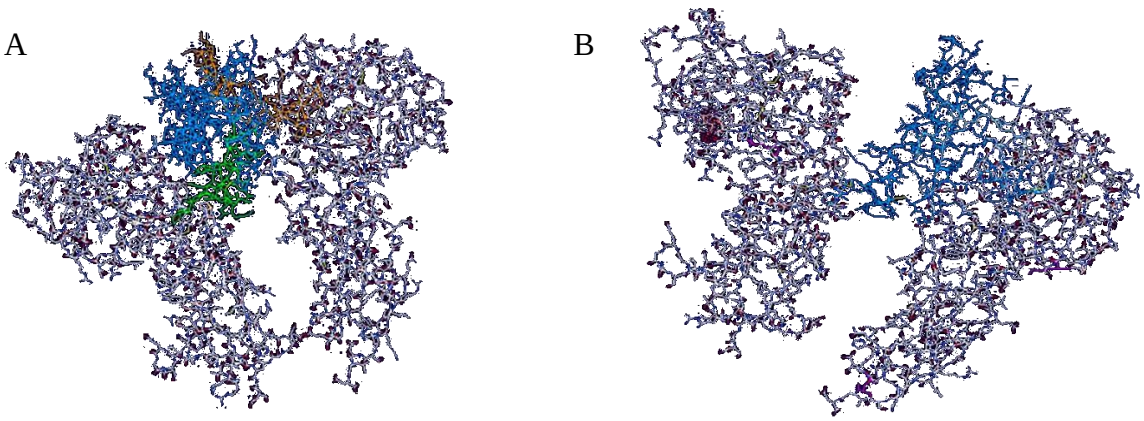

Figure 47: Crystal structure of human erythropoietin complexed to its receptor

A: Visualization of the human EPO-$(EPOR)_2$ complex. The AB-loop is highlighted in orange and the A helix is highlighted in green
B: Model of a putative mS-$(EPOR)_2$ complex derived from the crystal structure of human erythropoietin complexed to its receptor. The protein domains deleted in mS were hidden in the EPO-$(EPOR)_2$ complex.

4.9.3 BaF3 experiments: survival and proliferation assays

Putative $(EPOR)_2$ activation by EPO splice variants was tested exemplarily for the human splice form hS3 in a cell-based assay system. The BaF3 cell line is an interleukin 3 (IL-3)-dependent murine pro B cell line established from peripheral blood. BaF3/EPOR cells stably transfected with the EPOR were generously provided from PD Dr. rer. nat. Ursula Klingmüller from the Systems Biology of Signal Transduction lab at the Deutsches Krebsforschungszentrum Heidelberg. In contrast to wild-type BaF3 (BaF3 wt), BaF3/EPOR cells manifold overexpress EPOR as shown by real time PCR (Figure 48A). BaF3 cells also highly express the β-common chain (βcC) which is the signal transduction chain of the IL-3 receptor.

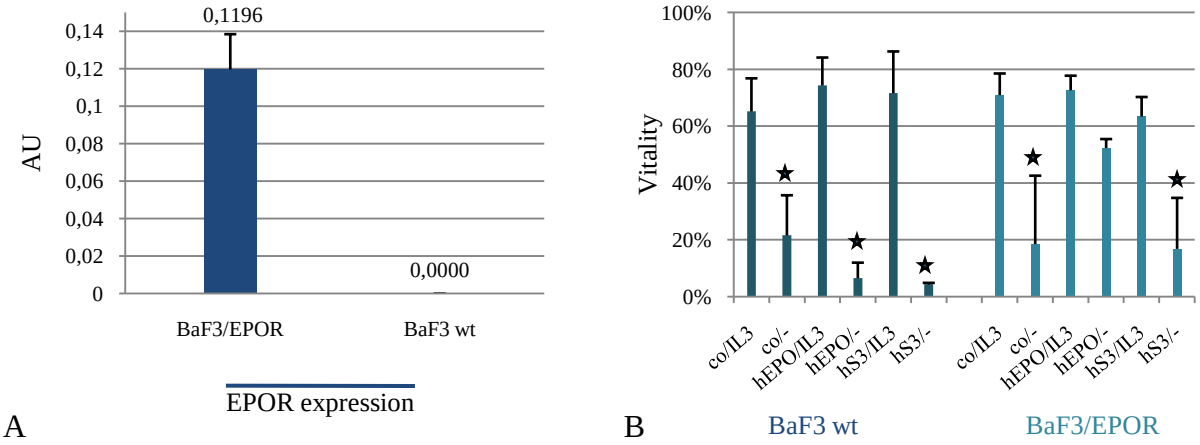

Figure 48: Functional assays on BaF3 cell lines

A: mRNA expression levels of EPOR using Real time PCR in non-transfected and EPOR-transfected BaF3 cell lines. Arbitrary units (AU) were obtained by comparison of the crossing-points of the EPOR-PCR with crossing-points of the beta-actin-PCR. EPOR transfected cells show significantly EPOR mRNA expression whereas the non-transfected cells do not express EPOR mRNA at all. Data are presented + s.d.
*B: Vitality assays were performed in BaF3 wt and BaF3/EPOR cells grown in presence or absence of EPO variants and/or IL-3. Vitality of BaF3 wt and BaF3/EPOR cultures was strongly declined in absence of IL-3. Vitality in IL-3 depleted cultures was only retained in EPOR overexpressing cells after addition of hEPO. Data from three independent experiments was pooled and plotted +s.d. Asterix: differences to co/IL-3-cultures (*p<0.05, ANOVA1, Bonferonni).*

BaF3/EPOR cells have been shown to survive and proliferate in absence of IL-3 when rhEPO was added in a dose-dependent manner (Jubinsky *et al.*, 1997). Furthermore, experimental evidence has been provided for functional interaction of EPOR and βcC in BaF3/EPOR cells (Jubinsky *et al.*, 1997). Therefore we chose this assay system to test $(EPOR)_2$ activation by recombinant purified hEPO and hS3 expressed in HEK293 cells. Vitality of IL-3 depleted BaF3/EPOR cultures grown in presence of EPO variants was used as a marker for $(EPOR)_2$ activation. Cells were plated in 96 well plates either in presence or absence of IL-3 and hEPO (300 pM) or hS3 (300 pM), respectively. Vitality of the cultures was analyzed 48 h after the onset of the experiment and calculated as percentage of healthy living cells to total number of

cells. Healthy round-shaped cells could easily be differentiated from smaller wrinkled apoptotic cells using microscopic techniques. Vitality of cells grown in presence of IL-3 was found to be independent from hEPO- or hS3-addition (Figure 48B). As expected, survival of BaF3/EPOR cells in absence of IL-3 was partially restored in presence of hEPO whereas hS3 had no effect (Figure 48B). In wild-type BaF3 cells neither hEPO nor hS3 provided any survival effects.
Our results suggest that hS3 is not able to activate the classical $(EPOR)_2$ in contrast to hEPO. In conclusion, the $(EPOR)_2$ appears not to be the receptor involved in neuroprotective effects mediated by hS3.

4.9.4 BAF3/EPOR Pulldown experiments

In the last years, the concept of alternative EPO binding sites apart from the homodimeric $(EPOR)_2$ was developed. For instance EPO may bind to a tissue-protective heteroreceptor comprised of one EPOR chain and the β-common chain (βcC) (M. Brines *et al.*, 2004).
To analyze the involvement of a putative heterodimeric receptor containing one EPOR chain in the effects mediated by the EPO splice variants, Pulldown assays were performed exemplarily for the murine splice variant mS. Lysates from BaF3/EPOR cells were used as source of putative binding partners, as they had previously been shown to highly express both EPOR and βcC.
The Pulldown assay is an *in vitro* method used to determine physical interaction between two or more proteins. Minimal requirements for Pulldown assays are the availability of tagged proteins (the bait) which will be used to capture and ‘pulldown’ a protein-binding partner (the prey). Pulldown experiments were performed with mEPO and mS expressed as mature proteins without the N-terminal secretion sequence in *E.coli* strains optimized for protein expression (matmEPO and matmS). Proteins were expressed as fusion proteins to an N-terminal glutathione-S-transferase (GST-tag) and bound to a GST-agarose for Pulldown experiments. Bacteria expressing only GST from the empty pGEX-6P-1 vector were used as negative controls (MOCK-lysate). Clones of three different *E.coli* strains suitable for recombinant protein production, namely BL21, BL21-RIL and BL21-RP, were tested for protein expression efficiencies (data not shown). Best clones were obtained from the BL21-RIL strain. Expression analysis of clones of this strain showed no leakage before induction of protein expression with Isopropyl β-D-1-thiogalactopyranoside (IPTG) (Figure 49A). IPTG is used as a molecular mimic of allolactose, a lactose metabolite that triggers transcription of the lac operon. In the pGEX-6P-1 vector the lacZ gene is replaced with the gene of interest and IPTG is then used to induce gene expression.

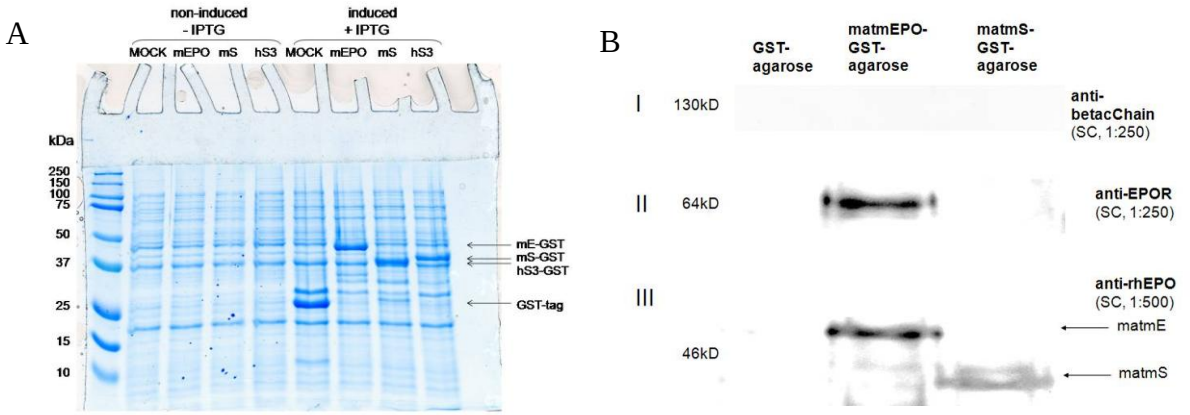

Figure 49: Pulldown of EPOR from BaF3/EPOR cells

A: Expression analysis of BL21-RIL E.coli clones expressing several EPO variants as GST fusion proteins. Cultures were lysed before and after induction of protein expression via IPTG. Protein lysates were analyzed on a protein gel stained with Coomassie Blue. Clones were not leaking, meaning no GST-protein expression was found before IPTG-induction, and showed high expression levels after IPTG induction (MOCK= BL21-RIL transfected with pGEX-6P1).
B: Pulldown experiment with GST-matmEPO and GST-matmS expressed in an E.coli strain bound to GST agarose. Lysates of the BAF3/EPOR cell lines were used as protein pool containing possible interaction partners. Analysis of pulldown eluates on Western Blots: I: no signal for the βcC detected; II: signal in matmEPO-pulldown for EPOR chain; III: staining of the GST-fusion proteins with the anti-rhEPO antibody from Santa-Cruz.

Expression of matmEPO and matmS was allowed for 3.5 h to 4 h after IPTG induction before lysis of the bacterial cultures. Lysates were incubated for minimum 1 h with GST-agarose to ensure binding of GST-tagged proteins. Then the protein-bound agaroses were incubated over-night with lysates of BAF3/EPOR cells. After washing and elution of captured proteins via boiling in an SDS sample buffer, proteins were separated on SDS-gels and stained for candidate proteins, namely EPOR and the beta common chain (βcC). Pulldowns using lysates of BAF3/EPOR cells as prey pool revealed interaction of EPOR with matmEPO but not with matmS (Figure 49B). Staining for the common beta chain (βcC) was negative for both Pulldown strategies.

In summary, interactions were identified between EPOR and mEPO but not between EPOR and mS. Also, no interaction was found to take place between the βcC and mEPO or mS. It should be noted that interactions with weak binding affinities (high dissociation constants) may not be recognized in Pulldown assays.

4.9.5 Radioactive binding experiments

From former experiments one cannot exclude that the EPO splice variants bind the $(EPOR)_2$ with low affinity but fail to activate the receptor. Therefore, a radioactive binding assay was established to test the ability of the EPO variants to displace rhEPO from its receptor binding

site. The principle behind this test was to saturate $(EPOR)_2$-binding sites on BaF3/EPOR cells with radioactive rhEPO before incubation of the cells with non-radioactive EPO or EPO variants. Binding of non-radioactive proteins to the EPOR displaces radioactive EPO thereby lowering radioactivity measured in the cell pellet.

BaF3/EPOR cells were grown to plateau phase and saturated with radioactive labeled rhEPO (^{125}I-rhEPO, Sigma). Saturated cells were incubated with different concentration of unlabelled EPO isoforms or control medium to test for displacement capacities of the variants. After thorough washing bound radioactivity was counted and displacement calculated as the difference between the amount of radioactivity in the absence of non-labeled EPO and the amount of radioactivity bound in the presence of non-labeled EPO or EPO variants. Counts measured in the absence of non-labeled EPO were defined as 100%.

Importantly, only hEPO was able to displace ^{125}I-rhEPO from BaF3/EPOR cells. In this study, maximal displacement was achieved with 6 nM unlabelled hEPO. Neither hS3, hS4 nor the control medium were able to displace ^{125}I-rhEPO from its binding site (Figure 50A).

In view of experimental results obtained in adult stem cells the binding site of the human A-helix derived peptide P16 was also of high interest. The peptide was tested at concentrations from 0 nM to 10 µM for the ability to displace rhEPO from $(EPOR)_2$. In two independent experiments even the highest dose was not able to displace ^{125}I-rhEPO from BaF3/EPOR cells (Figure 50B).

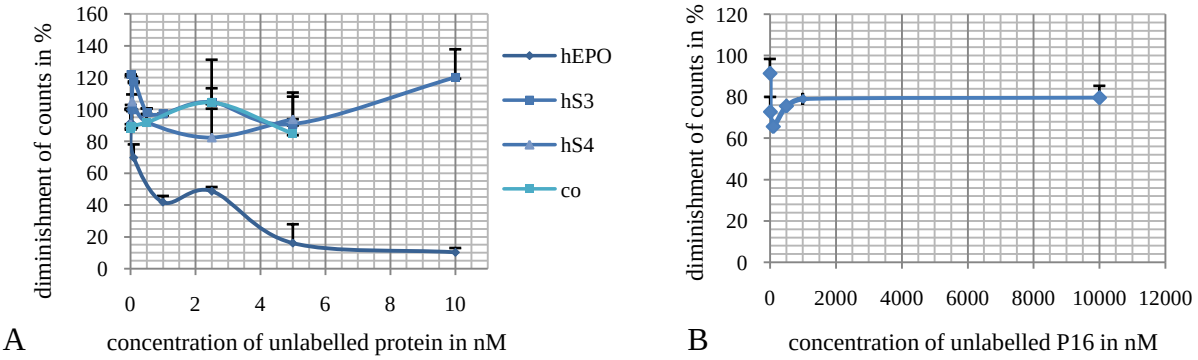

Figure 50: 125I-rhEPO competition assays

Displacement of radioactive rhEPO (^{125}I-rhEPO) from its receptor binding site by EPO variants. EPOR overexpressing BaF3 cells were saturated with iodinated rhEPO and incubated for 45 min with non-radioactive EPO variants. Cells were washed and content of bound radioactivity was subsequently measured. Absolute count numbers in samples incubated with 0 nM hEPO were considered as 100% counts and plotted + s.d. A decrease in radioactivity bound to cells indicates competitive displacement of ^{125}I-rhEPO by the non-radioactive EPO variant.
A: Saturated cells were incubated for 45 min with 0 – 10 nM hEPO, 0 – 10 nM hS3 or 0 – 5 nM hS4. In controls (co), cells were incubated with equivalent volumes of MOCK-samples. In three independent experiments we observed competitive displacement of ^{125}I-rhEPO only with hEPO. Maximal displacement was reached with approximately 6 nM hEPO. Even high concentrations of hS3 and hS4 failed to displace rhEPO.
B: Saturated cells were incubated for 45 min with 0 - 10,000 nM peptide P16. In two independent experiments even 10 µM P16 failed to displace ^{125}I-rhEPO from BaF3/EPOR. Because of negative displacement results experiments were not repeated to n=3.

4.9.6 Cytokine receptor screening in various cell types

The unknown receptor for the erythropoietin splice variants was postulated to be, alike $(EPOR)_2$, a member of the cytokine receptor family. The cytokine receptor family includes for example the interleukin receptors or the receptors for the ciliary neurotrohic factor (CNTFR), for oncostatin M (OSMR) or for the leukemia inhibitory factor (LIFR). Most of these receptors consist of a specific alpha chain and a non-specific signal-transduction chain, such as the common beta chain, the common gamma chain or the interleukin-6-transducer-chain gp130.

Hints for a receptor candidate mediating the effects of the EPO variants were obtained from NSC/NPC differentiation experiments. The hS3 supported astrocyte formation, a characteristic shared with factors signaling through the leukemia inhibitory factor receptor (Turnley *et al.*, 2000). Therefore, the LIFR or another receptor of this family were supposed to be very likely candidates.

Stronger evidence was obtained from expression analysis. Transcripts for LIFRα and gp130, the components of the LIFR, were found with high occurrence in all cell lines that were previously shown in this study to respond to the EPO variants, namely rat neurons, mouse NSC and the H9c2 cell line (Figure 51). Two neuronal cell lines, SY5Y and HT22, were analyzed in addition. OSMRα was equally tested since the OSM-receptor is also a member of the LIFR family. However, OSMRα-mRNA was not found to be expressed in all tested cell lines. Interestingly, the hS3-non-responsive Ba/F3 cell line neither express LIFRα, OSMRα nor gp130.

These results do not oppose the idea that the LIFR/gp130 complex might be an interesting candidate as receptor mediating the effects of the EPO variants.

Figure 51: Light cycler experiment: Receptor screening

mRNA expression levels of LIFR, OSMR and gp130 in different cell types. Arbitrary units (AU) were obtained by comparison of the crossing-points of the receptor PCRs with the crossing-points of the beta-actin PCRs.

4.9.7 Receptor blocking experiments

Suspecting that the LIFR and not the EPOR is the receptor responsible for the neuroprotective actions of the erythropoietin isoforms, it was tested if neuroprotection could be blocked in the OGD-model when hS3 and hEPO (30 pM) were coapplied with a soluble EPO receptor (sEPOR) or a soluble LIF receptor (sLIFR) in the preconditioning step. As expected, sEPOR blocked hEPO-mediated ischemic tolerance whereas coapplication of sLIFR no or only little inhibitory effects (Figure 52A). LDH release in sLIFR+hEPO treated cultures was found to be decreased by 20% compared to control cultures, similar to LDH reductions observed in hEPO-treated cultures. However, in sEPOR+hEPO treated cultures, absolute LDH release was equivalent to untreated controls. In the experiments using the human splice variant hS3 for preconditioning no blocking effect of sEPOR was found as expected from the BaF3 experiments. In the hS3- and sEPOR+hS3-pretreatment conditions LDH-release was found to be significantly decreased by 20% compared to control cultures, respectively. Importantly, the neuroprotective effect of hS3 was completely abolished by coapplication of sLIFR (Figure 52B).

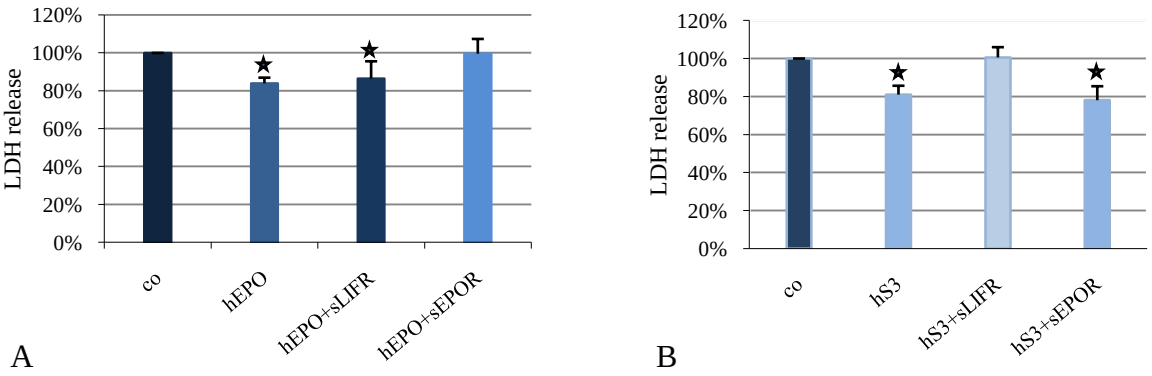

Figure 52: The soluble LIF receptor abolishes hS3 but not hEPO mediated tolerance against OGD in primary cortical neurons.

*The soluble LIF receptor abolishes hS3 but not hEPO mediated tolerance against OGD in primary cortical neurons. Primary cortical neurons were treated for 48 h with hEPO (30 pM) or hS3 (30 pM), respectively before exposure to 120 min OGD. OGD-induced cell death was evaluated by 24 h LDH release into the culture medium. A: Coapplication of soluble receptor EPOR (sEPOR) completely abrogated hEPO but not hS3 mediated neuroprotection. B: However, coapplication of soluble receptor LIFR (sLIFR) abolished neuroprotective actions of hS3 but not of hEPO. Data were obtained from five independent experiments. Data were normalized and plotted as means + s.d. Asterix: differences between treatment groups as indicated (*p<0.05, ANOVA1, Dunn's method)*

To strengthen these results the effects of LIFRα and gp130 blocking antibodies on neuroprotective effects mediated by the hS3 or hEPO were tested. As illustrated in Figure 53A neither the anti-gp130 antibody nor the anti-LIFRα antibody had any inhibitory effect on neuroprotection mediated by hEPO.

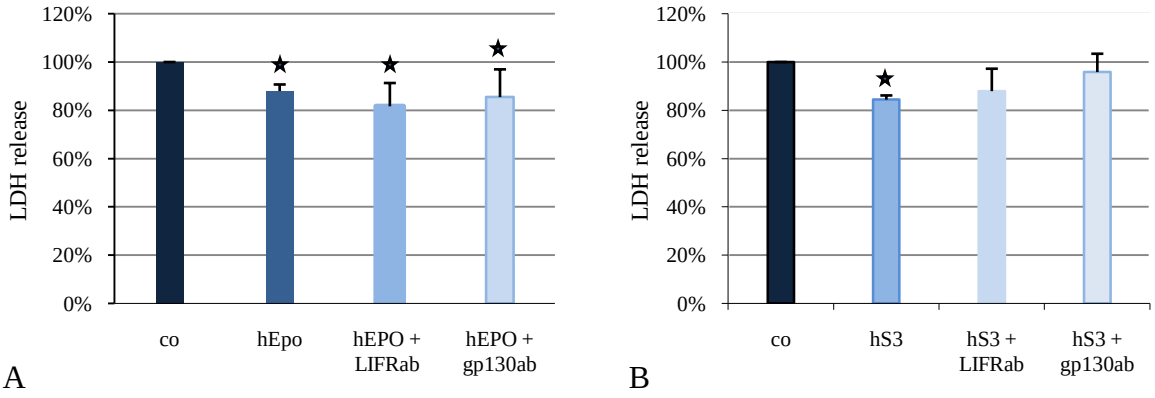

Figure 53: Neuroprotection conferred by hS3 is attenuated by coapplication of anti-LIFRα and anti-gp130 blocking antibodies.

*Primary cortical neurons were pre-incubated with anti-LIFRα (LIFR ab) or anti-gp130 (gp130ab) blocking antibodies for 1 h before application of hEPO (30 pM) or hS3 (30 pM), respectively. 120 min OGD was induced after 48 h treatment and cell death was evaluated by mean of LDH release 24 h after reoxygenation. Data were obtained from seven independent experiments. Data were normalized and plotted as means +s.d. Asterix: differences to control cultures (*p<0.05, ANOVA1, Dunn's method).*

In seven independent experiments significant reductions in LDH release of approximately 20% were measured in hEPO pretreated cultures compared to control cultures independent from coapplication of antibodies. In contrast, the anti-gp130 antibody was able to block the neuroprotective actions of hS3. Addition of anti-gp130 during hS3-preconditioning abolished antiapoptotic effects completely; in hS3+anti-gp130 treated cultures LDH release was found to be as high as in untreated cultures (Figure 53B). The anti-LIFRα antibody displayed only a weak blocking effect. LDH release was found to be reduced by nearly 10% compared to untreated cultures, however not to statistical significance. The incomplete blocking may be explained by an only partial inhibition of ligand binding to the receptor. One may also consider the higher expression level of the LIFRα chain compared to gp130 as shown previously by Real-time PCR. The dosing of the antibody may be insufficient and may therefore lead to incomplete blocking of all possible binding sites.

In summary, these experiments strongly suggest an involvement of LIFRα and gp130 in hS3-mediated neuroprotective effects.

4.9.8 Pulldown experiments LIFR

The functional assays in primary cortical neuronal cultures strongly suggested LIFRα and gp130 to be involved in the receptor complex mediating the neuroprotective effects of the human splice variant hS3. To confirm direct protein-protein interaction between the EPO splice variant and LIFRα or gp130, respectively, pulldown assays were performed. The assays were performed using the same protocol as in previous experiments except that hS3 was used in addition. Similar to mEPO and mS, hS3 was produced as mature protein in *E.coli*. As prey protein pools, lysates from cortical neurons containing rat LIFR, lysates from HEK293 cells containing human LIFR and supernatants from transfected HEK293 cells expressing the murine soluble LIFR (msLIFR) were used. In three independent experiments respectively, positive protein-protein interactions were identified between the murine splice variant mS and LIFRα of rat, human or murine origin. With hS3-bound agarose only human LIFRα was captured (Figure 54 A+B). Importantly, no interaction was found between mEPO and LIFRα of any species.

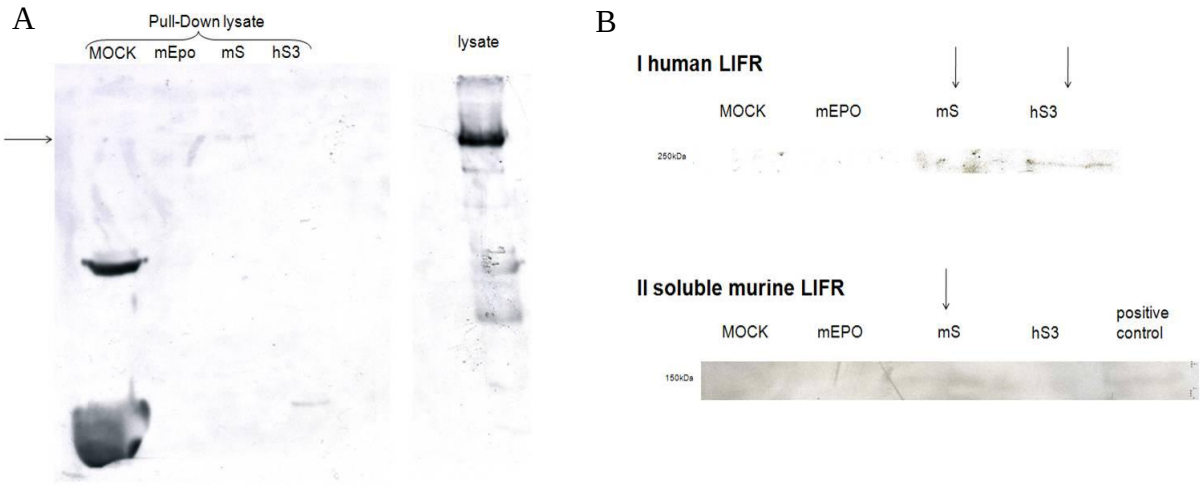

Figure 54: Pulldown assays show interacton of murine and human EPO splice variants with LIFRα species

GST-fusion proteins of the mature forms of mEPO, mS and hS3 were used to pulldown interacting proteins from cell lysates. Crude protein extracts, prepared from primary cortical neurons (A) or HEK 293 cells (B I), or supernatants of HEK 293 cultures expressing the V5-His-tagged murine soluble LIFR α (B II), were incubated with GST-fusion proteins mEPO, mS or hS3, respectively. Protein complexes were resolved on SDS-PAGE and immunoblotted with anti-LIFR antibody (A+B I) and anti-V5 antibody (B II). Each experiment was repeated three times. Representative Western Blots are shown.

Pulldown of the gp130 chain failed in all conditions (data not shown). These negative results do not exclude gp130 from the receptor complex. It is known from many receptor complexes that ligands bind the gp130 chain only with low affinity making pulldown assays very challenging.

4.9.9 M1 experiments: proliferation assays

The LIFR pulldown experiments and the functional assays on primary cortical neurons provided strong evidence implicating the LIFRα or gp130 in mediating the effect of the EPO splice variants. The glycoprotein LIF was initially identified based on its ability to induce suppression of proliferation and differentiation in the mouse myeloid leukemia cell line M1. To test if the EPO variants might also activate the LIFR, M1 cells were treated with murine LIF (mLIF, 50 ng/ml), hEPO (15 nM), hS3 (15 nM) or P16 (500 nM), respectively. The quantitative colorimetric MTT assay was used to measure proliferation of the cultures since the MTT-test was shown by Ohno *et al.* (Ohno *et al.*, 1991) to correlate with levels of LIF stimulation. The suppression of proliferation mediated by LIF was found to be maximal 72 h after onset of the stimulation.

Interestingly, in three independent experiments a weak but significant suppression of proliferation (around 10%) was observed in cultures treated with hS3 as single factor compared to MOCK-treated control cultures (Figure 55A). In contrast, hEPO- and P16-treated showed similar proliferation rates as control cultures. When cultures were treated with a combination of mLIF and EPO variants, no statistically significant differences were observed between treatment groups. Three days after seeding proliferation rates of the cultures had dropped by 30 – 55% compared to control cultures (MOCK-cultures without mLIF-treatment) (Figure 55B).

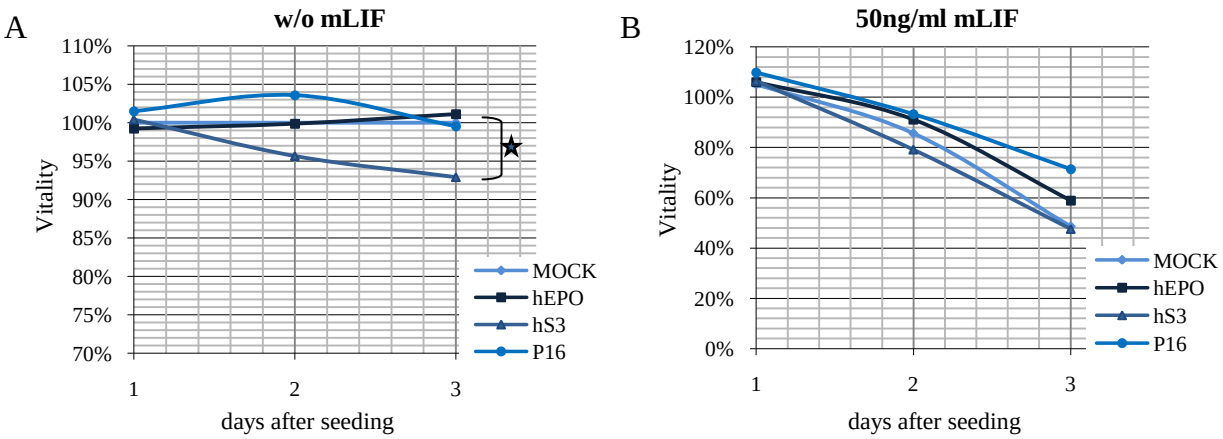

Figure 55: M1 proliferation assay

Mouse myeloid leukemia (M1) cells were seeded at the density of 150,000 cells/ml in presence or absence of 15 nM hEPO, hS3 or equivalent volumes of MOCK-medium or in presence or absence of 500 nM peptide P16 in 96- well plates. According to the experimental conditions murine LIF was added at a final concentration of 50 ng/ml. Proliferation of the cultures was measured by mean of the MTT-test 24 h, 48 h and 72 h after seeding. Mean proliferation rates in control conditions (=MOCK, w/o mLIF) were considered 100%. Experiments were repeated three times with 6 wells per condition and data was plotted + s.d.
A: M1 cells were grown in absence of murine LIF. In three independent experiments there was a weak but significant decrease in proliferation 72 h after seeding in presence of the splice variant hS3. Asterix: differences to MOCK-treatment (p<0.05, ANOVA1, Bonferroni t-test).*
B: M1 cells were grown in presence of 50 ng/ml murine LIF and EPO variants. mLIF was a potent inhibitor of M1 proliferation. No synergistic effects from EPO variants were observed. (no statistical significance, ANOVA1).

4.10 *In vivo* hematopoietic activity of vEPO

The main function of erythropoietin is the regulation of the levels of circulating erythrocytes by stimulating the maturation of late erythroid progenitor cells into proerythroblast. Administration of high amounts of *in vivo* biologically active exogenous EPO leads to an increase of hematocrit in the recipient. The *in vivo* biological activity of EPO is proportional to its *in vivo* half-life which is greatly dependent upon the presence or absence of sugar chains on the EPO molecule. As the type of sugar chains vary depending on the cell type, the biological activity of recombinant erythropoietins produced in different cell lines can vary dramatically depending on the type of the producer cell line. The hematocrit level can be used to determine the *in vivo* biological activity of recombinant EPO which is not necessarily equivalent to the *in vitro* biological activity.

4.10.1 *In vivo* biological activity of recombinant human erythropoietins

To evaluate the *in vivo* biological activity of our recombinant human erythropoietins produced in Freestyle HEK293 cells and in CHO-S cells that were shown beforehand not to differ significantly in their *in vitro* bioactivity (data not shown), an *in vivo* hematopoietic assay was performed. The hematocrit can easily be determined in a heparinized microhematocrit capillary after separation of the blood fractions as percentage of red blood cells to total blood volume (red blood cell zone, white blood cell zone, and plasma layer).

The experimental design for testing *in vivo* bioactivity of hEPO analogues produced in HEK293 or in CHO cells is shown in Figure 56A.

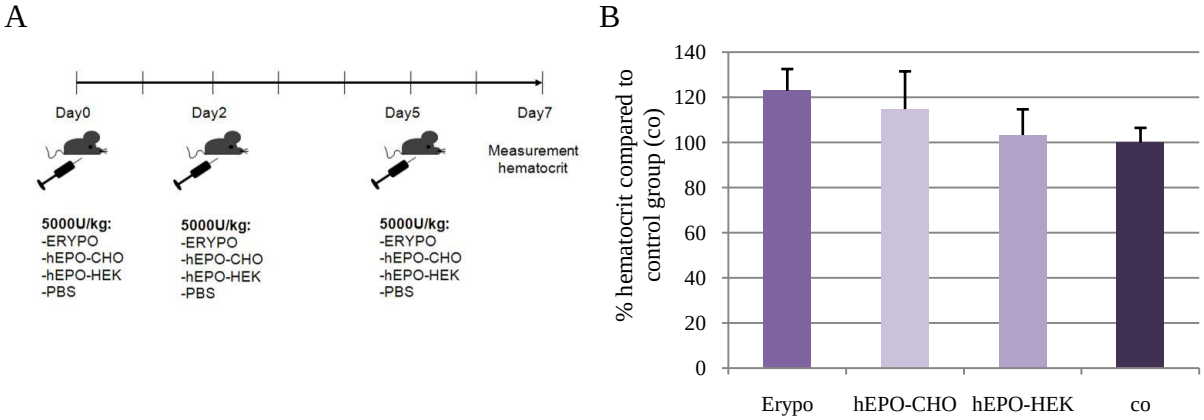

Figure 56: in vivo biological activities of recombinant hEPO analogues

A: Experimental setup. Male C57/Bl6 mice of age 8 – 10 weeks were injected intraperitoneally with 5000 U/kg recombinant human erythropoietin or equivalent amounts of PBS as control. Recombinant human erythropoietin was either commercial rhEPO (ERYPO), purified hEPO produced in Freestyle HEK293 (hEPO-HEK) or purified hEPO produced in CHO-S (hEPO-CHO). Injections were repeated three times (day 0, day 2, day 5) with 5 mice per group. Hematocrit was measured 48h after the last injection using microhematocrit capillaries.
B: In vivo biological activity of different human erythropoietins was plotted as normalized activity compared to PBS-control + s.d. Experiment was not repeated in order to obtain statistically significant differences.

Male C57Bl/6 mice were injected intraperitonelly with 42 µg/kg of our purified recombinant EPOs produced in Freestyle HEK293 (hEPO-HEK) or CHO cells (hEPO-CHO), with 5000 U/kg (= 42 µg/kg) commercial recombinant hEPO (ERYPO) as positive control or equal volumes of PBS as negative control. Injection was repeated every 2 to 3 days due to the known short plasma half-life of erythropoietin. Two days after the third and last injection hematocrit levels were determined using a microcapillary-based method. The hematocrit from each mouse was evaluated in duplicates.

In a pilot assay using 5 mice per group the mean hematocrits was found to be increased by approximately 20% in the experimental groups treated with ERYPO or hEPO produced in CHO-S cells, respectively, compared to the PBS group (Figure 56B).

Recombinant hEPO produced in Freestyle HEK293 cells seemed to have no or only little *in vivo* biological effect. For that reason recombinant proteins produced in CHO cells were used for later *in vivo* experiments.

4.10.2 *In vivo* hematopoietic activity of the EPO variants

In order to confirm the *in vitro* results of missing erythropoietic activity of the EPO variants (see chapter 4.3 Erythropoietic potential of the EPO variants) an *in vivo* hematopoietic activity assay was performed according to the protocol described previously. In view of the finding of different *in vivo* biological activities of HEK- and CHO- derived recombinant erythropoietins, experiments were performed with recombinant hEPO and hS3 produced in CHO-S cells. Mice were injected three times with 5000 U/kg (= 42 µg/kg) ERYPO or equivalent concentrations of hEPO and hS3 (Figure 57). Importantly, significant increases in mean hematocrit levels were only measured in hEPO and ERYPO-treated groups. The mean hematocrit increased up to 70% in EPO-groups whereas the mean hematocrit of the control group was in the normal range of hematocrit found in mice. The hS3-treatment had no effect on hematocrit levels; the mean hematocrit was about 50% and equivalent to the control group.

The mean blood hemoglobin levels in the treatment groups were found to correlate with hematocrit measurements. Hemoglobin (Hb) is carried by red blood cells and transports oxygen from the lungs to the peripheral tissues to maintain the viability of cells. Quantification of blood hemoglobin has been a key diagnostic parameter for anemia or polycythemia. Hemoglobin concentrations were easily quantified in a Colorimetric Assay Kit (Quantichrom). Mean Hb in the control group was found to be 13.53 ± 0.55 g/dl. Thrice injection of hS3 had no effect on Hb as expected from hematocrit levels, the mean Hb of this treatment group was 12.98 ± 0.56 g/dl.

In contrast, mice from both EPO-treated groups showed enhanced Hb-levels, namely 14.19 ± 0.77 g/dl in the hEPO-group and 15.64 ± 0.72 g/dl in the ERYPO-group.

This finding clearly supports the *in vitro* findings. The hS3 is a non-hematopoietic variant of human EPO.

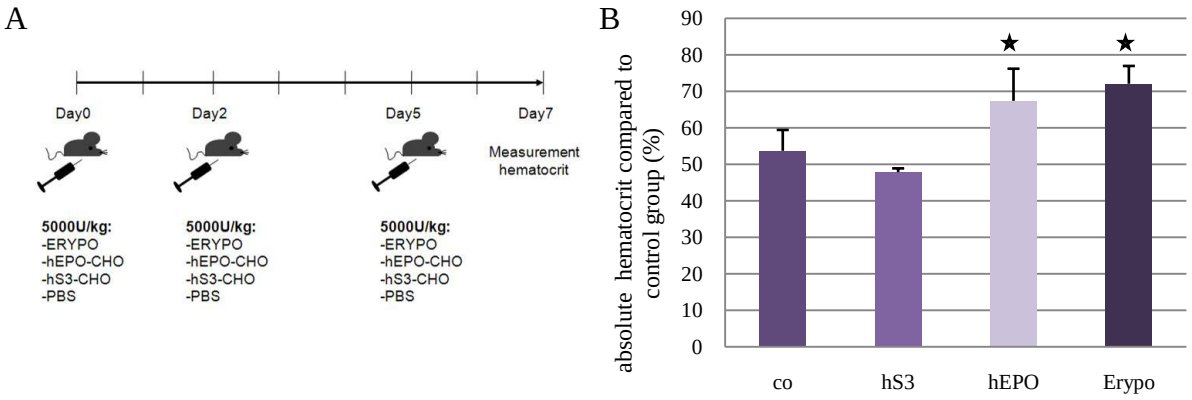

Figure 57: hS3 is non-erythropoietic in vivo

A: Experimental setup: Male C57Bl/6 mice of age 8 – 10 weeks were injected intraperitoneally with 5000 U/kg recombinant human erythropoietin or equivalent amounts of recombinant hS3 and PBS as control. Recombinant human erythropoietin was either commercial rhEPO (ERYPO), or purified hEPO produced in CHO-S (hEPO). Injections were repeated three times (day 0, day 2, day 5) with 5-10 mice per group. Hematocrit was measured 48h after the last injection using hematocrit capillaries.
*B: Mean hematocrit values of mice injected with ERYPO, hEPO, hS3 or PBS (co) + s.d. A significant increase of the mean hematocrit was only observed in hEPO- and ERYPO-groups. The hS3-group showed no effects. Asterix: differences from control group (*p<0.05, ANOVA1, Bonferroni).*

5 DISCUSSION

5.1 Identification of endogenous Erythropoietin variants

Alternative splicing plays an important role in the evolution of eukaryotes making adaptation to new environments much faster than for prokaryotes. Recent genome-wide studies predict that 40 - 60% of the human genes undergo alternative splicing. The frequency of alternative splicing in the mouse is estimated as 41% by analysis of full-length cDNAs (Okazaki *et al.*, 2002).

Thus, the discovery of human and murine erythropoietin splice variants is not astonishing as many proteins possess a large palette of isoforms due to splicing or post-translational processes. Nevertheless to this day no splice forms of EPO were reported in mammalians. The reason might be that erythropoietin is one of the lowest expressed proteins in mammalians making isolation of its mRNA very difficult. Only the Nested-PCR approach allowed the amplification of enough erythropoietin cDNA for further cloning in this study. By using Nested PCR approaches one has always to consider the risk of amplifying PCR-artefacts generated by the reverse transcriptase for example by skipping over looped-out regions in the secondary structure of the mRNA resulting in internal deletions in the generated cDNA (Korfhage *et al.*, 2000) or by template switching, a mechanism first described in retroviruses also occurring *in vitro* in RT-PCR reactions (Mader *et al.*, 2001) leading to internally deleted products. This mechanism is mediated by specific structural elements such as direct repeats.

It is therefore not surprising that not only the EPO cDNA was amplified in the Nested PCR approach but also additional smaller PCR products. An *in silico* analysis of the products obtained from murine and human erythropoietin PCRs revealed a common deletion pattern for most of the products (Table 17). Deletion occurred mainly between two short direct repeats with elimination of one of the repeated sequences. This pattern strongly suggests these variants to be products from template switching of the Moloney Murine Leukemia reverse transcription polymerase during cDNA synthesis.

Only three PCR products named hS3 (human isoform), hS4 (human isoform) and mS (murine isoform) do not follow this rule. Several lines of evidence suggest that these products are real splice variants of erythropoietin. An analysis of these variants revealed defined donor sites (GT) 3’ and defined acceptor sites (AG) 5’ of the deletion sites. When classifying the splice variants according the four major types of alternative splicing events, mS and hS3 result from exon skipping whereas hS4 results from an alternative acceptor site. Furthermore, the finding of the variants was reproducible using a second PCR approach with modified reaction conditions.

These are strong arguments in favor for the endogenous existence of these three alternatively spliced EPO transcripts.

Non-conserved alternatively spliced exons can cause a frame shift in the coding sequence or make the protein longer by suppressing a nearby stop codon. However in large-scale analysis of protein isoforms arising from alternative splicing it has been shown that alternative splicing tends to remove or insert complete protein domains rather than to disrupt domains (Kriventseva *et al.*, 2003). This observation was much more frequent than expected by chance, and was supposed to result from positive selection. Importantly, the alternatively spliced EPO variants contain also deletions of entire protein domains, namely the AB-loop in hS3, helix B in hS4 and helices B and C in the murine splice variants mS. Therefore the EPO spliced transcripts were supposed to be translated into proteins. Evidence for this was obtained in an immunoprecipitation setup directed against murine erythropoietin which revealed the existence of two proteins in murine tissue extracts having same molecular masses as our recombinant murine variants mEPO and mS (36 – 40 kDa and 30 kDa).

No alternative splicing of EPO has been reported in mammalians so far. However, a brain-specific EPO transcript was cloned from a teleost fish, the pufferfish *Fugu rubripes* (Chou *et al.*, 2004). The EPO transcripts in the *Fugu* brain are transcribed from another transcription site than in kidney and liver including an alternate first exon. Whether this alternatively spliced first exon conferred a different function to EPO in the brain has not been further analyzed, but a nonerythropoietic function of EPO in the central nervous as described in mammalian cannot be excluded. The alternatively spliced transcripts identified in this study are neither brain specific, as they were also found in the kidney, nor are they structurally similar to the brain EPO of *Fugu.* Interestingly, the murine EPO splice variant has also no structural similarities to the human EPO splice variants hS3 and hS3. However, low conservation of alternative splicing patterns in human and mouse genomes is well known, such as from Ras GTPase or from mucolipidosis type IV (Nurtdinov *et al.*, 2003). Half of the analyzed pairs of orthologous human and mouse genes were demonstrated to have species-specific isoforms. These evolutionary young, species-specific isoforms are thought to be the major mechanism for generation of species-specific proteome diversity. This would also explain the structural differences of the murine and human EPO variants.

Alternative splicing can result in protein isoforms with altered functions as for example in the case of the human IL-6 isoform resulting from a deletion of exon 2 (Kestler *et al.*, 1999). Same was shown to be true for the alternatively spliced EPO variants in our study.

5.2 *In vitro* functional analysis of the erythropoietin variants

5.2.1 Non-hematopoietic neuroprotective erythropoietin splice variants

Many authors describe beneficial effects of recombinant human erythropoietin (rhEPO) in *in vivo* (Bernaudin *et al.*, 1999; Brines *et al.*, 2000; Morishita *et al.*, 1997) and *in vitro* (Sinor *et al.*, 2000) models of brain ischemia. Furthermore endogenous EPO has also been shown to be a neuroprotective factor, as continuous cerebroventricular infusion of sEPOR in 2.5 min ischemic gerbils caused a significant reduction in learning ability and neuronal loss in the hippocampus (Sakanaka *et al.*, 1998), and to play a role in ischemic preconditioning as shown by Prass *et al.* (2003).

The results of the present study obtained with murine (mEPO) and human recombinant erythropoietin (hEPO and rhEPO) in the oxygen and glucose deprivation model of *in vitro* cerebral ischemia are in clear concordance with the literature. When pretreating rat cortical neuronal cultures with human and murine recombinant erythropoietin 48h before OGD significant neuroprotective effects were observed as described by Ruscher *et al* (Ruscher *et al.*, 2002). In this study, a maximum of 50% protection was observed compared to 75% protection in Ruscher's studies, but this might be explained by variations in experimental conditions. The antiapoptotic effect of erythropoietin in this study followed a U-shaped dose effect curve as also found by others in several cell culture models (Siren *et al.*, 2001; Weishaupt *et al.*, 2004). Increasing concentrations of erythropoietin beyond a maximal effective dose resulted in a decline of the neuroprotective effect down to control levels.

The key finding of this study was the discovery of endogenous murine and human splice forms of erythropoietin that provide equivalent neuroprotective actions as erythropoietin in our *in vitro* paradigm. Similar dose-effect curves were found for the human recombinant erythropoietins and human recombinant variants. From this data it was concluded that the splice variants hS3 and hS4 do not differ from wildtype erythropoietin in terms of neuroprotective effects *in vitro.* However, in contrast to the recombinant murine and human erythropoietins none of the splice variants were able to promote survival and proliferation of the erythroid progenitor cells derived from murine bone marrow in a classical methylcellulose assay. The non-erythropoietic feature of the human splice variant hS3 was furthermore reproduced *in vivo*. The finding that the hematopoietic and neuroprotective features of erythropoietin can be separated is not new as Leist showed this by carbamylation of erythropoietin in 2004 (Leist *et al.*, 2004). The striking innovation of this study is the finding of endogenous non-hematopoietic neuroprotective proteins that might play an important role in damaging events *in vivo.*

The tissue-protective actions of erythropoietin rely mainly on the inhibition of apoptosis. Several pathways responsible for these effects have been identified in the last years. The key pathway of antiapoptotic signaling of EPO in hematopoiesis involves STAT5 that enters the nucleus as a homodimeric and phosphorylated molecule where it enhances transcription of protective genes (Silva *et al.*, 1999). Another mechanism has been shown in kidney where erythropoietin induced the antiapoptotic heat shock protein 70 (C. W. Yang *et al.*, 2003). Two erythropoietin signaling pathways involve I-kB, the inhibitor of the transcription factor NF-κB, which is either directly phosphorylated after activation of the EPOR (Digicaylioglu *et al.*, 2001) or phosphorylated via the protein kinase B (PKB)/Akt (Kashii *et al.*, 2000). This analysis was focused on the signaling pathway described in primary cortical neurons of the rat (Ruscher *et al.*, 2002). In accordance to Ruscher significant activation of the Akt kinase was observed in EPO treated neuronal cultures. An EPO-induced phosphorylation of Akt was also described by Siren *et al.* in primary rat hippocampal neuronal cultures after exposure to hypoxia (Siren *et al.*, 2001). In our study, Western blot analysis showed enhanced phosphorylation of BAD at Ser 112 and 136 after EPO treatment. It is important to know that phosphorylated BAD prevents apoptosis. The unphosphorylated form of Bad is capable of forming heterodimers with the antiapoptotic proteins Bcl-XL or Bcl-2 and antagonizes thereby their antiapoptotic function (Zha *et al.*, 1996). An involvement of BAD phosphorylated at Ser136 in EPO-mediated neuroprotection was shown for the first time by Ruscher *et al.* and could be reproduced in the present study. Furthermore in the present study upregulation of BAD proteins phosphorylated at Ser112 was revealed. While phosphorylation of BAD at Ser 136 is mediated by the protein kinase Akt, phosphorylation at Ser112 was shown to be mediated by Ras and Raf (Fang *et al.*, 1999), which are upstream of mitogen-activated protein kinases (MAPK). An involvement of the Ras-MAPK pathway in EPO-mediated neuroprotection was also described in hippocampal neurons (Siren *et al.*, 2001).

In contrast to Ruscher *et al.*, hints for activation of the NF-κB pathway were revealed in this study. After hEPO- or hS3-treatment of neuronal cultures, a slightly enhanced phosphorylation of the IKK kinase was detected. IKK is the key kinase of the NF-κB pathway that, once activated, phosphorylates I-kB, the cytoplasmic inhibitor of NF-κB. This finding is in accordance with results of Digicaylioglu (Digicaylioglu *et al.*, 2001) who proposed involvement of the NF-kB-pathway in neuroprotection via phosphorylation of I-kB mediated by Akt. Both pathways are known to lead to expression of neuroprotective genes thereby enhancing cell survival.

The binding of erythropoietin to its receptor, which exists as a preformed dimer, induces a conformational change that brings constitutively associated Janus family tyrosine protein kinase 2 (Jak2) molecules in close proximity and stimulates their activation by transphosphorylation

(Witthuhn *et al.*, 1993). Upregulation of phosphorylated Jak2 was very weak in this study possibly due to rapid phosphorylation and dephosphorylation kinetics. Thus, involvement of this protein in the signaling pathway was shown via blocking experiments with the specific pJak2 inhibitor AG490. Interestingly, similar results were obtained in hS3 treated cultures. The levels of phosphorylated proteins pIKK, pBAD Ser112, pBAD Ser136, pJak2 and pAkt in hEPO and hS3 treated co-cultures were nearly identical. An involvement of Jak1 may be excluded for both proteins whereas Jak2 seems to play also a role in hS3-mediated signaling as treatment of neurons with AG490 blocked both hEPO and hS3 mediated neuroprotection.

In summary, the following pathway for hEPO and hS3 is proposed: Receptor activation leads to Akt activation after Jak2 phosphorylation. Two antiapoptotic pathways involving NF-κB and BAD are subsequently activated. An involvement of the Ras-MAPK may not be excluded due to phosphorylation of Bad at Ser112 but was not analyzed in more detail (Figure 58).

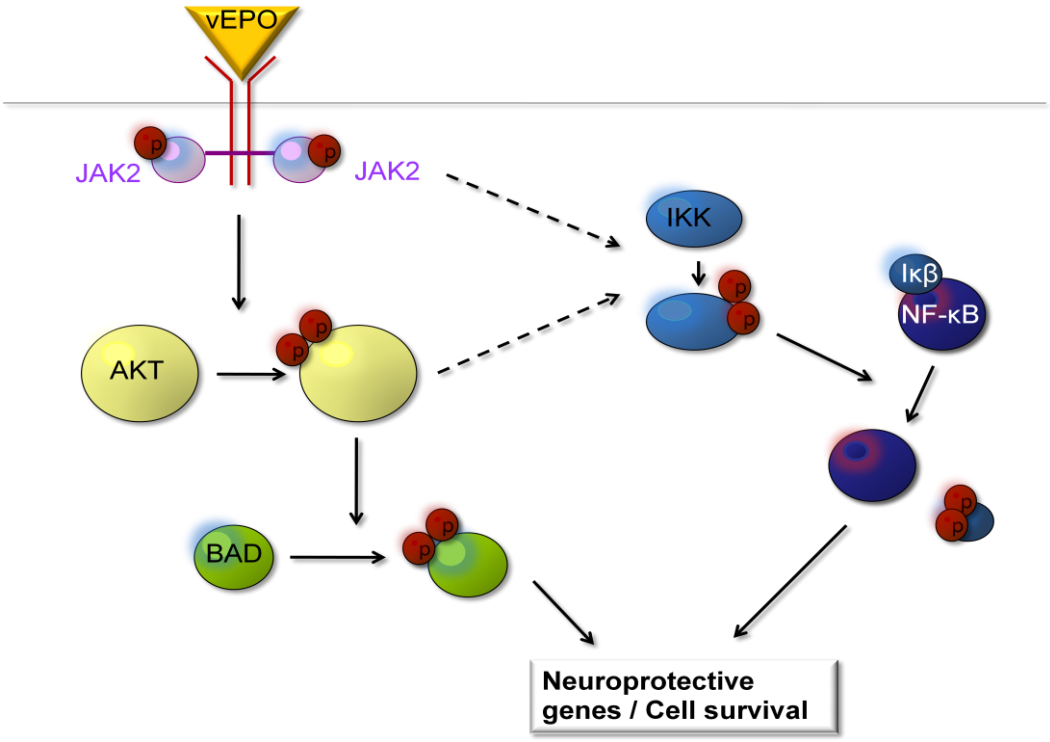

Figure 58: Signaling pathway of hEPO and hS3 in primary cortex neurons

We propose the following pathway for hEPO and hS3 in primary cortical neurons: hS3- or hEPO-binding to its specific receptor leads to Akt activation after Jak2 phosphorylation. Subsequent phosphorylation of BAD causes expression of neuroprotective genes. A second signaling pathway is activated after binding of hEPO or hS3, respectively, either via direct phosphorylation of IKK by pJak2 or via phosphorylation by pAKT. PIKK activates the NF-κB pathway promoting also cell survival.

5.2.2 Protective effects of hS3 in an *in vitro* model of myocardial ischemia

The present study reveals that not only hEPO but also the human splice variant hS3 is capable of protecting a myoblast cell line from rat (H9c2) in an *in vitro* model of myocardial ischemia.

An antiapoptotic effect of rhEPO in H9c2 myoblasts has already been shown in conditions where cell death was induced with H_2O_2 or with a long lasting anoxia (Parsa *et al.*, 2003). In H9c2-cells, EPO was shown to mediate its actions via induction of the Jak1-Stat3 pathway with additional activation of ERK-MAPK and Akt pathways. In accordance with Parsa increased survival of H9c2 cells was observed when cells were pretreated with hEPO. The antiapoptotic effect was less pronounced in the present study but this might be due to lower concentrations of EPO used for pretreatment. In this study 120 pM hEPO being approximately equivalent to 300U/l rhEPO (Roche) were used, instead of 1000 U/l as in Parsa's study. Furthermore, in the present experiments survival was evaluated at a later time point, namely at 24 h instead of 0 h after reoxygenation. In contrast to Parsa *et al.*, no proliferative effect of hEPO on H9c2 cells was detected. This may again be explained by the comparatively low dosing. The proliferative effect measured in Parsa's study was of about 9% compared with control after treatment with 4000 U/l EPO and explained via ERK activation.

The present study suggests that hEPO and the human splice variant hS3 are not only equal in their neuroprotective potential but also in their cytoprotective potential in our *in vitro* models. The *in vivo* situation has to be clarified. Signaling pathways are also still to be elucidated.

CEPO, the chemically generated nonerythropoietic derivative of EPO, has as well been shown to have comparable antiapoptotic effects as EPO in an *in vivo* model of isolated adult rat ventricular cardiomyocytes (Fiordaliso *et al.*, 2005). This is relevant for the present study as the authors postulate that cytoprotection by CEPO is not mediated via the classical EPOR.

5.3 Effects of EPO variants on adult stem cells

5.3.1 Hematopoietic stem and progenitor cells (HSC/HPC)

In the bone marrow (BM) a small number of HSC is responsible for the production of heterogeneous populations of actively dividing hematopoietic progenitors that generate millions of mature blood cells per day. *In vitro* assay systems are based on semi-solid culturing matrices in which individual colony-forming cells (CFCs) proliferate to form discrete clusters or colonies. The addition of specific nutrients and cytokines permits the growth of erythroid, granulocyte, monocyte or mixed colonies according to the specific requirements of the progenitors (Figure 59).

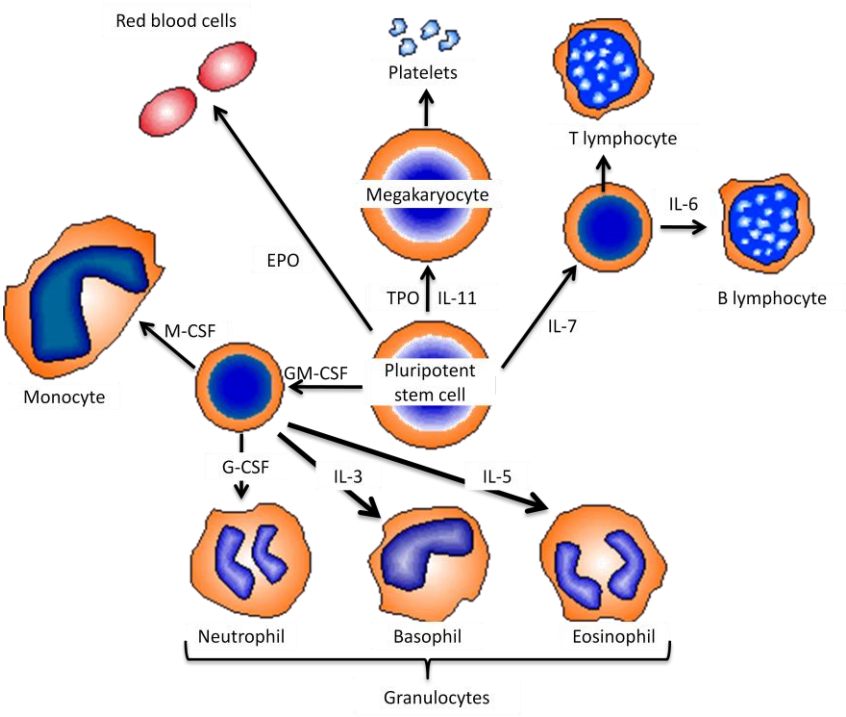

Figure 59: Diagram of the formation of blood cells
(Modified diagram from source: http://users.rcn.com/jkimball.ma.ultranet/BiologyPages/B/Blood.html)
Pluripotent stem cells can give rise to different cell populations regulated by the presence of different growth factors and cytokines. EPO alone is sufficient to trigger the differentiation towards red blood cells. Combinations of IL-3, IL-5, GM-CSF and G-CSF conduct maturation to cells of the granulocyte-type. Other factors are necessary for the differentiation into monocytes, megakaryocytes or the lymphocyte family.

Erythropoietin has long been known as the substance responsible for the regulation of red blood cell differentiation. The major mechanism in EPO action is thought to be promotion of survival of late erythroid progenitor cells via inhibition of apoptosis (Koury *et al.*, 1988) rather than a direct proliferative effect. If EPO is not present during the critical period the erythroid progenitor cells undergo apoptosis. In the methylcellulose-based assay system used in this study, erythroid colony forming units (CFU-E) were only detected after 2 days in culture when recombinant human or murine erythropoietins (rhEPO, hEPO or mEPO) were present. No significant numbers of CFU-E were detected in presence of all isolated erythropoietin variants of murine and human origin. *In vivo* biological activity of recombinant EPO can be shown by the elevation of hematocrit in experimental animals. Even though lower doses of rhEPO are effective in significantly raising hematocrit levels in mice by thrice week injections (Egrie *et al.*, 2001), the comparably high dose of 5000 U/kg (42 µg/kg) bodyweight was used, being the envisioned dose for future experiments in a stroke model of the mouse. In this study, only recombinant EPO expressed in CHO cells significantly increased hematocrit levels in mice, whereas hEPO produced in HEK293 cells had only little or no effect. However, the *in vivo* activity of recombinant EPO is strongly dependent on its carbohydrate moiety and therefore on the choice of the host-cell. Also other EPO analogues such as recombinant EPO produced in tobacco cells

(Matsumoto *et al.*, 1995) or in goat milk (Montesino *et al.*, 2008) have been shown to retain fully *in vitro* but only reduced *in vivo* biological activity. It has been demonstrated that recombinant glycoproteins produced in CHO cells possess sialylated carbohydrates that prolong the circulating half-life, whereas HEK293 cells seem to be limited in their ability to sialylate overexpressed proteins (Manna *et al.*, 2002). Fully active commercially available EPO analogues are only produced in CHO cells, baby hamster kidney cells (BHK-21) and mouse mammary cells (C127) (Hayakawa *et al.*, 1992). In view of this finding, the human splice variant hS3 was expressed in CHO cells and used in equivalent doses to hEPO and to the commercial recombinant EPO analogue ERYPO, both expressed in CHO cells. The result of this experiment demonstrated a striking difference in the biological activity of the EPO isoforms, confirming thereby the results obtained in the *in vitro* assays. By day 7, the group-mean hematocrits of animals injected thrice with 42 µ/kg hEPO or ERYPO increased to approximately 70% whereas the group-mean hematocrit of hS3-treated animals stayed at the level of the control group (approximately 50%). The very high hematocrit levels found in EPO treated animals are consistent with data obtained in rats treated with equal doses (Wang *et al.*, 2004). In summary, the results obtained from erythropoiesis experiments indicate that the EPO variants are not able to prevent apoptosis of the erythroid progenitor cells *in vitro* and presumably also *not in vivo*, as shown exemplarily for hS3.

Next, putative differentiation effects of the EPO variants on pluripotent HSC/HPC were investigated in combination with IL-3 or IL-3 + SCF as erythropoiesis experiments had suggested no direct colony-stimulating activity of the EPO variants as single factors. When analyzing the cultures after 2 days for CFU-E formation, no differences were observed in the number of CFU-E formed per 10,000 seeded cells between IL-3 + hEPO or IL-3 + SCF + hEPO. A synergistic effect of IL-3 and SCF with EPO on the differentiation of erythroid progenitors as described by Wang *et al.* (J. Wang, Tang *et al.*, 2007) was not observed in the present study. This might be due to the very high concentration of EPO used in our study, probably already stimulating the maximum of erythroid progenitors being present in the bone marrow. For the EPO isoforms hEPO, hS3 and P16 no clear effects on the differentiation of HSC/HPC were observed. In presence of IL-3 and SCF, hEPO and hS3 seemed to have a positive synergistic effect on myeloid colony formation of type CFU-G and CFU-GM. A weak, but significant stimulatory effect on murine splenic CFU-GM and granulocyte numbers was also described for recombinant human erythropoietin *in vivo* (Roeder *et al.*, 1998).

It is to note, that in this study additional analysis for colony-forming unit-megakaryocyte (CFU-Meg), e.g. via acetylcholinesterase (AchE) staining, was not performed. Hence, it is known that

IL-11 and LIF, although having no effect as single factors on normal murine bone marrow for cell colony formation *in vitro*, potentiate CFU-Meg-formation stimulated by IL-3 (E. Bruno *et al.*, 1991; Metcalf *et al.*, 1991). Thus, modulatory effects of the EPO variants on HPC cannot be totally excluded.

In the last years, research focused on the environmental and molecular requirements for HSC self-renewal, as *ex vivo* expanded populations of HSC are of therapeutical interest. HSC derived from bone marrow, peripheral blood or umbilical cord blood, are used for repopulation of the hematopoietic system after high-dose chemotherapy. For instance, umbilical cord blood is a promising source for HSC that can be used as an alternative to bone marrow. But, as the number of HSC in umbilical cord blood is limited, transplantation in adults is currently still a critical issue. Increasing the dose of HSC would shorten the time to engraftment of mature blood elements. Thus, a possibility to expand HSC via *ex vivo* cultivation is needed. But hematopoietic stem and progenitor cells are difficult to maintain in culture without loss of their original potency. Viability of committed and multipotent progenitor cells in liquid storage of bone marrow was extensively studied (Lasky *et al.*, 1986; Spivak *et al.*, 1985). Spivak observed a decline in cell numbers of non-adherent cells, containing the hematopoietic stem and progenitor cell population, to 20% after 96 h in cultures. Lasky described viability of stored hematopoietic progenitor cells (HPC) to be dramatically reduced from day 3 to day 7 days. This is consistent with the results in the present study, as a drastic decline of 80 % was observed in the numbers of non-adherent cells from day 2 to day 5 in our liquid bone marrow cultures. As well for the ability of colony formation a decline of approximately 40 CFU/20,000 seeded cells to 15 CFU/ 20,000 seeded was determined between cultivation periods of 2 days and 5 days. In addition, formation of CFU-E after seeding in rhEPO-supplemented methylcellulose was only observed when hEPO was present during the preceding starvation period. This finding can rather be explained by an antiapoptotic effect of EPO on erythroid progenitor cells than by a differentiation effect of EPO. This is in concordance with Koury's hypothesis of EPO's antiapoptotic action on erythroid HPC.

The key finding in this study is that recovery of myeloid progenitor cells can be significantly improved by addition of EPO isoforms in *ex vivo* bone marrow cultures. In a short cultivation period of 2 days this effect was nearly identical for hEPO, the splice variant hS3 and the peptide P16 whereas under prolonged starving conditions (5 days) the peptide P16 seemed to have the most pronounced effect. However, the peptide P16 was added in much higher concentrations than the proteins hEPO and hS3, the more pronounced effect might therefore be due to higher concentrations of this EPO isoform. Clinical studies suggest that the formation of CFU-GM from blood transplants is a reliable predictor of rapid engraftment (H. Yang *et al.*, 2005; Yoo *et al.*,

2007). In the past, many factors have been shown to preserve hematopoietic progenitor cells in *ex vivo* cultures such as IL-3, IL-6, SCF (stem cell factor), IL-11 or steel factor (SF) (Bodine *et al.*, 1991; Neben *et al.*, 1994). But transplantation experiments have suggested that addition of exogenous cytokines might diminish the long-term repopulating ability of the graft (Peters *et al.*, 1996; Tisdale *et al.*, 1998) leading to poorer graft rates. Cytokines such as IL-3, IL-6 or SCF do not act exclusively on HPC survival *in vitro* but have also effects on differentiation and act on proliferation via acceleration of cell-cycling (Tanaka *et al.*, 1995). IL-3 promotes growth of early myeloid progenitors of all lineages in combination with other cytokines. SCF is essential for growth of mast cells and promotes growth of lymphoid and myeloid progenitors in combination with other cytokines and IL-6 induces the maturation of megakaryocytes *in vitro*. These actions on differentiation and proliferation of HPS are thought to reduce the graft rates observed in many studies. Engraftable states of cultured hematopoietic progenitors might be maintained by cytokines that spare cell cycle activation and that do not promote differentiation.

Our methylcellulose-based assays suggest that the human splice variant hS3 and the peptide P16 have no differentiation effects on myeloid HPC. In combination with IL-3 and SCF a synergistic effect for hEPO and hS3 on CFU-G and CFU-GM formation was observed whereas P16 had no synergistic effect. Therefore, the peptide P16 might be an ideal candidate to maintain myeloid progenitor cells in *ex vivo* bone marrow cultures before transplantation as it (1) does not promote differentiation of myeloid CFU, (2) it does not expand HPC in our *in vitro* colony assay systems and (3) it promotes survival of progenitor cells under nutrient-deficient conditions. However, positive transplantation results are not only dependent on the status of the precursor cells but also on the quality of the HSC. Transplanted HSC have to home to the bone marrow of the host, to survive, to proliferate and to differentiate. Thus, future experiments have to clarify if the HSC retain full lympho-myeloid repopulating potential and an enhanced *in vivo* regenerative potential after treatment with P16. This is to be tested by grafting P16-pretreated murine bone marrow cells into heavily irradiated mice.

5.3.2 EPO variants effect on neural stem and progenitor cells

Neural stem cells continually generate new neurons in the adult mammalian central nervous system ensuring thereby neurogenesis – the process of giving birth to new neurons – throughout adulthood. Adult neurogenesis is normally restricted to the subventricular zone (SVZ), which lines the lateral ventricles of the brain, and the dendate gyrus. After stroke, neural stem cell proliferation was found to be enhanced in the SVZ and neuroblasts migrated into the degenerated areas. Multipotent progenitor cells isolated from adult brain and propagated *in vitro*, transform

into the three major cell types of the adult brain under the influence of various growth factors (Figure 60).

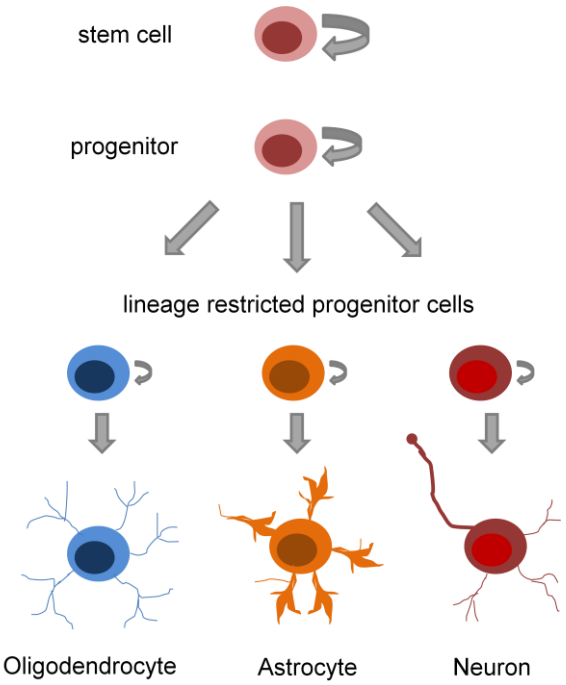

Figure 60: Differentiation potential of neural stem cells

Stem cells can undergo two types of cell division. Symmetric division gives rise to two identical daughter cells both having stem cell properties ensuring self-renewal. Asymmetric division, on the other hand, produces only one stem cell and a progenitor cell with limited self-renewal potential. Progenitors can go through several rounds of cell division before differentiation into a mature cell. Neural progenitor cells can give rise to three major cell types—astrocytes and oligodendrocytes, which are non-neuronal cells, and neurons or nerve cells.

An effect of erythropoietin on adult neural stem cells has been described for the first time in 2000 (Studer *et al.*, 2000). Studer *et al.* observed an increased yield in dopaminergic neurons in lowered oxygen conditions after EPO treatment of CNS precursors. The enhanced generation of neurons after exposure of NSC to EPO was also found by the group of Shingo (Shingo *et al.*, 2001) who showed that cultured neural stem cells (NSC) exposed to a modest hypoxia produced two- to threefold more neurons and that this effect could be mimicked by EPO administration. In Shingo's study, erythropoietin had only an enhancing effect on differentiation but not on proliferation. NSC cultures exposed to increasing concentrations of erythropoietin did not differ from control cultures in total cell numbers, but in a clonogenic assay spheres generated in the presence of EPO showed an increase in numbers of cells differentiating to neurons and a corresponding decrease in the number of secondary spheres. This result suggests that EPO acts on one hand as differentiating factor on NSC by pushing them to a neural phenotype but on the other hand reduces their self-renewal capability. In contrast to these findings, other authors indeed observed a stimulating effect of EPO on the proliferation of neural progenitor cells (NPC)

(Chen *et al.*, 2007). Chen described a dose-dependent effect of EPO on the proliferation of NPC leading to three times more NPC in β-FGF-depleted cultures containing 10 U/ml EPO compared to control cultures after 2 days in culture. A combination of β-FGF and EPO however, showed no synergistic effect on proliferation compared to β-FGF alone.

In the present study hS3 and the peptide P16 were found to have a proliferative effect on NSC/NPC cultures at high doses (100 ng/ml hS3 or 100,000 nM P16). A control experiment with hEPO supplemented NSC/NPC sphere cultures was not performed so that Chen's results can neither be opposed nor supported. Interestingly enough the proliferative effect of hS3 and P16 was observed in cultures supplemented with β-FGF and EGF. In contrast, EPO had no synergistic effect in presence of β-FGF (Chen *et al.*, 2007), but direct comparisons cannot be made. In the present study, neither the proliferative effect of hEPO in presence of β-FGF and EGF nor the proliferative effect of hS3 or P16 in growth factor depleted sphere cultures were tested. From these results, one might postulate a more pronounced proliferative effect mediated by the hS3 and P16 than by EPO. Interestingly, CEPO (carbamylated EPO) was also found to increase the number of NPC in growth medium supplemented with β-FGF and EGF (Wang, Zhang *et al.*, 2007). Approximately 25% more neurospheres were counted in cultures grown in presence of 100 ng/ml CEPO compared to control cultures. Also the size of neurospheres was found to be slightly increased. These results are similar to the findings in cultures grown in presence of 3 nM hS3 which is equivalent to 100 ng/ml hS3. Numbers of neurospheres were not evaluated, but total cell numbers were found to be increased by 25% compared to MOCK cultures. However, CEPO-treatment also increased the number of secondary neurospheres (Wang, Zhang *et al.*, 2007), whereas hS3 provided no significant changes in clonogenicity in the present study, although a weak tendency towards enhanced clonogenicity may exist. Promotion of clonogenicity of NPC was also described for ciliary neurotrophic factor (CNTF) and LIF (Pitman *et al.*, 2004; Shimazaki *et al.*, 2001). But in contrast to CEPO, neurospheres grew to a larger size in the absence of LIF (Pitman *et al.*, 2004). Importantly, differentiation of NSC/NPC in presence of CEPO was not found to decrease cell death (Wang, Zhang *et al.*, 2007). The present study indicates enhanced viability of differentiated cultures in presence of hS3 or after hS3 pretreatment, though noting that apoptosis detection methods have not been applied. In summary, the hS3 may have unlike LIF rather an effect on NSC/NPC survival or proliferation than on NSC/NPC self-renewal. Importantly, a proliferation- and survival-promoting effect on neural progenitor has also been suggested for exogenous ciliary neurotrophic factor (CNTF) *in vivo* (Emsley *et al.*, 2003).

When staining differentiated NSC/NPC cultures no changes were observed in the percentage of generated cells of neuronal phenotype in hEPO treated cultures compared to control cultures. This is in contrast to literature describing enhanced neurogenesis in presence of EPO (Shingo *et al.*, 2001; Studer *et al.*, 2000). Contradictory studies suggest EPO to be more a trophic factor acting on the maintenance of the NSC/NPC population than a differentiation factor for NPC (Chen *et al.*, 2007). The results obtained in NSC/NPC differentiation in this study are in favor for this hypothesis. Furthermore in hEPO treated cultures survival rates of differentiated cells were significantly higher than in control cultures suggesting also a trophic effect of erythropoietin in our model.

For high concentrations of the peptide P16 a trophic effect was observed as well but no differentiation effect on NPC. However the splice variant hS3 additionally promoted astrocyte-like formation. A differentiation promoting effect has also been described for CEPO (Wang, Zhang *et al.*, 2007), but in contrast to hS3 CEPO substantially increased the numbers of neurons but not of astrocytes. Promotion of astrocyte differentiation is quite well known for cytokines binding to the family of LIF receptors, such as LIF (Bonni *et al.*, 1997; Hermanson *et al.*, 2002; Johe *et al.*, 1996) or CNTF (Rajan *et al.*, 1998). Real-time PCR experiments performed on cDNA samples obtained from spheres treated for 4h with hS3 or P16 showed significant upregulation of GFAP-mRNA only in spheres treated with hS3. GFAP mRNA upregulation in neurospheres has also been shown after treatment with 100 ng/ml LIF (Pitman *et al.*, 2004). Indeed, the GFAP promoter contains a consensus binding site for STAT3, a transcription factor directly activated by LIFR signaling (Bonni *et al.*, 1997). For CNTF and LIF, the discrepancy between simultaneous self-renew and glial differentiation effects has been explained by the existence of diverse subpopulations in NSC/NPC. While uncommitted NSC are maintained, differentiation of progenitors is accelerated (Shimazaki *et al.*, 2001).

In summary, the key finding in the present study on NPC are (1) the EPO variants are trophic factors for NPC, (2) the hS3 acts predominantly on the glial lineage and (3) hS3 is not equivalent to CEPO in its functions. These findings are not only important for the question of which receptor mediates the effects of the EPO variants but suggest distinct actions of the different EPO variants on various cell types. The trophic actions and differentiation capacities of hS3 observed *in vitro* might also exist *in vivo* and will be analyzed in future experiments. The human splice variant hS3 might be a new factor promoting regeneration in the adult brain.

5.3.3 EPO variants promote survival of mesenchymal stem cells

Very little is known about EPO effects on mesenchymal stem cells (MSC), multipotent stem cells derived from the bone marrow, that have the capacity to differentiate for example into osteoblasts, chondrocytes or adipocytes.

Only recently, human MSC have been shown by flow cytometry, immunofluorescence and western blot analysis to express the EPOR (Zwezdaryk *et al.*, 2007). In the murine MSC used in our study we could also detect EPOR expression on an mRNA level (data not shown) suggesting that also murine MSC express the $(EPOR)_2$. Zwezdaryk demonstrated for the first time that EPO provides a proliferation effect in serum-starved human donor preparations of MSC. This finding is not consistent with the results obtained in the present study with murine MSC as EPO had no protective effects in serum-starved cultures. However, the splice variant hS3 drastically improved formation of colonies. These controversial results can be explained by the different experimental approaches. In the present study MSC were seeded at very low densities (50 cells/cm^2) compared to high density seeding of approximately 21,000 cells/cm^2 in Zwezdaryk's experiments. Furthermore, cells were directly seeded in low-serum medium whereas in Zwezdaryk's study cells were first allowed to attach before serum-removal. The experimental setup used in the present study is therefore more appropriate to study preservation of colony-formation capacities of single cells under starvation-periods whereas Zwezdaryk's model represents a better setup to study proliferation in dependence on added factors.

Another explanation is the use of different MSC sources. Not only species differences but also variations in preparation and isolation of stem cells have been found to be crucial and make results obtained in the stem cell field difficult to compare.

The interesting new finding in the present study is that the human splice variant hS3 seems to have a protective effect on starved MSC preserving their colony-forming capacities. This could be of use in the field of regenerative medicine where MSC are already employed because of their tissue repair functions and their immunosuppressive activities. MSC appear to have regenerative functions in a variety of tissues, such as liver, pancreatic islets, kidney or lung. Positive effects of MSC have already been shown in clinical trials for example in osteogenesis imperfecta, a genetic disorder of collagen I leading to bone fragility (Horwitz *et al.*, 2002; Horwitz *et al.*, 1999). The human splice variant hS3 might be used in the pre-treatment of MSC cultures in order to improve *in vivo* survival of MSC after infusion. Of course *in vivo* evidence has to be supplied. Moreover, one has to study possible differentiation effects of the hS3 on MSC as EPO has for example been shown to have pro-angiogenic effects on hMSC (Zwezdaryk *et al.*, 2007).

Another application of the hS3 may be the use as cell culture supplement. The expansion of mesenchymal stem cells (MSCs) strongly depends on the culture conditions and requires medium supplemented with 10 – 20% fetal calf serum (FCS) to generate relevant numbers of cells. However, the presence of FCS is a major obstacle for the clinical use of MSC raising potential hazards that cannot be neglected. Thus, the development of serum-free medium for MSC cultivation is of major interest. In our study the hS3 provided protective effects in medium containing very low serum contents. Recently, Invitrogen has launched the serum-free medium STEMPRO® MSC SFM for MSC cultivation. It has to be tested if the human splice variant hS3 may have additional positive effects in serum-free conditions.

5.4 The vEPO receptor

5.4.1 An alternate non-hematopoietic EPOR?

The homodimeric erythropoietin receptor $(EPOR)_2$ is not only expressed by erythroid colony-forming units, but also during CNS development and in the adult brain on neurons, astrocytes and endothelial cells. The importance of the EPO receptor in CNS development was revealed in EPOR knock-out mice. These mice die around embryonic day 13.5 (E13.5) due to severe anemia (Wu *et al.*, 1995). Besides of anemia and defective cardiac development the embryos show extensive apoptosis in fetal liver, endocardium, myocardium and brain by day E12.5 (Yu *et al.*, 2002). As early as E10.5, numbers of neuronal progenitor cells are reduced. Also EPO null mouse embryos have severely smaller and less-developed brains than control animals (Tsai *et al.*, 2006), suggesting an essential role of the EPO-EPOR system for early embryonic development.

The importance of the EPOR in EPO-mediated neuroprotection in cortical neurons cultures was shown by Ruscher *et al.* (Ruscher *et al.*, 2002). Coapplications of EPO with an EPOR blocking antibody or a soluble EPOR (sEPOR) were both able to diminish neuroprotection. These results were confirmed in our study in the OGD model on rat cortical neuronal cultures. Further evidence came from $EPOR^{-/-}$ cortical neurons isolated from knock-out mouse embryos. In the $EPOR^{-/-}$ cultures EPO failed to mediate neuroprotection in contrast to $EPOR^{+/+}$ cultures under hypoxic conditions. (Yu *et al.*, 2002). But although the EPOR has been clearly shown *in vitro* to be involved in EPO mediated neuroprotection, the question about an alternate receptor for EPOR has been raised in the last years.

In 2004, Leist *et al.* (Leist *et al.*, 2004) reported a new erythropoietin analogue (CEPO) missing hematopoietic characteristics and not binding the classical erythropoietin receptor. This brought up the question of an alternate EPO receptor. Only few months later Brines *et al.* suggested (M.

Brines *et al.*, 2004) a heteroreceptor composed of one EPOR chain and the beta common chain as non-hematopoietic receptor mediating EPO protection. *In vivo* evidence for an alternate EPO receptor came from EPOR conditional knockdown mice (Tsai *et al.*, 2006). Endogenous EPO in the adult brain was shown to promote cell proliferation in the subventricular zone (SVZ) and post-stroke neurogenesis. But the EPOR conditional knockdown mice did not display significant differences in infarct size versus control mice when exposed to stroke. Tsai suggested therefore alternative mechanisms underlying the neuroprotective functions of EPO than binding $(EPOR)_2$ on neurons such as increase of cerebral vasculature at infarct sites or upregulation of alternative receptor complexes mediating neuroprotective effects of EPO.

The results obtained in the present study are also in favor of an alternative non-hematopoietic receptor complex mediating neuroprotection, at least neuroprotection conferred by EPO variants. From the stem cell experiments (HPC, NPC), functional differences were deduced between erythropoietin and the human and murine splice forms in spite of nearly identical neuroprotective and cytoprotective characteristics. Therefore the erythropoietin splice variants were supposed not to bind the classical $(EPOR)_2$ involved in erythropoiesis but a so far unknown receptor. This hypothesis was supported by experimental data obtained from mutagenesis experiments of the A-helix, functional assays with an EPOR overexpressing cell line (Baf3/EPOR) and from radioactive displacement experiments (^{125}I-rhEPO).

The heteroreceptor composed of one EpoR chain and the beta common chain, suggested by Brines *et al.*, was therefore considered to be the receptor mediating neuroprotective effects of the EPO splice variants. A Pulldown experiment indeed provided evidence for a direct interaction of mEPO and the EPOR but the murine splice variant mS was neither able to pulldown the EPOR nor the beta common chain. These data suggest that the erythropoietin splice variants may not bind the heteroreceptor although CEPO does. Actually there is evidence for disparate receptor complexes binding CEPO or the erythropoietin splice variants, since they have opposite effects on neural stem cells.

5.4.2 LIFR as receptor candidate for the human splice variant hS3

The unknown receptor mediating the effects of the EPO splice variants was postulated to be a member of the cytokine receptor family. The cytokine superfamily is defined by shared structural feature of both ligands and receptors (Bravo *et al.*, 2000). The ligands share all the ‘four-helix-bundle’ such as EPO, the granulocyte colony-stimulating factor (G-CSF), the interleukins or the ‘gp-130’ cytokines. The receptors are characterized by a cytokine receptor homology domain (CHD) in the extracellular region containing a conserved WSXWS motif

(Bravo *et al.*, 2000). The cytokine receptor family can be classified into the hematopoietic cytokine receptor family, the interferon receptor family, the tumor necrosis factor receptor family and the chemokine receptor family (Boulanger *et al.*, 2004).

Having observed hS3-induced Glial promotion of murine NSC/NPC, members of the leukemia inhibitory factor receptor family (LIFR) were regarded as strong candidates for the unknown receptor. These receptors belong to the gp130 system, a set of ligands and receptors eliciting biological responses via oligomeric receptor complexes containing one or more copies of the common receptor chain gp130 (Bravo *et al.*, 2000). The glycoprotein gp130, also known as CD130, was first identified as signal transducing subunit of the IL-6 receptor. Knockout mice for gp130 are not viable revealing thereby the importance of gp130 as part of many different types of signaling complexes (Yoshida *et al.*, 1996). The LIF receptor subfamily consists of receptor complexes composed of the LIFR α-chain and the gp130 signaling chain and one or two more subunits (Bravo *et al.*, 2000) (Figure 61).

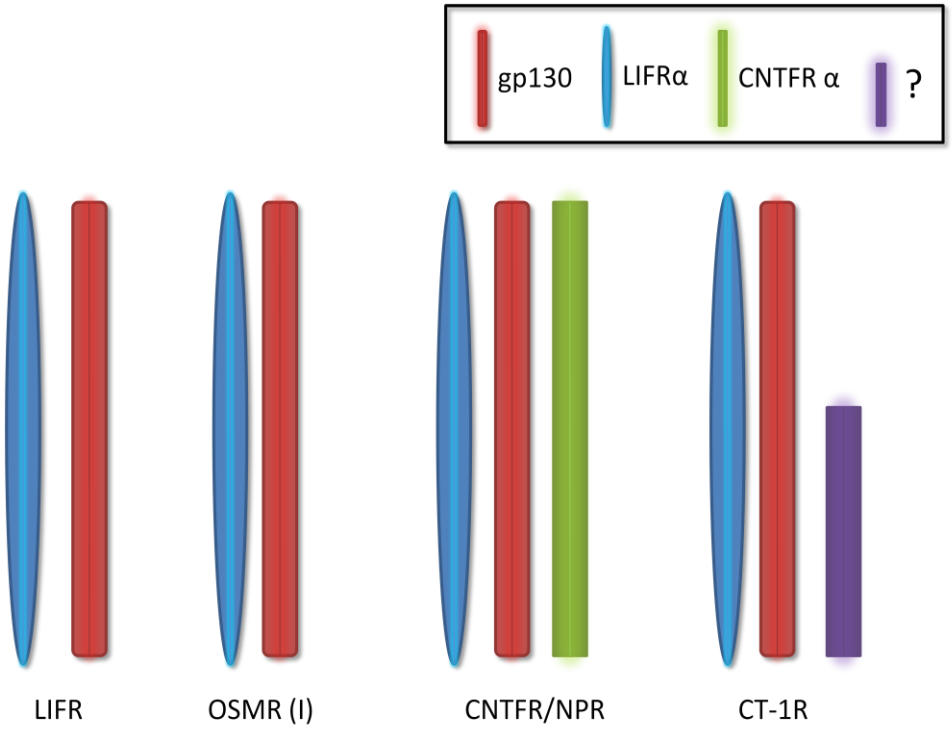

Figure 61: Subunit sharing in the receptors for the LIF-family of cytokines

LIF-specific receptor chains (blue) are present in the receptor complexes for LIF, OSM, CNTF, cardiotrophin-1 (CT-1), Neuropoietin (NP) and Cardiotrophin-like cytokine (CLC). The gp130 receptor subunit (red) is also present in these receptor complexes. OSM can additionally mediate its actions using a second OSMR complex consisting of gp130 and a OSM specific receptor chain (Mosley et al., 1996). CNTF uses the LIFR/gp130 complex after binding first a specific CNTFR α (green). The recently identified Neuropoietin uses also the CNTFR-complex. The receptor for CT-1 is presumably a tripartite receptor (Robledo et al., 1997) with an unknown third chain (violet).

Members of this subfamily are the receptors for LIF (LIFR), oncostatin M (OSMR) (Gearing *et al.*, 1992), ciliary neurotrophic factor (CNTFR) (Ip *et al.*, 1992), cardiotrophin 1 (CT-1R) (Pennica, King *et al.*, 1995), Cardiotrophin-like cytokine (CLCR) (Elson *et al.*, 2000) and the recently described neuropoietin (NPR) (Derouet *et al.*, 2004). The receptor mediating biological activities of LIF consists of the LIFR α-chain, which binds LIF with low affinity, and gp130, which does not itself bind LIF but is essential for high affinity complex formation and signal transduction (Gearing *et al.*, 1992). All cytokines binding to receptors of the LIFR family have multiple biological actions. Shared actions of this cytokine family include *in vitro* and *in vivo* neuroprotective potential and induction of astroglial differentiation of neural progenitor cells (Carpenter *et al.*, 1999; Derouet *et al.*, 2004; Murphy *et al.*, 1991; Ochiai *et al.*, 2001; Ohno *et al.*, 2006; Pennica, Shaw *et al.*, 1995; Rajan *et al.*, 1998; Rose *et al.*, 1994; Uemura *et al.*, 2002; Weiss *et al.*, 2006).

Several findings favor the hypothesis that the unknown receptor mediating the effects of the EPO splice variants is a member of the LIFR family. LIFR pulldown experiments revealed protein-protein interactions of LIFRα-chains derived from different species with the EPO splice variants hS3 and mS. Gp130 isoforms were not captured in these assays. However, this is in congruence with the finding that gp130 also does not bind LIF (Gearing *et al.*, 1992). Furthermore in receptor blocking and receptor competition experiments on primary cortical rat neurons we showed the biological importance of these protein-protein interactions. Both, soluble LIFR and antibodies directed towards the N-termini of the LIFRα-chain and gp130 blocked at least partially hS3-mediated neuroprotection in our OGD-model. Regarding their biological effects, the EPO splice variants fit perfectly into the group of cytokines binding to members of the LIFR family. In addition to neuroprotective and cytoprotective properties, the human splice variant hS3 promoted differentiation of murine NSC/NPC into the astroglial lineage. The signal transduction of hS3 in primary cortical neurons was found to involve Jak2-, Akt- and NF-κB-pathways. These pathways were not only described for EPOR-mediated signaling but also for LIFR-mediated signaling in neuronal cultures (Chang *et al.*, 2004; Middleton *et al.*, 2000).

However, in proliferation assays using murine M1 myeloid leukemic cells growth inhibition after hS3 treatment was found to be much less pronounced than after treatment with mLIF. Although LIF was shown to be the most potent inhibitor of growth of M1 cells, also other cytokines such as IL-6 or OSM share this ability. Half maximal inhibition is achieved with an approximately five time higher concentration of OSM or with an approximately 100 time higher concentration of IL-6 compared to LIF (Bruce *et al.*, 1992). The findings obtained in the present study may exclude the classical dipartite LIFR as receptor mediating the effects of the hS3. Another more

complex receptor involving LIFRα and gp130, such as CNTFR, the CT-1R or an unknown receptor, might be envisioned. However, weaker biological effects can also be explained by differing receptor binding affinities. The commercial mLIF was expressed as a fusion protein with glutathione-S-transferase (GST) in *E.coli* whereas hS3 was expressed as a fusion protein to a His-tag in an eukaryotic HEK cell line. Missing glycosylation might affect receptor binding kinetics as described for EPO (Darling *et al.*, 2002) with unglycosylated EPO having a higher receptor affinity than highly glycosylated EPO. This question might be answered in future radioactive displacement experiments with ^{125}I-LIF and hS3.

In the present study the question whether all identified EPO variants mediate their effects via the same receptor was not answered. The experiments on adult stem cells revealed disparate actions of the splice variant hS3 and the peptide P16. This might be explained by altered receptor binding kinetics or stability. However, the proteins of the EPO family are predicted to have very different tertiary protein structures. This suggests that we might have to deal with a whole non-hematopoietic (v)EPOR family.

5.5 Identification of a new neurotrophic sequence derived from erythropoietin

In 1998, a specific neurotrophic sequence of 17 amino acids within the EPO molecule has been identified which was shown to be neuroprotective but not hematopoietic *in vitro* (Campana *et al.*, 1998). Furthermore, this Epopeptide AB exerted in *vivo* neuroprotective functions when continuously infused over a period of 7 days into the lateral ventricle of Mongolian gerbils in which forebrain ischemia had been induced (Nagao *et al.*, 2005).

The human splice variant hS3 is structurally very interesting in respect to this data. The deleted sequence in hS3 comprises exactly the Epopeptide AB. We postulated therefore the existence of other EPO derived neurotrophic peptides relevant for the action of the splice variants. Comparing the protein structures of all EPO variants the A-helix was found to be the smallest peptide shared by all EPO variants. Thus, the A-helix was suggested to be alone sufficient as a neuroprotective non-hematopoietic EPO analogue. This hypothesis was not only confirmed in the present study but even smaller peptides generated from the N-terminus of the mature A-helix (without signal sequence) were identified as mediators of robust neuroprotection. Peptides P8, P10 and P16 encoding the first 8, 10 or 16 amino acids of the mature A-helix were found to be neuroprotective. The finding of neurotrophic peptides this short is not in conflict to literature as other very short neurotrophic peptides derived from other proteins have also been described. Examples are Prosapide^{TM}D5, a 11-mer derived from prosaposin, that was shown to protect dopaminergic neurons in a model of Parkinson's disease (Liu *et al.*, 2001) or the TrkA-selective

NGF peptidomimetic termed D3 (580 Da), that rescues cholinergic neurons in aged rats (M. A. Bruno *et al.*, 2004). Interestingly, very recently another non-erythropoietic peptide derived from the tertiary structure of erythropoietin has been described (M. Brines *et al.*, 2008). In contrast to the findings in the present study, the helix B and an 11-aa peptide composed of adjacent aminoacids in the helix B were found to be neuroprotective *in vitro* and tissue-protective *in vivo*. Contrary to the A-helix, the B-helix contains no interaction sites with $(EPOR)_2$, but faces the aqueous medium, when EPO is bound to the receptor homodimer. The 11-aa peptide has no sequence similarity to EPO at all, but mimics the external aqueous surface of EPO. The short plasma half-life of approximately 2 min indicates that already a very short contact with the effector is sufficient to promote tissue-protective effects (M. Brines *et al.*, 2008), as already claimed for asialo-EPO (Erbayraktar *et al.*, 2003). Same may be true for the A-helix derived peptides, having presumably plasma half-lifes of the same range. The finding, that also the B-helix mediates tissue-protective effects, complicates the definition of regions within the EPO molecule required for tissue-protection. Furthermore, it adds to the complexity of alternative EPO binding sites.

5.6 Conclusion and outlook

The finding of erythropoietin splice variants is highly interesting in many aspects:

(1) From a scientific view the finding of erythropoietin splice variants is of high importance. The endogenous proteins may play an important role in the organism. In the immunoprecipitation experiments, mEPO and mS were found to be co-upregulated in $CoCl_2$–treated mice. This indicates that the splice variants are induced via the same mechanisms as erythropoietin. Thus, the erythropoietin splice variants may be endogenous antiapoptotic molecules induced at low oxygen pressures in order to prevent or reduce damage to tissue caused by ischemic insults.

(2) In light of the successful separation of hematopoietic and cytoprotective properties of EPO, the existence of a tissue-protective heterodimeric EPO receptor has been suggested (M. Brines *et al.*, 2004). Complexity was added by an *in vivo* study, showing no involvement of the EPOR in protection of neurons from ischemic injury (Tsai *et al.*, 2006). The data of this study suggests an involvement of the LIFRα-chain and the gp130-chain in the tissue-protective receptor complex responsible for the cytoprotective effects of the EPO splice variants. Whether these two components are sufficient to form the ‘vEPO-R’ and whether the ‘vEPO-R’ is identical for all EPO variants remains unclear to this date. It is also to be notes, that other non-hematopoietic EPO variants, such as CEPO, may use alternative binding sites.

(3) The finding of cytoprotective and differentiation effects of the human splice variants hS3 on diverse stem and progenitor cell populations may indicate that the splice variant hS3 has not simply a cytoprotective role in ischemic insults but may also act in repair or regeneration of different tissues. Importantly the hS3 was isolated from fetal human brain mRNA. Thus, hS3 may also play a role in the growth and development of the fetus

(4) The non-erythropoietic EPO variants may be potential drug candidates for the treatment of acute neurological diseases and in particular of chronic neurological diseases as for example Parkinson’s or Huntington’s disease. As discussed earlier the major disadvantage of EPO as protective drug in neurodegenerative diseases is its effect on the formation of red blood cells. This feature required for the treatment of anemia can be a dangerous side-effect in chronic treatment of patients with non-pathological hematocrit levels resulting in changed blood rheologies and an enhanced risk for thromboses and strokes. This side-effect can be precluded for the erythropoietin splice variants as they

were shown to be non-erythropoietic. Focusing on the human splice variant hS3 as being most relevant in a therapeutic aspect, hS3 and hEPO were shown to be equipotent in mediating neuroprotective effects in the *in vitro* model of stroke and in mediating cytoprotective effects in the *in vitro* model of heart ischemia. From these results one can expect the hS3 to be a promising candidate for drug development even if the proof of principle has not been performed *in vivo* yet.

Future work has to be focused on pursuing the characterization of the erythropoietin variants *in vivo.* Besides providing *in vivo* evidence for cytoprotective effects of the EPO variants in animal models, one may also consider to characterize the expression levels of endogenous EPO splice variants under different pathological and non-pathological conditions. Assuming biological relevance of these splice variants it would be worth to analyze alternative splicing of EPO transcripts in evolutionary close species, e.g. rat, monkey or macaque (see: Figure 1). The analysis may indicate the evolutionary split leading to human- and mouse-specific isoforms.

As discussed previously the effects on diverse stem cell populations have to be analyzed in more detail, e.g. signaling pathways in NSC/NPC or effects on megakaryocytes. In view of a possible clinical application, putative immunological effects of the EPO variants have to be investigated.

6 SUMMARY

Erythropoietin (EPO) is a hematopoietic cytokine that functions as the main regulator of erythropoiesis. In the last years EPO was found to have multiple functions outside of the bone marrow. EPO acts as an antiapoptotic and tissue-protective cytokine in multiple *in vitro* and *in vivo* studies. Subcloning and sequencing of human and murine EPO-PCR products led to the discovery of alternative EPO transcripts in this study. Transcripts containing precise deletions between direct repeats were revealed to result from template-switching of the RT-polymerase, whereas the finding of three alternatively spliced transcripts was reproducible in an alternative RT-PCR approach. Two human splice forms, namely hS3 missing exon 3 and hS4 missing the first half of exon 4, were isolated from human brain and kidney polyA+ RNA. From murine tissue RNA I isolated one murine EPO splice variant missing exon 4 (mS). Evidence for the existence of the EPO splice variants on a protein level was provided by immunoprecipitation of two proteins from tissue-extracts of $CoCl_2$-treated mice, corresponding in size to murine EPO and mS.

The human and murine erythropoietin isoforms were expressed as recombinant proteins in mammalian cell lines and analyzed in cell culture assays for erythropoietic and cytoprotective characteristics. In an *in vitro* erythropoiesis assay, based on murine bone marrow, all EPO variants turned out to be non-hematopoietic. Neuroprotective potential was tested in an *in vitro* model of cerebral ischemia consisting of oxygen and glucose deprivation (OGD) in primary cortical cultures of the rat. In this experimental setup all EPO variants were shown to induce tolerance against OGD. Signaling pathways in primary cortical neurons were exemplarily studied for hEPO and hS3 and revealed to be identical. Protein sequence comparison of the murine and human EPO isoforms led to the hypothesis that the A-helix would be sufficient for mediating neuroprotective actions without stimulation of erythropoiesis. This hypothesis was confirmed in this study. Even smaller fragments of the A-helix were shown to be effective leading thereby to the discovery of neuroprotective non-hematopoietic EPO A-helix derived peptides.

The observation, that the EPO variants did not stimulate erythropoiesis but provided cytoprotective functions equivalent to EPO, suggested the existence of an alternative cytoprotection-mediating EPO receptor. Furthermore the EPO variants were shown in a variety of experimental setups not to bind the classical homodimeric $(EPOR)_2$. In this study I provide evidence, that the EPO splice variants mediate neuroprotection through an alternative binding site involving the LIF receptor family.

The second part is focused on putative effects of the EPO variants on adult stem cells. I could show the EPO variants to provide general survival effects on murine hematopoietic, neural and mesenchymal stem cells. Interestingly the hS3 was found to induce additional differentiation effects in neural stem and progenitor cells resulting in enhanced formation of astrocytes.

7 APPENDIX

7.1 List of human and murine EPO variants

Nb.	name	type of deletion	direct repeat	tissue	nucleotide deletion	amino acid deletion
1	hE (WT)	-	-	K + B	-	-
2	hS3	Splice-site (GT-AG)	-	K + B	exon 3	54 – 81
3	h1-4	Repeat (hexamer)	caggcc	K + B	intra-exon 4	87 – 105
4	h1-5	Repeat (triplet)	gcc	K	end exon 3 - half exon 4	77 – 105
5	hS4	Splice-site (GT-AG)	-	K	first half exon 4	83 – 113
6	h1-1	Repeat (tetramer)	ccag	B	half exon 3 - half exon 4	reading frame shift from pos.70; length:87
7	h2-1	Repeat (triplet)	gaa	K	half exon 3 - half exon 5	reading frame shift from pos. 66; length:68
8	mE (WT)	-	-	K + B	-	-
9	mS	Splice-site (GT-AG)	-	K + B	exon4	82 – 141
10	mG3	Repeat (pentamer)	gccaa	K + B	half exon4 - half exon5	110 – 173
11	mG5	Repeat (hexamer)	tctgca	K	intra-exon5	166 – 187
12	m300-1	Repeat (heptamer)	caacttc	B	end exon 3 - half exon5	175 – 174
13	mK3	Repeat (pentamer)	gaagc	K + B	half exon 4- half exon 5	reading frame shift from pos. 100

Table 17: Products from human and murine EPO PCR

List of EPO variants. K=kidney; B=brain; protein nomenclature: 1.Met=1; pos. = position

7.2 Multiple Alignments of human and murine EPO variants (cDNA)

7.2.1 Multiple Alignment of human EPO variants

```
hWT                 ATGGGGGTGCACGAATGTCCTGCCTGGCTGTGGCTTCTCCTGTCCCTGCTGTCGCTCCCT 60
hS3                 ATGGGGGTGCACGAATGTCCTGCCTGGCTGTGGCTTCTCCTGTCCCTGCTGTCGCTCCCT 60
hS4                 ATGGGGGTGCACGAATGTCCTGCCTGGCTGTGGCTTCTCCTGTCCCTGCTGTCGCTCCCT 60
h1-4                ATGGGGGTGCACGAATGTCCTGCCTGGCTGTGGCTTCTCCTGTCCCTGCTGTCGCTCCCT 60
h1-5                ATGGGGGTGCACGAATGTCCTGCCTGGCTGTGGCTTCTCCTGTCCCTGCTGTCGCTCCCT 60
h1-1                ATGGGGGTGCACGAATGTCCTGCCTGGCTGTGGCTTCTCCTGTCCCTGCTGTCGCTCCCT 60
h2-1                ATGGGGGTGCACGAATGTCCTGCCTGGCTGTGGCTTCTCCTGTCCCTGCTGTCGCTCCCT 60
                    ************************************************************

hWT                 CTGGGCCTCCCAGTCCTGGGCGCCCCACCACGCCTCATCTGTGACAGCCGAGTCCTGGAG 120
hS3                 CTGGGCCTCCCAGTCCTGGGCGCCCCACCACGCCTCATCTGTGACAGCCGAGTCCTGGAG 120
hS4                 CTGGGCCTCCCAGTCCTGGGCGCCCCACCACGCCTCATCTGTGACAGCCGAGTCCTGGAG 120
h1-4                CTGGGCCTCCCAGTCCTGGGCGCCCCACCACGCCTCATCTGTGACAGCCGAGTCCTGGAG 120
h1-5                CTGGGCCTCCCAGTCCTGGGCGCCCCACCACGCCTCATCTGTGACAGCCGAGTCCTGGAG 120
h1-1                CTGGGCCTCCCAGTCCTGGGCGCCCCACCACGCCTCATCTGTGACAGCCGAGTCCTGGAG 120
h2-1                CTGGGCCTCCCAGTCCTGGGCGCCCCACCACGCCTCATCTGTGACAGCCGAGTCCTGGAG 120
                    ************************************************************

hWT                 AGGTACCTCTTGGAGGCCAAGGAGGCCGAGAATATCACGACGGGCTGTGCTGAACACTGC 180
hS3                 AGGTACCTCTTGGAGGCCAAGGAGGCCGAGAATATCACG---------------------- 159
hS4                 AGGTACCTCTTGGAGGCCAAGGAGGCCGAGAATATCACGACGGGCTGTGCTGAACACTGC 180
h1-4                AGGTACCTCTTGGAGGCCAAGGAGGCCGAGAATATCACGACGGGCTGTGCTGAACACTGC 180
h1-5                AGGTACCTCTTGGAGGCCAAGGAGGCCGAGAATATCACGACGGGCTGTGCTGAACACTGC 180
h1-1                AGGTACCTCTTGGAGGCCAAGGAGGCCGAGAATATCACGACGGGCTGTGCTGAACACTGC 180
h2-1                AGGTACCTCTTGGAGGCCAAGGAGGCCGAGAATATCACGACGGGCTGTGCTGAACACTGC 180
                    ************************************

hWT                 AGCTTGAATGAGAATATCACTGTCCCAGACACCAAAGTTAATTTCTATGCCTGGAAGAGG 240
hS3                 ------------------------------------------------------------ 159
hS4                 AGCTTGAATGAGAATATCACTGTCCCAGACACCAAAGTTAATTTCTATGCCTGGAAGAGG 240
h1-4                AGCTTGAATGAGAATATCACTGTCCCAGACACCAAAGTTAATTTCTATGCCTGGAAGAGG 240
h1-5                AGCTTGAATGAGAATATCACTGTCCCAGACACCAAAGTTAATTTCTATGCC--------- 231
h1-1                AGCTTGAATGAGAATATCACTGTCCCAG------------------------------- 208
h2-1                AGCTTGAATGAGAA--------------------------------------------- 194

hWT                 ATGGAGGTCGGGCAGCAGGCCGTAGAAGTCTGGCAGGGCCTGGCCCTGCTGTCGGAAGCT 300
hS3                 ------GTCGGGCAGCAGGCCGTAGAAGTCTGGCAGGGCCTGGCCCTGCTGTCGGAAGCT 213
hS4                 ATGGAG---------------------------------------------------- 246
h1-4                ATGGAGGTCGGGCAGCAGGCC------------------------------------- 261
h1-5                ------------------------------------------------------------  -
h1-1                ------------------------------------------------------------  -
h2-1                ------------------------------------------------------------  -
```

```
hWT                 GTCCTGCGGGGCCAGGCCCTGTTGGTCAACTCTTCCCAGCCGTGGGAGCCCCTGCAGCTG 360
hS3                 GTCCTGCGGGGCCAGGCCCTGTTGGTCAACTCTTCCCAGCCGTGGGAGCCCCTGCAGCTG 273
hS4                 ----------------------------------------CCGTGGGAGCCCCTGCAGCTG 267
h1-4                ------------------CTGTTGGTCAACTCTTCCCAGCCGTGGGAGCCCCTGCAGCTG 303
h1-5                ------------------CTGTTGGTCAACTCTTCCCAGCCGTGGGAGCCCCTGCAGCTG 273
h1-1                ---------------GCCCTGTTGGTCAACTCTTCCCAGCCGTGGGAGCCCCTGCAGCTG 253
h2-1                ------------------------------------------------------------  -

hWT                 CATGTGGATAAAGCCGTCAGTGGCCTTCGCAGCCTCACCACTCTGCTTCGGGCTCTGGGA 420
hS3                 CATGTGGATAAAGCCGTCAGTGGCCTTCGCAGCCTCACCACTCTGCTTCGGGCTCTGGGA 333
hS4                 CATGTGGATAAAGCCGTCAGTGGCCTTCGCAGCCTCACCACTCTGCTTCGGGCTCTGGGA 327
h1-4                CATGTGGATAAAGCCGTCAGTGGCCTTCGCAGCCTCACCACTCTGCTTCGGGCTCTGGGA 363
h1-5                CATGTGGATAAAGCCGTCAGTGGCCTTCGCAGCCTCACCACTCTGCTTCGGGCTCTGGGA 333
h1-1                CATGTGGATAAAGCCGTCAGTGGCCTTCGCAGCCTCACCACTCTGCTTCGGGCTCTGGGA 313
h2-1                ------------------------------------------------------------  -

hWT                 GCCCAGAAGGAAGCCATCTCCCCTCCAGATGCGGCCTCAGCTGCTCCACTCCGAACAATC 480
hS3                 GCCCAGAAGGAAGCCATCTCCCCTCCAGATGCGGCCTCAGCTGCTCCACTCCGAACAATC 393
hS4                 GCCCAGAAGGAAGCCATCTCCCCTCCAGATGCGGCCTCAGCTGCTCCACTCCGAACAATC 387
h1-4                GCCCAGAAGGAAGCCATCTCCCCTCCAGATGCGGCCTCAGCTGCTCCACTCCGAACAATC 423
h1-5                GCCCAGAAGGAAGCCATCTCCCCTCCAGATGCGGCCTCAGCTGCTCCACTCCGAACAATC 393
h1-1                GCCCAGAAGGAAGCCATCTCCCCTCCAGATGCGGCCTCAGCTGCTCCACTCCGAACAATC 373
h2-1                ------------------------------------------------------------CAATC 199
                                                                                *****

hWT                 ACTGCTGACACTTTCCGCAAACTCTTCCGAGTCTACTCCAATTTCCTCCGGGGAAAGCTG 540
hS3                 ACTGCTGACACTTTCCGCAAACTCTTCCGAGTCTACTCCAATTTCCTCCGGGGAAAGCTG 453
hS4                 ACTGCTGACACTTTCCGCAAACTCTTCCGAGTCTACTCCAATTTCCTCCGGGGAAAGCTG 447
h1-4                ACTGCTGACACTTTCCGCAAACTCTTCCGAGTCTACTCCAATTTCCTCCGGGGAAAGCTG 483
h1-5                ACTGCTGACACTTTCCGCAAACTCTTCCGAGTCTACTCCAATTTCCTCCGGGGAAAGCTG 453
h1-1                ACTGCTGACACTTTCCGCAAACTCTTCCGAGTCTACTCCAATTTCCTCCGGGGAAAGCTG 433
h2-1                ACTGCTGACACTTTCCGCAAACTCTTCCGAGTCTACTCCAATTTCCTCCGGGGAAAGCTG 259
                    ************************************************************

hWT                 AAGCTGTACACAGGGGAGGCCTGCAGGACAGGGGACAGATGA 582
hS3                 AAGCTGTACACAGGGGAGGCCTGCAGGACAGGGGACAGATGA 495
hS4                 AAGCTGTACACAGGGGAGGCCTGCAGGACAGGGGACAGATGA 489
h1-4                AAGCTGTACACAGGGGAGGCCTGCAGGACAGGGGACAGATGA 525
h1-5                AAGCTGTACACAGGGGAGGCCTGCAGGACAGGGGACAGATGA 495
h1-1                AAGCTGTACACAGGGGAGGCCTGCAGGACAGGGGACAGATGA 475
h2-1                AAGCTGTACACAGGGGAGGCCTGCAGGACAGGGGACAGATGA 301
                    ******************************************
```

Figure 62: Multiple Alignment of cDNA sequences of human EPO variants

7.2.2 Multiple Alignment of murine EPO variants

```
mEPO                ATGGGGGTGCCCGAACGTCCCACCCTGCTGCTTTTACTCTCCTTGCTACTGATTCCTCTG 60
mS                  ATGGGGGTGCCCGAACGTCCCACCCTGCTGCTTTTACTCTCCTTGCTACTGATTCCTCTG 60
mG3                 ATGGGGGTGCCCGAACGTCCCACCCTGCTGCTTTTACTCTCCTTGCTACTGATTCCTCTG 60
mK3                 ATGGGGGTGCCCGAACGTCCCACCCTGCTGCTTTTACTCTCCTTGCTACTGATTCCTCTG 60
m300-1              ATGGGGGTGCCCGAACGTCCCACCCTGCTGCTTTTACTCTCCTTGCTACTGATTCCTCTG 60
mG5                 ATGGGGGTGCCCGAACGTCCCACCCTGCTGCTTTTACTCTCCTTGCTACTGATTCCTCTG 60
                    ************************************************************

mEPO                GGCCTCCCAGTCCTCTGTGCTCCCCCACGCCTCATCTGCGACAGTCGAGTTCTGGAGAGG 120
mS                  GGCCTCCCAGTCCTCTGTGCTCCCCCACGCCTCATCTGCGACAGTCGAGTTCTGGAGAGG 120
mG3                 GGCCTCCCAGTCCTCTGTGCTCCCCCACGCCTCATCTGCGACAGTCGAGTTCTGGAGAGG 120
mK3                 GGCCTCCCAGTCCTCTGTGCTCCCCCACGCCTCATCTGCGACAGTCGAGTTCTGGAGAGG 120
m300-1              GGCCTCCCAGTCCTCTGTGCTCCCCCACGCCTCATCTGCGACAGTCGAGTTCTGGAGAGG 120
mG5                 GGCCTCCCAGTCCTCTGTGCTCCCCCACGCCTCATCTGCGACAGTCGAGTTCTGGAGAGG 120
                    ************************************************************

mEPO                TACATCTTAGAGGCCAAGGAGGCAGAAAATGTCACGATGGGTTGTGCAGAAGGTCCCAGA 180
mS                  TACATCTTAGAGGCCAAGGAGGCAGAAAATGTCACGATGGGTTGTGCAGAAGGTCCCAGA 180
mG3                 TACATCTTAGAGGCCAAGGAGGCAGAAAATGTCACGATGGGTTGTGCAGAAGGTCCCAGA 180
mK3                 TACATCTTAGAGGCCAAGGAGGCAGAAAATGTCACGATGGGTTGTGCAGAAGGTCCCAGA 180
m300-1              TACATCTTAGAGGCCAAGGAGGCAGAAAATGTCACGATGGGTTGTGCAGAAGGTCCCAGA 180
mG5                 TACATCTTAGAGGCCAAGGAGGCAGAAAATGTCACGATGGGTTGTGCAGAAGGTCCCAGA 180
                    ************************************************************

mEPO                CTGAGTGAAAATATTACAGTCCCAGATACCAAAGTCAACTTCTATGCTTGGAAAAGAATG 240
mS                  CTGAGTGAAAATATTACAGTCCCAGATACCAAAGTCAACTTCTATGCTTGGAAAAGAATG 240
mG3                 CTGAGTGAAAATATTACAGTCCCAGATACCAAAGTCAACTTCTATGCTTGGAAAAGAATG 240
mK3                 CTGAGTGAAAATATTACAGTCCCAGATACCAAAGTCAACTTCTATGCTTGGAAAAGAATG 240
m300-1              CTGAGTGAAAATATTACAGTCCCAGATACCAAAGTCAACTTC------------------ 222
mG5                 CTGAGTGAAAATATTACAGTCCCAGATACCAAAGTCAACTTCTATGCTTGGAAAAGAATG 240
                    ****************************************

mEPO                GAGGTGGAAGAACAGGCCATAGAAGTTTGGCAAGGCCTGTCCCTGCTCTCAGAAGCCATC 300
mS                  GAG---------------------------------------------------------- 243
mG3                 GAGGTGGAAGAACAGGCCATAGAAGTTTGGCAAGGCCTGTCCCTGCTCTCAGAAGCCATC 300
mK3                 GAGGTGGAAGAACAGGCCATAGAAGTTTGGCAAGGCCTGTCCCTGCTCTCAGAAGC---- 296
m300-1              ------------------------------------------------------------  -
mG5                 GAGGTGGAAGAACAGGCCATAGAAGTTTGGCAAGGCCTGTCCCTGCTCTCAGAAGCCATC 300

mEPO                CTGCAGGCCCAGGCCCTGCTAGCCAATTCCTCCCAGCCACCAGAGACCCTTCAGCTTCAT 360
mS                  ------------------------------------------------------------  -
mG3                 CTGCAGGCCCAGGCCCTGCTAGCCAA---------------------------------- 326
mK3                 ------------------------------------------------------------  -
m300-1              ------------------------------------------------------------  -
mG5                 CTGCAGGCCCAGGCCCTGCTAGCCAATTCCTCCCAGCCACCAGAGACCCTTCAGCTTCAT 360
```

```
mEPO                ATAGACAAAGCCATCAGTGGTCTACGTAGCCTCACTTCACTGCTTCGGGTACTGGGAGCT 420
mS                  ------------------------------------------------------------  -
mG3                 ------------------------------------------------------------  -
mK3                 ------------------------------------------------------------  -
m300-1              ------------------------------------------------------------  -
mG5                 ATAGACAAAGCCATCAGTGGTCTACGTAGCCTCACTTCACTGCTTCGGGTACTGGGAGCT 420

mEPO                CAGAAGGAATTGATGTCGCCTCCAGATACCACCCCACCTGCTCCACTCCGAACACTCACA 480
mS                  ---AAGGAATTGATGTCGCCTCCAGATACCACCCCACCTGCTCCACTCCGAACACTCACA 300
mG3                 ------------------------------------------------------------  -
mK3                 ------------------------------------------------------------  -
m300-1              ------------------------------------------------------------  -
mG5                 CAGAAGGAATTGATGTCGCCTCCAGATACCACCCCACCTGCTCCACTCCGAACACTCACA 480

mEPO                GTGGATACTTTCTGCAAGCTCTTCCGGGTCTACGCCAACTTCCTCCGGGGGAAACTGAAG 540
mS                  GTGGATACTTTCTGCAAGCTCTTCCGGGTCTACGCCAACTTCCTCCGGGGGAAACTGAAG 360
mG3                 ------------------------------------CTTCCTCCGGGGGAAACTGAAG 348
mK3                 ------------------------------------------------------------ 296
m300-1              -------------------------------------------CTCCGGGGGAAACTGAAG 240
mG5                 GTGGATACTTTCTGCA-------------------------------------------- 496

mEPO                CTGTACACGGGAGAGGTCTGCAGGAGAGGGGACAGGTGA 579
mS                  CTGTACACGGGAGAGGTCTGCAGGAGAGGGGACAGGTGA 399
mG3                 CTGTACACGGGAGAGGTCTGCAGGAGAGGGGACAGGTGA 387
mK3                 -TGTACACGGGAGAGGTCTGCAGGAGAGGGGACAGGTGA 334
m30-1               CTGTACACGGGAGAGGTCTGCAGGAGAGGGGACAGGTGA 279
mG5                 ----------------------GGAGAGGGGACAGGTGA 513
                                           ******************
```

Figure 63: Multiple Alignment of cDNA sequences of murine EPO variants

7.3 Protein Sequences of murine and human EPO variants

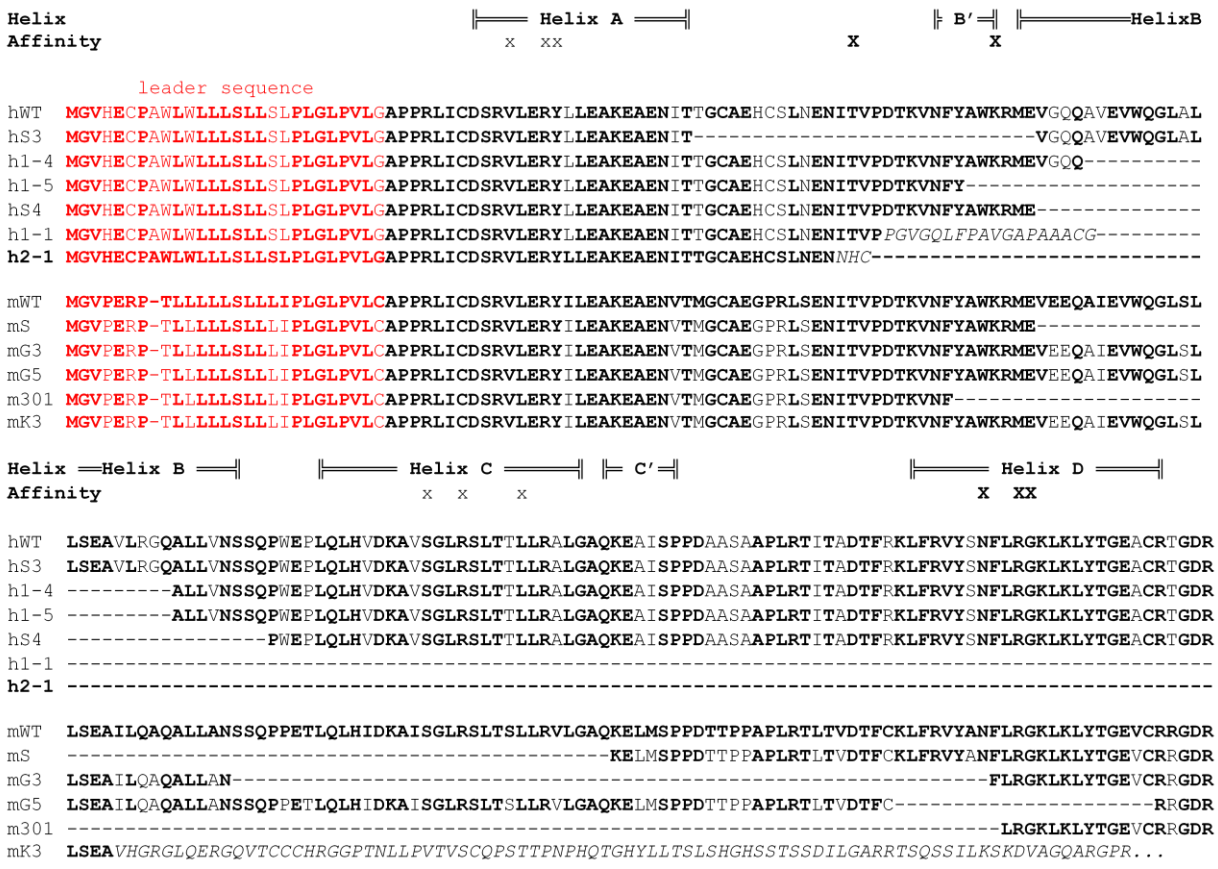

Figure 64: Protein sequence alignment of murine and human EPO variants

The figure shows a comparative alignment of the protein sequences of the murine and human EPO variants. The positions of helices A, B, B', C and D are indicated as horizontal bars. Conserved aminocids between murine and human EPO variants are highlighted (fat). The leader sequence for protein secretion is highlighted in red. The 'x' indicates amino acids involved in high and low affinity binding sites. Italic aminoacids indicate changes in protein sequences due to shifts in open-reading frames.

7.4 Summary: biological activities of the EPO variants and EPO peptides

vEPO	Neuroprotective potential	Hematopoietic potential
hEPO / hWT	+	+
hS3	+	-
hS4	+	-
h1-4	+	-/+ (weak)
h1-5	+	-
h1-1	+ (not significant)	not tested
h2-1	+ (not significant)	not tested
A-helix	+	-
P6 = '-20aa'	-	not tested
P8 (Bachem)	+	not tested
P10 (Bachem)	+	not tested
P12 (Bachem)	-	not tested
P14 (Bachem)	-	not tested
P16 (Bachem) / '-10aa'	+	-
mEPO / mWT	+	+
mS	+	-
mG3	+	-
mG5	+	-/+ (weak)
mK3	not tested	not tested
m301	+	-

Table 18: Summary of hematopoietic and neuroprotective properties of the EPO variants and EPO peptides

8 REFERENCES

AKISU, M., KULLAHCIOGLU GIRGIN, F., BAKA, M., HUSSEYINOV, A., et al. (2001). The role of recombinant human erythropoietin in lipid peroxidation and platelet-activating factor generation in a rat model of necrotizing enterocolitis. *Eur J Pediatr Surg, 11*(3), 167-172.

ANAGNOSTOU, A., LEE, E. S., KESSIMIAN, N., LEVINSON, R., et al. (1990). Erythropoietin has a mitogenic and positive chemotactic effect on endothelial cells. *Proc Natl Acad Sci U S A, 87*(15), 5978-5982.

ANAGNOSTOU, A., LIU, Z., STEINER, M., CHIN, K., et al. (1994). Erythropoietin receptor mRNA expression in human endothelial cells. *Proc Natl Acad Sci U S A, 91*(9), 3974-3978.

ARCASOY, M. O., JIANG, X., & HAROON, Z. A. (2003). Expression of erythropoietin receptor splice variants in human cancer. *Biochem Biophys Res Commun, 307*(4), 999-1007.

ARNOLD, K., BORDOLI, L., KOPP, J., & SCHWEDE, T. (2006). The SWISS-MODEL workspace: a web-based environment for protein structure homology modelling. *Bioinformatics, 22*(2), 195-201.

BERNAUDIN, M., BELLAIL, A., MARTI, H. H., YVON, A., et al. (2000). Neurons and astrocytes express EPO mRNA: oxygen-sensing mechanisms that involve the redox-state of the brain. *Glia, 30*(3), 271-278.

BERNAUDIN, M., MARTI, H. H., ROUSSEL, S., DIVOUX, D., et al. (1999). A potential role for erythropoietin in focal permanent cerebral ischemia in mice. *J Cereb Blood Flow Metab, 19*(6), 643-651.

BODINE, D. M., CROSIER, P. S., & CLARK, S. C. (1991). Effects of hematopoietic growth factors on the survival of primitive stem cells in liquid suspension culture. *Blood, 78*(4), 914-920.

BONNI, A., SUN, Y., NADAL-VICENS, M., BHATT, A., et al. (1997). Regulation of gliogenesis in the central nervous system by the JAK-STAT signaling pathway. *Science, 278*(5337), 477-483.

BOULANGER, M. J., & GARCIA, K. C. (2004). Shared cytokine signaling receptors: structural insights from the gp130 system. *Adv Protein Chem, 68*, 107-146.

BRAVO, J., & HEATH, J. K. (2000). Receptor recognition by gp130 cytokines. *Embo J, 19*(11), 2399-2411.

BREWER, G. J. (1995). Serum-free B27/neurobasal medium supports differentiated growth of neurons from the striatum, substantia nigra, septum, cerebral cortex, cerebellum, and dentate gyrus. *J Neurosci Res, 42*(5), 674-683.

BRINES, M., GRASSO, G., FIORDALISO, F., SFACTERIA, A., et al. (2004). Erythropoietin mediates tissue protection through an erythropoietin and common beta-subunit heteroreceptor. *Proc Natl Acad Sci U S A, 101*(41), 14907-14912.

BRINES, M., PATEL, N. S., VILLA, P., BRINES, C., et al. (2008). Nonerythropoietic, tissue-protective peptides derived from the tertiary structure of erythropoietin. *Proc Natl Acad Sci U S A, 105*(31), 10925-10930.

BRINES, M. L., GHEZZI, P., KEENAN, S., AGNELLO, D., et al. (2000). Erythropoietin crosses the blood-brain barrier to protect against experimental brain injury. *Proc Natl Acad Sci U S A, 97*(19), 10526-10531.

BRUCE, A. G., HOGGATT, I. H., & ROSE, T. M. (1992). Oncostatin M is a differentiation factor for myeloid leukemia cells. *J Immunol, 149*(4), 1271-1275.

BRUNO, E., BRIDDELL, R. A., COOPER, R. J., & HOFFMAN, R. (1991). Effects of recombinant interleukin 11 on human megakaryocyte progenitor cells. *Exp Hematol, 19*(5), 378-381.

BRUNO, M. A., CLARKE, P. B., SELTZER, A., QUIRION, R., et al. (2004). Long-lasting rescue of age-associated deficits in cognition and the CNS cholinergic phenotype by a partial agonist peptidomimetic ligand of TrkA. *J Neurosci, 24*(37), 8009-8018.

CAI, Z., MANALO, D. J., WEI, G., RODRIGUEZ, E. R., et al. (2003). Hearts from rodents exposed to intermittent hypoxia or erythropoietin are protected against ischemia-reperfusion injury. *Circulation, 108*(1), 79-85.

CALVILLO, L., LATINI, R., KAJSTURA, J., LERI, A., et al. (2003). Recombinant human erythropoietin protects the myocardium from ischemia-reperfusion injury and promotes beneficial remodeling. *Proc Natl Acad Sci U S A, 100*(8), 4802-4806.

CAMPANA, W. M., MISASI, R., & O'BRIEN, J. S. (1998). Identification of a neurotrophic sequence in erythropoietin. *Int J Mol Med, 1*(1), 235-241.

CARNOT, P., & DEFLANDRE, C. (1906). Sur l'activité hémopoiétique du sérum au cours de la regénération du sang. *C R Acad Sci (Paris), 143*, 384-386.

CARPENTER, M. K., CUI, X., HU, Z. Y., JACKSON, J., et al. (1999). In vitro expansion of a multipotent population of human neural progenitor cells. *Exp Neurol, 158*(2), 265-278.

CELIK, M., GOKMEN, N., ERBAYRAKTAR, S., AKHISAROGLU, M., et al. (2002). Erythropoietin prevents motor neuron apoptosis and neurologic disability in experimental spinal cord ischemic injury. *Proc Natl Acad Sci U S A, 99*(4), 2258-2263.

CHANG, M. Y., PARK, C. H., SON, H., LEE, Y. S., et al. (2004). Developmental stage-dependent self-regulation of embryonic cortical precursor cell survival and differentiation by leukemia inhibitory factor. *Cell Death Differ, 11*(9), 985-996.

CHEETHAM, J. C., SMITH, D. M., AOKI, K. H., STEVENSON, J. L., et al. (1998). NMR structure of human erythropoietin and a comparison with its receptor bound conformation. *Nat Struct Biol, 5*(10), 861-866.

CHEN, Z. Y., ASAVARITIKRAI, P., PRCHAL, J. T., & NOGUCHI, C. T. (2007). Endogenous erythropoietin signaling is required for normal neural progenitor cell proliferation. *J Biol Chem, 282*(35), 25875-25883.

CHIKUMA, M., MASUDA, S., KOBAYASHI, T., NAGAO, M., et al. (2000). Tissue-specific regulation of erythropoietin production in the murine kidney, brain, and uterus. *Am J Physiol Endocrinol Metab, 279*(6), E1242-1248.

CHOU, C. F., TOHARI, S., BRENNER, S., & VENKATESH, B. (2004). Erythropoietin gene from a teleost fish, Fugu rubripes. *Blood, 104*(5), 1498-1503.

D'ANDREA, A. D., LODISH, H. F., & WONG, G. G. (1989). Expression cloning of the murine erythropoietin receptor. *Cell, 57*(2), 277-285.

DARLING, R. J., KUCHIBHOTLA, U., GLAESNER, W., MICANOVIC, R., et al. (2002). Glycosylation of erythropoietin affects receptor binding kinetics: role of electrostatic interactions. *Biochemistry, 41*(49), 14524-14531.

DEROUET, D., ROUSSEAU, F., ALFONSI, F., FROGER, J., et al. (2004). Neuropoietin, a new IL-6-related cytokine signaling through the ciliary neurotrophic factor receptor. *Proc Natl Acad Sci U S A, 101*(14), 4827-4832.

DEXTER, T. M., ALLEN, T. D., & LAJTHA, L. G. (1977). Conditions controlling the proliferation of haemopoietic stem cells in vitro. *J Cell Physiol, 91*(3), 335-344.

DIGICAYLIOGLU, M., & LIPTON, S. A. (2001). Erythropoietin-mediated neuroprotection involves cross-talk between Jak2 and NF-kappaB signalling cascades. *Nature, 412*(6847), 641-647.

DIRNAGL, U., IADECOLA, C., & MOSKOWITZ, M. A. (1999). Pathobiology of ischaemic stroke: an integrated view. *Trends Neurosci, 22*(9), 391-397.

DUBE, S., FISHER, J. W., & POWELL, J. S. (1988). Glycosylation at specific sites of erythropoietin is essential for biosynthesis, secretion, and biological function. *J Biol Chem, 263*(33), 17516-17521.

DURAND, C., & DZIERZAK, E. (2005). Embryonic beginnings of adult hematopoietic stem cells. *Haematologica, 90*(1), 100-108.

EGRIE, J. C., & BROWNE, J. K. (2001). Development and characterization of novel erythropoiesis stimulating protein (NESP). *Br J Cancer, 84 Suppl 1*, 3-10.

EHRENREICH, H., HASSELBLATT, M., DEMBOWSKI, C., CEPEK, L., et al. (2002). Erythropoietin therapy for acute stroke is both safe and beneficial. *Mol Med, 8*(8), 495-505.

EHRENREICH, H., HINZE-SELCH, D., STAWICKI, S., AUST, C., et al. (2007). Improvement of cognitive functions in chronic schizophrenic patients by recombinant human erythropoietin. *Mol Psychiatry 12*, 206-220.

ELSON, G. C., LELIEVRE, E., GUILLET, C., CHEVALIER, S., et al. (2000). CLF associates with CLC to form a functional heteromeric ligand for the CNTF receptor complex. *Nat Neurosci, 3*(9), 867-872.

EMSLEY, J. G., & HAGG, T. (2003). Endogenous and exogenous ciliary neurotrophic factor enhances forebrain neurogenesis in adult mice. *Exp Neurol, 183*(2), 298-310.

EOM, T. Y., ROTH, K. A., & JOPE, R. S. (2007). Neural precursor cells are protected from apoptosis induced by trophic factor withdrawal or genotoxic stress by inhibitors of glycogen synthase kinase 3. *J Biol Chem, 282*(31), 22856-22864.

ERBAYRAKTAR, S., GRASSO, G., SFACTERIA, A., XIE, Q. W., et al. (2003). Asialoerythropoietin is a nonerythropoietic cytokine with broad neuroprotective activity in vivo. *Proc Natl Acad Sci U S A, 100*(11), 6741-6746.

FANDREY, J., & BUNN, H. F. (1993). In vivo and in vitro regulation of erythropoietin mRNA: measurement by competitive polymerase chain reaction. *Blood, 81*(3), 617-623.

FANG, X., YU, S., EDER, A., MAO, M., et al. (1999). Regulation of BAD phosphorylation at serine 112 by the Ras-mitogen-activated protein kinase pathway. *Oncogene, 18*(48), 6635-6640.

FIORDALISO, F., CHIMENTI, S., STASZEWSKY, L., BAI, A., et al. (2005). A nonerythropoietic derivative of erythropoietin protects the myocardium from ischemia-reperfusion injury. *Proc Natl Acad Sci U S A, 102*(6), 2046-2051.

GEARING, D. P., COMEAU, M. R., FRIEND, D. J., GIMPEL, S. D., et al. (1992). The IL-6 signal transducer, gp130: an oncostatin M receptor and affinity converter for the LIF receptor. *Science, 255*(5050), 1434-1437.

GUEX, N., & PEITSCH, M. C. (1997). SWISS-MODEL and the Swiss-PdbViewer: an environment for comparative protein modeling. *Electrophoresis, 18*(15), 2714-2723.

HAYAKAWA, T., WADA, M., MIZUNO, K., ABE, S., et al. (1992). In vivo biological activities of recombinant human erythropoietin analogues produced by CHO cells, BHK cells and C127 cells. *Biologicals, 20*(4), 253-257.

HE, T. C., JIANG, N., ZHUANG, H., & WOJCHOWSKI, D. M. (1995). Erythropoietin-induced recruitment of Shc via a receptor phosphotyrosine-independent, Jak2-associated pathway. *J Biol Chem, 270*(19), 11055-11061.

HERMANSON, O., JEPSEN, K., & ROSENFELD, M. G. (2002). N-CoR controls differentiation of neural stem cells into astrocytes. *Nature, 419*(6910), 934-939.

HORWITZ, E. M., GORDON, P. L., KOO, W. K., MARX, J. C., et al. (2002). Isolated allogeneic bone marrow-derived mesenchymal cells engraft and stimulate growth in children with osteogenesis imperfecta: Implications for cell therapy of bone. *Proc Natl Acad Sci U S A, 99*(13), 8932-8937.

HORWITZ, E. M., PROCKOP, D. J., FITZPATRICK, L. A., KOO, W. W., et al. (1999). Transplantability and therapeutic effects of bone marrow-derived mesenchymal cells in children with osteogenesis imperfecta. *Nat Med, 5*(3), 309-313.

HUANG, L. E., GU, J., SCHAU, M., & BUNN, H. F. (1998). Regulation of hypoxia-inducible factor 1alpha is mediated by an O2-dependent degradation domain via the ubiquitin-proteasome pathway. *Proc Natl Acad Sci U S A, 95*(14), 7987-7992.

IMAMURA, R., ISAKA, Y., ICHIMARU, N., TAKAHARA, S., et al. (2007). Carbamylated erythropoietin protects the kidneys from ischemia-reperfusion injury without stimulating erythropoiesis. *Biochem Biophys Res Commun, 353*(3), 786-792.

IMIELA, J., KORCZAK-KOWALSKA, G., MALECKI, R., NOWACZYK, M., et al. (1993). Immunomodulatory action of human recombinant erythropoietin in man. *Immunol Lett, 35*(3), 271-275.

IP, N. Y., NYE, S. H., BOULTON, T. G., DAVIS, S., et al. (1992). CNTF and LIF act on neuronal cells via shared signaling pathways that involve the IL-6 signal transducing receptor component gp130. *Cell, 69*(7), 1121-1132.

JACOBS, K., SHOEMAKER, C., RUDERSDORF, R., NEILL, S. D., et al. (1985). Isolation and characterization of genomic and cDNA clones of human erythropoietin. *Nature, 313*(6005), 806-810.

JELKMANN, W. (1992). Erythropoietin: structure, control of production, and function. *Physiol Rev, 72*(2), 449-489.

JOHE, K. K., HAZEL, T. G., MULLER, T., DUGICH-DJORDJEVIC, M. M., et al. (1996). Single factors direct the differentiation of stem cells from the fetal and adult central nervous system. *Genes Dev, 10*(24), 3129-3140.

JONES, S. S., D'ANDREA, A. D., HAINES, L. L., & WONG, G. G. (1990). Human erythropoietin receptor: cloning, expression, and biologic characterization. *Blood, 76*(1), 31-35.

JUBINSKY, P. T., KRIJANOVSKI, O. I., NATHAN, D. G., TAVERNIER, J., et al. (1997). The beta chain of the interleukin-3 receptor functionally associates with the erythropoietin receptor. *Blood, 90*(5), 1867-1873.

JUNK, A. K., MAMMIS, A., SAVITZ, S. I., SINGH, M., et al. (2002). Erythropoietin administration protects retinal neurons from acute ischemia-reperfusion injury. *Proc Natl Acad Sci U S A, 99*(16), 10659-10664.

KASHII, Y., UCHIDA, M., KIRITO, K., TANAKA, M., et al. (2000). A member of Forkhead family transcription factor, FKHRL1, is one of the downstream molecules of phosphatidylinositol 3-kinase-Akt activation pathway in erythropoietin signal transduction. *Blood, 96*(3), 941-949.

KATZ, O., GIL, L., LIFSHITZ, L., PRUTCHI-SAGIV, S., et al. (2007). Erythropoietin enhances immune responses in mice. *Eur J Immunol, 37*(6), 1584-1593.

KESTLER, D. P., GOLDSTEIN, K. M., AGARWAL, S., FUHR, J. E., et al. (1999). Hematopoietic differentiation activity of a recombinant human interleukin-6 (IL-6) isoform resulting from alternatively spliced deletion of the second exon. *Am J Hematol, 61*(3), 169-177.

KOLF, C. M., CHO, E., & TUAN, R. S. (2007). Mesenchymal stromal cells. Biology of adult mesenchymal stem cells: regulation of niche, self-renewal and differentiation. *Arthritis Res Ther, 9*(1), 204.

KOPP, J., & SCHWEDE, T. (2004). The SWISS-MODEL Repository of annotated three-dimensional protein structure homology models. *Nucleic Acids Res, 32*(Database issue), D230-234.

KORFHAGE, C., FISCH;E., SCHRÖDER-STUMBERGER, I., & OELMÜLLER, U. (2000). Solving difficult template problems in RT-PCR. *Qiagen News 1*, 12-14.

KOURY, M. J., & BONDURANT, M. C. (1988). Maintenance by erythropoietin of viability and maturation of murine erythroid precursor cells. *J Cell Physiol, 137*(1), 65-74.

KRIVENTSEVA, E. V., KOCH, I., APWEILER, R., VINGRON, M., et al. (2003). Increase of functional diversity by alternative splicing. *Trends Genet, 19*(3), 124-128.

LASKY, L. C., MCCULLOUGH, J., & ZANJANI, E. D. (1986). Liquid storage of unseparated human bone marrow. Evaluation of hematopoietic progenitors by clonal assay. *Transfusion, 26*(4), 331-334.

LEIST, M., GHEZZI, P., GRASSO, G., BIANCHI, R., et al. (2004). Derivatives of erythropoietin that are tissue protective but not erythropoietic. *Science, 305*(5681), 239-242.

LIU, J., WANG, C. Y., & O'BRIEN, J. S. (2001). Prosaptide D5, a retro-inverso 11-mer peptidomimetic, rescued dopaminergic neurons in a model of Parkinson's disease. *Faseb J, 15*(6), 1080-1082.

MADER, R. M., SCHMIDT, W. M., SEDIVY, R., RIZOVSKI, B., et al. (2001). Reverse transcriptase template switching during reverse transcriptase-polymerase chain reaction: artificial generation of deletions in ribonucleotide reductase mRNA. *J Lab Clin Med, 137*(6), 422-428.

MANNA, P. R., JOSHI, L., REINHOLD, V. N., AUBERT, M. L., et al. (2002). Synthesis, purification and structural and functional characterization of recombinant form of a common genetic variant of human luteinizing hormone. *Hum Mol Genet, 11*(3), 301-315.

MARTI, H. H. (2004). Erythropoietin and the hypoxic brain. *J Exp Biol, 207*(Pt 18), 3233-3242.

MARTI, H. H., BERNAUDIN, M., PETIT, E., & BAUER, C. (2000). Neuroprotection and Angiogenesis: Dual Role of Erythropoietin in Brain Ischemia. *News Physiol Sci, 15*, 225-229.

MARTI, H. H., WENGER, R. H., RIVAS, L. A., STRAUMANN, U., et al. (1996). Erythropoietin gene expression in human, monkey and murine brain. *Eur J Neurosci, 8*(4), 666-676.

MATSUMOTO, S., IKURA, K., UEDA, M., & SASAKI, R. (1995). Characterization of a human glycoprotein (erythropoietin) produced in cultured tobacco cells. *Plant Mol Biol, 27*(6), 1163-1172.

METCALF, D., HILTON, D., & NICOLA, N. A. (1991). Leukemia inhibitory factor can potentiate murine megakaryocyte production in vitro. *Blood, 77*(10), 2150-2153.

MIDDLETON, G., HAMANOUE, M., ENOKIDO, Y., WYATT, S., et al. (2000). Cytokine-induced nuclear factor kappa B activation promotes the survival of developing neurons. *J Cell Biol, 148*(2), 325-332.

MIYAKE, T., KUNG, C. K., & GOLDWASSER, E. (1977). Purification of human erythropoietin. *J Biol Chem, 252*(15), 5558-5564.

MONTESINO, R., TOLEDO, J. R., SANCHEZ, O., SANCHEZ, A., et al. (2008). Monosialylated biantennary N-glycoforms containing GalNAc-GlcNAc antennae predominate when human EPO is expressed in goat milk. *Arch Biochem Biophys, 470*(2), 163-175.

MORISHITA, E., MASUDA, S., NAGAO, M., YASUDA, Y., et al. (1997). Erythropoietin receptor is expressed in rat hippocampal and cerebral cortical neurons, and erythropoietin prevents in vitro glutamate-induced neuronal death. *Neuroscience, 76*(1), 105-116.

MOSLEY, B., DE IMUS, C., FRIEND, D., BOIANI, N., et al. (1996). Dual oncostatin M (OSM) receptors. Cloning and characterization of an alternative signaling subunit conferring OSM-specific receptor activation. *J Biol Chem, 271*(51), 32635-32643.

MURPHY, M., REID, K., HILTON, D. J., & BARTLETT, P. F. (1991). Generation of sensory neurons is stimulated by leukemia inhibitory factor. *Proc Natl Acad Sci U S A, 88*(8), 3498-3501.

NAGAO, M., WEN, T. C., OKAMOTO, M., IRIE, K., et al. (2005). In vivo neuroprotective activity of Epopeptide AB against ischemic damage. *Cytotech, 47*, 139-144.

NARHI, L. O., ARAKAWA, T., AOKI, K. H., ELMORE, R., et al. (1991). The effect of carbohydrate on the structure and stability of erythropoietin. *J Biol Chem, 266*(34), 23022-23026.

NEBEN, S., DONALDSON, D., SIEFF, C., MAUCH, P., et al. (1994). Synergistic effects of interleukin-11 with other growth factors on the expansion of murine hematopoietic progenitors and maintenance of stem cells in liquid culture. *Exp Hematol, 22*(4), 353-359.

NIWA, H., YAMAMURA, K., & MIYAZAKI, J. (1991). Efficient selection for high-expression transfectants with a novel eukaryotic vector. *Gene, 108*(2), 193-199.

NURTDINOV, R. N., ARTAMONOVA, II, MIRONOV, A. A., & GELFAND, M. S. (2003). Low conservation of alternative splicing patterns in the human and mouse genomes. *Hum Mol Genet, 12*(11), 1313-1320.

OCHIAI, W., YANAGISAWA, M., TAKIZAWA, T., NAKASHIMA, K., et al. (2001). Astrocyte differentiation of fetal neuroepithelial cells involving cardiotrophin-1-induced activation of STAT3. *Cytokine, 14*(5), 264-271.

OHNO, M., & ABE, T. (1991). Rapid colorimetric assay for the quantification of leukemia inhibitory factor (LIF) and interleukin-6 (IL-6). *J Immunol Methods, 145*(1-2), 199-203.

OHNO, M., KOHYAMA, J., NAMIHIRA, M., SANOSAKA, T., et al. (2006). Neuropoietin induces neuroepithelial cells to differentiate into astrocytes via activation of STAT3. *Cytokine, 36*(1-2), 17-22.

OKAZAKI, Y., FURUNO, M., KASUKAWA, T., ADACHI, J., et al. (2002). Analysis of the mouse transcriptome based on functional annotation of 60,770 full-length cDNAs. *Nature, 420*(6915), 563-573.

PARSA, C. J., MATSUMOTO, A., KIM, J., RIEL, R. U., et al. (2003). A novel protective effect of erythropoietin in the infarcted heart. *J Clin Invest, 112*(7), 999-1007.

PEITSCH, M. C. (1995). Protein modeling by E-mail. *Bio/Technology 13*, 658-660.

PENNICA, D., KING, K. L., SHAW, K. J., LUIS, E., et al. (1995). Expression cloning of cardiotrophin 1, a cytokine that induces cardiac myocyte hypertrophy. *Proc Natl Acad Sci U S A, 92*(4), 1142-1146.

PENNICA, D., SHAW, K. J., SWANSON, T. A., MOORE, M. W., et al. (1995). Cardiotrophin-1. Biological activities and binding to the leukemia inhibitory factor receptor/gp130 signaling complex. *J Biol Chem, 270*(18), 10915-10922.

PESCHLE, C., MARONE, G., GENOVESE, A., CILLO, C., et al. (1975). Erythropoietin production by the liver in fetal-neonatal life. *Life Sci, 17*(8), 1325-1330.

PETERS, S. O., KITTLER, E. L., RAMSHAW, H. S., & QUESENBERRY, P. J. (1996). Ex vivo expansion of murine marrow cells with interleukin-3 (IL-3), IL-6, IL-11, and stem cell factor leads to impaired engraftment in irradiated hosts. *Blood, 87*(1), 30-37.

PITMAN, M., EMERY, B., BINDER, M., WANG, S., et al. (2004). LIF receptor signaling modulates neural stem cell renewal. *Mol Cell Neurosci, 27*(3), 255-266.

PRASS, K., RUSCHER, K., KARSCH, M., ISAEV, N., et al. (2002). Desferrioxamine induces delayed tolerance against cerebral ischemia in vivo and in vitro. *J Cereb Blood Flow Metab, 22*(5), 520-525.

RAJAN, P., & MCKAY, R. D. (1998). Multiple routes to astrocytic differentiation in the CNS. *J Neurosci, 18*(10), 3620-3629.

RATAJCZAK, M. Z., ZUBA-SURMA, E. K., MACHALINSKI, B., & KUCIA, M. (2007). Bone-marrow-derived stem cells--our key to longevity? *J Appl Genet, 48*(4), 307-319.

REMY, I., WILSON, I. A., & MICHNICK, S. W. (1999). Erythropoietin receptor activation by a ligand-induced conformation change. *Science, 283*(5404), 990-993.

REUTER, C. W., MORGAN, M. A., & BERGMANN, L. (2000). Targeting the Ras signaling pathway: a rational, mechanism-based treatment for hematologic malignancies? *Blood, 96*(5), 1655-1669.

ROBLEDO, O., FOURCIN, M., CHEVALIER, S., GUILLET, C., et al. (1997). Signaling of the cardiotrophin-1 receptor. Evidence for a third receptor component. *J Biol Chem, 272*(8), 4855-4863.

ROEDER, I., DE HAAN, G., ENGEL, C., NIJHOF, W., et al. (1998). Interactions of erythropoietin, granulocyte colony-stimulating factor, stem cell factor, and interleukin-11 on murine hematopoiesis during simultaneous administration. *Blood, 91*(9), 3222-3229.

ROSE, T. M., WEIFORD, D. M., GUNDERSON, N. L., & BRUCE, A. G. (1994). Oncostatin M (OSM) inhibits the differentiation of pluripotent embryonic stem cells in vitro. *Cytokine, 6*(1), 48-54.

ROSSERT, J., & ECKARDT, K. U. (2005). Erythropoietin receptors: their role beyond erythropoiesis. *Nephrol Dial Transplant, 20*(6), 1025-1028.

RUSCHER, K., FREYER, D., KARSCH, M., ISAEV, N., et al. (2002). Erythropoietin is a paracrine mediator of ischemic tolerance in the brain: evidence from an in vitro model. *J Neurosci, 22*(23), 10291-10301.

SAITOU, N., & NEI, M. (1987). The neighbor-joining method: a new method for reconstructing phylogenetic trees. *Mol Biol Evol, 4*(4), 406-425.

SAKANAKA, M., WEN, T. C., MATSUDA, S., MASUDA, S., et al. (1998). In vivo evidence that erythropoietin protects neurons from ischemic damage. *Proc Natl Acad Sci U S A, 95*(8), 4635-4640.

SALMONSON, T. (1990). Pharmacokinetic and pharmacodynamic studies on recombinant human erythropoietin. *Scand J Urol Nephrol Suppl, 129*, 1-66.

SARAY, A., OZAKPINAR, R., KOC, C., SEREL, S., et al. (2003). Effect of chronic and short-term erythropoietin treatment on random flap survival in rats: an experimental study. *Laryngoscope, 113*(1), 85-89.

SAVINO, C., PEDOTTI, R., BAGGI, F., UBIALI, F., et al. (2006). Delayed administration of erythropoietin and its non-erythropoietic derivatives ameliorates chronic murine autoimmune encephalomyelitis. *J Neuroimmunol, 172*(1-2), 27-37.

SAWYER, S. T., KRANTZ, S. B., & LUNA, J. (1987). Identification of the receptor for erythropoietin by cross-linking to Friend virus-infected erythroid cells. *Proc Natl Acad Sci U S A, 84*(11), 3690-3694.

SCHUSTER, S. J., WILSON, J. H., ERSLEV, A. J., & CARO, J. (1987). Physiologic regulation and tissue localization of renal erythropoietin messenger RNA. *Blood, 70*(1), 316-318.

SCHWEDE, T., KOPP, J., GUEX, N., & PEITSCH, M. C. (2003). SWISS-MODEL: An automated protein homology-modeling server. *Nucleic Acids Res, 31*(13), 3381-3385.

SEMENZA, G. L., NEJFELT, M. K., CHI, S. M., & ANTONARAKIS, S. E. (1991). Hypoxia-inducible nuclear factors bind to an enhancer element located 3' to the human erythropoietin gene. *Proc Natl Acad Sci U S A, 88*(13), 5680-5684.

SEMENZA, G. L., & WANG, G. L. (1992). A nuclear factor induced by hypoxia via de novo protein synthesis binds to the human erythropoietin gene enhancer at a site required for transcriptional activation. *Mol Cell Biol, 12*(12), 5447-5454.

SHIMAZAKI, T., SHINGO, T., & WEISS, S. (2001). The ciliary neurotrophic factor/leukemia inhibitory factor/gp130 receptor complex operates in the maintenance of mammalian forebrain neural stem cells. *J Neurosci, 21*(19), 7642-7653.

SHINGO, T., SOROKAN, S. T., SHIMAZAKI, T., & WEISS, S. (2001). Erythropoietin regulates the in vitro and in vivo production of neuronal progenitors by mammalian forebrain neural stem cells. *J Neurosci, 21*(24), 9733-9743.

SILVA, M., BENITO, A., SANZ, C., PROSPER, F., et al. (1999). Erythropoietin can induce the expression of bcl-x(L) through Stat5 in erythropoietin-dependent progenitor cell lines. *J Biol Chem, 274*(32), 22165-22169.

SINOR, A. D., & GREENBERG, D. A. (2000). Erythropoietin protects cultured cortical neurons, but not astroglia, from hypoxia and AMPA toxicity. *Neurosci Lett, 290*(3), 213-215.

SIREN, A. L., FRATELLI, M., BRINES, M., GOEMANS, C., et al. (2001). Erythropoietin prevents neuronal apoptosis after cerebral ischemia and metabolic stress. *Proc Natl Acad Sci U S A, 98*(7), 4044-4049.

SPIVAK, J. L., SMITH, R. R., & IHLE, J. N. (1985). Interleukin 3 promotes the in vitro proliferation of murine pluripotent hematopoietic stem cells. *J Clin Invest, 76*(4), 1613-1621.

STUDER, L., CSETE, M., LEE, S. H., KABBANI, N., et al. (2000). Enhanced proliferation, survival, and dopaminergic differentiation of CNS precursors in lowered oxygen. *J Neurosci, 20*(19), 7377-7383.

STUTE, N., HOLTZ, K., BUBENHEIM, M., LANGE, C., et al. (2004). Autologous serum for isolation and expansion of human mesenchymal stem cells for clinical use. *Exp Hematol, 32*(12), 1212-1225.

SYED, R. S., REID, S. W., LI, C., CHEETHAM, J. C., et al. (1998). Efficiency of signalling through cytokine receptors depends critically on receptor orientation. *Nature, 395*(6701), 511-516.

SYTKOWSKI, A. J., FELDMAN, L., & ZURBUCH, D. J. (1991). Biological activity and structural stability of N-deglycosylated recombinant human erythropoietin. *Biochem Biophys Res Commun, 176*(2), 698-704.

TANAKA, R., KATAYAMA, N., OHISHI, K., MAHMUD, N., et al. (1995). Accelerated cell-cycling of hematopoietic progenitor cells by growth factors. *Blood, 86*(1), 73-79.

TISDALE, J. F., HANAZONO, Y., SELLERS, S. E., AGRICOLA, B. A., et al. (1998). Ex vivo expansion of genetically marked rhesus peripheral blood progenitor cells results in diminished long-term repopulating ability. *Blood, 92*(4), 1131-1141.

TSAI, P. T., OHAB, J. J., KERTESZ, N., GROSZER, M., et al. (2006). A critical role of erythropoietin receptor in neurogenesis and post-stroke recovery. *J Neurosci, 26*(4), 1269-1274.

TSUDA, E., KAWANISHI, G., UEDA, M., MASUDA, S., et al. (1990). The role of carbohydrate in recombinant human erythropoietin. *Eur J Biochem, 188*(2), 405-411.

TURNLEY, A. M., & BARTLETT, P. F. (2000). Cytokines that signal through the leukemia inhibitory factor receptor-beta complex in the nervous system. *J Neurochem, 74*(3), 889-899.

UEMURA, A., TAKIZAWA, T., OCHIAI, W., YANAGISAWA, M., et al. (2002). Cardiotrophin-like cytokine induces astrocyte differentiation of fetal neuroepithelial cells via activation of STAT3. *Cytokine, 18*(1), 1-7.

WANG, J., TANG, Z. Y., KA, W., SUN, D., et al. (2007). Synergistic effect of cytokines EPO, IL-3 and SCF on the proliferation, differentiation and apoptosis of erythroid progenitor cells. *Clin Hemorheol Microcirc, 37*(4), 291-299.

WANG, L., ZHANG, Z., WANG, Y., ZHANG, R., et al. (2004). Treatment of stroke with erythropoietin enhances neurogenesis and angiogenesis and improves neurological function in rats. *Stroke, 35*(7), 1732-1737.

WANG, L., ZHANG, Z. G., GREGG, S. R., ZHANG, R. L., et al. (2007). The Sonic hedgehog pathway mediates carbamylated erythropoietin-enhanced proliferation and differentiation of adult neural progenitor cells. *J Biol Chem, 282*(44), 32462-32470.

WATOWICH, S. S., HILTON, D. J., & LODISH, H. F. (1994). Activation and inhibition of erythropoietin receptor function: role of receptor dimerization. *Mol Cell Biol, 14*(6), 3535-3549.

WEISHAUPT, J. H., ROHDE, G., POLKING, E., SIREN, A. L., et al. (2004). Effect of erythropoietin axotomy-induced apoptosis in rat retinal ganglion cells. *Invest Ophthalmol Vis Sci, 45*(5), 1514-1522.

WEISS, T. W., SAMSON, A. L., NIEGO, B., DANIEL, P. B., et al. (2006). Oncostatin M is a neuroprotective cytokine that inhibits excitotoxic injury in vitro and in vivo. *Faseb J, 20*(13), 2369-2371.

WEN, D., BOISSEL, J. P., SHOWERS, M., RUCH, B. C., et al. (1994). Erythropoietin structure-function relationships. Identification of functionally important domains. *J Biol Chem, 269*(36), 22839-22846.

WEN, D., BOISSEL, J. P., TRACY, T. E., GRUNINGER, R. H., et al. (1993). Erythropoietin structure-function relationships: high degree of sequence homology among mammals. *Blood, 82*(5), 1507-1516.

WITTHUHN, B. A., QUELLE, F. W., SILVENNOINEN, O., YI, T., et al. (1993). JAK2 associates with the erythropoietin receptor and is tyrosine phosphorylated and activated following stimulation with erythropoietin. *Cell, 74*(2), 227-236.

WU, H., LIU, X., JAENISCH, R., & LODISH, H. F. (1995). Generation of committed erythroid BFU-E and CFU-E progenitors does not require erythropoietin or the erythropoietin receptor. *Cell, 83*(1), 59-67.

YANG, C. W., LI, C., JUNG, J. Y., SHIN, S. J., et al. (2003). Preconditioning with erythropoietin protects against subsequent ischemia-reperfusion injury in rat kidney. *Faseb J, 17*(12), 1754-1755.

YANG, H., ACKER, J. P., CABUHAT, M., LETCHER, B., et al. (2005). Association of post-thaw viable CD34+ cells and CFU-GM with time to hematopoietic engraftment. *Bone Marrow Transplant, 35*(9), 881-887.

YOO, K. H., LEE, S. H., KIM, H. J., SUNG, K. W., et al. (2007). The impact of post-thaw colony-forming units-granulocyte/macrophage on engraftment following unrelated cord blood transplantation in pediatric recipients. *Bone Marrow Transplant, 39*(9), 515-521.

YOSHIDA, K., TAGA, T., SAITO, M., SUEMATSU, S., et al. (1996). Targeted disruption of gp130, a common signal transducer for the interleukin 6 family of cytokines, leads to myocardial and hematological disorders. *Proc Natl Acad Sci U S A, 93*(1), 407-411.

YU, X., SHACKA, J. J., EELLS, J. B., SUAREZ-QUIAN, C., et al. (2002). Erythropoietin receptor signalling is required for normal brain development. *Development, 129*(2), 505-516.

ZHA, J., HARADA, H., YANG, E., JOCKEL, J., et al. (1996). Serine phosphorylation of death agonist BAD in response to survival factor results in binding to 14-3-3 not BCL-X(L). *Cell, 87*(4), 619-628.

ZHANG, R., ZHANG, Z., WANG, L., WANG, Y., et al. (2004). Activated neural stem cells contribute to stroke-induced neurogenesis and neuroblast migration toward the infarct boundary in adult rats. *J Cereb Blood Flow Metab, 24*(4), 441-448.

ZHAO, C., DENG, W., & GAGE, F. H. (2008). Mechanisms and functional implications of adult neurogenesis. *Cell, 132*(4), 645-660.

ZWEZDARYK, K. J., COFFELT, S. B., FIGUEROA, Y. G., LIU, J., et al. (2007). Erythropoietin, a hypoxia-regulated factor, elicits a pro-angiogenic program in human mesenchymal stem cells. *Exp Hematol, 35*(4), 640-652.

9 LIST OF FIGURES AND TABLES

9.1 List of Tables

Table 1: List of Chemicals and Reagents 20
Table 2: List of commercial Kits 21
Table 3: List of antibodies 21
Table 4: List of Cell Culture Media and Supplements 22
Table 5: List of Laboratory Equipment 23
Table 6: List of media used for Microbiology 23
Table 7: List of standard buffers 24
Table 8: List of PCR strategies used to amplify the EPO variants 26
Table 9: List of primers used for the generation of the His-tag expression vectors 28
Table 10: List of primers used for the generation of the A-helix mutants 29
Table 11: List of primers used for the generation of the GST-tag expression vectors 30
Table 12: List of primers used for the generation of the murine LIFR- and gp130-constructs 31
Table 13: Cultivation protocols of cell lines 40
Table 14: Primers used in LightCycler experiments for the establishment of receptor expression profiles of different cell lines 40
Table 15: Primers used in LightCycler experiments for quantification of GFAP-mRNA levels in NSC sphere cultures 43
Table 16: Improvements in protein expression systems 56
Table 17: Products from human and murine EPO PCR 128
Table 18: Summary of hematopoietic and neuroprotective properties of the EPO variants and EPO peptides 134

9.2 List of Figures

Figure 1: Phylogenetic tree of erythropoietin ... 8
Figure 2: The average minimized NMR structure of EPO ... 9
Figure 3: Spliceosome catalyses removal of introns in pre-mRNAs ... 12
Figure 4: Workflow: protein purification of His-tagged proteins expressed in HEK293 cells ... 32
Figure 5: Oxygen glucose deprivation (OGD) assay as model of cerebral ischemia ... 35
Figure 6: Serum and oxygen deprivation in the H9c2 myoblast cell line ... 38
Figure 7: Experimental Design 1 of NSC experiments ... 41
Figure 8: Experimental Design 2 of NSC experiments ... 42
Figure 9: Survival paradigm in a hematopoietic stem cell system derived from murine bone marrow ... 46
Figure 10: Differentiation assay with hematopoietic stem cells derived from murine bone marrow ... 47
Figure 11: Agarose gels visualizing products of EPO-PCRs on murine and human tissues ... 51
Figure 12: cDNA structure of EPO splice variants ... 52
Figure 13: Predicted secondary protein structures of EPO splice variants ... 53
Figure 14: Structure prediction of hS3 and mS using an automated comparative protein modeling approach ... 54
Figure 15: Purification of His-tagged murine and human EPO variants ... 57
Figure 16: Colony forming assays ... 59
Figure 17: Human and murine EPO variants are neuroprotective. ... 60
Figure 18: The EPO variants induce a more robust tolerance against OGD compared to EPO ... 61
Figure 19: Human EPO and EPO splice variants have similar dose-survival curves ... 62
Figure 20: Primary protein structures of the EPO variants ... 63
Figure 21: The A-helix of erythropoietin is sufficient to induce ischemic tolerance in neuronal cultures 64
Figure 22: Erythropoietin A-helix deletion variants are neuroprotective ... 65
Figure 23: Neuroprotective EPO peptides ... 66
Figure 24: hEPO and hS3 mediated cytoprotection in an in vitro model of myocard ischemia ... 67
Figure 25: Anti-EPO antibodies immunoprecipitate two proteins from murine tissue extracts ... 68
Figure 26: The expression of the smaller protein seems to be co-regulated with mEPO-expression ... 68
Figure 27: Akt kinase assay ... 70
Figure 28: Signaling in primary cortical neurons ... 71
Figure 29: AG490 treatment of cortical neurons inhibits neuroprotection mediated by hS3 and hEPO .. 71
Figure 30: Recombinant EPO isoforms effect on cell viability of NSC/NPC ... 72
Figure 31: hS3 mediates survival and differentiation effects on NSC/NPC ... 73
Figure 32: Sphere cultures cultivated in presence of hS3 contain higher cell numbers ... 74
Figure 33: Clonogenic assay on neural stem cell cultures pretreated with hS3. ... 75
Figure 34: hS3 influences the differentiation of NSC/NPC ... 76

Figure 35: MAP2 and DCX staining of cultures derived from hS3 treated spheres 78
Figure 36: NSC/NPC exposure to hS3 enhances GFAP mRNA expression..... 79
Figure 37: Human A-helix derived peptide P16 protects NSC/NPC from growth factor withdrawal in a dose-dependent manner 79
Figure 38: Effects of peptide P16 on NSC/NPC cultures..... 80
Figure 39: Light cycler real time PCR experiment for 4 h treatment of spheres with peptide P16..... 81
Figure 40: Influence of IL-3 or IL-3+SCF in combination with vEPO on the formation of CFU-E and myeloid CFU 82
Figure 41: EPO isoforms enhance survival of HPC in 2 day liquid bone marrow cultures 84
Figure 42: P16 is most effective in enhancing survival of HPC in 5 day liquid bone marrow cultures.... 86
Figure 43: Colonies grown from P16-treated cultures are on average larger and denser..... 87
Figure 44: The splice variant hS3 mediates survival effects on murine mesenchymal stem cells. 88
Figure 45: P16 provides survival effects on murine mesenchymal stem cells in a feeding paradigm. 89
Figure 46: Neuroprotection mediated by A-helix mutants..... 90
Figure 47: Crystal structure of human erythropoietin complexed to its receptor..... 91
Figure 48: Functional assays on BaF3 cell lines 92
Figure 49: Pulldown of EPOR from BaF3/EPOR cells..... 94
Figure 50: 125I-rhEPO competition assays..... 95
Figure 51: Light cycler experiment: Receptor screening 96
Figure 52: The soluble LIF receptor abolishes hS3 but not hEPO mediated tolerance against OGD in primary cortical neurons. 97
Figure 53: Neuroprotection conferred by hS3 is attenuated by coapplication of anti-LIFRα and anti-gp130 blocking antibodies. 98
Figure 54: Pulldown assays show interacton of murine and human EPO splice variants with LIFRα species 99
Figure 55: M1 proliferation assay 100
Figure 56: in vivo biological activities of recombinant hEPO analogues 101
Figure 57: hS3 is non-erythropoietic in vivo..... 103
Figure 58: Signaling pathway of hEPO and hS3 in primary cortex neurons..... 108
Figure 59: Diagram of the formation of blood cells..... 110
Figure 60: Differentiation potential of neural stem cells..... 114
Figure 61: Subunit sharing in the receptors for the LIF-family of cytokines..... 120
Figure 62: Multiple Alignment of cDNA sequences of human EPO variants 130
Figure 63: Multiple Alignment of cDNA sequences of murine EPO variants..... 132
Figure 64: Protein sequence alignment of murine and human EPO variants..... 133

ACKNOWLEDGEMENTS

I thankfully acknowledge my supervisors Prof. Dr. Josef Priller and Prof. Dr. Andreas Meisel for their support and advice in this particular project.

I wish to thank Dr. Dorette Freyer for her helpful suggestions in cell culture techniques and Renate Gusinda for her immense help in preparation of primary neurons.

I also thank Claudia Muselmann, Carena Teufelhart, Sonja Blumenau and Christian Boettcher for their technical assistance in the vEPO project and especially Anna Hegele, a former technical assistance in our lab for her patient entering guides in many techniques of the molecular biology during my diploma thesis time. I am grateful to Katharina Stohlmann and Sabine Cho for help in the animal experiments.

Furthermore I would like to thank Thomas Götz, Franziska Scheibe, Dr. Chotima Boettcher, Dr. Stefanie Maerschenz and Nicolas Coquery for critical comments and their readiness to provide assistance. Thanks also to Dr. Ulrich Schweizer for providing advice. I would like to thank Dr. Stefanie Maerschenz and Michael Quinn for proofreading of my dissertation. Thanks to all members of my lab for their friendship and encouragements.

Special thanks to the International Graduate Program Medical Neurosciences.

Finally many thanks to my husband Peter Saiger for his support and understanding during his own PhD thesis time.

CURRICULUM VITAE

“Mein Lebenslauf wird aus datenschutzrechtlichen Gründen in der elektronischen Version meiner Arbeit nicht veröffentlicht.“

LIST OF PRESENTATIONS AND PUBLICATIONS

PATENTS

MEISEL, A., PRILLER, J., BONNAS, C. & DIRNAGL, U. (2006). Erythropoietin variants (C07/K 14/435 ed.). AE, AG, AL, AM, AT, AU, AZ, BA, BB, BG, BR, BW, BY, BZ, CA, CH, CN, CO, CR, CU, CZ, DE, DK, DM, DZ, EC, EE, EG, ES, FI, GB, GD, GE, GH, GM, HR, HU, ID, IL, IN, IS, JP, KE, KG, KM, KN, KP, KR, KZ, LC, LK, LR, LS, LT, LU, LV, LY, MA, MD, MG, MK, MN, MW, MX, MZ, NA, NG, NI, NO, NZ, OM, PG, PH, PL, PT, RO, RU, SC, SD, SE, SG, SK, SL, SM, SY, TJ, TM, TN, TR, TT, TZ, UA, UG, US, UZ, VC, VN, YU, ZA, ZM, ZW.

PRILLER, J., BONNAS, C. & MEISEL, A. (2007). Method of cell culture and method of treatment comprising a vEPO protein variant (C07K 14/505 (2006.01), A61K 38/18 (2006.01) ed.). AE, AG, AL, AM, AT, AU, AZ, BA, BB, BG, BH, BR, BW, BY, BZ, CA, CH, CN, CO, CR, CU, CZ, DE, DK, DM, DO, DZ, EC, EE, EG, ES, FI, GB, GD, GE, GH, GM, GT, HN, HR, HU, ID, IL, IN, IS, JP, KE, KG, KM, KN, KP, KR, KZ, LA, LC, LK, LR, LS, LT, LU, LY, MA, MD, ME, MG, MK, MN, MW, MX, MY, MZ, NA, NG, NI, NO, NZ, OM, PG, PH, PL, PT, RO, RS, RU, SC, SD, SE, SG, SK, SL, SM, SV, SY, TJ, TM, TN, TR, TT, TZ, UA, UG, US, UZ, VC, VN, ZA, ZM, ZW.

PRILLER, J., BONNAS, C. & MEISEL, A. (2008). In preparation.

PUBLICATIONS

BONNAS, C., MEISEL, A. & PRILLER, J. (2008). Endogenous non-hematopoietic erythropoietin splice variants with cytoprotective properties. *submitted*.

BONNAS, C., MAERSCHENZ, S., GÖTZ, T., MEISEL, A. & PRILLER, J. (manuscript in preparation). An endogenous EPO splice variant promotes survival in diverse stem cell populations.

ORAL PRESENTATIONS AND POSTERS

BONNAS, C. (2006). The cytoprotective role of erythropoietin in different cell types., *Route 28*. Frauenchiemsee (Germany). Poster.

BONNAS, C., MEISEL, A. & PRILLER, J. (2007). Neuroprotection by novel endogenous non-hematopoietic erythropoietin derivatives. , *Society for Neuroscience annual meeting*. San Diego (USA). Oral presentation.

BONNAS, C., MEISEL, A. & PRILLER, J. (2008). Neuroprotection by novel endogenous non-hematopoietic erythropoietin derivatives, *Berlin Neuroscience Forum*. Liebenwalde (Germany). Oral presentation.

BONNAS, C., MEISEL, A. & PRILLER, J. (2008). Identification of endogenous, non-hematopoietic erythropoietin splice variants with cytoprotective activities, *Society for Neuroscience annual meeting*. Washington, DC (USA). Poster accepted.

EIDESSTATTLICHE ERKLÄRUNG

Ich versichere an Eides statt, dass ich die vorliegende Dissertation

In vitro characterization of unknown isoforms of erythropoietin and evaluation of their biological importance.

selbst und ohne unzulässige Hilfe Dritter verfasst habe, dass sie auch in Teilen keine Kopie anderer Arbeiten darstellt und die benutzen Hilfsmittel sowie Literatur vollständig angegeben sind.

Berlin, den 22.09.2008

Christel Bonnas